

LINE-OF-SIGHT GUIDANCE  
TECHNIQUES FOR MANNED  
ORBITAL RENDEZVOUS

by

Edwin Eugene Aldrin, Jr.

January 1963

degree of Doctor of Science

Archives  
MASS. INST. OF TECHNOLOGY  
AUG 11 1967  
LIBRARIES

LINE-OF-SIGHT GUIDANCE TECHNIQUES  
FOR MANNED ORBITAL RENDEZVOUS

by

Edwin Eugene Aldrin, Jr.  
Major, USAF

B. S. , United States Military Academy  
(1951)

SUBMITTED IN PARTIAL FULFILLMENT  
OF THE REQUIREMENTS FOR THE  
DEGREE OF DOCTOR OF SCIENCE

at the

MASSACHUSETTS INSTITUTE OF TECHNOLOGY  
January, 1963

Signature of Author \_\_\_\_\_  
Department of Aeronautics and  
Astronautics, January, 1963

Certified by \_\_\_\_\_  
Thesis Supervisor

Certified by \_\_\_\_\_

Certified by \_\_\_\_\_

Certified by \_\_\_\_\_

Accepted by \_\_\_\_\_  
Chairman, Departmental  
Graduate Committee

MASS. INST. OF TECHNOLOGY  
APR 17 1968



Room 14-0551  
77 Massachusetts Avenue  
Cambridge, MA 02139  
Ph: 617.253.2800  
Email: docs@mit.edu  
<http://libraries.mit.edu/docs>

## **DISCLAIMER**

### **MISSING PAGE(S)**

Page 69 is missing from the Archives copy of this thesis. This is the most complete version available.

MRL  
P69  
Penny

Phis  
Geo.  
1963  
S.C.D.

LINE-OF-SIGHT GUIDANCE TECHNIQUES  
FOR MANNED ORBITAL RENDEZVOUS

by

Edwin Eugene Aldrin, Jr.  
Major, USAF

Submitted to the Department of Aeronautics and Astronautics on January 7, 1963, in partial fulfillment of the requirements for the degree of Doctor of Science.

ABSTRACT

A study is made of the inertial rotation of the line of sight throughout three dimensional Keplerian rendezvous trajectories. A simple, yet very meaningful method of classifying rendezvous trajectories through the use of "Rendezvous Parameters" is presented. Simple approximate expressions are derived in terms of these parameters which greatly facilitate the analysis of rendezvous guidance.

The noncoplanar aspects of rendezvous are analyzed by a method, valid for low relative inclinations, which, based on two brief target position observations, permits the simple calculation of the out-of-plane velocity change required to shift the relative line of nodes to a predetermined point.

These principles are then applied to a specific rendezvous mission situation, namely the NASA Gemini rendezvous mission. A rendezvous guidance technique, designed to extend man's control capabilities, is derived, whereby, through a sight reticle programmed to vary inertially for a selected exact nominal Keplerian trajectory, the astronaut can initiate, monitor and correct his intercept to maintain a collision course up to the braking or velocity matching maneuver.



This optical method of rendezvous is thoroughly analyzed and, through a digital computer simulation, found capable of performing successful rendezvous within prescribed velocity change limitations for significantly large uncertainties in the knowledge of initial orbit conditions and for significant errors in observations, tracking, and thrust correction application. The results of the study of the specific mission application are then demonstrated to be directly extendible both to a wide range of near-Earth manned orbital operations including targets of extreme ellipticity, and to orbital operations in the vicinity of the Moon.

Thesis Supervisors:

Title: Dr. Walter Wrigley  
Professor of Instrumentation and  
Astronautics

Title: Robert L. Halfman  
Associate Professor of Aeronautics  
and Astronautics

Title: Dr. Myron A. Hoffman  
Assistant Professor of Aeronautics  
and Astronautics

Title: Norman E. Sears  
Group Leader, Apollo Space  
Guidance Analysis Division,  
M. I. T. Instrumentation Laboratory





## DEDICATION

In the hopes that this work may in some way contribute to their exploration of space, this is dedicated to the crew members of this country's present and future manned space programs. If only I could join them in their exciting endeavors!



## TABLE OF CONTENTS

<u>Chapter No.</u>		<u>Page No.</u>
1	Introduction	1
2	Review of Current Rendezvous Concepts	4
3	Specific Mission Application	21
4	The Approach Phase	37
5	Intercept Trajectories - Rendezvous Parameters	65
6	Derivation of Guidance Philosophy	125
7	Rendezvous Simulations	141
8	Complete Results of Simulations	181
9	General Theory of Rendezvous	231
10	Summary and Conclusions	243
<u>Appendices</u>		
A	Derivation of Exact and Approximate Orbital and Relative Motion Expression	261
B	Description of Computer Subroutine ORBIT POS	299
References		305
Biography		311



## INDEX OF FIGURES

<u>Figure No.</u>		<u>Page No.</u>
3-1	Gemini Spacecraft Maneuver Capabilities and Visibility	25
3-2	Launch Out-of-Plane Conditions	27
3-3	Gemini Closed Loop Guidance - Typical Example, Inertial and Rotating Coordinate Frames	29
3-4	Suggested Gemini Rendezvous - Typical Example, Inertial and Rotating Coordinate Frames	33
4-1a	An Elliptic Orbit in Rotating Coordinates	39
4-1b	Anomaly Diagram	39
4-2a	Other Orbits in Rotating Coordinates	45
4-2b	Intercept Trajectories in Rotating Coordinates	45
4-3	Phase Rate versus Range	47
4-4	The Concept of Parking and Waiting Orbits	49
4-5	Coapsidal Elliptic Waiting Orbits for Elliptic Target Orbits	53
4-6	Circular Waiting Orbits for Elliptic Target Orbits	54
4-7	Ideal Gemini Phase Angle versus Time	57
4-8	Practical Gemini Phase Angle versus Time	59
4-9	Quasi-Direct Ascent for Gemini	61
4-10	Angle in Orbit versus Launch Delay Time	62

<u>Figure No.</u>		<u>Page No.</u>
5-1	Typical Intercept - Circular Coplanar Orbits	67
5-2	Multiple Intersecting Intercepts - Circular Coplanar Orbits	75
5-3	Approximate True Anomalies and Total Velocity Changes as Functions of Rendezvous Parameters b and k	76
5-4	Approximate Initial and Final Line of Sight and $\Delta V$ Angles as Functions of Rendezvous Parameters b and k	77
5-5	Approximate Initial, Final and Total Velocity Changes as Functions of Rendezvous Parameters b and k	78
5-6	Target Initiated Intercept Trajectories	87
5-7	Radial Error Insensitivity for Elliptic Target Orbits	89
5-8	Non-Coplanar Effects	92
5-9	$\Delta V_{iz}$ Determination by Observation	95
5-10	Out-of-Plane Motion during Intercept Trajectories	105
5-11	Line-of-Sight $\phi$ and $\psi$ Angles for Hohmann Transfer and k = 0.6	111
5-12	Line-of-Sight $\phi$ and $\psi$ Angles for k = 0.7	112
5-13	Line-of-Sight $\phi$ and $\psi$ Angles for k = 0.8	113
5-14	Line-of-Sight $\phi$ and $\psi$ Angles for k = 0.9	114
5-15	Line-of-Sight $\phi$ and $\psi$ Angles for k = 1.0	115
5-16	Line-of-Sight $\phi$ and $\psi$ Angles for k = 1.1	116
5-17	Line-of-Sight $\phi$ and $\psi$ Angles for k = 1.2	117

<u>Figure No.</u>		<u>Page No.</u>
5-18	Selected Standard Trajectory $\phi$ vs $t$ , $\psi$ vs $t$ , and $\tan_N \psi$ vs $t$	118
6-1	Optical Plane-of-Orbit Determination	127
6-2	The Optical Rendezvous Sight	131
6-3	Velocity Correction Coupling Effects	135
6-4	Guidance Equation Approximation - No Radar Option	137
7-1	Analytical Determination of Initial Pitch Down Angle $a_p$	155
7-2	Analytical Determination of Subsequent Pitch Down Angle $a_p$	157
7-3	Effects of Variable $\gamma_i$	165
7-4	Effects of Waiting Orbit Errors	167
7-5	Effects of Target Orbit Errors	169
7-6	Target Orbit Errors Reflecting Combined Errors	171
7-7	Rendezvous Between Coapsidal Elliptic Orbits - No Errors	175
7-8	Rendezvous Between Extreme Coapsidal Elliptic Orbits - No Errors	177
8-1	Effects of Measurement and Action Errors on the Standard Trajectory	183
8-2a	Detailed Presentation of a Rendezvous Simulation	186
8-2b	Detailed Presentation of a Rendezvous Simulation (cont.)	187

<u>Figure No.</u>		<u>Page No.</u>
8-3	Comparison of Modes of Operation	191
8-4	Standard Trajectory Compared with Other Trajectories	193
8-5	Effects of Variations in Pitch Down Angle Angle $\alpha_p$	197
8-6	Effects of Variations in Nominal Radial Distance d	199
8-7	Effects of Variations in Size of Square Reticle	201
8-8	Effects of a Circular Reticle	203
8-9	Effects of Variations in $\gamma_i$ on a Critical Orbit Error	205
8-10	Extension of Results to Other Earth Orbit Missions	207
8-11	Extension of Results to Lunar Orbit Missions	211
8-12	Error Effects on Extreme Coapsidal Elliptic Orbits	215
8-13	Initial Maneuver for Standard Intercept Line-of-Sight Motion - Intercepts from Circular Waiting Orbit to Elliptic Target Orbit	219
8-14a -	Error Effects on Intercepts from Circular	220 -
8-14h	Waiting Orbits to Elliptic Target Orbit	227
9-1	Generalized Approach for Rendezvous Intercept	233
9-2	Intentional No-coplanar Injection	237
10-1	Applications to Lunar Orbit Rendezvous Mission	253
A-1	Approximate Relative Motion in a Rotating Coordinate Frame	291



## DEFINITION OF TERMS AND SYMBOLS

- a - semi-major axis
- b - rendezvous parameter
- c - fictitious vehicle in circular orbit
- d - radial difference between initial and final radii  
of intercept
- e - eccentricity
- E - eccentric anomaly
- f - true anomaly
- h - massless angular momentum
- i - relative inclination between orbits, interceptor vehicle
- k - rendezvous parameter
- K - guidance sensitivity
- M - mean anomaly
- n - mean motion
- p - semilatus rectum
- P - orbital period
- r - interceptor radius
- R - target radius
- Rng - range from interceptor to target
- S - circular arc distance

- t - time, target vehicle
- V - velocity
- X - coordinate axis - usually coplanar with specified velocity vector
- Y - coordinate axis - usually extends from center of attracting body and passes through a specified vehicle
- Z - coordinate axis - usually aligned with specified angular momentum vector
- $\alpha$  - velocity change angle measured in interceptor plane from the local vertical, or planar pitch angle relative to the line of sight
- $\beta$  - line-of-sight angle measured in interceptor plane from the local vertical
- $\gamma$  - central angle in target orbit plane measured from relative line of nodes unless doubly subscripted
- $\delta$  - incremental quantity representing an error
- $\Delta$  - incremental quantity or deviation
- $\theta$  - central phase angle between interceptor and target, usually in interceptor's plane
- $\mu$  - gravitational constant
- $\pi$  - angular radian measure
- $\rho$  - projection of Rng vector into interceptor plane

- $\phi$  - inertial line-of-sight angle measured in interceptor plane
- $\chi$  - initial velocity change angle measured normal to interceptor plane
- $\psi$  - ~~line-of-sight~~ angle measured normal to interceptor plane
- $\omega$  - mean phase rate or difference in mean motions

Subscripts - pertaining to

- a - target acquisition point, apogee
- b - braking condition
- c - circular orbit
- f - final condition, fictitious satellite in circular orbit
- H - Hohmann transfer
- i - initial condition at start of intercept, interceptor vehicle
- N - a normalization of a function
- p - planar component, parking orbit, perigee, phase shift
- r - radial component
- T - total
- t - target vehicle
- w - waiting orbit

- $z$  - out-of-plane component
- $\epsilon$  - error condition
- $\theta$  - component in the plane of motion and normal to the radius vector
- $\phi$  - planar correction
- $\psi$  - out-of-plane correction
- 1 - first  $\psi$  observation condition
- 2 - second  $\psi$  observation condition

## CHAPTER 1

### INTRODUCTION

#### 1.1 The Rendezvous Problem

The rendezvous problem as treated herein is concerned with the maneuvers required of one space vehicle, termed the interceptor, to establish and maintain a collision course with another space vehicle, termed the target, up to the final braking or velocity-matching maneuver. In general, the target is assumed to be non-maneuvering and in an orbit in the near vicinity of a central attracting body such as the Earth. Further, subsequent to orbit injection of the interceptor, both vehicles are assumed to be essentially free from the effects of atmospheric drag.

The motion of the two vehicles, treated as point masses, is considered primarily from the geometrical aspect of the relative motion of the target vehicle as seen from the interceptor. This motion is considered to consist of relative range changes and angular rotation of the LOS (line-of-sight) relative to some convenient coordinate frame.

The guidance techniques for achieving rendezvous, as developed in this investigation, are based on the premise that angular LOS motion of the target may at times be the only tracking information available to the interceptor. Only the orbital injection and perhaps initial corrective maneuvering of the interceptor are based on ground tracking and a knowledge of the target orbit ephemeris. The guidance equipment required for initiating and completing the intercept, however, is self-contained in the interceptor vehicle.

#### 1.2 Potentialities of Line-of-Sight Guidance Techniques

In general, the ability to perform rendezvous missions in space utilizing only LOS angular tracking information has two potential applications. Either the range information is intentionally absent due to equipment limitations, or some component failure in the primary guidance

system prevents the use of the anticipated complete automatic tracking information.

The first case is usually characteristic of intercepts of a passive or uncooperative target. The complexity of radar equipment to acquire a target and supply range and angle tracking information is considerably increased when the target is not equipped with a transponder beacon. Weight and power considerations also may prohibit the use of such radar systems at the ranges desired for intercept initiation. Alternatives to microwaves involve the use of angle trackers varying from the ultraviolet to the infrared spectrum. Eventually such devices may be coupled with laser or simple radar ranging equipment. It is quite probable that angle tracking information would be available at considerably greater ranges than range tracking information. As a result, it may very well be desirable to perform initial intercept maneuvers utilizing only LOS angular tracking data. Operational missions in this category would include rescue, repair or inspection of disabled or alien space vehicles.

The second case for the application of LOS guidance techniques implies a back-up guidance mode to complete a rendezvous intercept of a cooperative target in the face of primary guidance equipment malfunctions. Requirements for such a back-up might stem from a desire to increase the probability of overall mission success by protecting against failures of radar tracking or data processing and computation equipment. Angle tracking data for LOS guidance might consist of astronaut observations of a flashing light on the target through a referenced optical sight or the output of an automatic tracker of some target spectral emissions. Since such equipment would be of a back-up nature, it should be as simple and reliable as possible and ideally independent of the primary guidance system components. The exact form of mechanization and degree of complexity of the back-up mode will be subject to many trade-off considerations, the spacecraft configuration and specific mission requirements. Operational missions which might employ such a back-up mode of rendezvous guidance are the Gemini mission, the Apollo landing abort maneuvers or rendezvous from the lunar surface and various future space station ferry missions.

The guidance techniques and orbit considerations discussed in this investigation are generally applicable to either the passive target situation or the back-up mode application. The prime emphasis, however, is directed toward back-up utilization to enhance the chances of mission success. In particular, the Gemini mission has been selected as a specific illustrative application.

## CHAPTER 2

## REVIEW OF CURRENT RENDEZVOUS CONCEPTS

2.1 General

Rendezvous of space vehicles has received widespread attention in the past several years. Many of our national space programs, both civilian and military, are involved intimately with the problems of rendezvous. Of the many published works, the references by Houbolt (23) and Thompson (51) offer excellent general treatment and summaries.

The basic rendezvous problem is usually subdivided into maneuvering phases. Though these phases vary considerably depending on specific approaches and in many cases overlap, they may be categorized as follows:

- (1) Ascent or Approach Phase
- (2) Intercept or Terminal Phase
- (3) Braking and Docking Phase

The distinction that separates the first two phases is that for the ascent or approach phase, the relative motion is inferred from the separately determined motion of the two vehicles; whereas during the intercept or terminal phase, the relative motion is obtained directly from observations of the target made by the interceptor. The approach phase, which can be considered to start at interceptor lift-off, may be either a direct or indirect ascent type, and the desired end conditions may or may not be a near-collision course. The desired end condition of the intercept phase is to maneuver the interceptor onto a precise collision course with the target. In some concepts this may be combined with a portion of the final braking maneuver. The rendezvous culminates in the last phase with the vehicles at zero relative velocity either in soft contact or a prescribed station-keeping orientation.

2.2 The Ascent or Approach Phase

As the earth's rotation causes the interceptor launch site to approach the target orbit plane, there are two position variations that strongly



influence the launch timing and subsequent interceptor maneuvering during the approach phase. The first is the position or "phase angle" of the target in its orbit relative to the interceptor, and the second is the position of the interceptor relative to the target orbit plane or "planar displacement".

When the phase angle determines the launch time, direct ascent maneuvers may be executed. In this case the orbit injection or termination of the thrusting ascent of the interceptor is planned to occur either in the close vicinity of the target or in such a way that the interceptor is on a coasting near-collision course with the target. In general, a planar displacement will exist for a direct ascent, and can be compensated for by a combination of a turning maneuver of the booster, which is termed "yaw steering", and a plane change of the interceptor as it passes through the target orbit plane.

On the other hand, when a small tolerance in the planar displacement determines a time period for acceptable launches and phase angle dictates only a desired but not required launch time, then an indirect ascent utilizing an intermediate near-coplanar interceptor orbit is employed. This intermediate orbit is caused to have a period different from the target orbit so that a catch-up or phase rate exists between the two vehicles. Then at some subsequent time, perhaps following an interceptor orbit change, acquisition of the target by the interceptor is made and the intercept or terminal phase is begun.

In the special case of target orbits for which a zero planer displacement exists simultaneously with a favorable phase angle, a coplanar direct ascent maneuver may be accomplished. These target orbits which have a particular period or semi-major axis length are termed "Rendezvous Compatible Orbits". A rather complete treatment of these special situations is given by Petersen in reference (37).

## 2.21 Direct Ascent

Direct ascent affords the opportunity to complete the rendezvous maneuver in a minimum amount of time, yet the demands on the launching

operation are quite stringent and the fuel penalties associated with delays, inaccuracies and non-optimum target orbit conditions may be quite high. Since a target in a near Earth orbit is travelling at a rate of almost 5 miles per second, relative to the Earth, it is obvious that any launch delays or guidance variations will necessitate either changes in the nominal boost trajectory or considerable corrections in the subsequent phases of the rendezvous maneuver. Unfortunately, last second changes in the booster guidance programs are a bit beyond the current state of the art; therefore, launch inaccuracies are usually envisioned as being absorbed in subsequent corrective thrusting maneuvers of the interceptor. The situation is further compounded when planar displacements require significant plane change maneuvers, since these maneuvers are most efficiently performed at the relative line of nodes and launch delays may require shifting the nominal rendezvous location away from this point. The period of time during which a direct ascent rendezvous launch can be initiated and not exceed the maneuver capabilities of the interceptor is usually termed the "launch window".

#### 2.211 Near Orbit Matching Direct Ascent

In some cases of direct ascent, the desired end conditions of the first phase of rendezvous may not be the attainment of a collision course with the target. If the target orbit altitude is in the vicinity of a desirable orbit injection altitude of the interceptor, then a continuous thrusting boost profile can inject the interceptor into a near matching orbit in close proximity to the target. Injection errors or possible intentional mismatching of position and velocity will result in a small relative velocity between the vehicles but not necessarily a collision course. Then at some subsequent favorable time a terminal intercept may be initiated. The "group flights" of the Russian Vostoks provide good examples of this type of direct ascent orbit matching. In these flights it appears as though the injection profiles of both vehicles were very nearly identical with the possible exception of the use of yaw steering in the second vehicle since the target orbit was not precisely a rendezvous compatible orbit. The second vehicle was injected slightly ahead of the first and with a slightly greater semi-major axis so that the

first vehicle would soon overtake it. The period difference in the orbits was probably due more to orbital decay from atmospheric effects than anything else. This technique of orbit-matching direct ascent is limited to rather low altitude target orbits whose lifetimes may not exceed much more than a week. Perhaps of more importance is the critical requirement to launch on time. Launch windows on the order of a few seconds would exist for preprogrammed injection profiles. With variable injection programs, the window could be extended to tens of seconds.

#### 2.212 Coasting Orbit Direct Ascent

The more general case of direct ascent employs a coasting period between the powered ascent phase and the time that the interceptor approaches the close vicinity of the target. A near collision course is the goal of the ascent phase in these cases. The coasting orbit travel may vary from somewhat less than  $90^{\circ}$  to about  $270^{\circ}$  and this variation can be used to absorb considerably greater launch delays than are possible in the previous case. A boost trajectory can be selected which will compensate for delays by simply changing the cut-off of the final booster engine; i. e. , the altitude and flight path would remain essentially the same but the magnitude of the velocity vector would be varied. Planar displacements, however, would require more involved changes in yaw steering so that the relative line of nodes of the coasting orbit would occur at the nominal rendezvous point.

The optimum conditions of relative position and velocity at the end of the coasting period stem from the desire to further reduce the effects of timing and guidance inaccuracies during the ascent phase. It has generally been found that an interceptor position ahead and above the target with a fairly high relative closing velocity (underspeed condition) near collision course is most tolerant to injection errors. This might be likened to a "lob" maneuver where the interceptor, with a considerably lower velocity near the top of the arc, awaits the rapidly approaching target.

The work done by Sears (40, 41) and Duke, Goldberg and Pfeffer (11) is typical for this case of direct ascent. This coasting orbit maneuver can be employed for a much wider range of target orbit altitudes than for the orbit matching maneuver; however, the launch window is still on the order of several tens of seconds.

## 2.22 Indirect Ascent

Indirect ascent is employed as a basic maneuver technique during the ascent or approach phase when the time from launch to rendezvous is deemed to be generally less important than the desire to minimize fuel expenditures and to avoid critical launch times and sensitivity to variations in the boost trajectory. In this technique the desired launch time is no longer based on the rapidly changing phase angle as in direct ascent maneuvers. Instead, the more slowly changing planar displacement determines the desired launch time. The phase angle errors that result from this increased freedom in the launch timing are then gradually reduced by virtue of the period differences between the intermediate injection orbit of the interceptor and the target orbit. The interceptor, usually at a lower average altitude than the target, then catches up with the target a certain number of degrees per target revolution at a rate which is termed the phase rate. Though the fuel penalties associated with small planar displacements are rather modest and the reduction of phase angle errors is accomplished at essentially no fuel cost, the time from launch to rendezvous may be quite long, especially for large phase angles and low phase rates.

The launch window for indirect ascent rendezvous is limited by the interceptor capabilities to remove planar displacements by yaw steering during boost and/or plane change maneuvers in orbit, and is a function of the target orbit inclination and the launch site latitude. For the same general maneuver capability considered for the direct ascent profiles, indirect ascent launch windows are measured in tens or even hundreds of minutes. For high inclination or near polar target orbits the launch windows will be shorter, but two will exist each day as the launch site

passes through the target orbit plane twice in 24 hours. Range safety launch azimuth restrictions may, however, preclude the use of one of these windows.

For target orbit inclinations that are equal to or just slightly greater than the latitude of the launch site, as might be the case when one can choose the target orbit such as for the Gemini mission, space station missions, or the Apollo lunar orbit rendezvous problem, the two daily windows lengthen and blend into one large launch window. If the interceptor is launched at any time within the launch window into an intermediate orbit with an inertial velocity vector at injection that is parallel to the target orbit plane, then the relative inclination between the orbits will not exceed the value of  $0.4$  of a degree and the relative line of nodes will occur at a point  $90^{\circ}$  past the injection point. Yaw steering, naturally, may be used during boost to reduce or possibly eliminate the relative inclination between the orbits.

When such a launch window exceeds the orbit period of the target, a time will always exist during the window when the phase angle will be favorable for a short time to rendezvous or a "near direct ascent" maneuver. If further, a maximum time is specified for the interceptor to wait in the intermediate orbit to catch up to a favorable phase angle with respect to the target, then an acceptable launch period can be specified within the planar launch window. The final selection of a nominal target orbit is indeed a complex problem which depends on such things as the booster capabilities and optimum launch profiles, spacecraft maneuver capability, range restrictions, recovery areas, maximum wait times, window panes on successive days, and possible target maneuvers to compensate for errors or to facilitate the overall rendezvous problem. At the time of the original writing of this thesis, the Gemini mission planned to have a target orbit inclination about  $0.4^{\circ}$  greater than the launch site latitude which resulted in a launch window for the interceptor of about  $1\frac{1}{2}$  hours and a window pane one day later based on a one day maximum catch-up that was near the center of the window and lasted about 15-20 minutes.

Intermediate orbits for indirect ascent are generally considered to be one of two types:

- (1) A chasing orbit which is nominally tangent to the target orbit,
- (2) An intermediate orbit that does not intersect the target orbit and is usually at a lower altitude.

#### 2.221 Chasing Orbits

A chasing orbit is obtained usually by injecting the interceptor into an elliptic orbit at perigee with an excess over circular orbit velocity such that the orbit is just tangent to the target orbit. When the target orbit is circular, the point of tangency is at apogee. As the interceptor catches up to the target, the phase angle is reduced at successive points of tangency. When this phase angle becomes less than the phase rate per orbit, a tangential velocity is added by the interceptor so that a perfect phase match will occur in one or more orbits. An analysis of this technique as it applies to circular target orbits is given by Straly (48).

When a planar displacement exists for a perigee injection into a chasing orbit nominally tangent to a circular target orbit at apogee, a conflict exists between the in-plane and out-of-plane motion. The relative line of nodes for minimum planar displacement will occur  $90^\circ$  after perigee whereas the planar rendezvous is constrained by chasing orbit adjustment to the  $180^\circ$  point. This noncoplanar condition can either be corrected by a separate plane change maneuver at the line of nodes or absorbed by the terminal phase maneuvers. A possibility exists for alleviating this conflict by injecting the interceptor with a vertical velocity component so that the apogee point would coincide with the relative line of nodes  $90^\circ$  after insertion. The required total velocity at insertion would be less and naturally the subsequent perigee altitude would be lowered. A combined plane change and velocity addition at first apogee, however, could raise perigee up to within safe limits.

The current Gemini mission plan uses the chasing orbit approach with the Agena target vehicle in a nominally circular orbit at an altitude of 161 nm and the spacecraft injected at perigee with altitudes ranging from 87 to 161 nm. At present the option is being retained for a precise on time launch to perform the terminal phase rendezvous at first apogee. If anticipated launch uncertainties or holds prevent this, then the phase rate will be adjusted based on ground tracking information so that a low phase rate orbit with small relative velocity differences will exist for the orbit leading to a phase match situation.

Chasing orbits have several general characteristics which can be summarized as follows:

- (1) An optimum coplanar approach to the target,
- (2) A constrained location of the phase match point,
- (3) A relative nodal point that is out of phase with the point of tangency,
- (4) A limited final approach to the target that is nominally tangent to the target orbit
- (5) The interceptor is committed to a collision course based on ground tracking and prior to the terminal phase.

## 2.222 Intermediate Orbits

Alternatives to the use of the chasing orbit technique imply a catch-up orbit that is not tangential to the target orbit. Of the infinite possibilities that exist, the circular target orbit and a lower circular intermediate orbit will serve as a simple illustrative example. The circular intermediate orbit could be entered directly at insertion but considering the low burn-out altitudes of present boosters, orbit lifetime and various safety considerations, this orbit would most probably be entered by a circularizing maneuver at the first or some subsequent apogee. From this orbit a classical Hohmann transfer or many other types of intercepts could be initiated when the appropriate phase angle is reached.

The original Apollo concept based on Earth orbit rendezvous planned to use these types of intermediate orbits. One vehicle, perhaps the tanker, would be placed in a circular orbit at 300 nm and the spacecraft, launched into a circular orbit at 150 nm, would then perform a transfer intercept to 300 nm for the rendezvous.

Recently in several informal meetings an interesting variation to the approach phase using intermediate orbits has been discussed. This maneuver, termed a bi-elliptic transfer, has not as yet appeared in the open literature but appears worthy of brief note here. Basically it combines optimum planar maneuvers with plane changes at the nodal point. For two vehicles in circular orbits, the phase angle when one is at the nodal point may be arbitrary. To compensate for this, two successive Hohmann transfers are made at the nodes with the plane change being made at the midpoint of the complete  $360^\circ$  maneuver. The altitude gain during the first transfer is a variable and its proper selection will compensate for the variable initial phase angle. This maneuver seems to be highly efficient but rather complicated and perhaps quite sensitive to errors.

The intermediate orbit approach to rendezvous in contrast to the chasing orbit approach has been selected by the author to best exploit the potentialities of LOS guidance. The general characteristics of the intermediate orbit approach can be summarized as follows:

- (1) A rendezvous as early as first apogee is not possible,
- (2) Less velocity is required from the booster, therefore allowing a greater payload,
- (3) More velocity is required from the interceptor, thereby decreasing the payload,
- (4) An optimum coplanar approach to the target is possible if desired,
- (5) The rendezvous point can be adjusted,
- (6) The intercept initiation point or the rendezvous point can be adjusted to occur near a nodal point,



- (7) A wide range of final approach intercepts to the target is available,
- (8) The initiation of the intercept phase can be delayed until terminal phase observations of the target are available.

### 2.3 The Intercept or Terminal Phase

The intercept phase is that critical transition phase of rendezvous guidance between the periods of indirect relative motion determination during the ascent phase and the maneuvers performed in the close vicinity of the target that result in velocity matching. Starting as soon as direct measurements of the target motion by the interceptor become available, the objective is to insure that a collision course exists between the vehicles for the final braking maneuver.

By far the large preponderance of the literature that has appeared on the general subject of rendezvous has been devoted to this critical terminal phase. Direct comparison of the many proposed guidance techniques is most difficult due to the wide variety of assumed initial conditions, vehicle performance and equipment requirements. To be valid, such a comparison would involve a complete systems analysis. Most techniques, however, can be categorized as belonging to one of two basic guidance correction concepts: those employing the principles of proportional navigation, and those using orbit mechanics to describe relative motion.

#### 2.31 Proportional Navigation

Proportional navigation for rendezvous guidance is similar to the fire control problem of controlling the motion of the line-of-sight. For rendezvous, thrust accelerations or velocity changes are made normal to the LOS and proportional to some function of the angular velocity of the LOS. In an early reference Wrigley (55) pointed out the uses of proportional navigation for satellite rendezvous. Connors (8) used similar techniques for a constant bearing simplified guidance technique for interplanetary navigation. In all of the rendezvous papers to date dealing with proportional navigation, the function of angular velocity of the

LOS used for guidance corrections has been the angular velocity itself measured with respect to inertial space. For perfect orbital collision courses, the LOS motion goes to zero in the final stages, but earlier, at greater ranges, the direction of motion depends upon the direction of approach as will be seen in Chapter 5. Almost all of the techniques encountered have assumed that for the ideal case the two vehicles were essentially on a collision course prior to initiating proportional navigation techniques.

Several authors have proposed automatic terminal guidance schemes employing the above techniques of proportional navigation. These maneuvers have usually been assumed to be the culmination of a coasting orbit direct ascent approach and as such the relative velocities have been on the order of 1000 ft/sec. or higher. Such relative velocities would tend to indicate that if the final maneuver were not executed due to engine failure or other reasons, the resulting interceptor trajectory would lose altitude and probably reenter the atmosphere - a situation not wholly acceptable for manned operations. The relative vehicle orientation most conducive to proportional navigation techniques is to have the interceptor above and ahead of the target in a descending orbital condition slightly past the apogee point. As will be seen in Chapter 5, these conditions result in rather long periods of near-stationary LOS motion. In the techniques advanced by Sears (40, 41) LOS control is accomplished in conjunction with the braking or relative velocity reduction maneuver. Range rate is reduced as a function of the square root of range as a one-dimensional problem and simultaneously the thrust vector is set at a computed angle to the LOS to drive the LOS motion gradually to zero. The techniques of Duke, et al (11) are essentially similar except for an adaptation maneuver executed prior to terminal guidance to prolong the period that the interceptor remains above the orbit of the target.

Other terminal rendezvous guidance techniques, employing manual pilot control, also follow the essential principles of proportional navigation. Much of the work done in this area was pioneered at the Langley Research Center by Brissenden (3, 4), Kurbjun (24), and Lineberry (27). In their

simulations, a target equipped with a flashing light beacon was projected along with a star field background onto a planetarium type screen and the relative motion as seen from the interceptor was maintained by an analog computer. With a closing velocity controlled by the pilot through reference to a simulated radar range and range rate meter, a collision course was maintained by thrusting perpendicular to the LOS to hold the flashing light essentially fixed with respect to the inertial star background. When a motion of the target was discerned, a velocity change was added in the direction of motion until the target again appeared stationary. The complete relative motion situation was not covered in these simulations in that the dynamic attitude control of the interceptor in pitch, roll and yaw was not simulated. The results of these preliminary studies seem to indicate that for intercepts initiated at about 40 miles with relative velocities of about 1000 ft/sec, manual control to compensate for undisturbed miss distances of about 15 miles could accomplish rendezvous with only small penalties above the theoretical minimum fuel.

As an extension to these studies, Lineberry (27) investigated an all-optical technique that replaced the radar measured range and range rate with optically determined values. Basically the technique involved making two LOS angular rate measurements and then performing a velocity change normal to the LOS to null its rotation. Range and range rate can then be calculated with a simple linear relationship, valid for straight line motion. The conclusions stated that reasonable performance could be expected with angular rate measurements on the order of 0.1 milliradian per sec. To obtain these accuracies would require a stabilized sighting device with rather good optical quality.

Current planning for the NASA Gemini missions includes an alternate or back-up rendezvous technique termed "semi-optical" rendezvous which is essentially the same as the Langley work with out-the-window observations of a flashing light target against the star background and radar supplied range and range rate presentations. As a result of adjusted chasing orbits the vehicles are on a near-collision course with relative velocities between 50 and 150 ft/sec. Proportional navigation

corrections are initiated at about 20 miles and it is hoped that miss distances greater than 10 miles can be eliminated without exceeding vehicle capabilities. (It should be noted that the ratio of desired miss distance tolerance to closing velocity is considerably greater for Gemini than that originally studied by Langley.)

Recent pilot controlled simulations of the semi-optical rendezvous technique conducted at McDonnell Aircraft Corporation have uncovered two potential problem areas. The first is concerned with correctly discerning and correcting for actual target translation while the interceptor is experiencing expected body attitude rates and disturbance torques. The use of a fixed sight reticle of some sort is viewed as a possible aid in assisting the pilot in distinguishing between target translation with respect to the stars and his own spacecraft attitude motions. The second is that the inefficiencies associated with thrusting the LOS rate continually to zero are higher than many had originally envisioned. Velocity change capabilities in excess of 500 ft/sec were required to compensate for errors in the intercept that would have missed the target by less than 10 miles, and this approaches the maneuver limit of the Gemini spacecraft.

## 2.32 Orbit Mechanics

In contrast to proportional navigation techniques which usually assume an undisturbed straight line relative motion between the target and interceptor, terminal guidance techniques based on various approximations to true orbital motions can be categorized under the general heading of orbit mechanics. Due to the more exact descriptions of body motions inherent in orbit mechanics guidance, these techniques are useful at greater relative ranges and over greater periods of orbital travel. Proportional navigation is usually limited to about  $30^{\circ}$  of orbit travel whereas orbit mechanics guidance may be useful throughout a complete orbit.

Some orbit mechanics techniques are based on a complete orbit determination of both vehicles and the subsequent computation of the maneuvers required of one vehicle to establish an intercept orbit where-

as other techniques deal only with the relative motion of the two bodies without actually determining their respective orbits. The former approach has been taken by M.I.T. in developing the primary rendezvous guidance for the Lunar Excursion Module (LEM) in the Apollo mission. Current thinking is to have as a back-up a duplicate redundant system on board the Command Module (CM) to continually solve the rendezvous problem in a similar manner. Unfortunately, to date the full details of this system are not available in the open literature.

The relative motion approach to orbit mechanics rendezvous guidance stems from work pioneered by Hollister and Spradlin (20, 44) of M.I.T. and Clohessey and Wiltshire (7). The names of the latter individuals have generally been associated with a set of approximate linear differential equations which describe the motions of an interceptor with respect to a target in a circular orbit. These equations are derived in a coordinate frame centered in the target and rotating with its uniform angular velocity. The gravity terms are expanded in a series and the non-linear terms discarded. The resulting equations can be solved and rearranged to indicate the required relative velocity as a function of initial displacement to result in an intercept after a specified angular orbit travel. The equations can be used to provide mid-course corrections to a previously established near-collision course or to initiate an intercept course from the general vicinity of the target. Though the equations were derived assuming a target in a circular orbit, informal studies conducted by NASA seem to indicate that the relative motion description is not appreciably degraded for low ellipticity target orbits in the near vicinity of Earth.

Several evaluations have appeared on variations of these relative motion equations and many simulations have been conducted since their original disclosure. The basic equations remain the same for rectangular, cylindrical or spherical rotating reference coordinate frames; however, the motions differ in their validity as the time to rendezvous is increased. A report by Stapleford (46) concludes that each of the above coordinate frames has its advantageous regions of application but in general the

original rectangular frame seems to offer the best all-around solutions. Eggleston (14) of NASA has claimed that, for the rectangular coordinate frame, the solutions are only reasonably valid if the initial relative ranges are less than 200 nm and the time to complete the rendezvous is of the order of one quarter of a period or less. Swanson and Peterson (50) have proposed an alternative to the basic two-impulse technique of Clohessy and Wiltshire which is also based on the approximate linearized equations of motion and utilizes five horizontal velocity changes to complete the rendezvous in one complete orbit. This technique has been termed by the authors as a Quasi Optimal Rendezvous Guidance System yet no complete performance or error analysis has been published to date.

The primary on-board guidance for the NASA Gemini rendezvous missions employs the orbit mechanics approach with the Clohessy-Wiltshire equations and a modified cylindrical coordinate system. Many details of the techniques are continually being modified, but a general description is given by Czarnik (9). The terminal phase is initiated from a chasing orbit which has been adjusted to a near-collision course. Under the current plan, the intercept maneuver traverses a fixed  $270^{\circ}$  of orbit travel up to the final rendezvous point. The  $270^{\circ}$  was selected as a result of studies that indicated it to be a near optimum fuel maneuver to compensate for errors in the chasing orbit. The overall technique has been given the name "closed-loop guidance" since four intermediate corrections are scheduled every  $60^{\circ}$  of orbit travel; the last occurring  $30^{\circ}$  prior to rendezvous. Besides trimming the intercept to a collision course, these corrections compensate for errors introduced by the approximations in the guidance equations.

Prior to initiating the intercept, the astronaut must track the target with the on-board radar system for a period of 1000 sec while range and bearings information plus the platform orientation are periodically fed to the computer. Relative velocities are then computed and averaged over the last 1000 sec and the sum of the initial and final velocity changes required for rendezvous is displayed. When this sum is within the spacecraft capability and passes through a minimum, the intercept is initiated. After the last intermediate correction  $30^{\circ}$  prior to rendezvous the astronaut proceeds as in the semi-optical technique and manually with visual

references executes the braking and docking maneuver.

One final technique under the category of orbit mechanics terminal guidance systems appears worthy of mention since in many respects it is similar to the approach taken in this investigation. Sears of M.I.T. (41) has considered the problem of conducting a coplanar rendezvous between two vehicles in circular orbits under conditions of incomplete tracking. Of the two cases examined of either only range tracking or angle tracking information available to the interceptor, the latter case appeared to be distinctly superior. In this case a preplanned intercept was initiated when the target reached a predetermined elevation angle above the local horizontal. A single midcourse velocity change correction was then made in the radial direction based on a comparison of the actual LOS rotation rate and the rate expected for the preplanned intercept. Only coplanar Hohmann transfers were considered in this study.

#### 2.4 The Braking and Docking Phase

The final phase of orbital rendezvous consists of maneuvering the interceptor as it approaches the target so that their velocities are identical at some small displacement distance, then following this by small changes in position and velocity to establish physical contact and effect docking. With no significant exception, this phase of rendezvous has been treated as strictly a relative motion problem wherein a braking thrust is applied to control the closing velocity as a function of the range to the target according to some guidance law which will produce a velocity matching or zero relative velocity as the range goes to zero. Since the maneuvers take place in the close vicinity of the target with small amounts of orbital travel involved and the differential gravity forces are small in comparison to vehicle thrust accelerations, proportional navigation techniques are normally employed to obtain and maintain a collision course. The thrust vector producing relative motion deceleration (usually increasing the interceptor's absolute velocity) can be tilted away from the LOS inertial angular rate. For direct ascent or other approaches where the closing velocity is high, rather large miss distances can be eliminated with only a small increase in fuel expenditures.

To take advantage of this savings, the terminal phase can be delayed until the braking maneuver commences, in which case the two phases become one and the same.

Many guidance techniques have been proposed for accomplishing the braking maneuver, ranging from the fully automatic to complete manual pilot-controlled maneuvers. The investigations of Felleman and Sears (17, 18) are typical of the automatic approach. They have developed guidance logic for both variable thrust and constant thrust rocket engines wherein the commanded thrust is proportional to a function of range and the square of range rate such that engine capabilities are not exceeded. Intermediate acceleration levels below the maximum vehicle capability are used in a phase-plane plot of range and range rate to command increases or decreases in thrust levels or engine start and stop in the case of constant thrust engines. While the closing velocity is being reduced, a collision course is maintained by commanding the thrust to some angle to the LOS so that undesired inertial angular rotations of the LOS will gradually be nulled to zero.

Manual control of the braking phase has been studied by Brissenden and others (3, 4) with simulations employing transverse thrusters and observations of the target against a star background for proportional navigation course control and longitudinal thrusters and a simple range vs. range rate schedule for closing velocity reductions. Thrust accelerations of one or two  $\text{ft}/\text{sec}^2$  were used for the manual studies. These are considerably lower than the levels usually envisioned for the automatic systems. The efficiencies of the manual systems as measured in fuel consumption appear to approach those of the automatic systems; however, as indicated previously, these manual studies did not fully simulate the vehicle dynamics.

Analysis of the close-in maneuvering and docking of spacecraft is highly dependent upon specific vehicle configurations, thrust levels, look-angles, etc. Many detailed studies and simulations are currently being conducted by NASA and the general space industry, however, few reports are presently available. The Gemini docking maneuver will be completely manual based on visual observations and the Apollo procedures will most likely be very similar. Since the scope of this investigation includes only the maneuvers up to the braking phase no analysis will be made of docking techniques.



## CHAPTER 3

## SPECIFIC MISSION APPLICATION

3.1 Selection of the Gemini Mission for Application

Though the rendezvous principles and techniques presented in this investigation are valid for application to a wide range of space missions, it was felt that an application to a specific mission would be more enlightening and understandable to the reader. In addition, considering the large number of variables associated with rendezvous missions, an application to a specific mission with realistic boundaries and constraints would help to uncover basic methods and steps to be taken to solve rendezvous problems in general. Once the capabilities and limitations of a rendezvous technique have been uncovered for a specific mission, it is relatively simple to gradually change the mission and observe the effects on the capabilities and limitations of the system, thereby gaining an insight as to its applications in general.

When the study was first started, Apollo Earth orbit rendezvous maneuvers were considered as the specific application. Several factors soon became apparent to argue against this choice. The complexity and precision of the subsequent mission maneuvers seemed incompatible with an attempt to simplify greatly the rendezvous

maneuver. The large size of the vehicles requiring long burning time for velocity changes seemed to complicate unduly an attempt to apply a wholly new technique. There seemed to be little inherent design provision for pilot control of the vehicle especially by visual observations. When the Apollo mission concept was shifted to the Lunar Orbit Rendezvous approach, further consideration of this application was dropped.

Attention was then shifted to rendezvous missions associated with the NASA Gemini program. This spacecraft seemed far better suited to direct pilot control efforts. In fact as will be pointed out later, the preliminary design has incorporated specific provisions for man's direct participation in the rendezvous guidance. Since one of the primary missions of Gemini is to test specifically various rendezvous techniques, this alone should make it an ideal choice. After considerable study the author has come to the conclusion that if his suggestions and techniques are ever to be tested, then Gemini would be the most likely candidate.

In the subsequent investigation the author will attempt to be as general as possible and, when a solution to the Gemini problem appears to be in hand, extensions of these techniques will be discussed.

### 3.2 Limitations and Constraints of the Gemini Mission

The basic mission problem consists of launching an Atlas Agena D target vehicle into orbit from Cape Canaveral and following this by about one day with the launch of the two-man Gemini capsule,

boosted by a Titan II, into another orbit from which rendezvous and docking can be carried out as soon as practicable. Once the vehicles have been connected together, various maneuvers powered by the Agena will then take place. Following this the vehicles will uncouple and the Gemini will prepare for re-entry.

The initial tentative orbit altitudes are based on a desire for achieving a maximum payload in orbit, yet at the same time having sufficient orbit lifetime for a duration of several days. These considerations would place the rendezvous maneuvering in the close vicinity of 150 nm. The optimum burn trajectory for injecting the Gemini capsule into orbit has a cutoff altitude in the vicinity of 87 nm.

The target is to be equipped with a radar transponder, a high intensity flashing light beacon, an attitude control system, and a radio link so that velocity changes can be commanded from the ground or from the spacecraft. An adapter section has been fitted to the vehicle for docking and mooring purposes.

The spacecraft has a complete attitude control system rather similar to that used in the Mercury capsule. An adapter section for the rendezvous missions provides maneuver capability in six directions as shown in Fig. 3-1. The acceleration levels are fixed at  $1 \text{ ft/sec}^2$  forward and to the rear and  $1/2 \text{ ft/sec}^2$  in the transverse directions. It seems reasonable to assume that the velocity change capacity for

maneuvering, after subtracting out a quantity for docking and possible booster supplement, is somewhere in the region of 500 ft/sec. From a study of drawings of the capsule and from observing photographs of mock up models, it appears that the astronaut's visibility out the window as measured from the forward direction is about  $10^{\circ}$  down,  $30^{\circ}$  -  $40^{\circ}$  up and  $30^{\circ}$  -  $40^{\circ}$  to either side. Some of the special equipment planned to handle the presently proposed rendezvous techniques include a stabilized platform as part of an inertial measurement unit (IMU) package, a full tracking radar capable of measuring range and angles and their respective rates, and a special-purpose digital computer for solving the guidance problem. (9, 55)

It is within the framework of these limitations and constraints that the line-of-sight techniques developed in this investigation will be applied to the specific Gemini rendezvous mission.

### 3.3 Review of Present Approaches to Gemini Rendezvous

At present there are provisions for both automatic and manual modes of relative motion guidance to bring about a rendezvous situation. Both of these utilize the same initial orbital injection plan and subsequent preliminary maneuvering. First the Agena target is launched into a circular orbit 150 nm above the Earth with an inclination about  $.4^{\circ}$  greater than the latitude of the launch site ( $28.5^{\circ}$ ). This orbit would be corrected as required to within some, as yet unspecified, tolerance of circularity. Then about one day later as the launch site again approaches the target plane, the Gemini spacecraft would

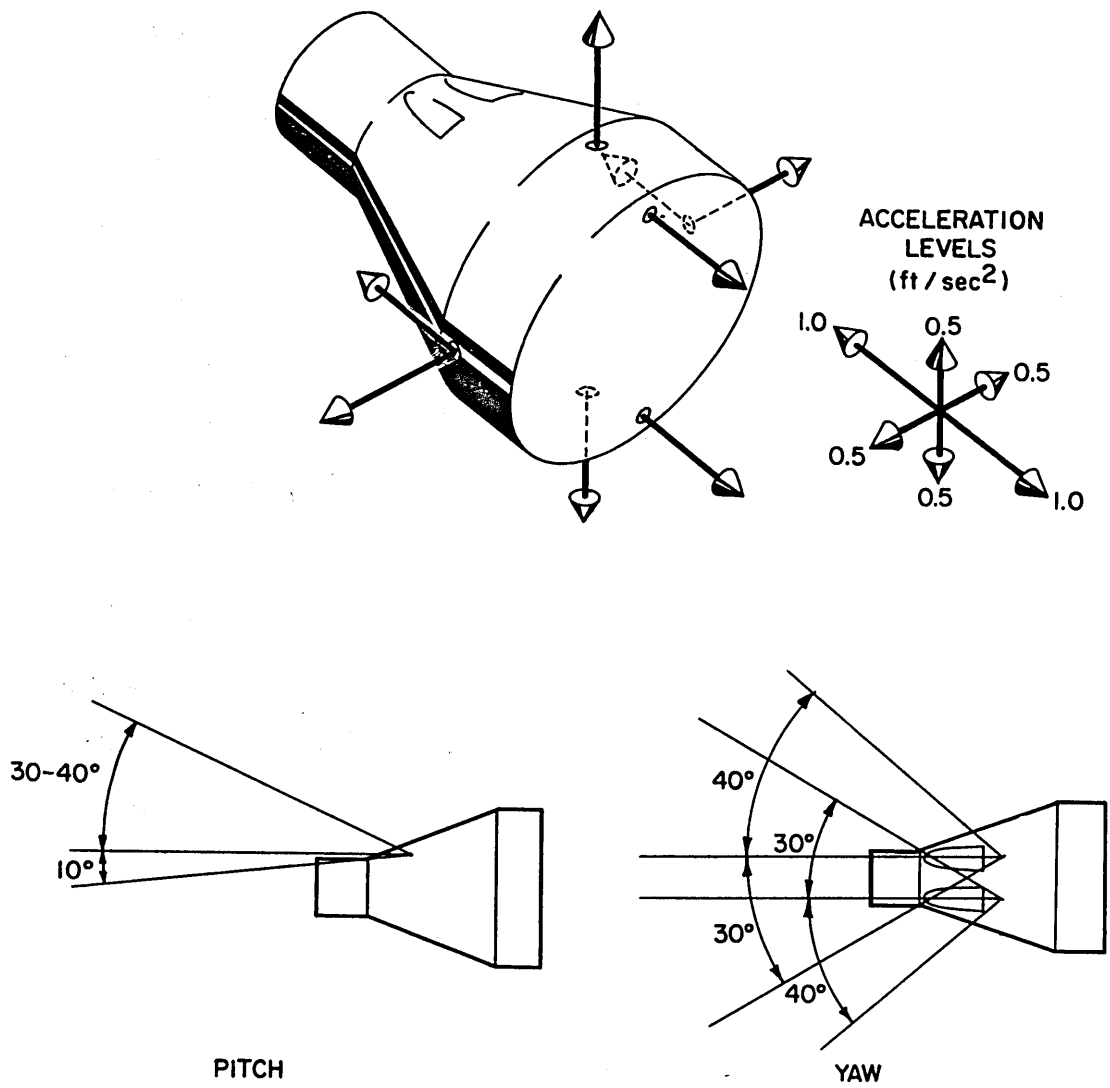


Fig. 3-1 Gemini Spacecraft Maneuver Capabilities and Visibility

be launched. Realizing that the launch site will pass through the target orbit plane twice with a time interval of about one hour, it can be seen from Fig. 3-2, that if the spacecraft is injected with a velocity vector parallel to the target plane at any time from slightly before the first intersection of the launch site with the target plane until slightly after the second intersection, then the resulting relative inclination between the two orbits will never be greater than  $.4^{\circ}$ . It is anticipated at present that this can be kept to less than  $.3^{\circ}$ . The orbit into which it is hoped that the spacecraft will be injected is an elliptic one with a perigee at the burn out altitude of 87 nm (indicating a horizontal injection velocity vector) and an apogee at the height of the target orbit of 150 nm. The launch of the spacecraft will be made primarily with regard to the resulting plane relationship, but consideration will also be given to the phase relationship between the two vehicles in their respective orbits so that an excessive time will not be required to wait for a phase relationship favorable to continued rendezvous maneuvering.

It is hoped that the phase relationship at injection will place the spacecraft less than  $70^{\circ}$  behind the target which corresponds to a catch-up time of about 18 hours. If the relative inclination is greater than about  $.4^{\circ}$  or the phase angle is greater than  $70^{\circ}$ , a plane change or period change followed by a recircularization at 150 nm will be made by the target vehicle.

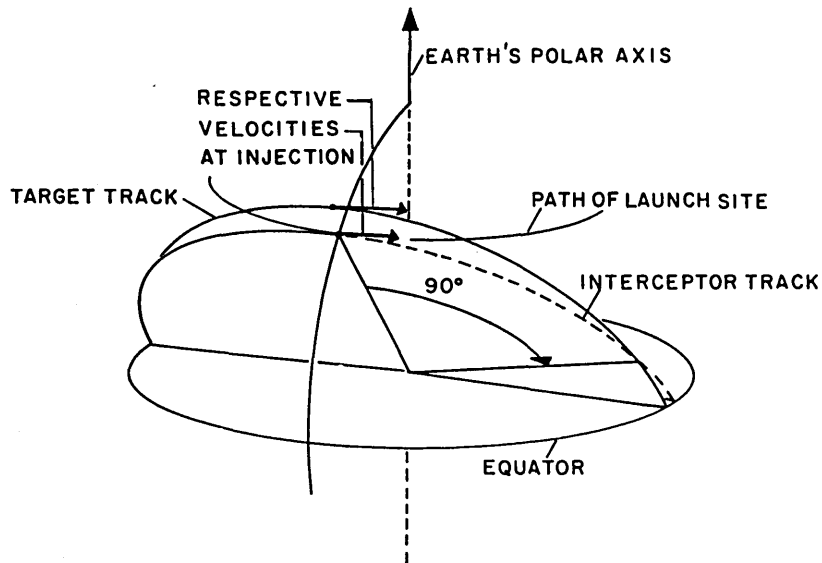
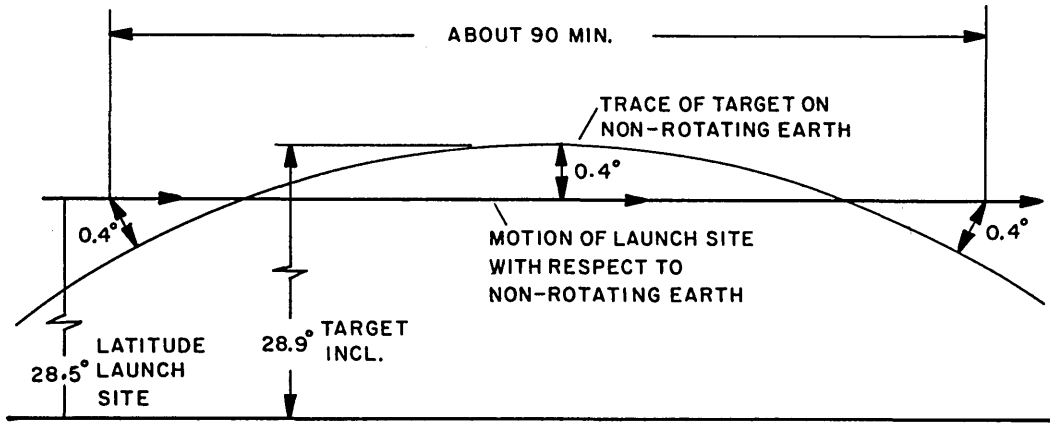


Fig. 3-2 Launch Out-of-Plane Conditions

The phase rate is planned to be modified as the phase angle is decreased. The phase rate in the injection orbit of the spacecraft is about  $5.3^\circ$  per revolution. As the phase angle decreases to  $10^\circ$ , a horizontal velocity increment will be applied at the apogee of the interceptor orbit which will increase the semi-major axis of the orbit, raise the perigee altitude to about 113 nm, and decrease the phase rate. While the original orbit is termed a standard catch-up orbit, the modified orbit is termed a slow catch-up orbit. Figure 3-3 depicts the idealized situation.

Now that the vehicles are in relatively close proximity to each other, there are three methods proposed for continuing the intercept maneuver. The first of these is called closed loop guidance and utilizes the full tracking radar, a digital computer, and the shell coordinate approximate linearized equations. The procedure is generally as follows. When the relative ranges at any point in their orbits decrease to less than 200 nm, the radar is used to measure the three components of relative position and velocity. These are then fed into the computer along with any existing eccentricity and true anomaly of the target. Since the rendezvous maneuver, once initiated, is to cover about  $270^\circ$  of Earth travel, the computer then solves the problem and displays to the astronaut the needed velocity change at that instant and the total nominal velocity change needed to complete the maneuver. Either an iterative technique to look at the velocities required for



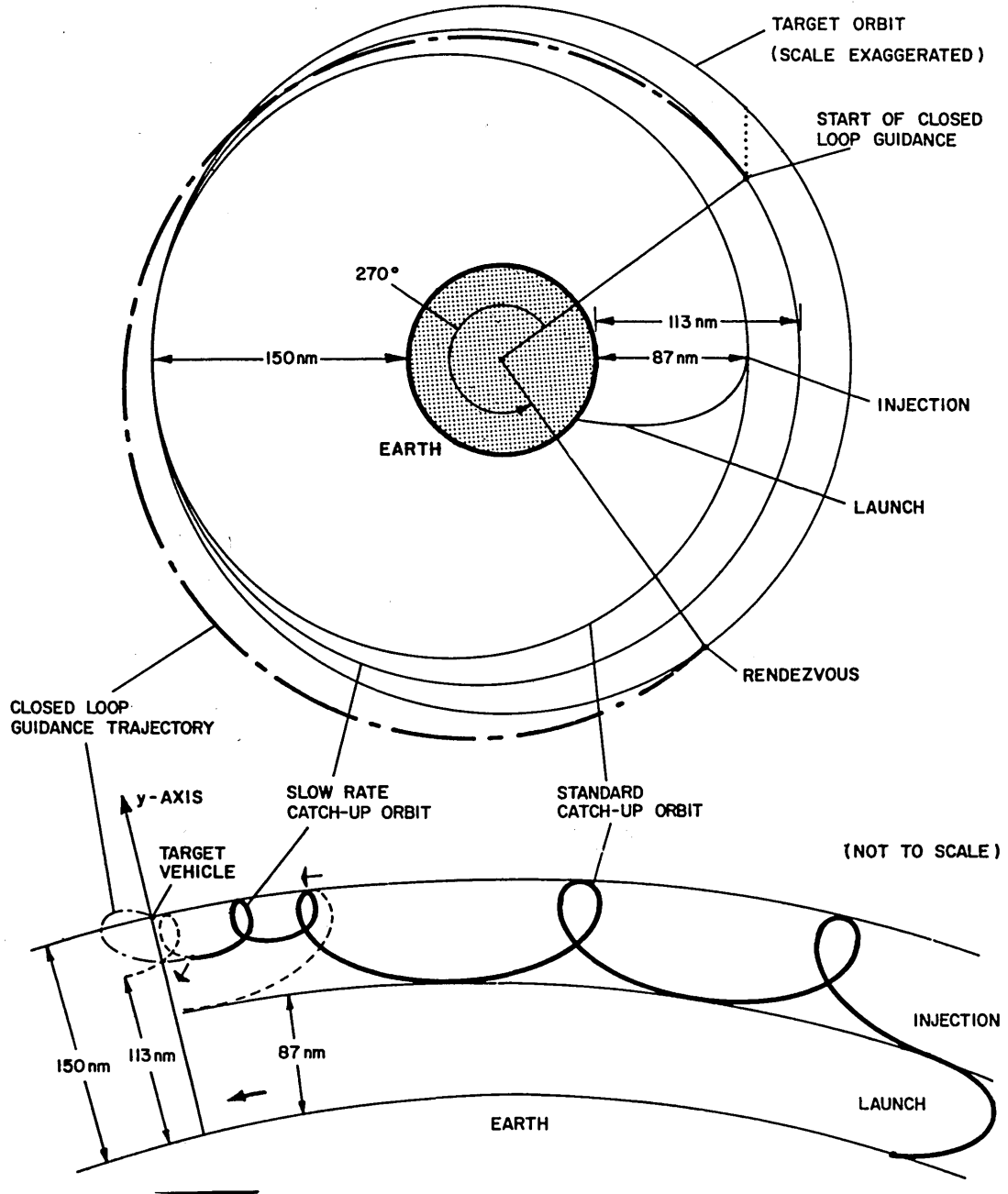


Fig. 3-3 Gemini Closed Loop Guidance - Typical Example, Inertial and Rotating Coordinate Frames

future times or a process of waiting until the velocities are within the capability of the spacecraft is employed. Once a solution is selected the in-plane components of velocity are applied and, from subsequent solutions, corrections are made at five or six preselected times. At about  $90^\circ$  prior to rendezvous the out-of-plane corrections are brought in for the remainder of the intercept. As the range decreases to a point where the braking or velocity matching should begin, the astronaut takes over visually to reduce the relative velocities and guides the spacecraft through the docking maneuver. This rendezvous technique could be briefly described as a three-impulse (the out-of-plane correction  $90^\circ$  prior to rendezvous is the second impulse) maneuver with mid-course corrections made at preselected time intervals. Due to the variations in the initial conditions the actual trajectory to be followed cannot be anticipated prior to launch. A typical maneuver is portrayed in Fig. 3-3 both in an inertial reference and in a rotating coordinate frame. The latter usage will be explained in the next chapter.

The second method of relative motion guidance is called semi-optical guidance and makes use of radar range and range rate information and the motion of the flashing light beacon against the star background (which is hopefully available when needed). This is initiated when the vehicles are within 20 nm of each other. ( $3^\circ$  out of plane at 150 nm altitude could be as large as 18.8 nm.) From the radar range rate a closing velocity is established and the rotation of the line of sight is simultaneously brought to zero. As the range then

decreases, the rotation of the line of sight is again periodically brought to zero and when a braking range is reached the rendezvous terminates as before. The reason for the initial 20 nm restriction is that investigations at NASA and McDonnell Aircraft Corporation have indicated that application of these constant line-of-sight techniques at greater ranges is beyond the velocity capability of the spacecraft. As will be seen later, the errors in initial conditions applied to the technique presented by the author, if applied here, would place the vehicles well outside the 20 nm limit.

The third method of relative motion guidance is called back-up optical guidance and is similar to the second method except that radar is not employed. Instead, range and range rate are inferred optically by the method outlined in Reference (27). Unfortunately, in order to determine range the rotation of the line of sight must be stopped, and as mentioned, this could be disastrous if the range turned out to be much greater than 20 nm.

It should not be inferred that the author is suggesting that these methods will not work. What is suggested is that the over-all system complexity and reliability should be carefully weighed against other rendezvous techniques which in some respects may be more tolerant of initial orbit errors.

#### 3.4 Characteristics of Suggested Approach for Gemini Rendezvous

To serve as a basis for comparison and as a preview of the subsequent analysis, it seems pertinent at this point to outline briefly how

the techniques suggested in this investigation would be employed for the Gemini rendezvous mission.

The target would be injected into the same nominally circular orbit at 150 nm. The interceptor launch would be subject to the same out-of-plane considerations as before and the phase relations are nearly comparable as will be seen. Instead of an initial elliptical orbit ranging from 87 nm to 150 nm, the injection would be into an initial orbit called a parking orbit which again has a perigee of 87 nm, or whatever the optimum burn out altitude is, but with an apogee now in the vicinity of 130 nm. Then, as the phase angle is decreased, this orbit would be circularized into a waiting orbit at 125 nm. (The reasons for this choice and the timing considerations for circularization will be evident later.)

Now, as the interceptor closes on the target, due to its shorter period and lower altitude, visual acquisition of the target's light beacon takes place at ranges of 80 - 100 nm. When the angular relationship of the target to the interceptor's local vertical reaches a preselected value, various out-of-plane angular measurements are made. When the angle to the local vertical reaches another value, a velocity change consisting of a nominal in-plane component and an out-of-plane component based on a simple calculation from the previous out-of-plane angles is made. In the absence of errors, this would result in a free-fall trajectory that would rendezvous with the target  $90^{\circ}$  later. A

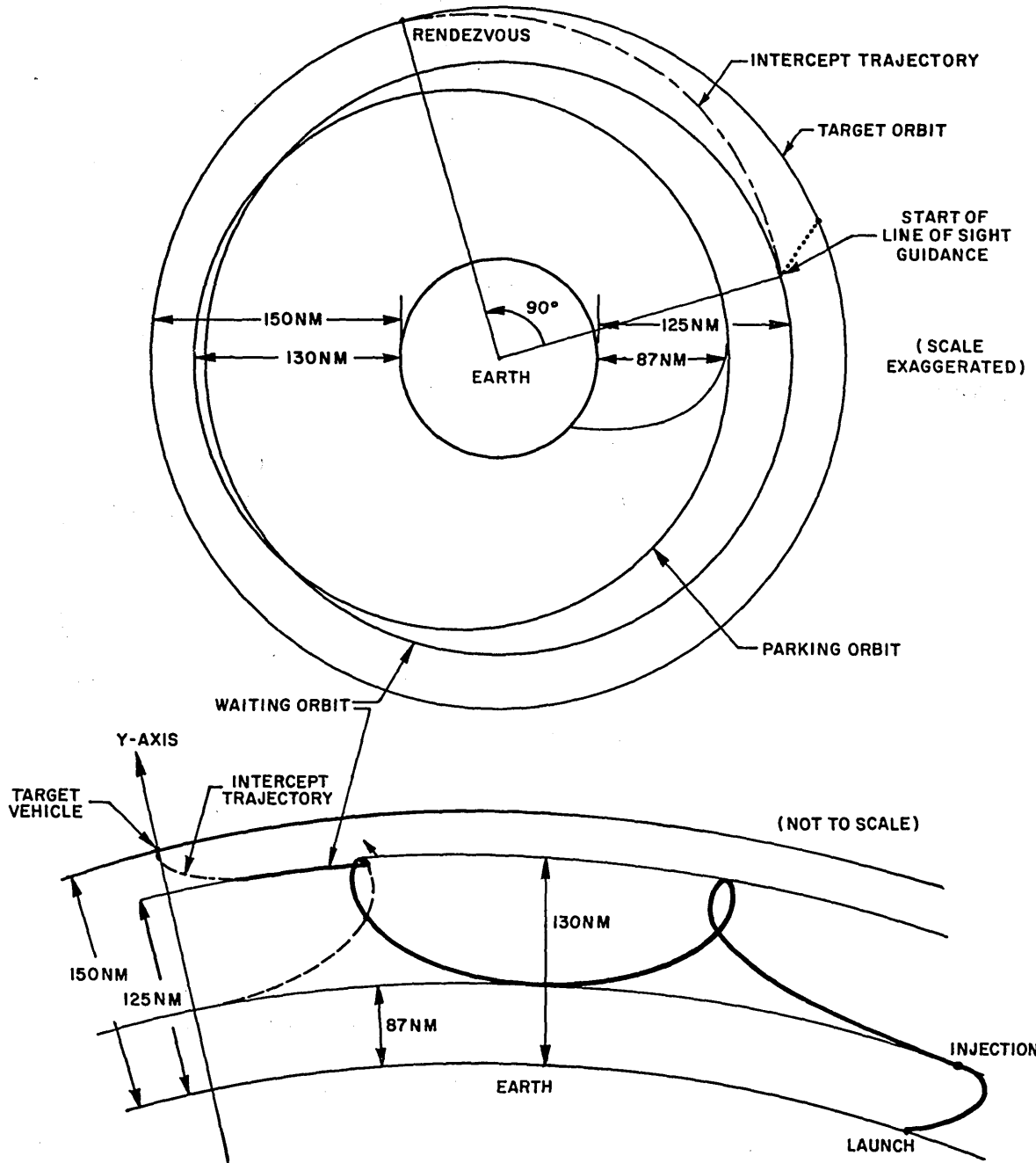


Fig. 3-4 Suggested Gemini Rendezvous - Typical Example, Inertial and Rotating Coordinate Frames

sight reticle that is varied with respect to inertial space according to predetermined functions of time is centered on the target vehicle. The interceptor is pointed directly toward the target and a certain pitch down attitude is then established. As the target drifts from the center of the sight reticle, velocity changes are made using the transverse thrusters to correct for the error in the rotation of the line of sight, and the reticle is recentered on the target. This process is continued until a braking range is reached at which time a velocity matching maneuver takes place as in the present proposed system. The amount of velocity change needed to correct the rotation of the line of sight is obtained from simple guidance equations that are easily mechanized functions, or, if future pilot simulation establishes that motion of the target relative to the reticle can be effectively used as a correction cutoff, the guidance equations could be dispensed with completely. A typical rendezvous maneuver is portrayed in Fig. 3-4, again in both inertial and rotating coordinate frames.

In addition to the sight, this maneuver can be conducted using only slide-rule-type calculations and without the use of radar by using the optical range determination for braking as was referred to earlier. With radar range only and a slightly more involved single computation, the error tolerances are increased somewhat, and the braking range determination obviously is considerably simplified.

It should be noted in passing that since the phase rates in the

parking and waiting orbits are slightly greater than in the proposed standard catch-up and slow rate catch-up orbits and since the guidance maneuver covers  $90^\circ$  instead of  $270^\circ$ , for a given phase angle at injection, the total time until rendezvous would be less. To put it another way, a greater phase angle could be tolerated before resorting to target maneuvers.

### 3.5 Limitations of this Investigation

Certain basic assumptions and limitations that apply to the general investigation as a whole should be pointed out now; more will be mentioned later as they arise. The basic approach deals with methods and techniques of rendezvous rather than a feasibility design of component equipment. For example, much as the author would like to design the sight for patent purposes, he has dealt mainly with what it should be capable of doing and pointed out only briefly how this might be accomplished. The guidance phase of rendezvous from optical acquisition to the start of the braking maneuver has been the primary concern of this investigation. Little effort of comparison in a direct, qualitative manner has been made, since it is felt that further simulation including man's direct participation is necessary before any true comparison would be valid.

Visual acquisition ranges of the flashing light beacon on the order of 100 nm have been assumed and the power requirements for this have not been investigated. In the simulation phase of the study,

impulsive velocity changes have been assumed (more will be said of this later) and since the work was of a digital nature, discrete time sampling intervals were necessary. Throughout the work a two-body, spherical Earth has been assumed, which from the many references consulted seems to be fully justified for the close relative motions involved in rendezvous. Human reactions have not been incorporated directly into the simulations. However, in the final simulation analysis, rather pessimistic random and bias errors associated with measurement, tracking, attitude control and thrust control have been used and their effects noted. Throughout the work the reader will not be bored by the derivation of basic orbital mechanics relations that are available in any standard text book. (29, 42)



## CHAPTER 4

## THE APPROACH PHASE

4.1 Rotating Coordinates as a Visualization Aid

Frequent use throughout this investigation will be made of rendezvous maneuvers as seen in rotating coordinate frames, especially in this chapter that deals with maneuvers made by the interceptor in orbit subsequent to injection and prior to the guidance phase. It should be stressed at the outset that these frames are used only as an aid to visualization. When use is made of approximations that may or may not be derived from rotating coordinates, it is only to assist in the corrections that are made in the guidance phase. Trajectories that are used as a basis for the nominal trajectory are obtained by an exact solution of the problem in inertial coordinates.

When use is made of these axes, they will, unless otherwise specified, have an origin at the center of the Earth and rotate uniformly with a real or fictitious circular satellite, with the Y-axis passing through this satellite, the Z-axis aligned with the angular momentum vector and, naturally, the X-axis directed opposite to the actual motion of the satellite. When coplanar elliptical satellites with

a semi-major axis equal to the radius of the fictitious satellite or, which is the same, with identical mean motions are viewed in this frame they trace out an approximate 2 by 1 ellipse as shown in Fig. 4-1a. The approximation is better, the smaller the eccentricity is. To show that this is true, use is made of the standard circle which defines the eccentric anomaly  $E$ , but to this is added another circle to show the mean anomaly  $M$  as in Fig. 4-1b. The situation shown is with  $E = \pi/2$ . A dotted line is added to the  $M$  circle which again portrays the angle  $E = \pi/2$ . From the diagram it is clear that at perigee or apogee, or where  $f = M = E = 0$  or  $\pi$ , the arc distance that the elliptical satellite is from the fictitious satellite on the  $M$  circle is  $\pm a e$ . To establish that the arc 1-2-3 is approximated by  $2 a e$ , one proceeds as follows (complete treatment in Appendix A. 7):

For the arc 1-2, use is made of Kepler's equation,

$$M = E - e \sin E$$

which for  $E = \pi/2$  gives

$$M = \pi/2 - e$$

and the arc 1-2 is exactly  $a e$ . Now, from the diagram

$$\sin (f - E) = \cos (\pi - f) = e$$

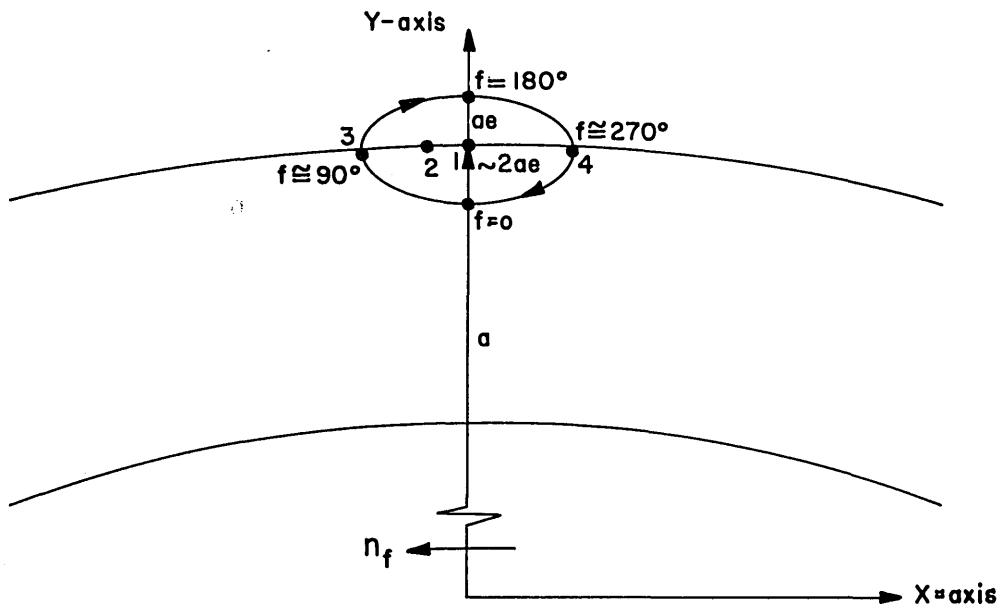


Fig. 4-1a An Elliptic Orbit in Rotating Coordinates

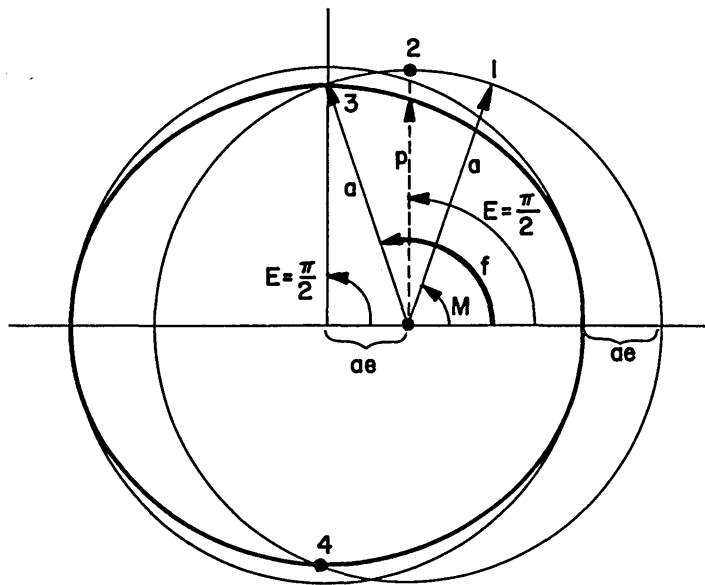


Fig. 4-1b Anomaly Diagram

which for small  $e$  gives:

$$f - E = e$$

and the arc 2-3 is also  $a e$  for small  $e$ . Also for small  $e$ , the points 3 and 4, where the radius is equal to the semi-major axis  $a$ , correspond very nearly to the true anomalies of  $90^\circ$  and  $270^\circ$ .

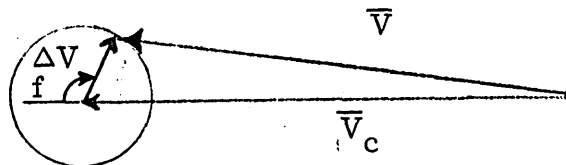
While the diagram is available, two more very useful relations will be developed. If  $\Delta r$  is designated as the maximum radial deviation of the elliptic satellite from a circular orbit then from Fig. 4-1b,

$$e = \frac{\Delta r}{a}$$

It will now be shown that for small  $e$ , a useful approximate vector diagram for the velocity vector in the elliptic orbit can be derived, and that to this approximation:

$$e = \frac{\Delta r}{a} = \frac{\Delta V}{V_c}$$

where  $V_c$  is the circular velocity at  $r = a$ . The diagram is:



To show this, the standard conic equation  $r = \frac{p}{1 + e \cos f}$  is differentiated giving ,

$$\dot{r} = \frac{p e \sin f \dot{f}}{(1 + e \cos f)^2} = \frac{r^2 \dot{f}}{p} e \sin f$$

but  $r^2 \dot{f} = h$  the massless angular momentum, and  $h = \sqrt{\mu p}$ , so:

$$\begin{aligned} \dot{r} &= \sqrt{\frac{\mu}{p}} e \sin f = \sqrt{\frac{\mu}{a}} e \sin f (1 - e^2)^{-1/2} \\ &= V_c e \sin f \left(1 + \frac{e^2}{2} + \dots\right) \end{aligned}$$

Hence, the approximation for small  $e$ ,

$$\dot{r} \cong V_c e \sin f$$

Now the tangential velocity  $V_\theta$  is given by:

$$\begin{aligned} V_\theta &= r \dot{f} = \frac{h}{r} = \frac{h}{p} (1 + e \cos f) \\ &= \sqrt{\frac{\mu}{p}} (1 + e \cos f) \\ &= V_c (1 + e \cos f) \left(1 - \frac{e^2}{2} + \dots\right) \end{aligned}$$

and the approximation for small  $e$ :

$$V_\theta \cong V_c + V_c e \cos f$$

Hence the diagram holds for small  $e$  and:

$$e = \frac{\Delta r}{a} = \frac{\Delta V}{V_c}$$

Going back to the rotating frames, a circular satellite at a smaller radius than the fictitious satellite will trace out a circular arc centered at the origin moving in the direction of rotation. On the other hand, if its radius is greater, then it will move opposite to the rotation. If now this satellite orbit is elliptical, then a moving 2 by 1 ellipse will be superimposed on the arcs centered at the origin.

To get a feel for these rates of motion, let us consider a coplanar circular satellite in a waiting orbit at a distance  $d$  lower than the fictitious satellite at a radius of  $r_f$ .

$$r_w = r_f - d$$

The angular rate of the fictitious satellite is:

$$n_f = \frac{\sqrt{\mu}}{r_f^{3/2}}$$

and that of the satellite in the waiting orbit is:

$$n_w = \frac{\sqrt{\mu}}{r_w^{3/2}}$$

The phase rate now is given by:

$$\begin{aligned}
 \omega_{wf} &= n_w - n_f \\
 &= \frac{\sqrt{\mu}}{r_w^{3/2}} - \frac{\sqrt{\mu}}{r_f^{3/2}} = \frac{\sqrt{\mu}}{(r_f - d)^{3/2}} - \frac{\sqrt{\mu}}{r_f^{3/2}} \\
 &= \frac{\sqrt{\mu}}{r_f^{3/2}} (1 - d/r_f)^{-3/2} - \frac{\sqrt{\mu}}{r_f^{3/2}} \\
 &= n_f \left( \frac{3d}{2r_f} + \frac{15d^2}{8r_f^2} + \dots \right)
 \end{aligned}$$

Or the approximation:

$$\omega_{wf} \approx n_f \frac{3d}{2r_f}$$

which holds for small radius  $d/r_f$ . (This ratio,  $d/r_f$ , will be most prominent in the next chapter.) So, it can be said that for small ratios  $d/r_f$ , the phase rate varies in direct proportion with the distance,  $d$ .

Another useful aid in visualizing the motion in rotating coordinates would be to obtain an approximate expression for the arc distance travelled by the interceptor in a waiting orbit during one target

period. This can easily be obtained by substituting  $2\pi$  for  $n_f$  in the above expression and multiplying by  $r_f$ .

$$\begin{aligned} S_f &= \omega_{wf} r_f \\ &= 2\pi \frac{3}{2} \frac{d}{r_f} r_f \end{aligned}$$

$$S_f = 3\pi d$$

Since the periods of the target and interceptor are nearly the same, the distance  $3\pi d$  can also be taken as very nearly the arc distances between periodic points in an elliptic waiting orbit with a semi-major axis located the distance  $d$  from the semi-major axis of the fictitious target.

In Fig. 4-2a are shown examples of such elliptic motion portrayed in a rotating frame. Orbit 2 might be similar to that for the proposed standard catch-up orbit or slow rate catch-up orbit in the Gemini mission.

Various intercept trajectories can also be nicely portrayed in the rotating frame. Consider the three different intercepts in Fig. 4-2b. Intercept 1 is a Hohmann transfer with an initial true anomaly  $f_i = 0$  and a final true anomaly  $f_f = 180^\circ$ . Intercept 2 has an  $f_i = 0^\circ$  and  $f_f = 90^\circ$ , while intercept 3 covers an angle of  $270^\circ$  going outside the target orbit with  $f_i = -45^\circ$  and  $f_f = 225^\circ$ . It can readily be seen that the



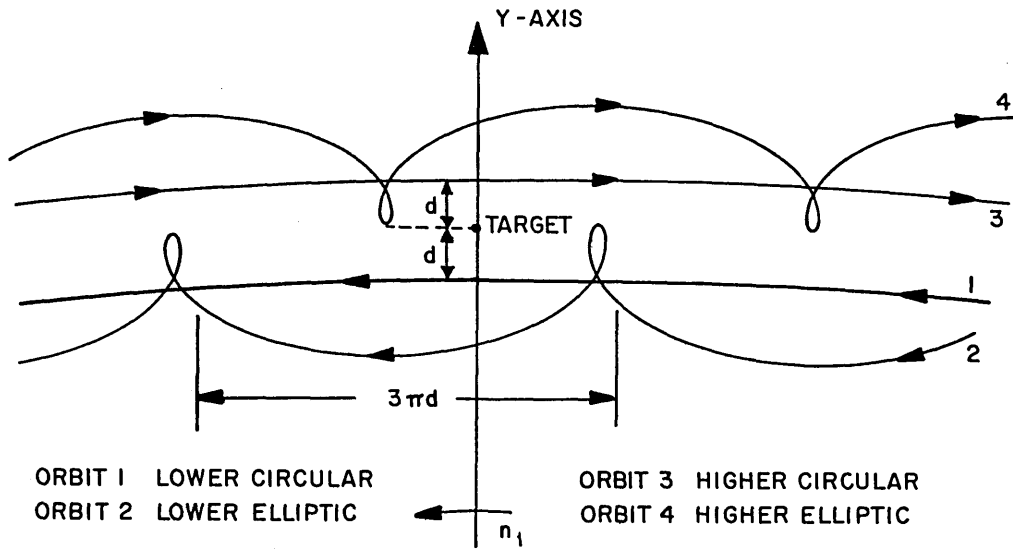


Fig. 4-2a Other Orbits in Rotating Coordinates

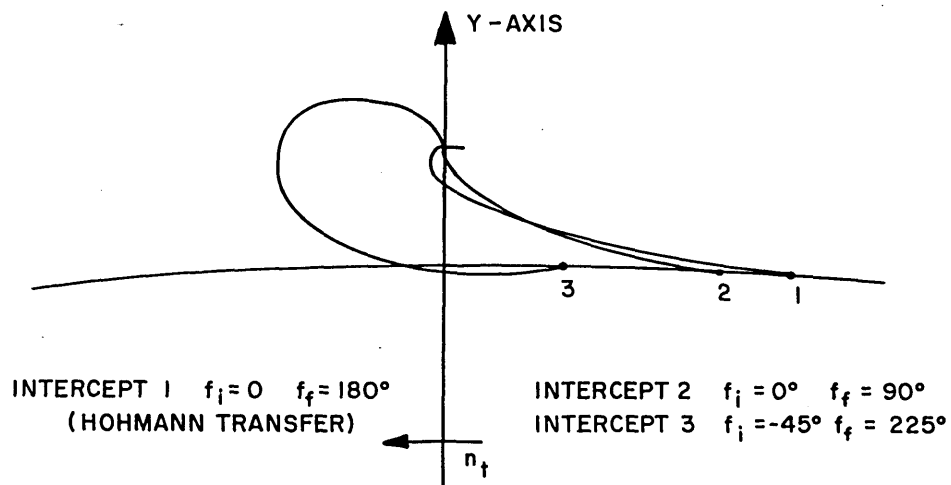


Fig. 4-2b Intercept Trajectories in Rotating Coordinates

local vertical indication is well preserved for both vehicles throughout, and the relative velocity vector is tangent to the path.

#### 4.2 Phase Rate vs Acquisition Range - Single Parking Orbit

Since, in the preceding paragraph, the phase rate was shown to be very nearly proportional to the distance between the semi-major axes of the target and the interceptor, an obvious conflict exists between acquisition ranges and an adequate phase rate closure. Consider the simple situations portrayed in Fig. 4-3. In both cases the target is in a circular orbit at an altitude of 300 nm. In Fig. 4-3a, the interceptor is in a circular parking orbit at an altitude of 275 nm with a phase rate of about  $3.6^\circ$  per revolution of the target. In Fig. 4-3b, the interceptor is now in a lower circular parking orbit at 150 nm with a phase rate of about  $21.6^\circ$  per target revolution. Now, for reasonable intercept trajectories, when the interceptor is at 275 nm, the required acquisition ranges are considerably less than 100 nm. In contrast, when the interceptor is at 150 nm, the acquisition ranges might well be in excess of 300 nm, especially since to cover the larger radial distance a near optimum maneuver would be desired.

However, the low phase rate at 275 nm would involve either a limited launch window (remembering that the target is travelling over the earth at about  $4^\circ$  per minute) or possible unacceptably long waiting times at 275 nm before a favorable phase relation for intercept occurred. As one attempts to lower the parking orbit from 275 nm, the limits of

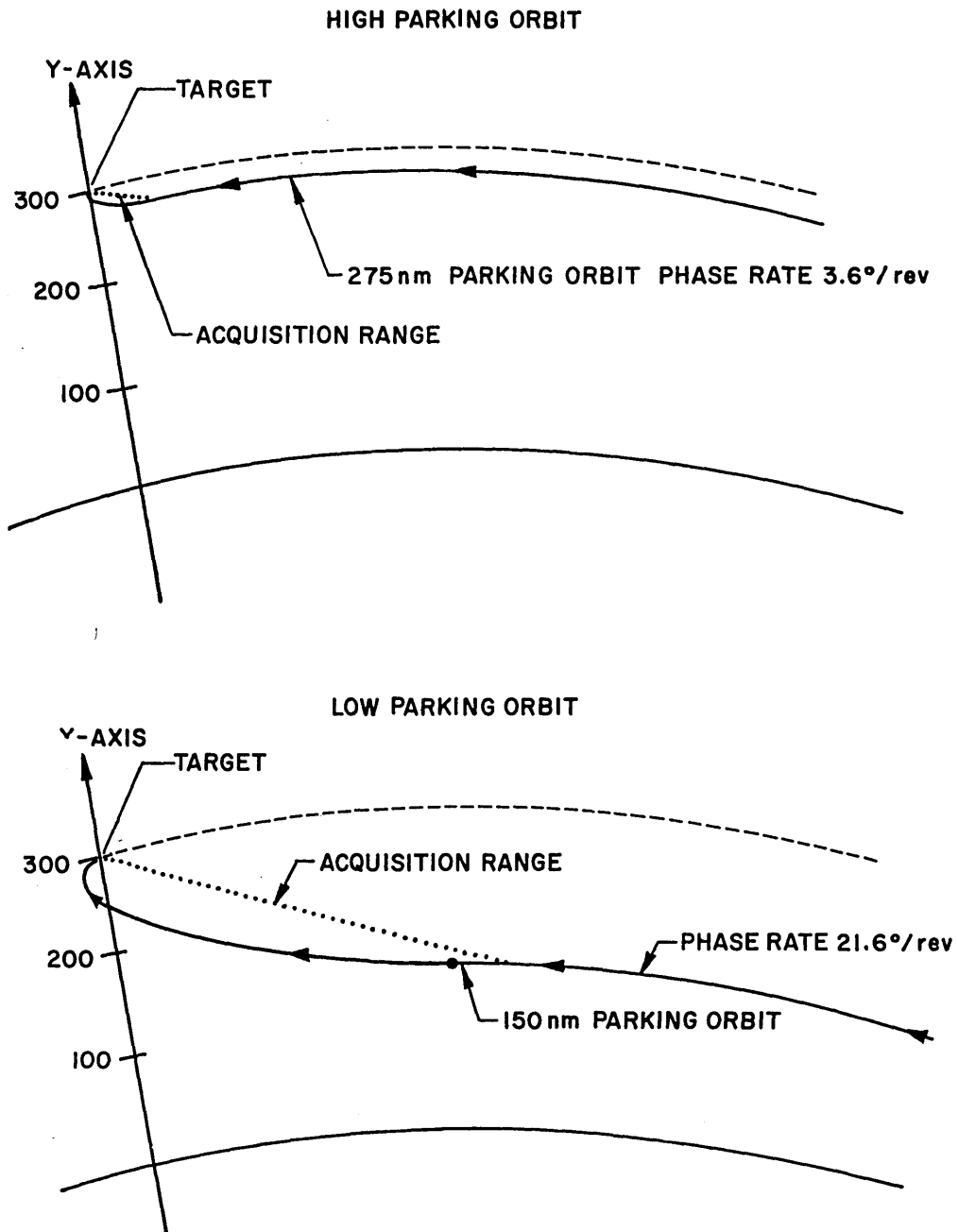


Fig. 4-3 Phase Rate vs Range

optical acquisition ranges are soon reached and the fuel required to perform the intercept maneuver increases.

In addition, if the target is in an elliptic orbit and it is desired to terminate the intercept at a particular target true anomaly, there is no way to adjust the phase relation so that a nominal intercept may be followed unless the parking orbit is varied. The same would hold true if the rendezvous was desired to take place over a particular region of the earth.

#### 4.3 The Use of Parking and Waiting Orbits

To alleviate the conflict between phase rate and acquisition ranges, a combination of two parking orbits, or as they will be termed subsequently, a parking and a waiting orbit, can be utilized in the approach phase. An example of this concept is shown in Fig. 4-4. The interceptor is injected into a circular parking orbit at 150 nm to take advantage of the larger phase rate, then as the phase angle is decreased, a transfer is made through optimum tangential velocity increments to a waiting orbit at 275 nm. By this time the remaining phase angle is small and the low phase rate is not as bothersome. From these ranges the interceptor can optically acquire the target and initiate the intercept trajectory.

Due to the smaller radial distance to be covered during the intercept, a trajectory can be selected more to suit optical guidance considerations than to be a near optimum fuel maneuver. Considering only coplanar aspects, the fuel needed to go from 150 nm to the

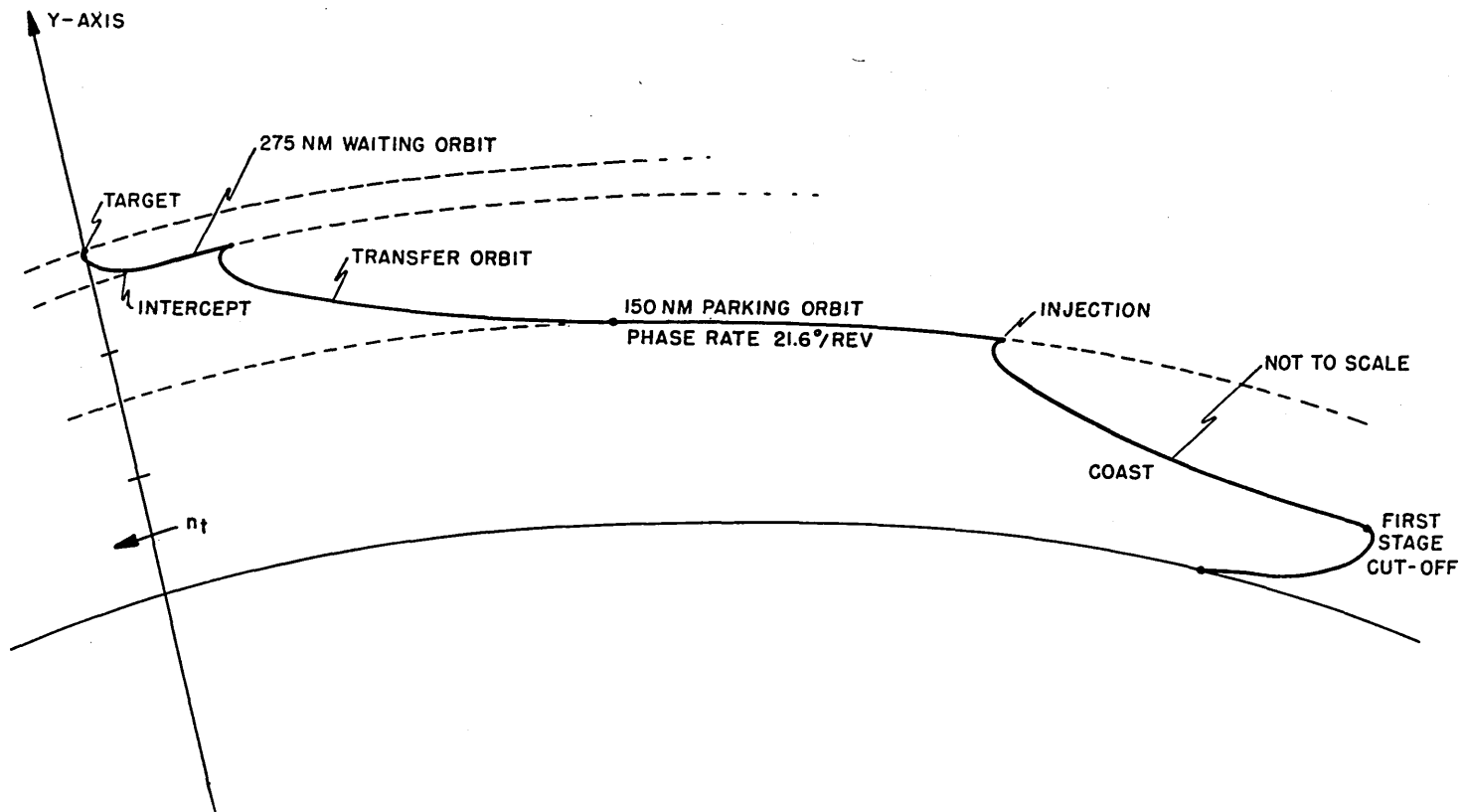


Fig. 4-4 The Concept of Parking and Waiting Orbits

target in a one and one-half times Hohmann fuel intercept would enable a four times Hohmann fuel intercept from 275 nm since the radial distance from 150 nm to 275 nm or  $5/6$  of the total distance would be traversed in the optimum manner.

Now if consideration is given to the number of velocity changes required subsequent to injection to get the interceptor into the waiting orbit, then the use of an elliptic parking orbit can be seen to have certain advantages. The attainment of a circular parking orbit high enough to avoid rapid atmospheric decay usually involves a circularizing velocity increment at the apogee of a coasting elliptic orbit that results from booster cutoff. Two more velocity changes are required then to reach the circular waiting orbit making a total of three velocity changes. If instead, however, the coasting elliptic orbit is planned to have an apogee at the desired altitude of the waiting orbit with a perigee at the cutoff altitude, then this coasting elliptic orbit can be considered as a parking orbit and only one velocity change is required. Since the change to the waiting orbit can only be made at or near apogee, the ability to adjust the phase relation to reach a predetermined phase angle at a specified epoch of the target orbit is considerably reduced. This will be explained in somewhat more detail in Section 4.5. A typical example of the use of an elliptic parking orbit and a circular waiting orbit been shown in Fig. 3-4 as the suggested approach to Gemini rendezvous. As long as the target orbit is circular and it is

desired to make use of a nominal intercept trajectory, there appears to be no advantage in having the waiting orbit other than circular. The next section will mention the possibility of using elliptic waiting orbits in the approach phase for elliptic targets. This will then be further investigated in Chapter 5 and finally established to provide distinct advantages of simplification in Chapters 7 and 8.

#### 4.4 The Approach Phase for Elliptic Target Orbits

When the target orbit is elliptic, there appear to be two general methods of maneuvering the interceptor into favorable position for initiating the intercept maneuver. The first method uses a circular waiting orbit and, as will be seen, is only useful when the ellipticity of the target is quite small. The waiting orbit is located at a somewhat lower altitude than the perigee of the target orbit and as the interceptor approaches a favorable phase angle either a different intercept trajectory is used for various target true anomalies or a standard line-of-sight motion trajectory with variable entry velocity changes is employed. The second method which was developed in the latter stages of this investigation makes use of a coapsidal elliptic waiting orbit with a combination of eccentricity and semi-major axis that results in a near constant radial separation of the orbits. As will be established later, this approach enables the use of a standard nominal intercept trajectory with constant entry conditions regardless of the true anomaly that exists when the proper phase angle is reached. In effect, once

the interceptor is in this elliptic waiting orbit, the astronaut can neglect completely the fact that the orbits are elliptical and treat the situations as if the intercept were being performed from a circular waiting orbit to a target in a circular orbit.

As seen in Fig. 4-5, in order to enter this coapsidal orbit from an elliptic parking orbit, a circular transfer orbit is used to connect the apogee of the parking orbit with the perigee of the waiting orbit. Though this procedure involves the application of an additional velocity change, the benefits of simplicity to be derived are well worth the effort. A nominally circular transfer orbit is selected since this minimizes the velocity change requirements. If the target orbit eccentricity results in a  $\Delta r$  of more than about 50 nm, the time and magnitude of the velocity change needed to enter the coapsidal elliptic waiting orbit should be based on accurate ground tracking. Otherwise this maneuver, like the entry into the transfer orbit, could be based on a nominal time from injection. Naturally the lower the perigee of the target the lower the eccentricity of the parking orbit.

Figure 4-6 shows the technique that could be employed for small eccentricity target orbits using a circular waiting orbit. The intercept trajectories shown by dashed lines traverse slightly more than  $90^\circ$  and are initiated when the target is at the indicated true anomaly. These trajectories all have essentially the same line-of-sight motion as will be evident in the next chapter; however, the initial velocity



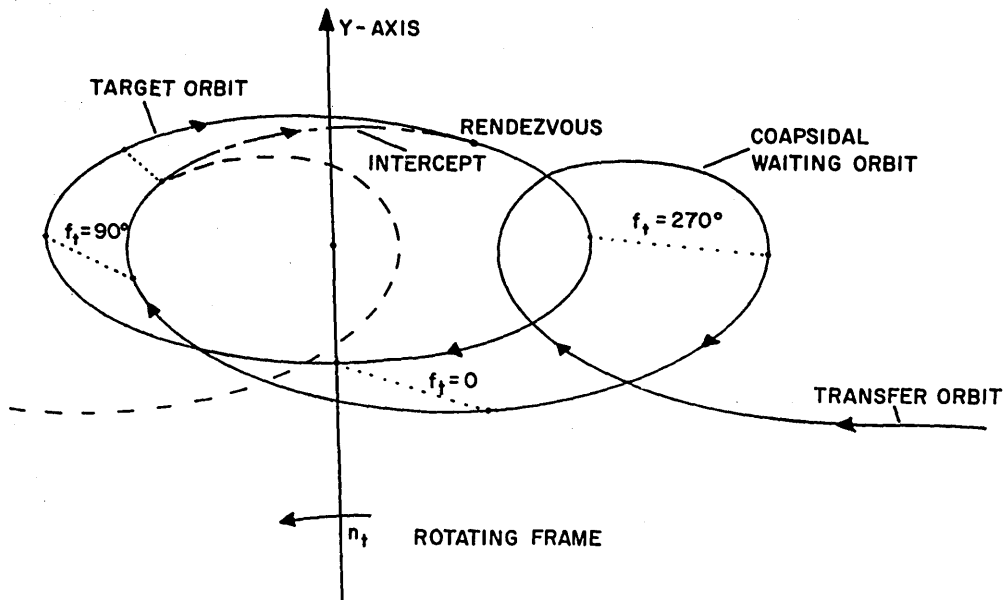
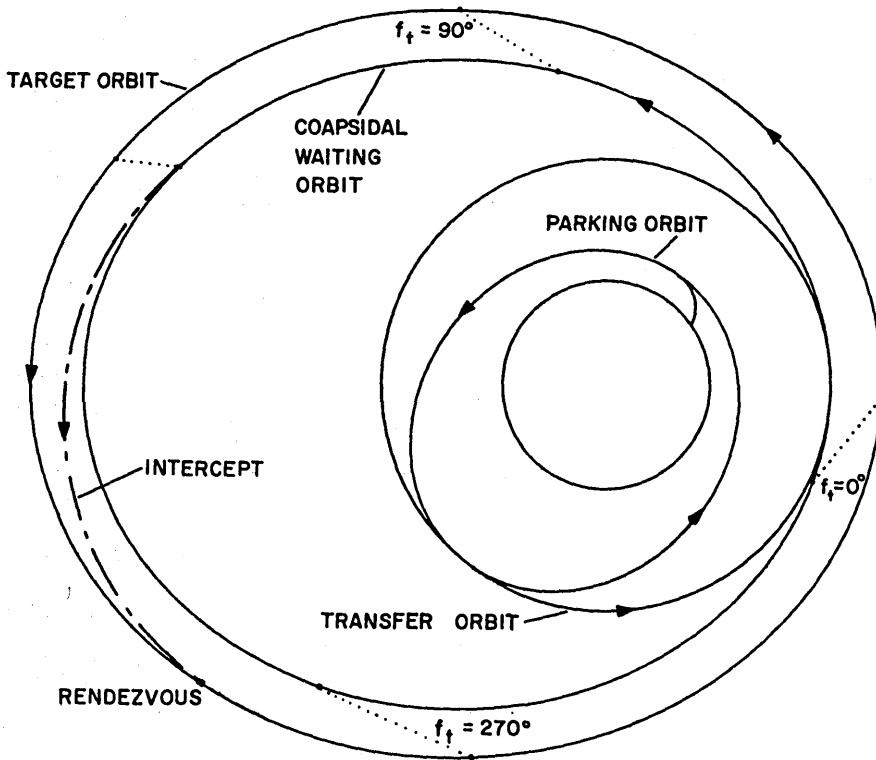


Fig. 4-5 Coapsidal Elliptic Waiting Orbits for Elliptic Target Orbits

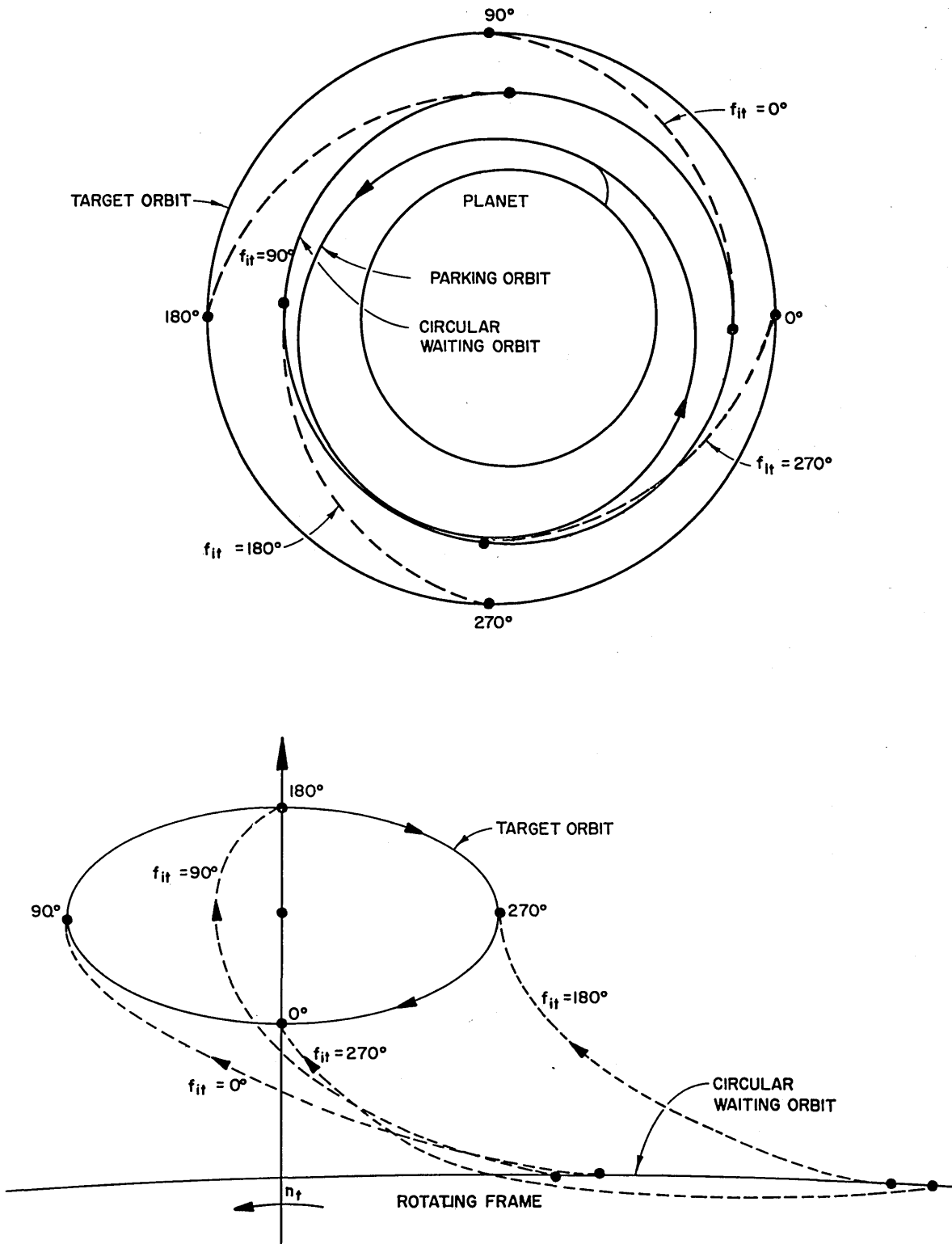


Fig. 4-6 Circular Waiting Orbits for Elliptic Target Orbits

change directions and magnitudes naturally vary considerably. The reason for the eccentricity limit on the target is now evident, in that with the circular waiting orbit and no attempt at phase angle control, the interceptor must be capable of conducting an intercept to any point in the target orbit. Line-of-sight range could also be a problem if the target eccentricity was large.

A rigorous examination of the approach phase maneuvering will not be pursued since the prime emphasis of this investigation is on the intercept guidance phase. However, one comment does appear appropriate and that concerns the entry into the coapsidal elliptic waiting orbit. Unless the ellipticity of the target is quite large, this velocity change is no more critical than the circularizing of an elliptic orbit since both require a specific amount of velocity change in a given direction at a specified time. In this case, if the target eccentricity is large, the parking orbit will most likely be less elliptic, making its circularization less critical.

The author would like to remark here that the concept of the parking and the waiting orbits used in the approach phase was derived by him prior to learning of the proposed standard and slow catch-up rate orbits of the Gemini mission which bear striking resemblance, yet are used in different ways.

#### 4.5 Application to the Gemini Rendezvous Mission

From the preceding discussion, the Gemini rendezvous mission

with the target in a nominally circular orbit at an altitude of 150 nm would call for a circular waiting orbit. If the target orbit turned out to be slightly elliptic either a circular or coapsidal elliptic waiting orbit could be used; however, the simulation results indicate the latter to be preferable. For the circular target, the guidance simulations in Chapter 8 seem to indicate that considering optical ranges, reasonable uncertainties in the orbits and the velocity change capability of the spacecraft, the waiting orbit should be in the vicinity of 125 nm. Again, it will be pointed out that the intercept technique to be employed is that whenever the phase angle (or more correctly, the in-plane angle of the line of sight from the interceptor's local vertical) reaches a predetermined value, the nominal intercept trajectory is entered by changing the spacecraft's velocity by a preselected increment in a preselected direction. The elliptic parking orbit would now have, in the ideal case, a perigee at booster cutoff or 87 nm and an apogee at 125 nm.

By referring to a plot of phase angle vs time in terms of target periods for this ideal case, as shown in Fig. 4-7, the progress of the phase relationship for any situation can be readily seen. The steeper sloping guide lines represent the mean phase rate of  $6.6^{\circ}/\text{rev}$  for the parking orbit and the shallower sloping guide lines are for the phase rate of  $3.75^{\circ}/\text{rev}$  for the waiting orbit. The horizontal line at  $\theta_i$  is the phase angle required to start the nominal intercept trajectory and

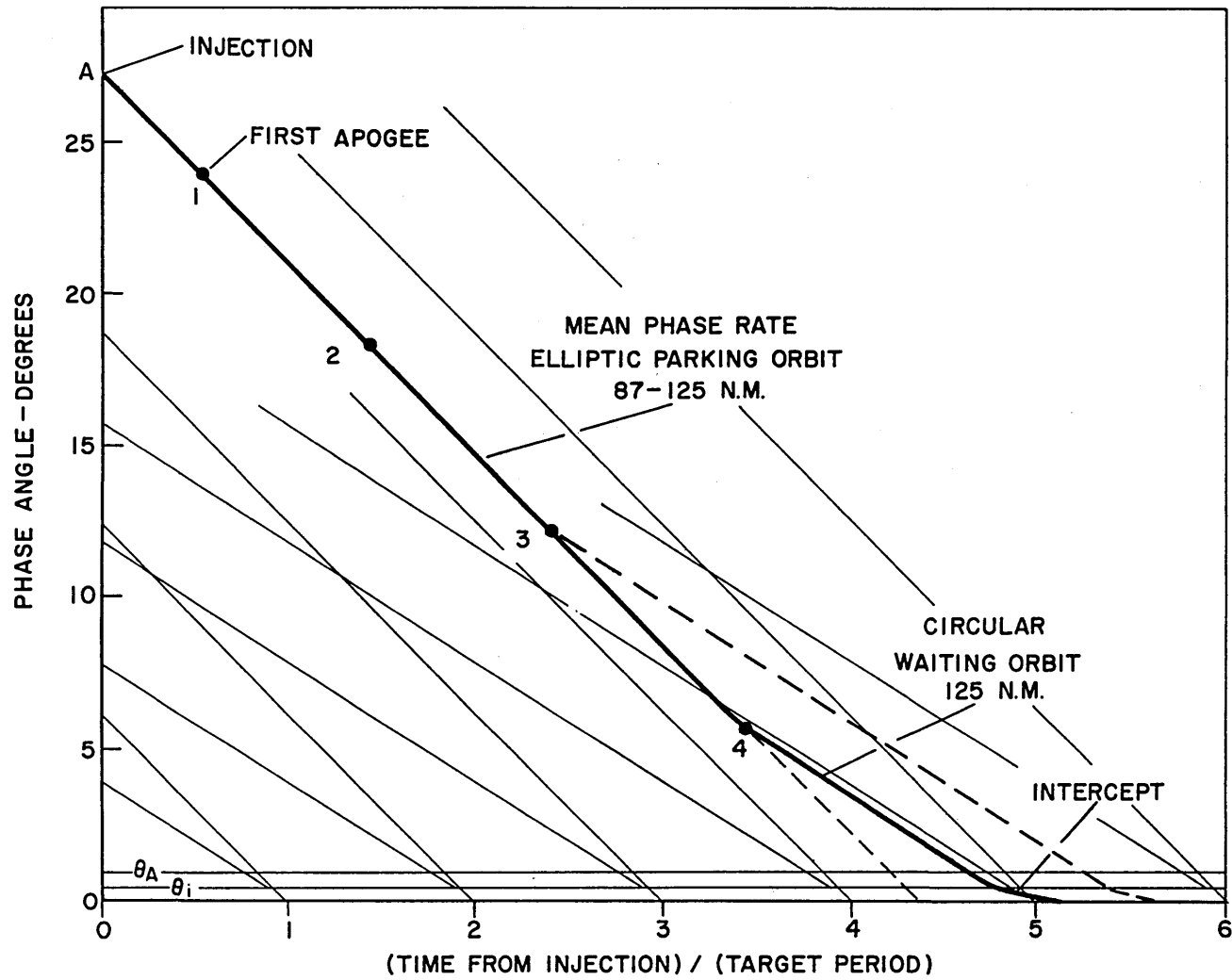


Fig. 4-7 Ideal Gemini Phase Angle vs Time

$\theta_A$  is the minimum phase angle to allow for target acquisition and the various out-of-plane measurements that are to be made. The transfer to the circular waiting orbit must be completed prior to reaching  $\theta_A$ . Associated with a given parking orbit such as A are points 1, 2, 3, 4 at which it reaches apogee and transfer to the waiting orbit can be made. Clearly the sooner this is done the longer it will take to complete the rendezvous maneuver. Unless it is desired to correct the waiting orbit based on ground tracking, to minimize the total time, the time spent in the parking orbit should be as long as the injection conditions will allow.

In order to be assured of having a waiting orbit at 125 nm, it would seem only natural to allow for some errors in the apogee of the parking orbit and plan it to be at about 130 nm. It would be unwise to plan the apogee too high since it requires more velocity change to circularize an elliptic orbit at points other than perigee or apogee, reaching a factor of about two at the semi-major axis. In addition, a higher apogee would also mean a decrease in the phase rate of the parking orbit. In Fig. 4-8 is shown the varying phase rate of a typical parking orbit varying from 87 to 130 nm. Points 1, 2, 3, and 4 may now be chosen to enter the waiting orbit. It can be seen that each of these results in a slightly different epoch or true anomaly of the target when the interceptor reaches  $\theta_i$ , and so some degree of phase adjustment is available. It is not difficult to visualize that if the parking orbit was

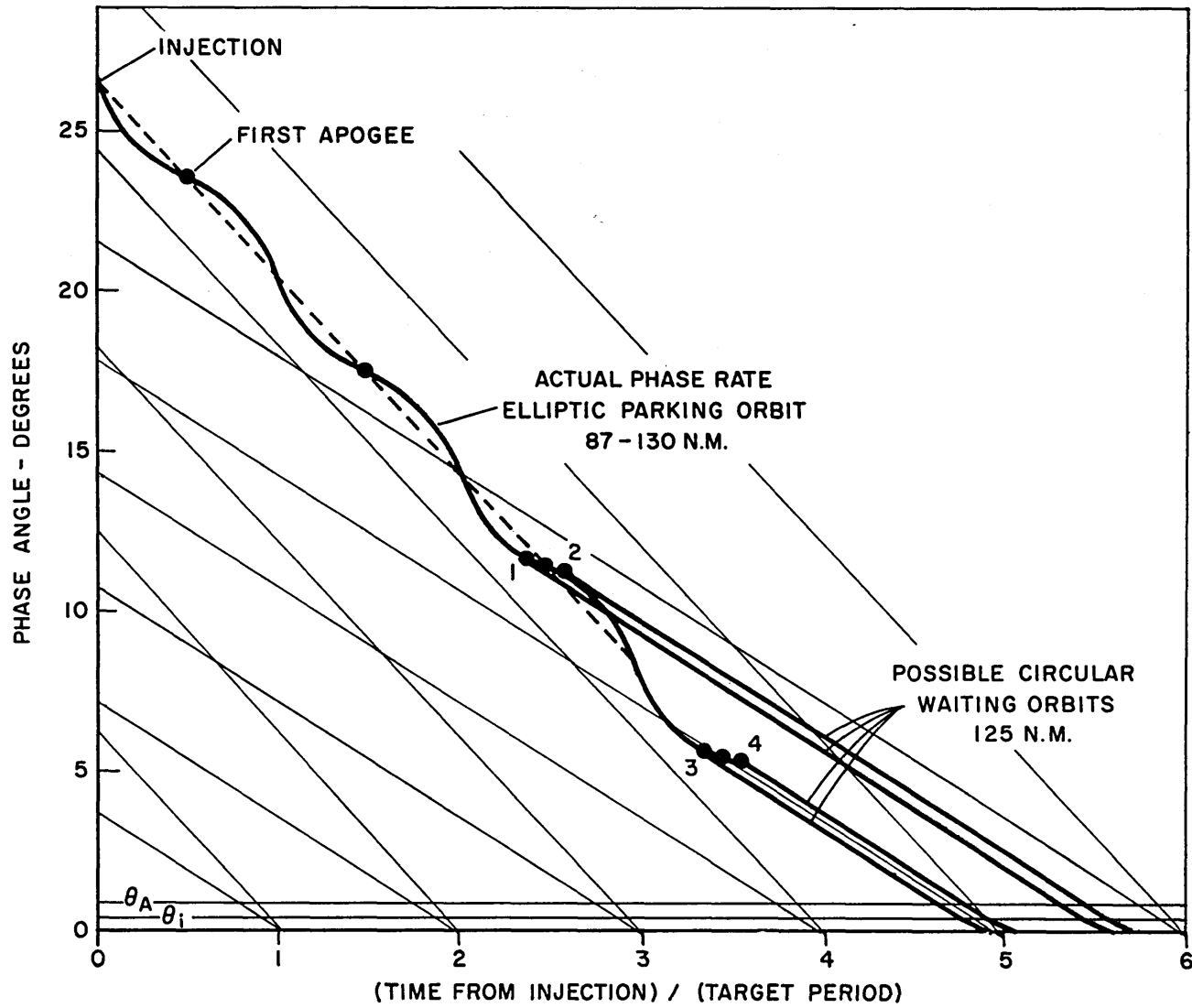


Fig. 4-8 Practical Gemini Phase Angle vs Time

instead merely a  $180^\circ$  transfer from a lower circular parking orbit (in this case at 87 nm) then, if the initial phase angle was large enough, any target true anomaly at  $\theta_1$  could be obtained. It is also rather easy to see that this procedure could be rather sensitive to measurement and action errors and that the longer time spent in the waiting orbit, the greater the effects would be.

Fortunately for the Gemini mission, phase control is not required, since as will be explained in Chapter 9, the location of the sun in relation to the line of sight is of no concern providing the target is launched at certain times of the day.

Since the question of injection for minimum time to rendezvous is of concern, the potentialities of such a "quasi-direct ascent" will now be briefly explained. The intercept trajectories suggested for this mission cover a nominal  $90^\circ$  of orbit and the acquisition and measurement phase should be at least  $30^\circ$ . To allow for errors in the parking orbit, the second or descending passage through 125 nm should be selected to transfer to the waiting orbit. The parking orbit would then cover about  $190^\circ$  making the entire quasi-direct ascent maneuver cover about  $310^\circ$ . This short a time to rendezvous could scarcely be beaten by the presently proposed closed loop guidance technique even if the intercept maneuver were initiated from the lower standard catch-up rate orbit, since certain operational delays following injection are required and the intercept maneuver itself covers



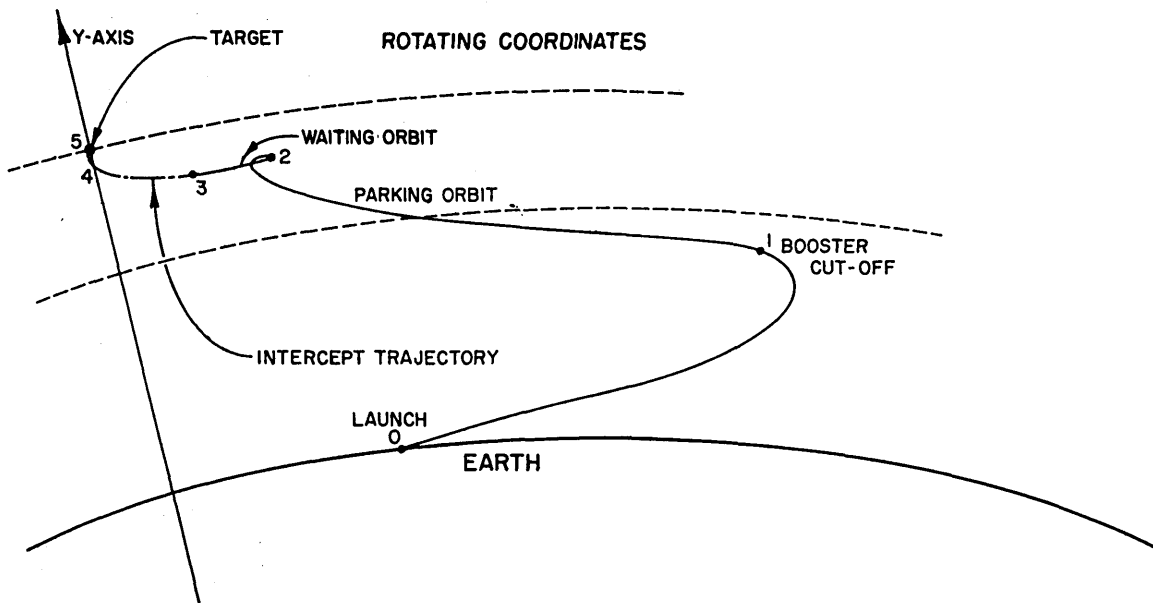
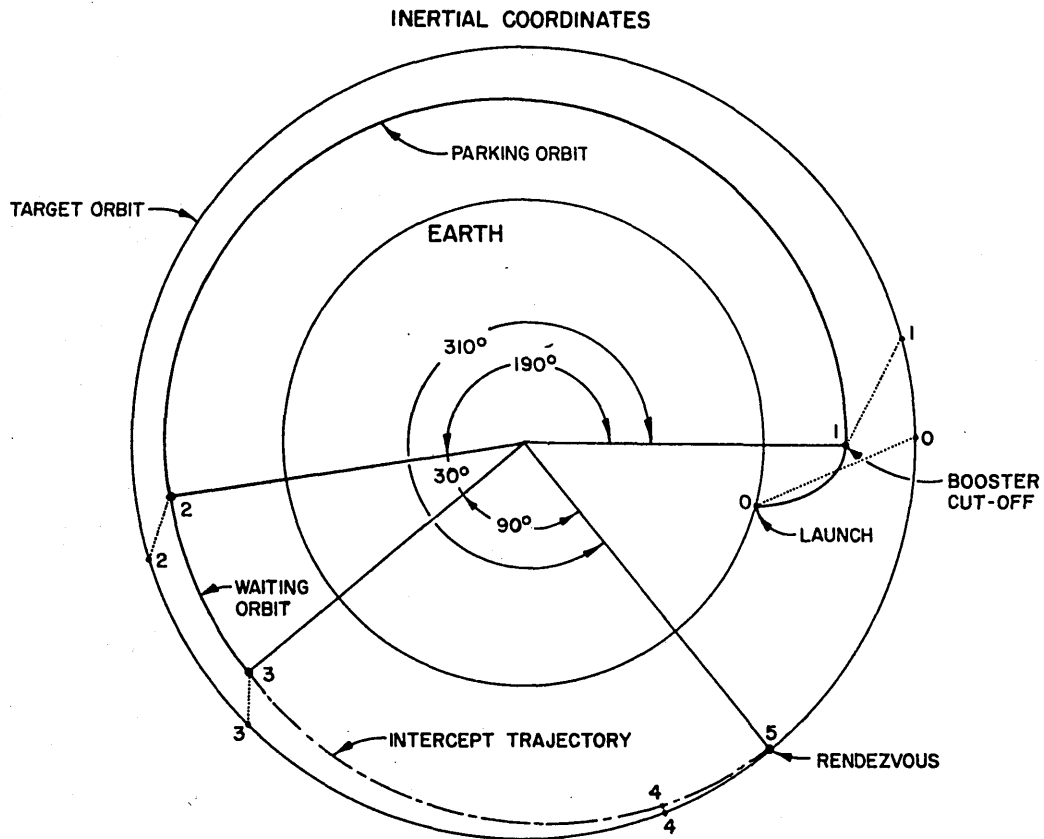


Fig. 4-9 Quasi-Direct Ascent for Gemini

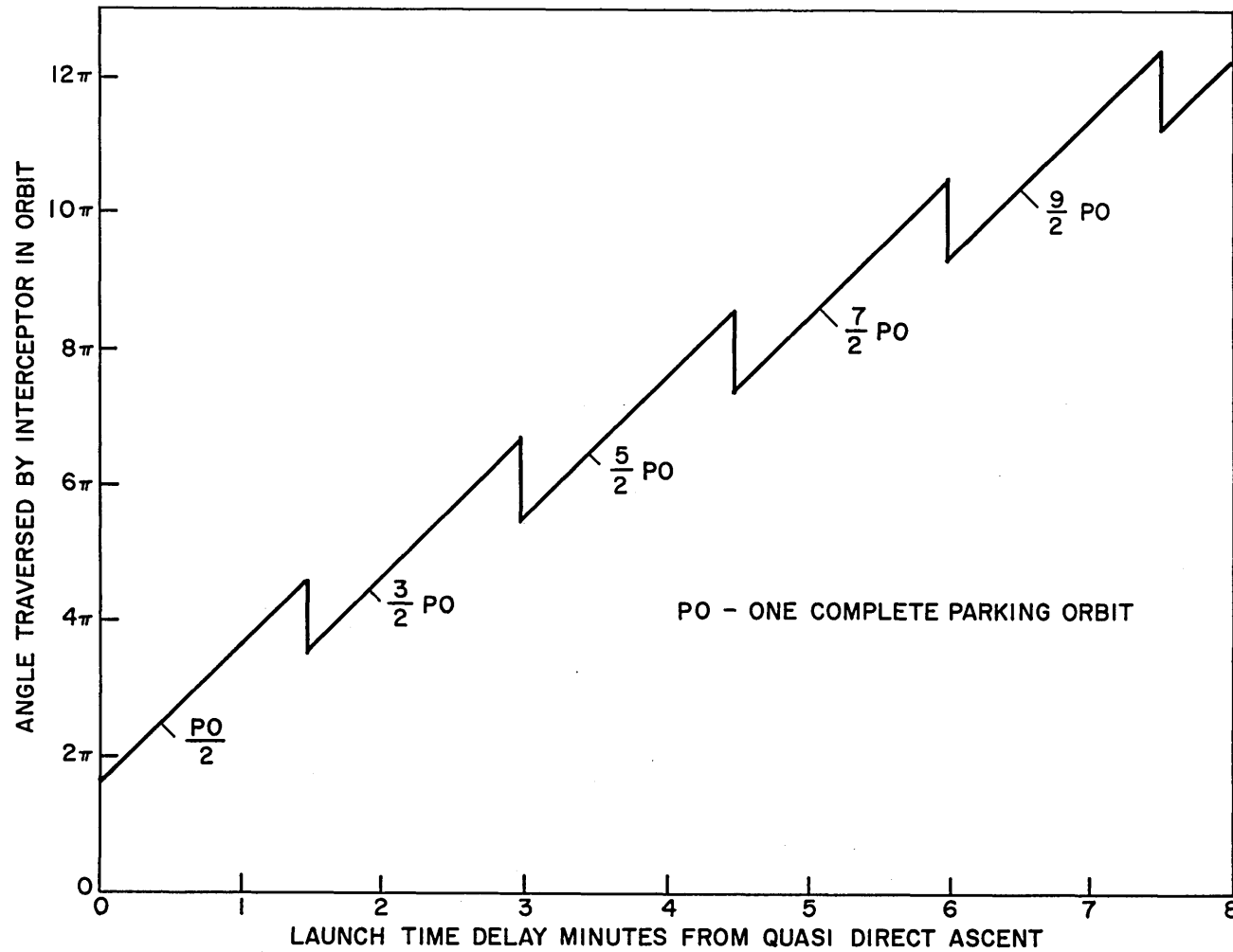


Fig. 4-10 Angle in Orbit vs Launch Delay Time

270°. For the suggested approach of this thesis, delays in launch would increase the time spent in the waiting orbit until an additional period could be spent in the parking orbit. An inertial and rotating frame depiction of the "quasi-direct ascent" is presented in Fig. 4-9, and a plot of the nominal angle traversed in orbit as a function of delay time from the "quasi-direct ascent" launch time is presented in Fig. 4-10. The author would hesitate to recommend this maneuver unless the expected apogee errors for the parking orbit are less than 5 nm and ground tracking could supply the astronaut the times and velocity changes required to attain a reasonably accurate waiting orbit prior to reaching the first apogee passage.



## CHAPTER 5

## INTERCEPT TRAJECTORIES - RENDEZVOUS PARAMETERS

5.1 Inertial Analysis

In the previous chapter dealing with the approach phase, extensive use was made of rotating coordinates as a visualization aid. In this chapter dealing with intercept trajectories, since the goal is to study the line-of-sight variation relative to inertial space, almost exclusive use will be made of inertial reference frames.

Since, for a given intercept trajectory between orbits, the point of initiating the maneuver depends upon satisfying the required relative positions of the vehicles in their orbits, and this time may be unpredictable, a convenient inertial reference direction should have some fixed relationship to the desired intercept trajectory. The inertial reference direction used for the remainder of this analysis will be the direction of perigee of the intercept trajectory. As previously mentioned, the study will be based on the assumption of Keplerian orbits or unperturbed two-body motion about a spherical earth whose center is inertially unaccelerated. The convenient artifice of having the two vehicles coincide at the rendezvous point and

then running time backwards to determine relative motion for exact nominal intercept trajectories will also be used.

Initially, the problem will be restricted to intercepts between two vehicles in circular coplanar orbits. The circular restrictions will next be removed and finally the non-coplanar aspects of the relative motion will be investigated.

Figure 5-1 portrays a typical intercept between circular coplanar orbits using the intercept perigee as the reference direction. Note that the angle  $\phi = f + \beta$  gives the line-of-sight angular variation with respect to inertial space throughout the intercept trajectory. A complete definition of terms and symbols appears just before Chapter 1. Where ambiguities exist and the meaning is not obvious, it is hoped that the text will resolve the difficulty.

Single intersecting intercept trajectories, that is, trajectories that neither go inside the waiting orbit nor outside the target orbit, will be considered almost exclusively. Many of the reasons for this will be evident later but the more important ones will be mentioned now (Reference Fig. 5-3). If the intercept goes outside the target orbit, the line of sight passes through the horizon and terminates with the earth as a background. Visual observation of the target's flashing light beacon would be most difficult under these circumstances. If the intercept does not go outside the target but does go inside the waiting orbit, acquisition and intercept initiation ranges must be increased. For large out-of-plane velocities relative to fuel capabilities,

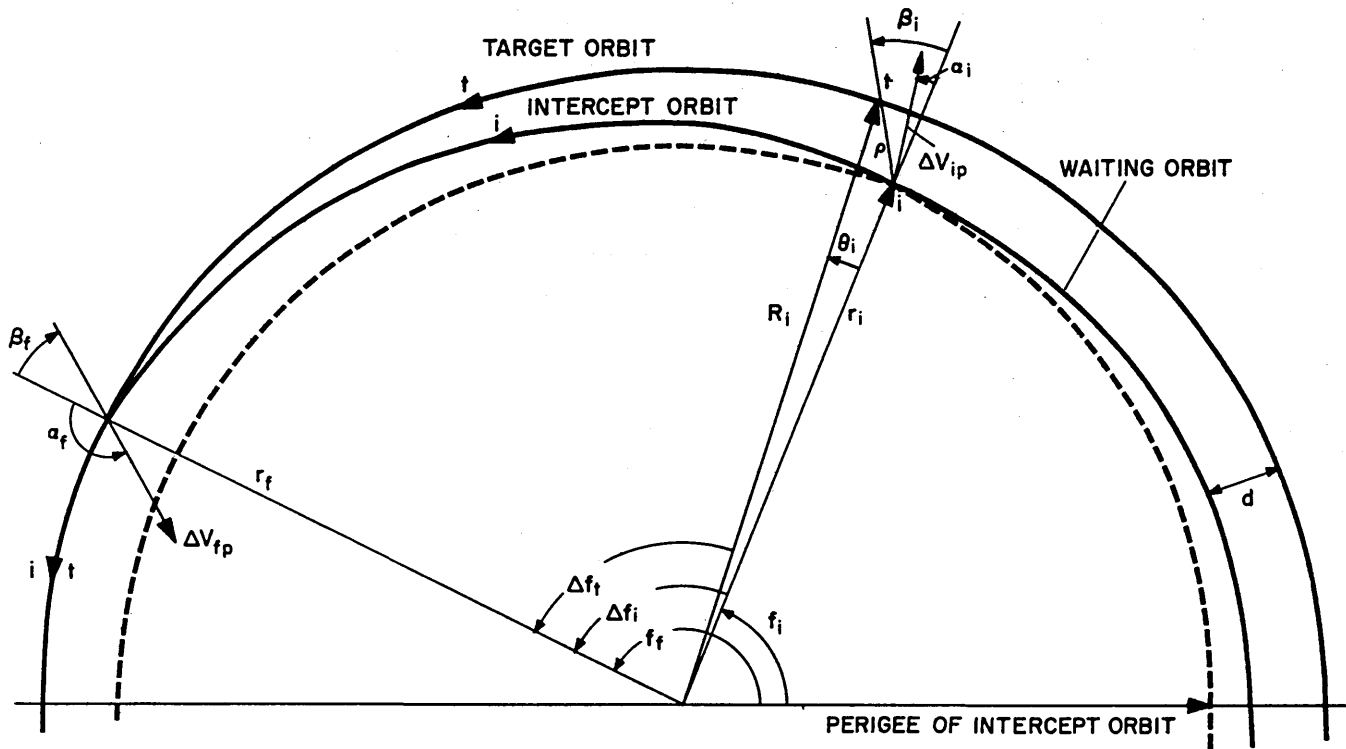


Fig. 5-1 Typical Intercept - Circular Coplanar Orbits

which are fully anticipated, optimum fuel intercepts traverse either near  $90^\circ$  or near  $270^\circ$ , and the latter  $270^\circ$  intercept would have to go outside the target. Finally, single intersecting trajectories are usually completed in a shorter time for a given fuel expenditure.

The study of the spectrums of available single intersecting intercept trajectories could be carried out in terms of the usual two parameters of classical mechanics, the semi-major axis  $a_i$  and the eccentricity  $e_i$  which together completely specify a trajectory in a plane with respect to the perigee direction. Instead, the author has found it most convenient and meaningful, both for exact and approximate analyses, to adopt two new constants  $b$  and  $k$  to replace  $a_i$  and  $e_i$ . These two parameters, for lack of imagination, will be termed "rendezvous parameters". Their definitions and significance will form the subject of the following section.

## 5.2 Rendezvous Parameters

Very early in the author's study of the rendezvous problem, the need became quite evident for classifying intercept trajectories in terms of some numbers that had much more significance to the rendezvous situation than do  $a$  and  $e$ . The idea for such a classification was somewhat prompted and inspired by a paper on rendezvous by Miller et al., of Astronautics Corporation of America (28). Though the rendezvous parameters  $b$  and  $k$  are initially derived for transfers between circular coplanar orbits, it will be shown that with proper





Room 14-0551  
77 Massachusetts Avenue  
Cambridge, MA 02139  
Ph: 617.253.2800  
Email: docs@mit.edu  
<http://libraries.mit.edu/docs>

## **DISCLAIMER**

**MISSING PAGE(S)**

69

However, the former expressions are usually handier for recalling the significance of  $b$  and  $k$ .

A few observations may make the use of these parameters clearer and point out the simplicity and utility they afford.

- (1) For the Hohmann transfer:

$$b = 1/2; k = \frac{1}{2 - d/r_f} \quad \text{or nearly } 1/2$$

(For any admissible solution,  $k$  must always be equal to or greater than this.)

- (2) For a tangential departure from the circular waiting orbit:

$$b = \frac{1 - k}{1 - kd/r_f} \quad \text{or nearly } 1 - k$$

(For an admissible solution,  $b$  must be equal to or greater than this.)

- (3) For a tangential arrival at the circular target orbit:

$$b = \frac{k}{1 + kd/r_f} \quad \text{or nearly } k$$

(For an admissible solution,  $b$  must be equal to or less than this.)

(4) For constant  $b$ , as  $k$  increases:

$f_i$  increases,

$f_f$  decreases,

intercept time decreases

(5) For constant  $k$ , as  $b$  increases,

$f_i$  increases,

$f_f$  increases,

intercept time decreases if  $b < 1/2$ ,

intercept time increases if  $b > 1/2$ .

(6) For illustration, some approximate values are:

$b$	$k$	$f_i$	$f_f$
0	1	$0^\circ$	$\sim 90^\circ$
1/2	1	$\sim 60^\circ$	$\sim 120^\circ$
$\sim 1$	1	$\sim 90^\circ$	$180^\circ$

If the expressions for  $a_i$  and  $e_i$  in terms of  $b$ ,  $k$ ,  $d$ , and  $r_f$  are substituted into standard conic formulas and the resulting expressions expanded in power series of the ratio  $d/r_f$ , some very useful relations are obtained. All these expressions are derived in complete detail in Appendix A. Since, for optical guidance purposes, the ratio  $d/r_f$  is rather small (about 0.007 for the Gemini application), terms of this

order and higher can be neglected to obtain to within about one percent the following:

$$\cos f_i = (1 - b)/k$$

$$\cos f_f = -b/k$$

$$\tan \alpha_i = \frac{1}{2} \cot f_i = \frac{1 - b}{2 \sqrt{k^2 - (1 - b)^2}}$$

$$\tan \alpha_f = \tan \beta_f = \frac{1}{2} \cot f_f = -\frac{b}{2 \sqrt{k^2 - b^2}}$$

$$\Delta V_H = V_{\text{cir. at } r_f} \quad d/2 \quad r_f$$

$$\Delta V_i = \Delta V_H \sqrt{4k^2 - 3(1 - b)^2}$$

$$\Delta V_f = \Delta V_H \sqrt{4k^2 - 3b^2}$$

$$\tan \beta_i = \frac{\frac{3}{2} (f_f - f_i) \cos f_f - 2(\sin f_f - \sin f_i)}{\cos f_f - \cos f_i}$$

$$= \frac{3}{2} b(f_f - f_i) + 2 \sqrt{k^2 - b^2} - 2 \sqrt{k^2 - (1 - b)^2}$$

For multiple intersecting intercepts, it is seen from Fig. 5-2 that one need only appropriately change the sign of some of the expressions. The expression for  $\tan \beta_i$  would require considerable interpretation, however.

Additional approximate analytical expressions for  $\phi$ ,  $\dot{\phi}$ , and  $\psi$  as functions of the true anomaly in the selected trajectory are also given in Appendix A. These expressions are valid for either a target in a circular orbit or a target in an elliptic orbit where the final target true anomaly is specified. These expressions might be useful if it were ever necessary to derive  $\phi$  and  $\psi$  curves in orbit instead of using the exact curves for a nominal intercept which would naturally be computed on the ground prior to launch.

To avoid the possible conclusion by the reader that the above approximations underlie the guidance techniques to be developed later, it should be pointed out that the prime usefulness of these expressions is to facilitate the examination of the spectrum of intercept trajectories and to get a feel for what exactly will change and in what direction as one looks at different trajectories. In essence, they serve as a handy visualization crutch for intercept trajectories in the way that rotating coordinates assisted in the approach phase. Once a trajectory is selected by choosing values of  $b$  and  $k$ , the exact line-of-sight variation will be obtained to the highest order of precision that could possibly be desired. This then will form the basis for the guidance techniques to be later derived.

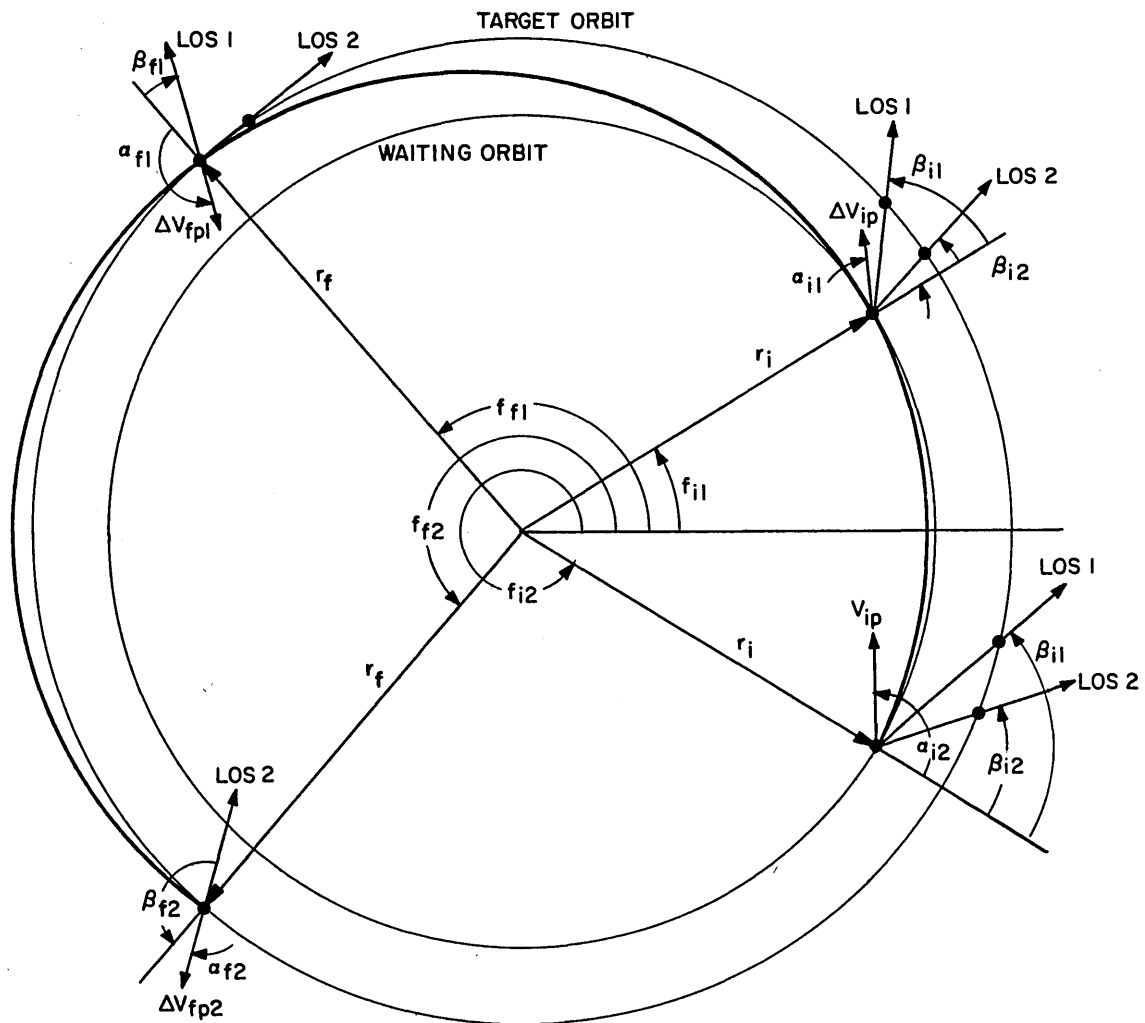
One important conclusion, however, can immediately be derived from the approximate expressions. For rather large radial errors in the waiting orbit (errors in  $d$ ), the properties of the trajectory are essentially unchanged. However, the velocity change needed in the  $a_1$  direction is directly proportional to those errors in  $d$ . From the above conclusions, the first guiding rule for initiating the transition from the waiting orbit to the intercept trajectory can be

formulated: Simply stay in the waiting orbit until the target reaches the angle  $\beta_i$  from the local vertical, then apply the nominal  $\Delta V_i$  in the direction  $\alpha_i$ .

By using the approximate expressions in terms of  $b$  and  $k$ , accurate to order  $d/r_f$ , three very useful graphs can be constructed to portray how various angles and velocity changes vary as a function of rendezvous parameters  $b$  and  $k$ . Actually, all the variables could be put on one graph but its usefulness would obviously be reduced. In Fig. 5-3,  $f_i$ ,  $f_f$ ,  $\Delta f_i$  and  $\Delta V_T/\Delta V_H$  are given as functions of  $b$  and  $k$ . In Fig. 5-4,  $\alpha_i$ ,  $\beta_i$ , and  $\beta_f$  are given as functions of  $b$  and  $k$ , and finally, Fig. 5-5 gives  $\Delta V_i/\Delta V_H$ ,  $\Delta V_f/\Delta V_H$  and  $\Delta V_T/\Delta V_H$  in terms of  $b$  and  $k$ . The author has personally found these charts invaluable in his search for trajectories that utilize to the fullest advantage the line-of-sight technique for rendezvous.

### 5.3 Extension to Non-circular Orbits

For intercepts to a circular target orbit from an elliptic waiting orbit, the condition of insensitivity to radial errors can be employed to considerable advantage. If the ephemeris of the waiting orbit is known, a nominal intercept trajectory can still be selected and when the line of sight to the target reaches the angle  $\beta_i$  from the local vertical, the intercept would be initiated as before. However, in this case instead of  $\alpha_i$  and  $\Delta V_i$  being constant values, they would be time varying with the true anomaly of the waiting orbit. To account



$$f_{f2} = 360^\circ - f_{f1}$$

$$a_{f2} = 180^\circ - a_{f1}$$

$$|\Delta V_{fp2}| = |\Delta V_{fp1}|$$

$$\beta_f = \alpha_f - 180^\circ$$

$$f_{i2} = 360^\circ - f_{i1}$$

$$a_{i2} = 180^\circ - a_{i1}$$

$$|\Delta V_{ip2}| = |\Delta V_{ip1}|$$

Fig. 5-2 Multiple Intersecting Intercepts - Circular Coplanar Orbits

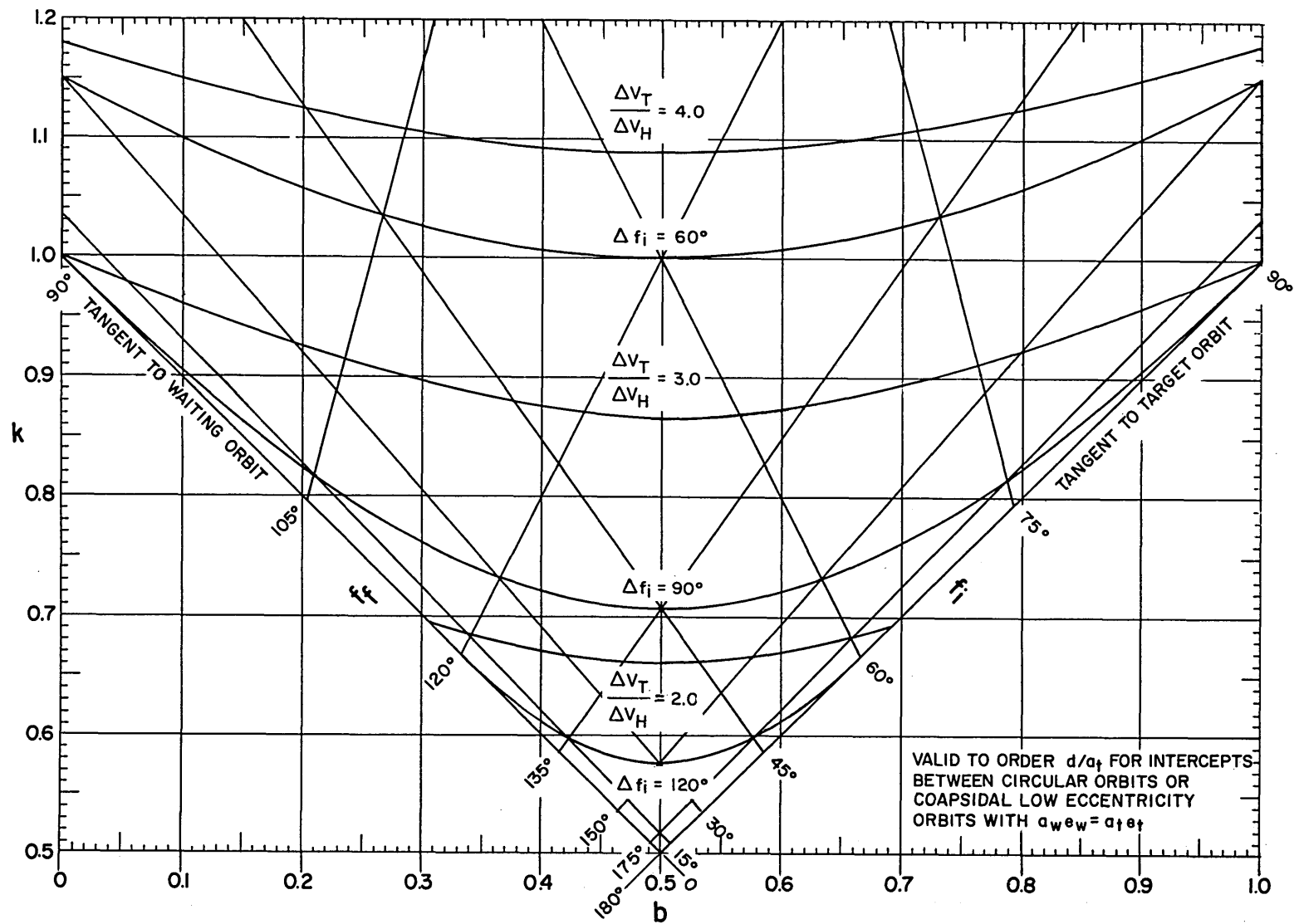


Fig. 5-3 Approximate True Anomalies and Total Velocity Changes as Functions of Rendezvous Parameters  $b$  and  $k$



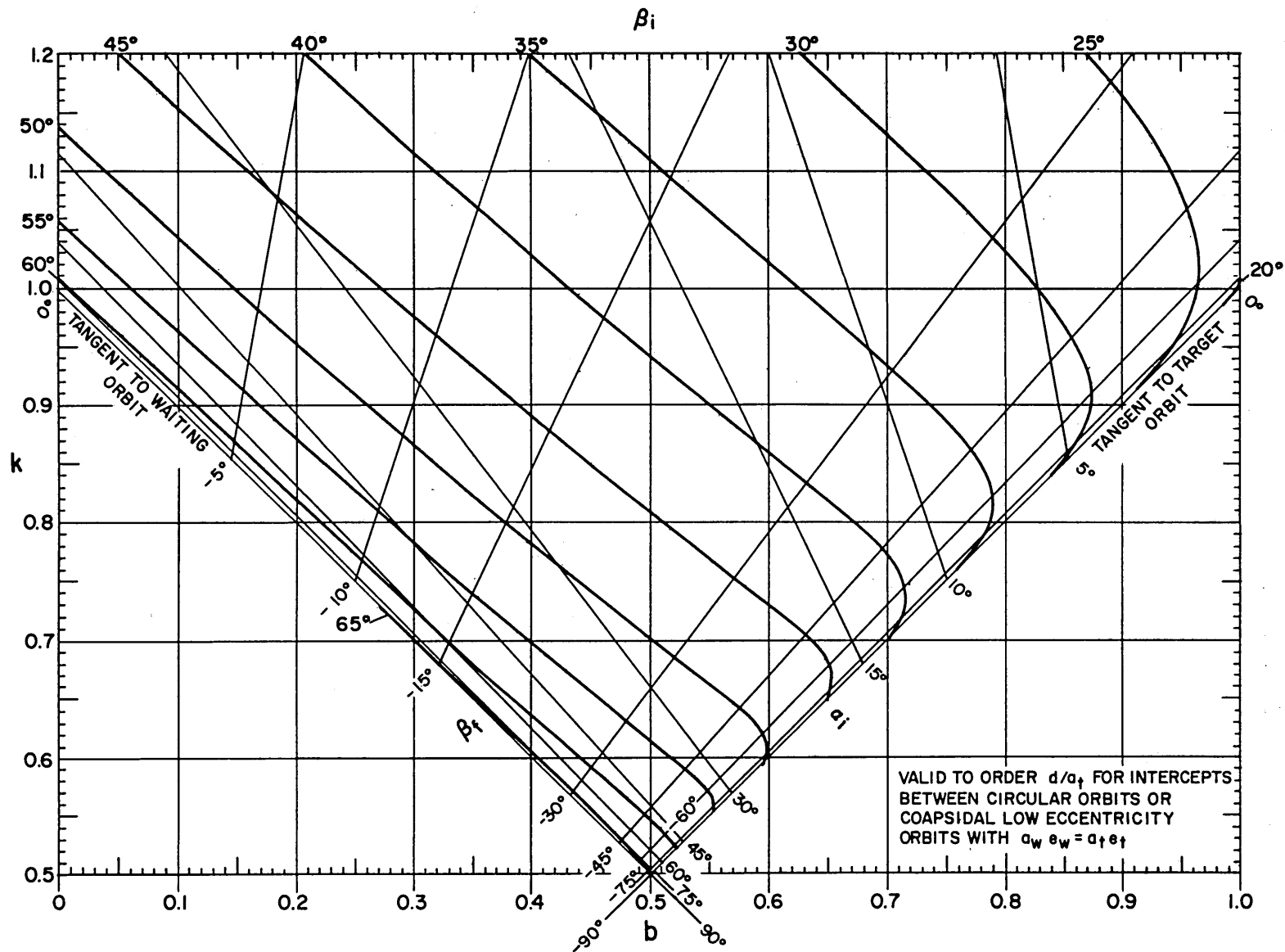


Fig. 5-4 Approximate Initial and Final Line-of-Sight and  $\Delta V$  Angles as Functions of Rendezvous Parameters  $b$  and  $k$

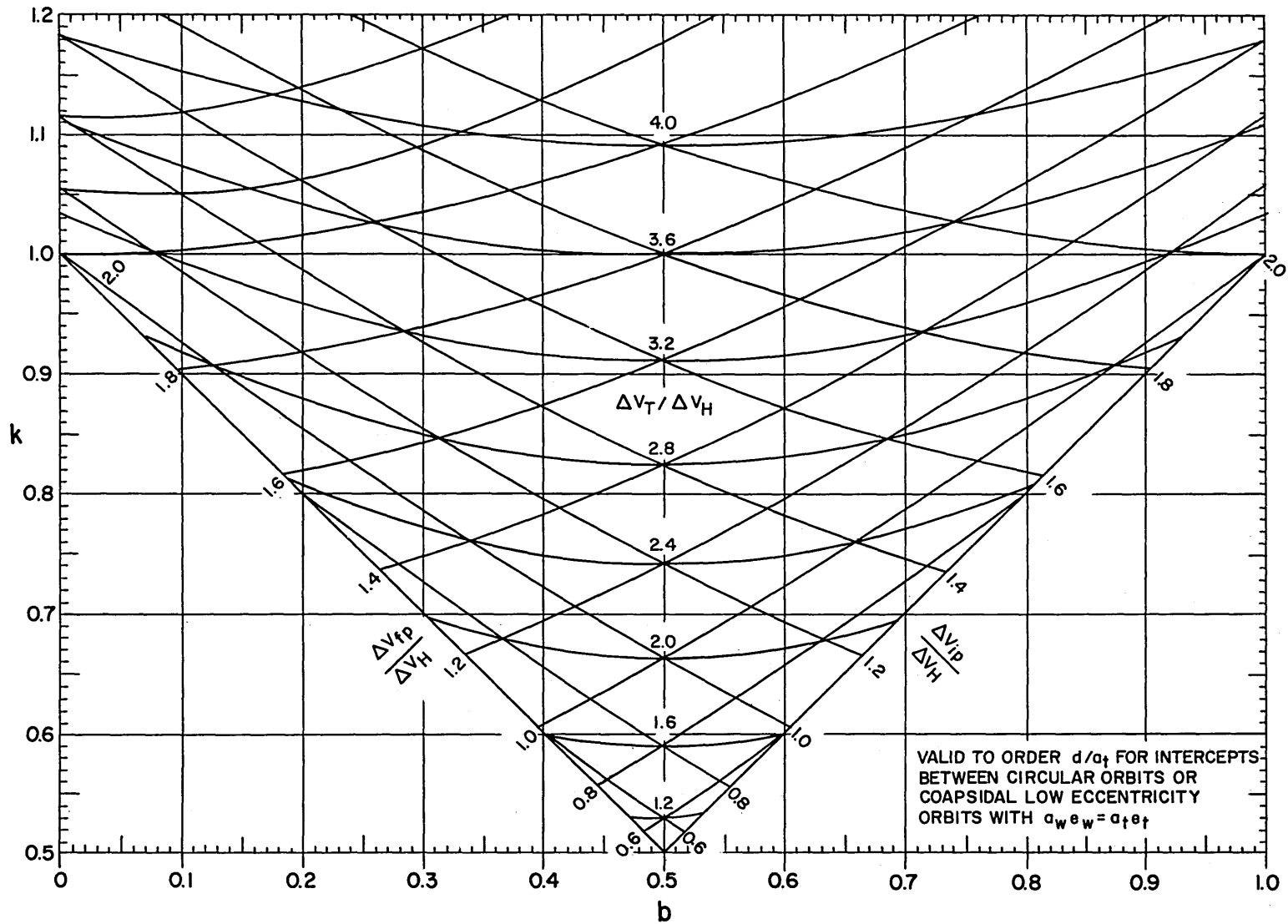


Fig. 5-5 Approximate Initial, Final and Total Velocity Changes as Functions of Rendezvous Parameters  $b$  and  $k$

for this would be a simple question of vector subtraction of the existing velocity deviation of the waiting orbit from circular velocity from the required  $\Delta V_i$  for initiating the intercept from a circular orbit at the existing radial distance,  $d$ . The general mechanics of this calculation are illustrated in Fig. 7-1 where the results are used for slightly different purposes. Whereas this procedure might have application to other rendezvous missions, it is felt by the author that the use of an intentional elliptic waiting orbit adds an unwarranted complication to the Gemini mission, or for any mission where the coapsidal elliptic waiting orbit technique is not used. As will be evident later, the assumption of a nominal circular waiting orbit for the guidance simulation results in no loss in generality, since the initial condition orbit errors could instead be interpreted as errors in the knowledge of the ephemeris of the elliptic waiting orbit resulting in an incorrect application of the velocity change to initiate the intercept.

For intercepts to elliptic target orbits, as mentioned in the previous chapter, two concepts have evolved. The first retains the uniformity advantages of the circular waiting orbit and is useful when the target orbit eccentricity is not large relative to the velocity change capability of the interceptor, and the second rather recently derived technique, which has very significant implications, makes use of the near uniformity of relative motion afforded by a coapsidal elliptic waiting orbit of near-constant radial separation from the target orbit.

For any intercept from a circular orbit to an elliptic orbit, with a specified true anomaly of the target at rendezvous, a transformation of the associated rendezvous parameters for this actual trajectory can be made to yield a  $b'$ ,  $k'$ , and  $d'$  of a pseudo intercept between circular orbits that has very nearly identical line-of-sight motion properties as the actual intercept. Conversely, if the line-of-sight motion for the actual intercept, terminating at a specified target true anomaly, is desired to be like a pseudo intercept between circular orbits, then a similar transformation of  $b'$  and  $k'$  will yield the  $b$  and  $k$  of the actual intercept. The latter transformation has greater practical significance since it would enable the use of a single set of driving functions for the sight regardless of the position of the target in its elliptic orbit; this would enable the selection of the single pseudo intercept that affords a near-optimum guidance with the greatest demonstrated tolerance to orbit errors. These transformations are based on certain approximations which assume low values of  $e_t$  and  $d/r_f$  and are derived in Appendix A. The mechanics of accomplishing these transformations are as follows:

- (1) To find the pseudo intercept rendezvous parameters  $b'$ ,  $k'$ , and the radial distance  $d'$  between circular orbits which correspond to the actual intercept described by  $b$  and  $k$  and the final target true anomaly  $f_{ft}$  with  $a_w$ ,  $a_t$ , and  $e_t$  specified, one proceeds as

follows:

$$d = a_t - a_w = a_t e_t \cos f_{ft}$$

$$d' = a_t - a_w = a_t e_t \cos (f_{ft} - \Delta f_i)$$

where;

$$\begin{aligned} \Delta f_i &= f_f - f_i \\ &= \cos^{-1} \left( \frac{-b}{k} \right) - \cos^{-1} \left( \frac{1-b}{k} \right) \end{aligned}$$

then;

$$k' = \frac{1}{\cos (f_i + \Delta f_p) - \cos (f_f + \Delta f_p)}$$

$$b' = -k' \cos (f_f + \Delta f_p)$$

where;

$$\Delta f_p = \tan^{-1} \left( \frac{-a_t e_t \sin (f_{ft} - f_f)}{kd - a_t e_t \cos (f_{ft} - f_f)} \right)$$

$\Delta f_p$  is essentially a phase shifting of the intercept initial and final true anomalies.

- (2) To find the actual intercept rendezvous parameters  $b$  and  $k$ , for an intercept to an elliptic target orbit with the final target true anomaly  $f_{ft}$  and  $a_w$ ,  $a_t$  and  $e_t$  specified, so that this actual intercept will have line-of-sight motion similar to that of a pseudo intercept between circular orbits described by  $b'$  and  $k'$ , one proceeds as follows:

$$d' = a_t - a_w - a_t e_t \cos (f_{ft} - \Delta f_i')$$

where;

$$\begin{aligned} \Delta f_i' &= f_f - f_i \\ &= \cos^{-1} \left( \frac{-b'}{k'} \right) - \cos^{-1} \left( \frac{1 - b'}{k'} \right) \end{aligned}$$

then;

$$k = \frac{1}{\cos (f_i' - \Delta f_p') - \cos (f_f' - \Delta f_p')}$$

$$b = -k \cos (f_f' - \Delta f_p')$$

where;

$$\Delta f_p' = \tan^{-1} \left( \frac{-a_t e_t \sin (f_{ft}' - f_f')}{k' d' + a_t e_t \cos (f_{ft}' - f_f')} \right)$$

It should be noted in both the transformations that when  $e_t$  is zero or when  $(f_{ft}' - f_f')$  or  $(f_{ft} - f_f)$  is  $0^\circ$  or  $180^\circ$ , no change is made in the rendezvous parameters.

The use of the above transformations to a pseudo intercept with a target in a circular orbit are only valid for line-of-sight relative motion considerations. Naturally, the magnitude  $\Delta V_i$  and direction  $\alpha_i$  must be obtained from the actual situation. The exact line-of-sight motions, when obtained by the analysis to be described in Section 5.6, agree so closely for the pseudo and actual intercepts that in a graphical comparison the differences are barely detectable. In fact, when this technique using the transformations of (2) above is tested by actual simulations, the  $\phi$  and  $\psi$  functions used for intercepts to elliptic orbit targets at various target true anomalies are those actually derived from a single intercept between circular orbits with only  $\Delta V_i$  and  $\alpha_i$  varying with target true anomaly at intercept initiation. The variations of  $b$ ,  $k$ , and  $\Delta V_{ip}$ , and  $\alpha_i$  for an intercept to an elliptically orbiting target to produce line-of-sight relative motion similar to a standard circular orbit intercept are given in Fig. 8-13 for various

values of target true anomaly. This technique of intercepting a target in an elliptic orbit from a circular waiting orbit appears to have some merit and does establish the comparison analogy with intercepts to targets in circular orbits; yet, it is rather limited in application and considerably inferior in results to the concept of employing a coapsidal elliptic waiting orbit which will now be briefly described.

The basic purpose of placing the interceptor into a coapsidal elliptic waiting orbit with near-constant radial separation from the elliptic target orbit is so that as the two vehicles approach each other in their respective orbits, the deviation of each vehicle from conditions of orbit circularity will be very nearly identical and the tendency to have these deviations cancel each other out for relative motion purposes will exist. Then, to the extent that this cancellation does occur, the ensuing intercept can be treated as if the orbits were indeed circular and the point of initiating the intercept will have no effect on the subsequent relative motion. A rigorous proof of this concept which appears to have far-reaching consequences will not be attempted analytically but rather will be left to the results of rendezvous simulation for verification. Certain effects of orbit errors for intercepts between nominally circular orbits which tend to substantiate the validity of this concept will be noted in Chapter 7 followed by actual simulations of intercepts between coapsidal elliptic orbits ranging to the extremes of near-Earth operation under conditions of no errors in the orbits.



Finally, then in Chapter 8, simulation under error conditions will compare this coapsidal elliptic orbit technique with the other alternative of departing a circular waiting orbit. In order to provide near-constant radial separation of the coapsidal elliptic orbits, the eccentricity of the waiting orbit is defined from:

$$a_w e_w = a_t e_t$$

which insures that the radial separations at apogee and perigee are equal. Then, since the radial separation is small in comparison with the orbital radii, the separation at other true anomalies will also be very nearly the same as this. The resulting deviations from a constant radial separation are quite small in comparison with the orbit errors used in testing the simulations.

A slight diversion which will assist in further analyzing the elliptic target situation appears now in order. Suppose that instead of the interceptor embarking upon an intercept trajectory to rendezvous with the target, the target itself is commanded to change its orbit to make the rendezvous with the interceptor in the circular waiting orbit. This situation is shown in Fig. 5-6. Now, for ease of comparison and to assist in drawing an analogy, the reference direction will be the direction of apogee and the angles  $f$  will be measured from that direction. If the same values of  $b$  and  $k$  are used but now defined as:

$$a_i = r_f + bd$$

$$e_i = kd/r_f$$

then, it is found that the approximate expression for the angles and velocities are identical and the exact expressions are very nearly the same. In fact, in every way, except that the target applies the velocity change in the opposite direction, the rendezvous maneuver proceeds in a relative motion manner that is essentially undistinguishable from the rendezvous in which the interceptor applies the velocity change. As will be mentioned later, for actual rendezvous simulations conducted for this type of a mission, the deviations and corrections due to orbit errors are almost identical.

Going back now to the discussion of the conventional interceptor initiated intercepts from a circular waiting orbit to an elliptic target orbit, it should be recalled that for the circular target orbit, the line-of-sight variation was shown to be rather insensitive to radial errors in the waiting orbit (errors in  $d$ ). One might now logically ask the question: Under what conditions would one get the same insensitivity to radial errors if the target is in an elliptic orbit? To carry out this analysis, use will be made of a phantom target C in a circular orbit, elliptic targets  $t$  and  $t'$  and the interceptor  $i$ . If one works backwards in time from a condition of rendezvous of all four vehicles at a radial distance  $r_f$ , to the point where  $i$  initiates the intercept,  $i$  has

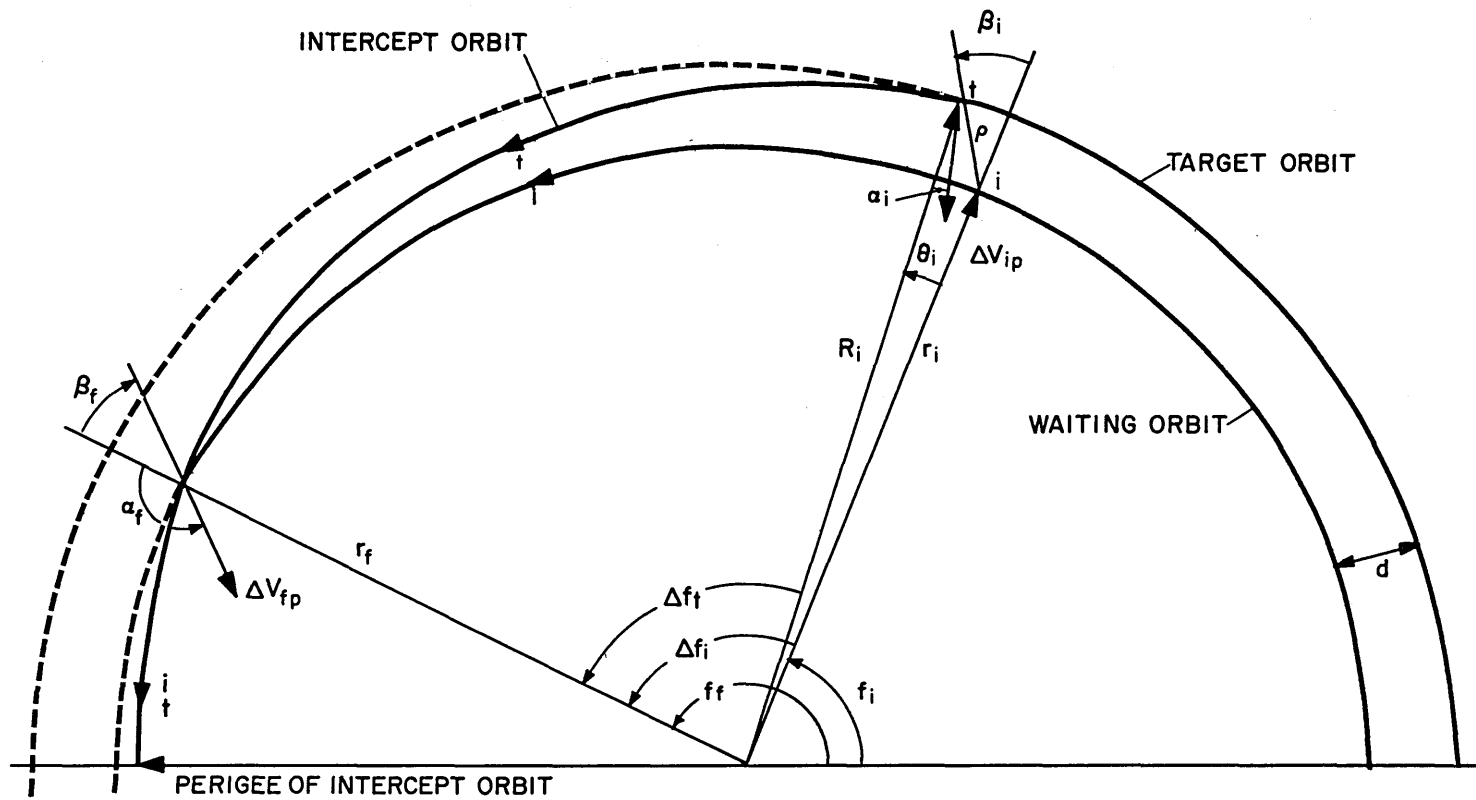


Fig. 5-6 Target Initiated Intercept Trajectories

a radial separation from  $c$  of  $d_i$  and  $t$  and  $t'$  have corresponding radial distances,  $d_t$  and  $d_{t'}$ , from  $c$ . Figure 5-7 is a sketch of this situation. After some thought, the conclusion is reached that if the line of sight from  $i$  to  $c$  is to pass through  $t$  and  $t'$ , then the rendezvous parameters for the  $t$  to  $c$  and  $t'$  to  $c$  intercepts with respect to the distance  $d_t$  and  $d_{t'}$  should be the same as the values of  $b$  and  $k$  for the  $i$  to  $c$  intercept. When this is done, the result is that the perigee direction of the  $i$  intercept very nearly coincides with the perigee of  $t$  and the apogee of  $t'$ . Now it can be stated that if the final true anomaly of the intercept trajectory to an elliptic target orbit is equal to the final target true anomaly plus  $n 180^\circ$  where  $n$  is 0 or 1, then the same insensitivity to radial errors in the waiting orbit will result.

The basic conclusion to be drawn from all this discussion of rendezvous with targets in elliptic orbits is that, since the recommended techniques of intercepting such targets all stem from the similarity and analogies through transformation to intercepts of targets in circular orbits, all the succeeding analyses pertaining to intercepts between circular orbits are directly applicable through the same similarities and transformations to targets in elliptic orbits.

In a like manner, the line-of-sight variations considered in this investigation of intercepts could also be applied to the coasting portion of a true direct ascent rendezvous since the primary concern is the variations that take place after injection into a free-fall intercept trajectory. As will be pointed out in Chapter 10, this entire study could

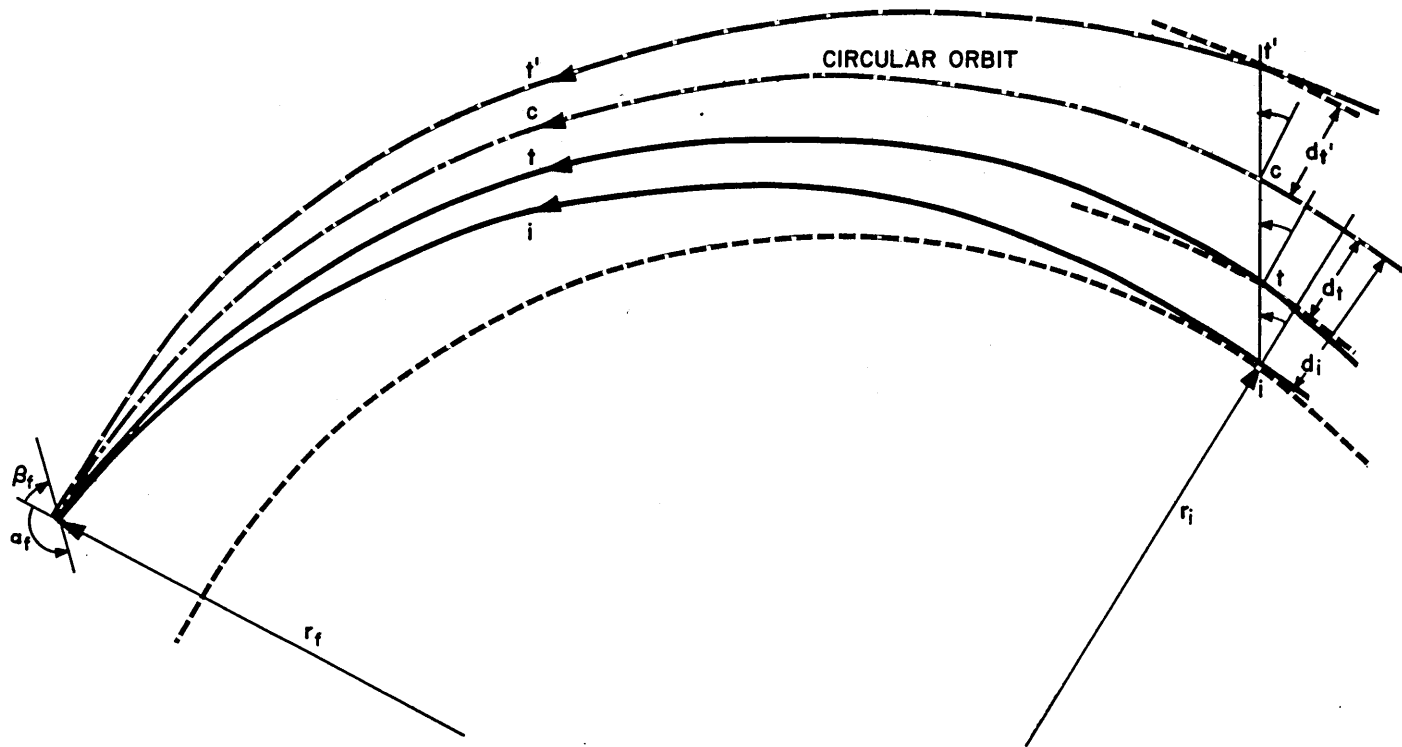


Fig. 5-7 Radial Error Insensitivity for Elliptic Target Orbits

be applied to the Apollo Lunar Orbit Rendezvous using either the direct-ascent or parking-orbit approach.

#### 5.4 Non-Coplanar Effects on the Line of Sight

In considering the out-of-plane problem, as in previous sections, certain approximations will be made to derive a simple model from which a simple visualization of the problem can be made. However, also as before, when the actual out-of-plane line-of-sight variation is desired for a selected intercept trajectory, all the exact relations will be employed. Since the magnitude and orientation of the out-of-plane situation may be somewhat arbitrary, some approximations must necessarily be carried over into the implementation of line-of-sight guidance philosophy if a simple solution is to be readily attainable. Where these are necessary, a brief description of their effects will be noted.

Consider a waiting orbit of arbitrary ellipticity and a target orbit also of arbitrary ellipticity with a relative inclination  $i_t$  and the Z-axis perpendicular to the waiting orbit plane as shown in Fig. 5-8a. The  $\gamma$  angles are measured in the target orbit plane and unless doubly subscripted are measured in the direction of motion from the ascending line of nodes. Thus the  $Z_t$  displacement and  $\dot{Z}_t$  velocity of the target relative to the waiting orbit plane can be written as:

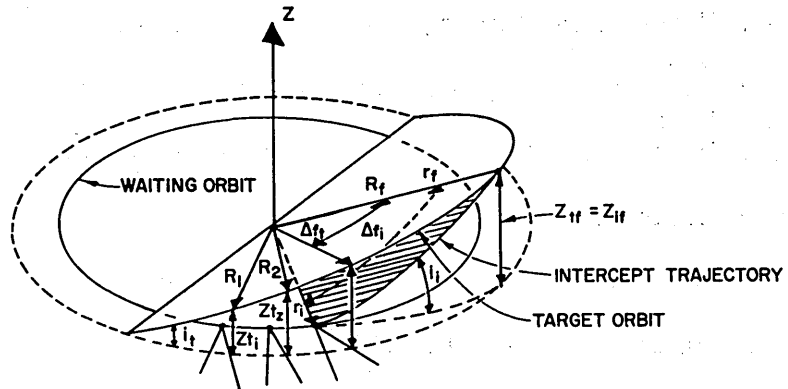
$$Z_t = R_t \sin i_t \sin \gamma$$

$$\dot{Z}_t = \dot{R}_t \sin i_t \sin \gamma + R_t \dot{i}_t \sin i_t \cos \gamma$$

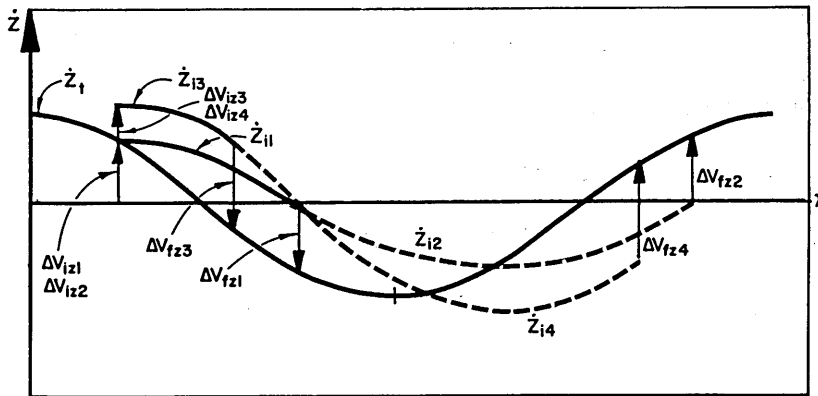
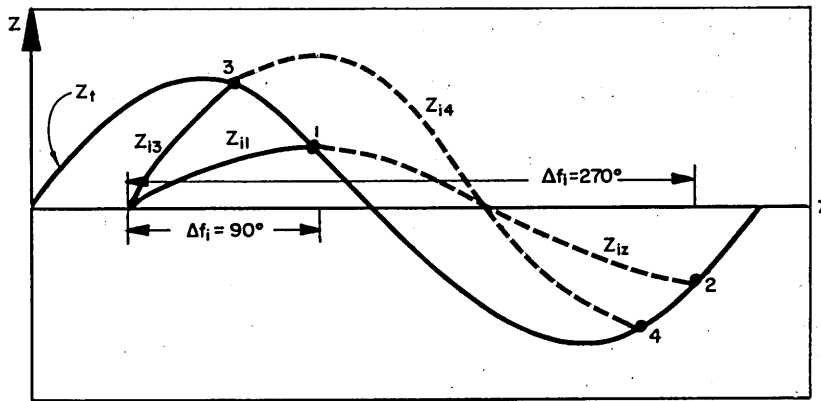
and their variations with  $\gamma$  might be as shown in Fig. 5-8b. If the target orbit was circular,  $\dot{f}_t$  would be constant,  $\dot{R}_t$  would be zero and the variations would be purely sinusoidal. For elliptic target orbits, the periodicity would be the same but the variations would not be purely sinusoidal.

Now if the relative motion due to the in-plane situation were such that the target would be within visual range for more than  $180^\circ$ , or, if it were known that a nodal crossing would occur while it was within visual range and prior to rendezvous, then it would be a simple matter to wait until the nodal crossing occurred and at that time change the velocity of the interceptor so that it would remain in the target plane. Unfortunately, unless long time trajectories are used, the target will not be in sight for  $180^\circ$  and unless phase rate control is employed, the line of nodes may occur anywhere. There are specific cases such as direct ascent where this procedure might have merit but the author has chosen to study the more general case.

For arbitrary location of the line of nodes, it will usually be necessary to adjust the nodal crossing so that it will occur before or at rendezvous. The most advantageous time to do this will be at the time when the in-plane velocity change is made so that a fuel saving can be realized by the application of the resultant of the vector sum of the corrections required. If the desired new nodal crossing is at the rendezvous point, then the line of sight must be controlled in the



- a -



- b -

Fig. 5-8 Non-Coplanar Effects



Z direction to insure that this does happen. An alternative to this is to adjust the new nodal crossing so that it will occur at a certain angle prior to the expected rendezvous. In this case, the line of sight need not be controlled unless large errors are evident and, when the crossing does occur, a velocity change is made in the Z direction to cause the interceptor to change its plane to coincide with that of the target. Z guidance would be needed subsequent to this and maintained until rendezvous. This latter method was investigated to a considerable degree by the author as explained in Chapter 7 and ultimately rejected for the Gemini mission application. It should be obvious that the second Z correction does not enjoy the fuel saving inherent in the vector addition of components that planning for the nodal crossing at rendezvous would involve.

Regardless of which method is employed at the time for applying the initial planar component,  $\Delta V_{ip}$ , some angle  $\gamma_i$  will exist, and it will usually be desired to apply a Z component,  $\Delta V_{iz}$ , so that the new line of nodes will occur some angle  $\Delta f_i$  later. From a brief study of rendezvous conditions 1, 2, 3, and 4 of Fig. 5-8b, it is readily seen that if the angle  $\Delta f_i$  is equal to  $90^\circ$  or  $270^\circ$ , then the new relative inclination will never be increased. Such is not the case in certain instances if  $\Delta f_i$  is greater or less than  $90^\circ$  or  $270^\circ$ . To be more precise, if:

$$\left| \sin \gamma_i \right| > \left| \sin \Delta f_t \right|$$

then, an increase in relative inclination will result. The difficulties associated with a  $\Delta f_i$  of near  $180^\circ$  are now clearly apparent. For the worst value of  $\gamma$ , the sum of the Z corrections needed are smallest when  $\Delta f_i$  is near  $90^\circ$  or  $270^\circ$  and for these values of  $\Delta f_i$ , a value of  $45^\circ + n90^\circ$  ( $n = 0, 1, 2, \dots$ ) gives the sum of the Z corrections which is very nearly greatest. Naturally, the total maximum velocity change would involve the vector additions of the required in-plane components and this will be analyzed later including guidance and error effects for a nominally selected trajectory.

By making an observation at an angle  $\gamma_{2i}$  prior to  $\gamma_i$ , the displacement  $Z_{t2}$  can be calculated and, if an earlier observation at  $\gamma_{12} + \gamma_{2i}$  prior to  $\gamma_i$  is made, the displacement  $Z_{t1}$  can likewise be calculated. With these two values, an expression can be derived to give the required Z component of velocity change,  $\Delta f_i$  later. Refer to Figs. 5-8 and 5-9 and note that the following derivation applies to both elliptic target and waiting orbits as well as circular orbits.

For any angle  $\gamma$ , the following holds:

$$Z_t = R \sin i_t \sin \gamma$$

therefore;

$$Z_{t1} = R_1 \sin i_t \sin (\gamma_2 - \gamma_{12})$$

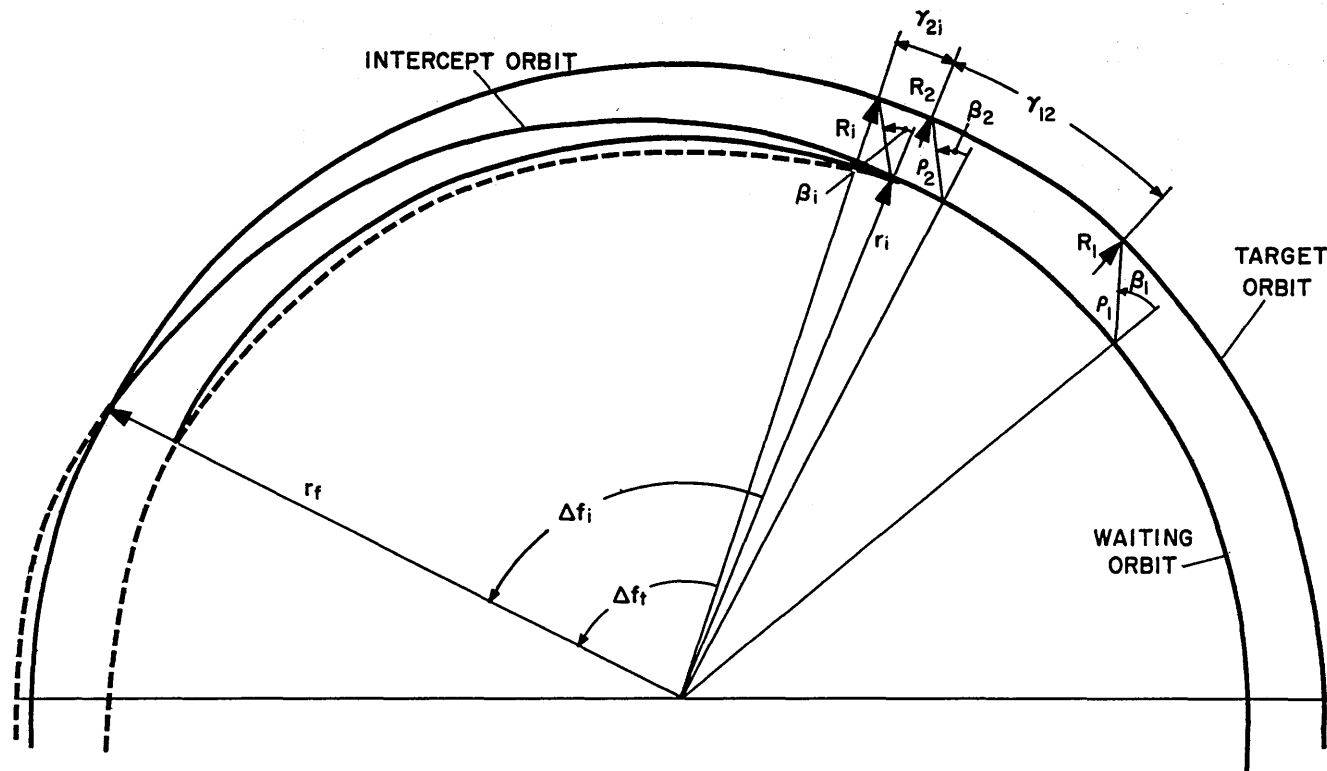


Fig. 5-9  $\Delta V_{iz}$  Determination by Observation

and;

$$Z_{t2} = R_2 \sin i_t \sin \gamma_2$$

so;

$$\frac{Z_{t1}}{Z_{t2}} = \frac{R_1}{R_2} \frac{(\sin \gamma_2 \cos \gamma_{12} + \cos \gamma_2 \sin \gamma_{12})}{\sin \gamma_2}$$

$$\cot \gamma_2 = \cot \gamma_{12} - \frac{Z_{t1} R_2}{Z_{t2} R_1 \sin \gamma_{12}}$$

Now, for the interceptor, at any time after the impulsive initial velocity change;

$$Z_i = r \sin i_i \sin (f - f_i)$$

and;

$$\dot{Z}_i = \dot{r} \sin i_i \sin (f - f_i) + r \dot{f} \sin i_i \cos (f - f_i)$$

Since at rendezvous it is desired that;

$$Z_{tf} = Z_{if}$$

and;

$$R_f = r_f$$

then, since;

$$Z_{tf} = R_f \sin i_t \sin (\gamma_i + \Delta f_t)$$

and;

$$Z_{if} = r_f \sin i_i \sin \Delta f_i$$

then;

$$\sin i_i = \sin i_t \frac{\sin (\gamma_i + \Delta f_t)}{\sin \Delta f_i}$$

At  $\gamma_i$  or when  $f = f_i$ , immediately after the impulsive velocity change of the interceptor;

$$\dot{Z}_{ii} = r_i \dot{f}_i \sin i_i$$

Since prior to this the Z velocity of the interceptor was zero:

$$\begin{aligned} \Delta V_{iz} &= r_i \dot{f}_i \sin i_i \\ &= r_i \dot{f}_i \sin i_t \frac{\sin (\gamma_i + \Delta f_t)}{\sin \Delta f_i} \end{aligned}$$

Substituting for  $\sin i_t$  from the third equation of the derivation and expanding:

$$\Delta V_{iz} = \frac{r_i \dot{f}_i Z_{t2}}{R_2 \sin \gamma_2 \sin \Delta f_i} (\sin \gamma_i \cos \Delta f_t + \cos \gamma_i \sin \Delta t_t)$$

$$= \frac{r_i \dot{f}_i Z_{t2}}{\sin \Delta f_i R_2 \sin \gamma_2} [\sin \gamma_2 \cos \gamma_{2i} \cos \Delta f_t + \dots]$$

$$+ \cos \gamma_2 \sin \gamma_{2i} \cos \Delta f_t + \cos \gamma_2 \cos \gamma_{2i} \sin \Delta f_t$$

$$- \sin \gamma_2 \sin \gamma_{2i} \sin \Delta f_t]$$

$$= \frac{r_i \dot{f}_i}{\sin \Delta f_i} \frac{Z_{t2}}{R_2} (\cos \gamma_{2i} \cos \Delta f_t + \cot \gamma_2 \sin \gamma_{2i} \cos \Delta f_t$$

$$+ \cot \gamma_2 \cos \gamma_{2i} \sin \Delta f_t - \sin \gamma_{2i} \sin \Delta f_t)$$

$$= r_i \dot{f}_i \frac{\sin \Delta f_t}{\sin \Delta f_i} \frac{Z_{t2}}{R_2} [(\cos \gamma_{2i} \cot \Delta f_t - \sin \gamma_{2i})$$

$$+ \cot \gamma_2 (\sin \gamma_{2i} \cot \Delta f_t + \cos \gamma_{2i})]$$

$$= r_i \dot{f}_i A \frac{Z_{t2}}{R_2} (B + \cot \gamma_2 C)$$

where;

$$A = \frac{\sin \Delta f_t}{\sin \Delta f_i}$$

$$B = \cos \gamma_{2i} \cot \Delta f_t - \sin \gamma_{2i}$$

$$C = \sin \gamma_{2i} \cot \Delta f_t + \cos \gamma_{2i}$$

Now, substituting in the previously derived expression for  $\cot \gamma_2$  in terms of  $Z_{t1}$  and  $Z_{t2}$ :

$$\Delta V_{iz} = r_i \dot{f}_i A \frac{Z_{t2}}{R_2} (B + C \cot \gamma_{12} - C \frac{R_2}{R_1 \sin \gamma_{12}} \frac{Z_{t1}}{Z_{t2}})$$

or;

$$\Delta V_{iz} = - \left[ r_i \dot{f}_i \frac{AC}{R_1 \sin \gamma_{12}} \right] Z_{t1} + \left[ r_i \dot{f}_i \frac{A}{R_2} (B + \cot \gamma_{12}) \right] Z_{t2}$$

From the above it can be seen that once a nominal trajectory is selected for rendezvous with either a circular or elliptic target orbit and the angles  $\gamma_{12}$  and  $\gamma_{2i}$  specified for making the  $Z_1$  and  $Z_2$  measurements from either a circular or elliptic waiting orbit, the  $\Delta V_{iz}$  required can readily be computed once the  $Z_{t1}$  and  $Z_{t2}$  measurements

are made.

There are numerous options available for spacing and measuring the Z displacements at the appropriate times depending on the equipment available and the degree of sophistication desired to overcome the errors in the calculations due to uncertainties in the target and waiting orbits. If radar range information is available, the Z displacement at any time can be obtained quite accurately despite orbit errors by combining the range with the out-of-plane line-of-sight angle,  $\psi$ , according to the expression:

$$Z = Rng \sin \psi$$

and if radar is not available, the expression:

$$Z = \rho \tan \psi$$

can be used where  $\rho$  is the projection of the line of sight on the waiting orbit plane. When the relative inclination of the orbits is not large,  $\rho$  can be considered equal to the expected range for a coplanar situation. Naturally, this method without radar does not correct for uncertainties in the target and interceptor orbits.

For the spacing of the  $\psi$  measurements, since the reaching of a preselected  $\beta$  angle is to be used to apply the  $\Delta V_i$  needed to initiate the intercept trajectory, it seems only logical to specify a  $\beta_1$  angle for making the  $\psi_1$  observation. Due to the uncertainties of the orbits, the central angle traversed between  $\beta_1$  and  $\beta_i$  may vary



considerably and the resultant  $\Delta V_{iz}$  computation will be in error if nominal values of  $\gamma_{12}$  and  $\gamma_{2i}$  are used. As will be explained later in Chapter 7, if a simple slide-rule-type calculation is desired, less errors result if the  $\psi_2$  angle is measured at a specified time after the  $\psi_1$  measurement rather than upon reaching a specified  $\beta_2$  angle. This is merely another way of saying that errors in  $\gamma_{2i}$  are less significant than errors in  $\gamma_{12}$ . If the equipment is available to make a more involved  $\Delta V_{iz}$  calculation, then  $\gamma_{12}$  can be treated as a variable to be determined approximately by the time interval between reading  $\beta_1$  and  $\beta_2$ . Then, since the nominal  $\beta_2$  need differ from  $\beta_1$  only by the time needed to make the calculation, errors in  $\gamma_{2i}$  will be small. The term "computation" will be henceforth applied to this more involved calculation of  $\Delta V_{iz}$ . The primary guidance analysis of this study assumes the use of both radar and computation; however, the effects of radar and no computation, no radar and computation, and no radar and no computation will be examined for selected trajectories.

A very possible alternative to this  $\Delta V_{iz}$  calculation would be to employ a nominal anticipated relative inclination and line of nodes location based on launch or ground supplied information together with the simple previously derived relation:

$$\Delta V_{iz} = r_i \dot{f}_i \frac{\sin i_t}{\sin \Delta f_i} \sin (\gamma_i + \Delta f_t)$$

where  $\gamma_i$  would be the only variable for a circular waiting orbit and uniformly dependent only upon time or angular position in orbit. For the quasi-direct ascent approach, the relative orbit plane precession due to the Earth's bulge would be small; however, ground supplied information would not be as precise for such a short time in orbit. Though the author feels that the use of a nominal  $i_t$  and location of the line of nodes may very well be preferable for the Gemini missions, in the interest of generality, the calculation method based on relative observations has been pursued exclusively. Further potentialities of this alternative will be pointed out in Chapters 9 and 10.

#### 5.5 Relative Motion for Noncoplanar Rendezvous

For convenience and uniformity, the inertial reference direction for the in-plane line-of-sight motion was taken as the direction of perigee of the intercept trajectory. In practice, any direction could be selected and the most obvious would be the in-plane line-of-sight direction at the time of the completion of the  $\Delta V_i$  application. As a reference for out-of-plane motion, the most logical one is the plane of the intercept orbit, since target motions relative to this are more easily obtained and more meaningful. This plane deviates from the original waiting orbit plane by the angle  $i_i$  which is readily obtained from the expression:

$$\sin i_i = \frac{\dot{Z}_{ii}}{r_i \dot{f}_i}$$

If the Z-axis is now oriented perpendicular to the intercept plane as shown in Fig. 5-10a with  $i_f$  being the angle of inclination of this plane with the target plane, then the following relations apply:

$$Z = R \sin i_f (\gamma_f - \gamma)$$

$$Z_i = R_i \sin i_f \sin \Delta f_t$$

$$\dot{Z}_f = R_f \dot{f}_t \sin i_f$$

Now using a plane passing through both vehicles and perpendicular to the intercept plane:

$$\tan \psi = \frac{Z}{\rho}$$

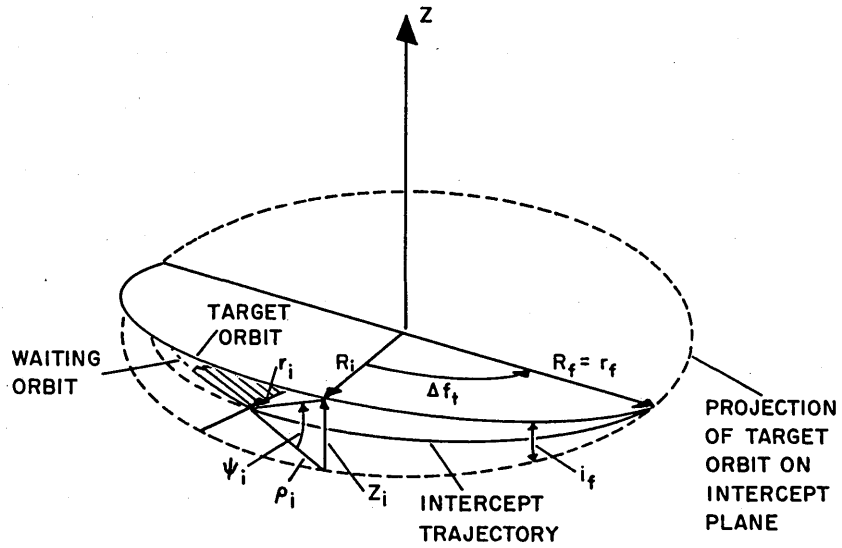
then;

$$\tan \psi_i = \frac{R_i \sin i_f \sin \Delta f_t}{\rho_i}$$

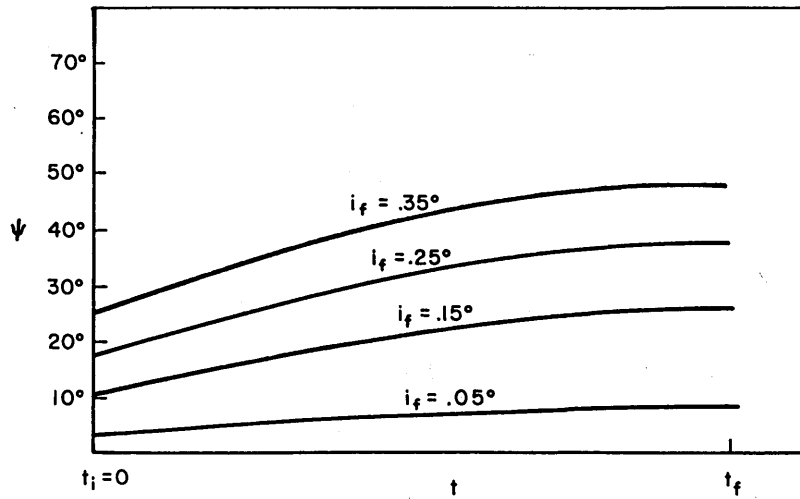
$$\tan \psi_f = \frac{-\dot{Z}_f}{-\Delta V_{fp}} = \frac{R_f \dot{f}_t \sin i_f}{\Delta V_{fp}}$$

where  $\rho$  again is the projection of the line of sight on the intercept plane and  $\Delta V_{fp}$  is the final velocity increment needed for a coplanar rendezvous. The general shape of various  $\psi$  versus time curves for various  $i_f$  for a given nominal trajectory are shown in Figure 5-10b. Rather than requiring a variety of  $\psi$  versus  $t$  curves to go with a selected nominal trajectory, the problem would be greatly simplified if a single function of time could be derived that could be easily converted to produce the desired  $\psi$  versus  $t$  for the existing  $\psi_i$  at the start of the guidance phase. If a  $\tan \psi$  versus  $t$  function were normalized by dividing by  $\tan \psi_i$ , the  $\sin i_f$  dependence would cancel out and the resulting  $\tan_N \psi$  function would vary from a value of one to  $\tan \psi_f / \tan \psi_i$ . If this normalized  $\tan_N \psi$  function was then multiplied by the tangent of the actual existing  $\psi_i$ , then the resulting  $\tan \psi$  functions would hold to the degree that the projections of the actual line of sight,  $\rho$ , on the intercept plane agree with corresponding  $\rho$  values of the intercept used to derive the normalized function. For the relative inclinations that are commensurate with realistic rendezvous capabilities, this approximation is very close. Since the solution is trivial for  $\psi_i = 0$  and the errors plus corrections increase for larger inclinations, the approximations can be made even closer by choosing an inclination, slightly less than the maximum expected, to derive the normalization curve. More will be said concerning this approximation in Chapter 7.

Again it should be emphasized that this analysis applies equally to elliptic as well as circular target orbits. While on the subject of



- a -



- b -

Fig. 5-10 Out-of-Plane Motion during Intercept Trajectories

elliptic orbits, it should be recalled from the discussion on coplanar elliptic target orbits and reference to Figure 5-7. that if the perigee of the intercept trajectory was nearly aligned with the perigee or apogee of the target then the  $\rho$  distance to the target remained in a near-direct proportion to the  $\rho$  distance to a phantom circular target and a condition of near insensitivity to errors in the radial distance  $d$  existed. After a little thought, one can conclude that when this condition is also met for noncoplanar rendezvous, the  $\psi$  variation again is nearly identical for the elliptic target and the phantom target in a circular orbit and the same insensitivity to errors in the distance  $d$  exists. (The phantom target merely has a different relative inclination.)

As a brief summary of this treatment of noncoplanar rendezvous it can be stated that for elliptic as well as circular target orbits, when the relative inclination is a few degrees or less, then the velocity change needed to shift the line of nodes to a predetermined relative point can be simply calculated based on two angular observations of the target, and the subsequent out-of-plane motion can be simply and accurately predicted.

#### 5.6 Analysis of Line of Sight Variation for Possible Intercept Trajectories

In order to study the line-of-sight variations for space vehicles in collision course orbits two programs were written for the MH800

computer at the M. I. T. Instrumentation Laboratory. Both these programs used the exact equations of motion and an iterative solution to Kepler's equation, starting from a condition of rendezvous and working back in time examining the relative positions of the two vehicles. One program was designed to examine in detail the variations for a particular trajectory and target orbit and to produce the data required for a subsequent rendezvous simulation program to be run forward in time. The other program produced in lesser detail the line-of-sight motion for a wide range of trajectories between circular orbits separated by a distance ratio  $d/r_f$  and a specified inclination  $i_f$ . In both cases the intercept trajectory was specified in terms of the rendezvous parameters  $b$  and  $k$ .

In both programs the solution to the orbital motion was embodied in a subroutine which had for inputs the position and velocity vectors in any inertial reference coordinate system, the gravitational constant and a time interval. The output of the subroutine was a new set of position and velocity vectors at the end of the time interval, in a new inertial coordinate system having its  $y$ -axis passing through one of the vehicles and the  $z$ -axis along that vehicle's angular momentum vector. In addition the original position vector of that vehicle is also given in the new coordinate system. The general principles of operation of this subroutine are given in Appendix B.

The initial position and velocity vectors of the interceptor and the target at the starting point or rendezvous point are first calculated, then, at 15-second intervals the inertial angles  $\phi$  and  $\psi$  are obtained through simple trigonometric relationships and this process is continued until the true anomaly of the interceptor becomes less than the desired initial true anomaly  $f_i$ . At this point the interceptor's orbit is circularized by changing its velocity to be that of a circular orbit at the existing radial distance. Up to this point the initial conditions for the subroutine have always been those of the rendezvous condition and the time interval has been increased by 15 sec. each time. With the interceptor in a circular waiting orbit the line-of-sight angle to the local vertical,  $\beta_i$ , as well as the velocity change angle  $\alpha_i$ ,  $\Delta V_{ip}$ ,  $\Delta f_t$  and  $\Delta f_i$  are noted and time is further incremented to obtain  $\gamma_{2i}$ ,  $\beta_2$ ,  $\rho_2$ ,  $R_2$ , and  $\gamma_{12}$ ,  $\beta_1$ ,  $\rho_1$ , and  $R_1$  at predetermined time intervals. The data consisting of discrete values of  $\phi$ ,  $\psi$  and  $\rho$  are then processed by reversing the order and subtracting  $\phi_i$  from all the  $\phi$  values so that they represent changes from the initial in-plane line-of-sight direction. The  $\psi$  values are reversed and their tangents normalized by dividing by  $\tan \psi_i$ , and the  $\rho$  values are merely reversed. All the above data is then punched on cards to serve as inputs to the rendezvous simulation and the entire program is printed out.

The trajectory spectrum analysis is similar except the radii and velocities are normalized to the circular target conditions and



The trajectory spectrum analysis is similar except the radii and velocities are normalized to the circular target condition and the time interval is considerably greater, representing 2-1/2 degrees of travel of the circular target. This program is run and adjusted to make the initial true anomaly exactly that desired and the program goes to a new trajectory after the velocity and angle needed to circularize the interceptor's orbit are noted. The velocity changes are normalized by dividing by the Hohmann transfer characteristic velocity.

Figures 5-11 to 5-17 present the  $\phi$  and  $\psi$  angles versus true anomaly for a wide range of values of  $b$  and  $k$  for a relative inclination of  $.35^\circ$  and a radius change ratio of .00695 which corresponds to transfers from 125 n. m. to 150 n. m. altitude circular orbits.

Figure 5-11 shows the Hohmann transfer and several values of  $b$  for a constant  $k = .6$ . Succeeding figures show various values of  $b$  for constant  $k$  with each figure having  $k$  larger by .1. For each value of  $k$  one line-of-sight variation is given for a trajectory that goes outside the target orbit. The value of  $b$  for these cases is always  $k - .05$ . Due to the similarities in the  $\psi$  curves only four  $\psi$  curves are shown for each value of  $k$  and these correspond to a tangential departure from the waiting orbit,  $b = .5$ , tangential arrival at the target orbit, and the outside-the-target-orbit case. It should be noted that all trajectories terminate as expected with an essentially constant

line of sight. Also it is interesting to note that all the  $\phi$  curves reach a peak indicating a change in the direction of the angular rate. The multiple intersecting trajectories consistently exhibit greater angular rates and usually a greater total angular variation, in addition obviously, to having the line-of-sight pass through the horizon.

The angles and velocities obtained by these exact methods compare generally to within one percent or to order  $d/r_f = 0.00695$  with those derived in the approximate manner by using the expressions in terms of the rendezvous parameters and neglecting terms of order  $d/r_f$  and higher.

Whereas the trajectory spectrum program was used for Figs. 5-11 to 5-17, Fig. 18 was obtained from the more detailed trajectory program and shows the  $\phi$  vs  $t$  curve and various  $\psi$  versus  $t$  curves corresponding to  $i_f$  values of  $0.5^\circ$ ,  $1.5^\circ$ ,  $2.5^\circ$ ,  $3.5^\circ$  for transfers from 125 nm to 150 nm for the standard trajectory selected as well-suited to the Gemini mission. The rendezvous parameter values for this trajectory are:

$$b = 0.2115$$

$$k = 0.8175$$

The normalized true  $\psi$  curve is also shown by the dotted line.

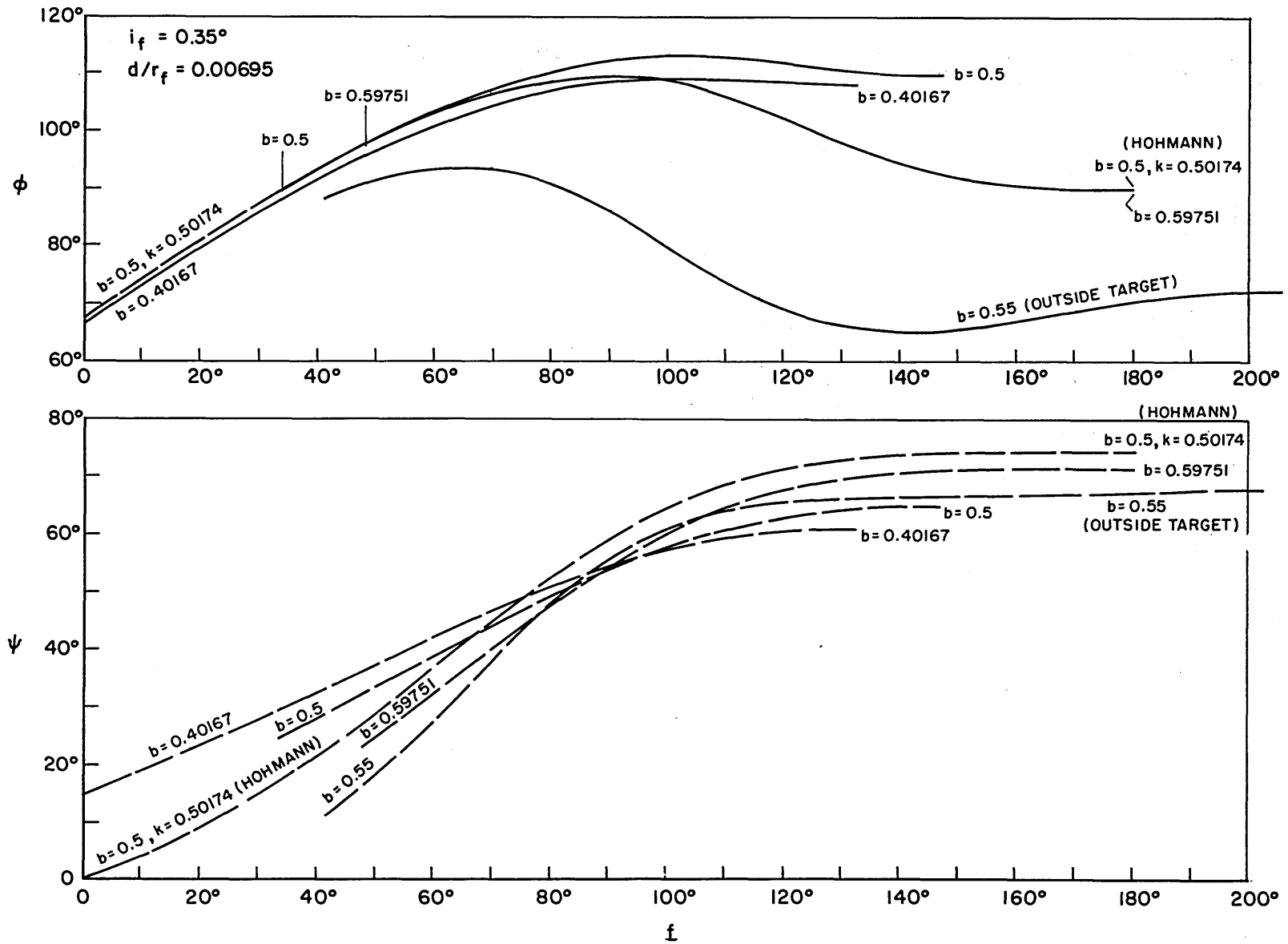


Fig. 5-11 Line-of-Sight  $\phi$  and  $\psi$  Angles for Hohmann Transfer and  $k = .6$

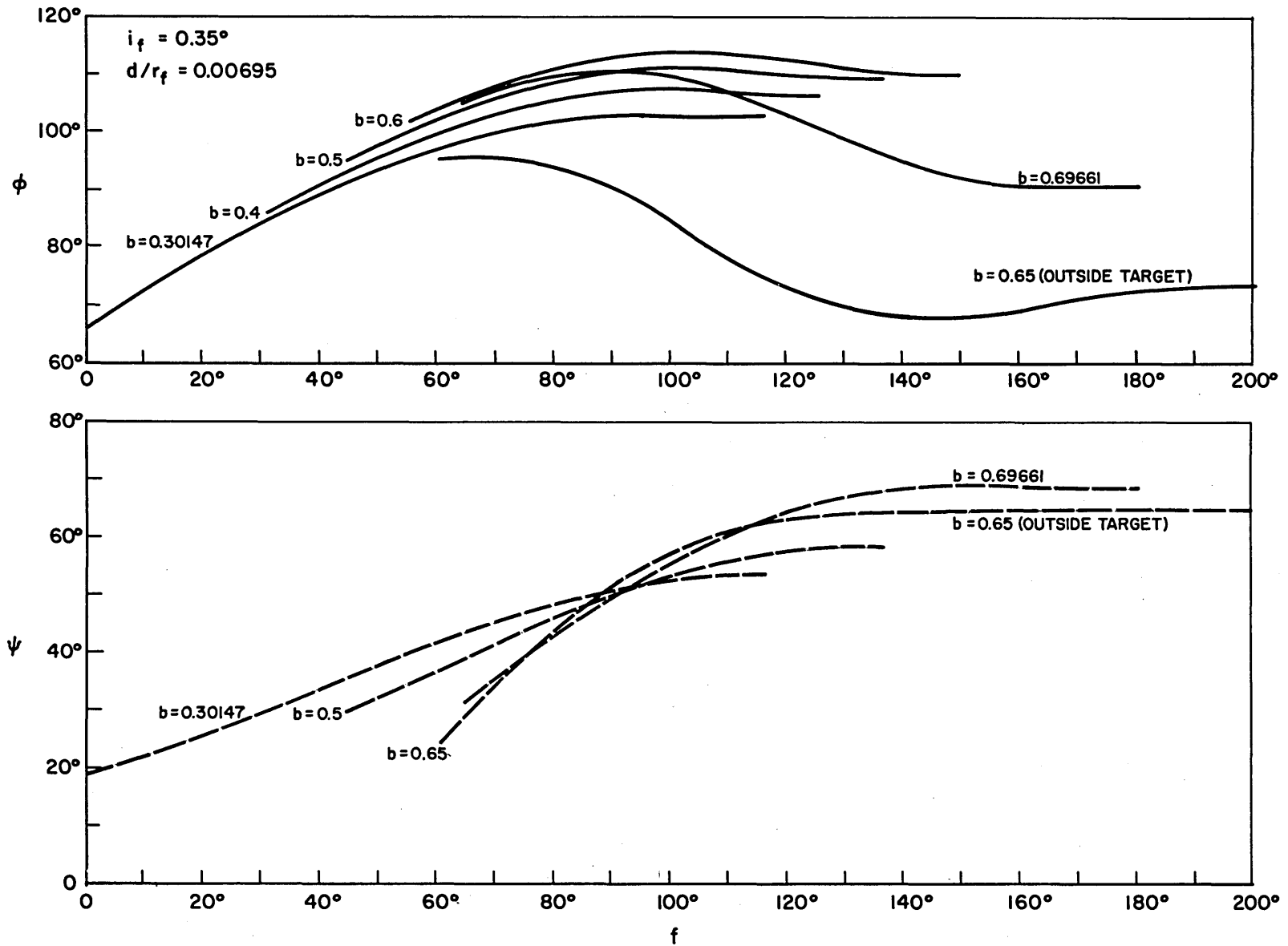


Fig. 5-12 Line-of-Sight  $\phi$  and  $\psi$  Angles for  $k = .7$

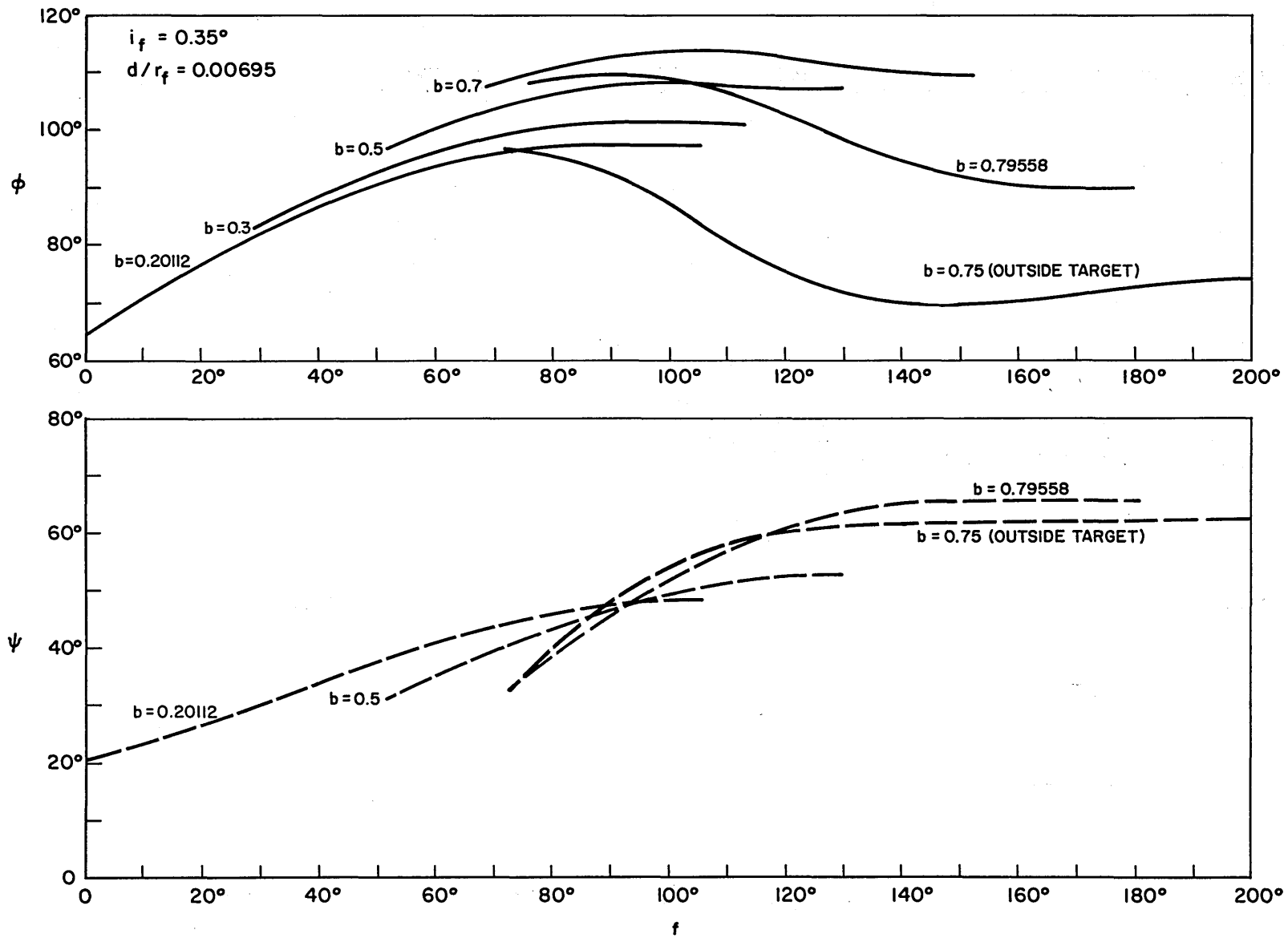


Fig. 5-13 Line-of-Sight  $\phi$  and  $\psi$  Angles for  $k = .8$

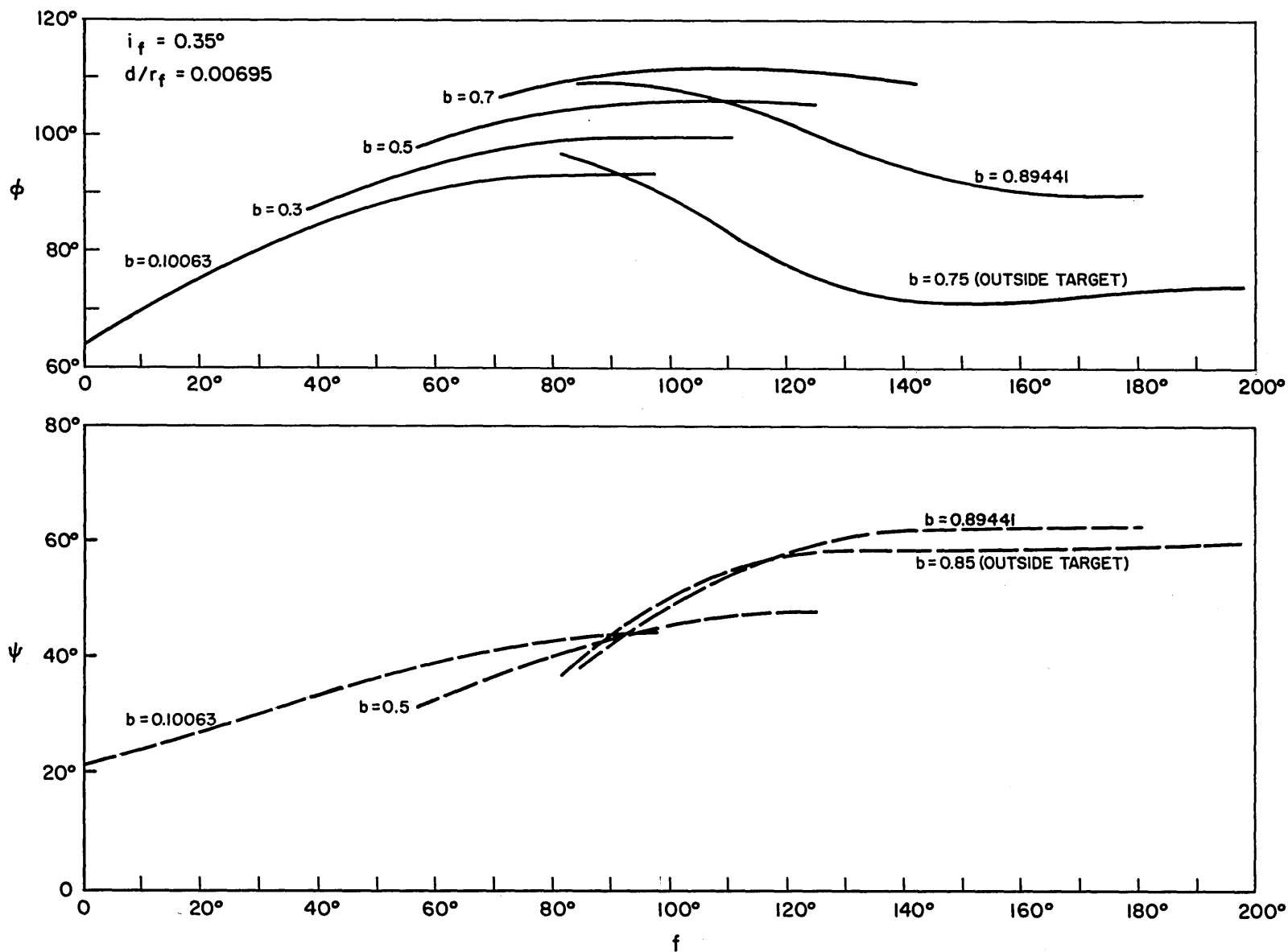


Fig. 5-14 Line-of-Sight  $\phi$  and  $\psi$  Angles for  $k = .9$

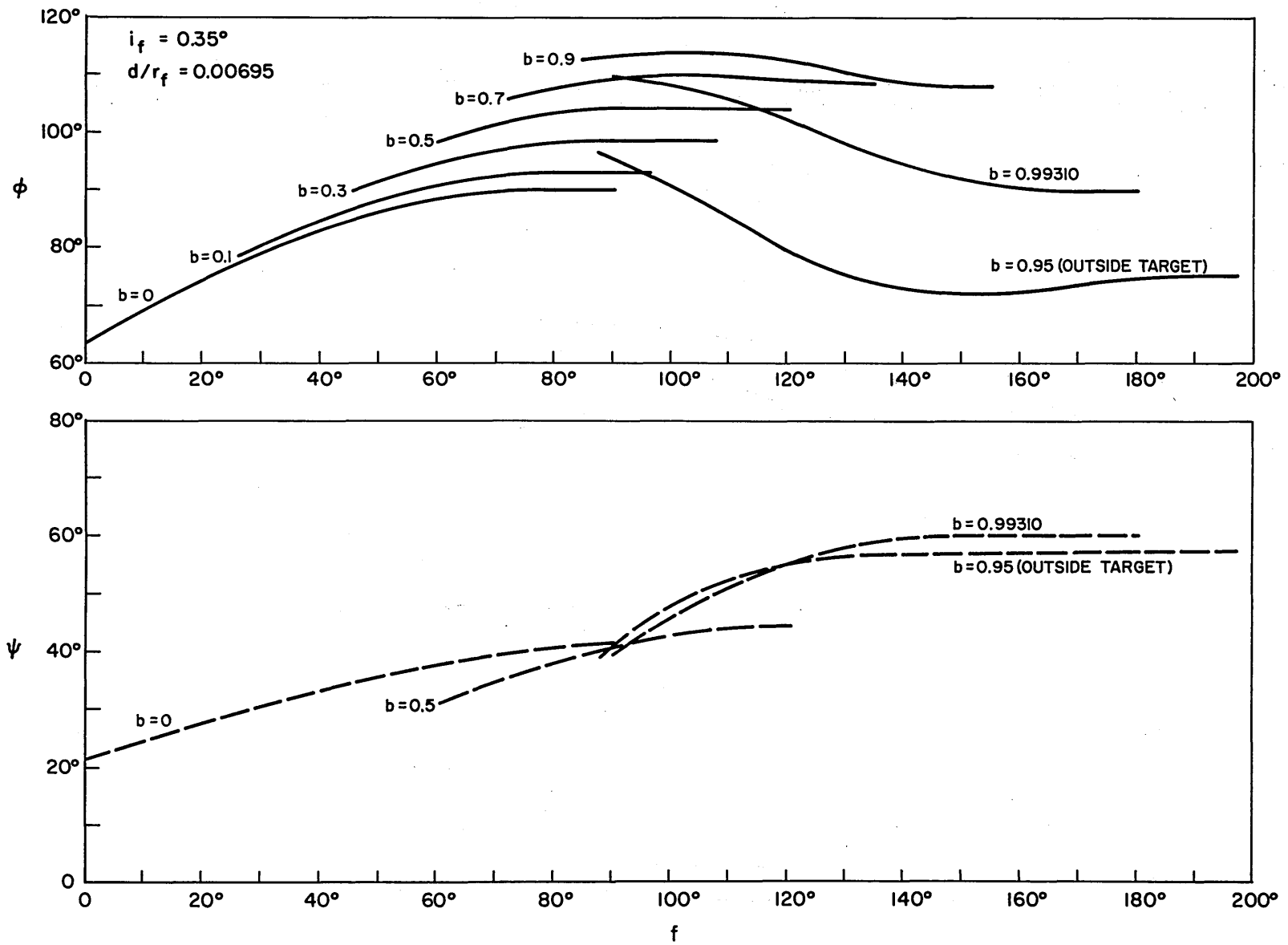


Fig. 5-15 Line-of-Sight  $\phi$  and  $\psi$  Angles for  $k = 1.0$

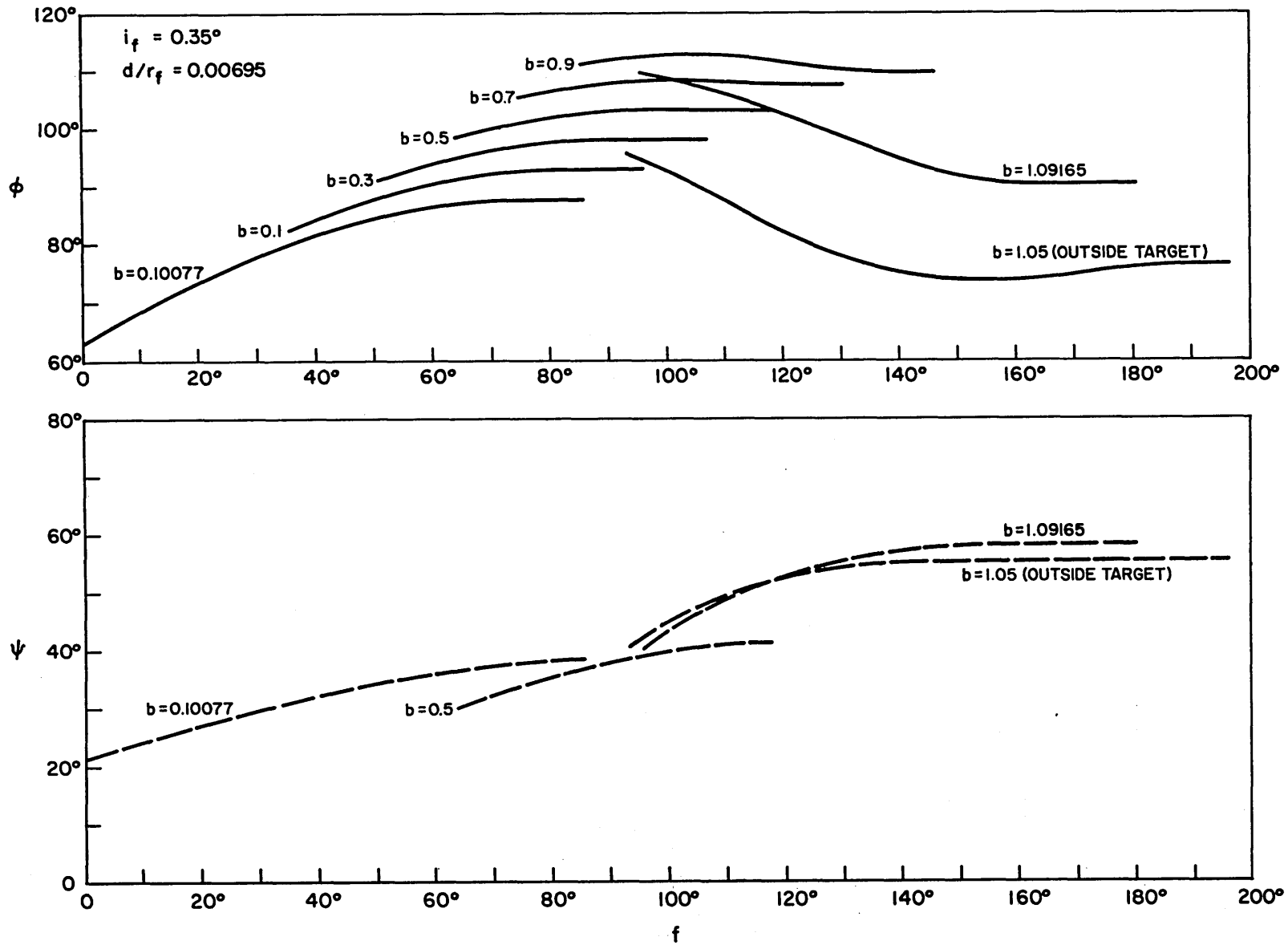


Fig. 5-16 Line-of-Sight  $\phi$  and  $\psi$  Angles for  $k = 1.1$



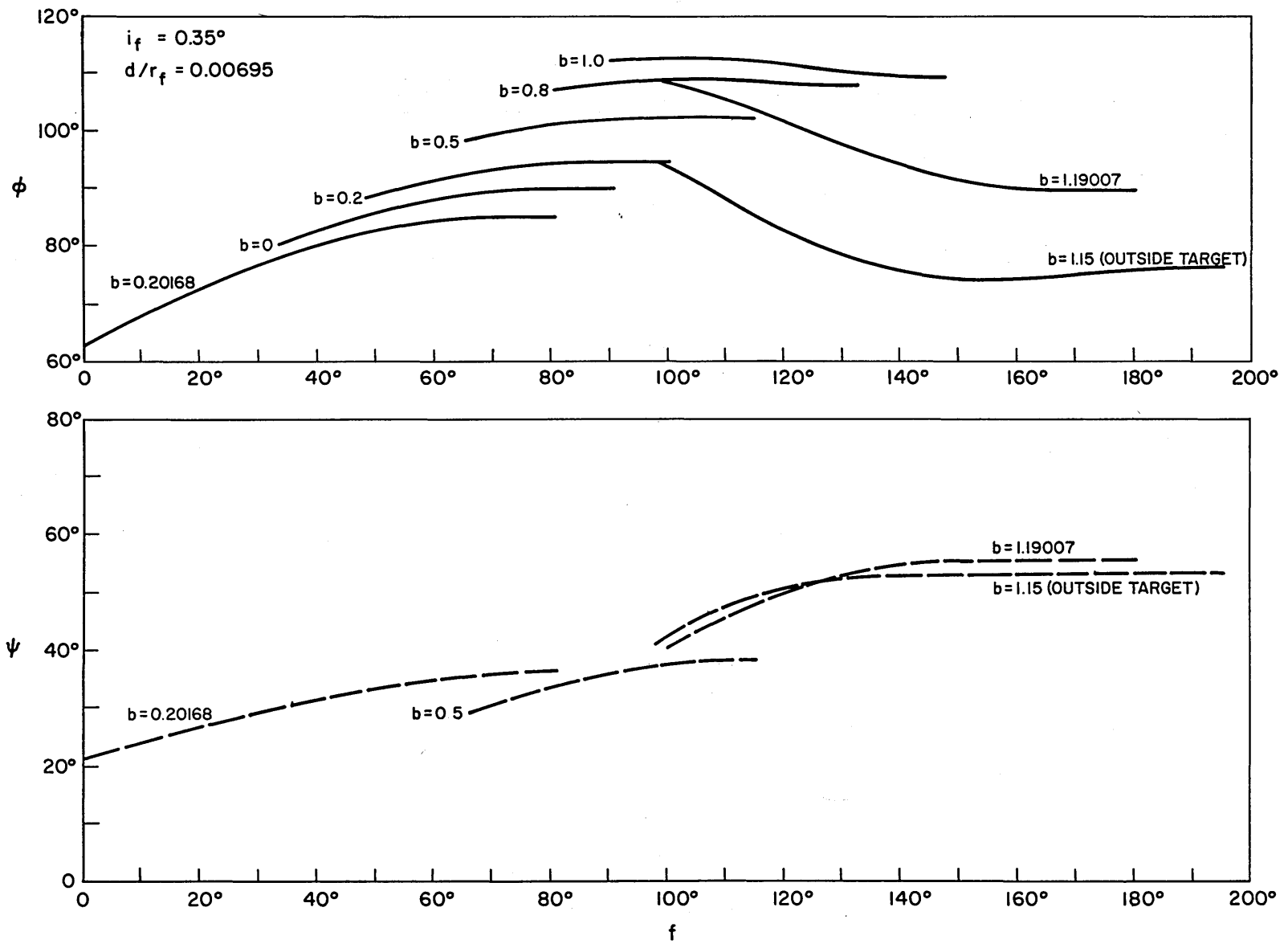


Fig. 5-17 Line-of-Sight  $\phi$  and  $\psi$  Angles for  $k = 1.2$

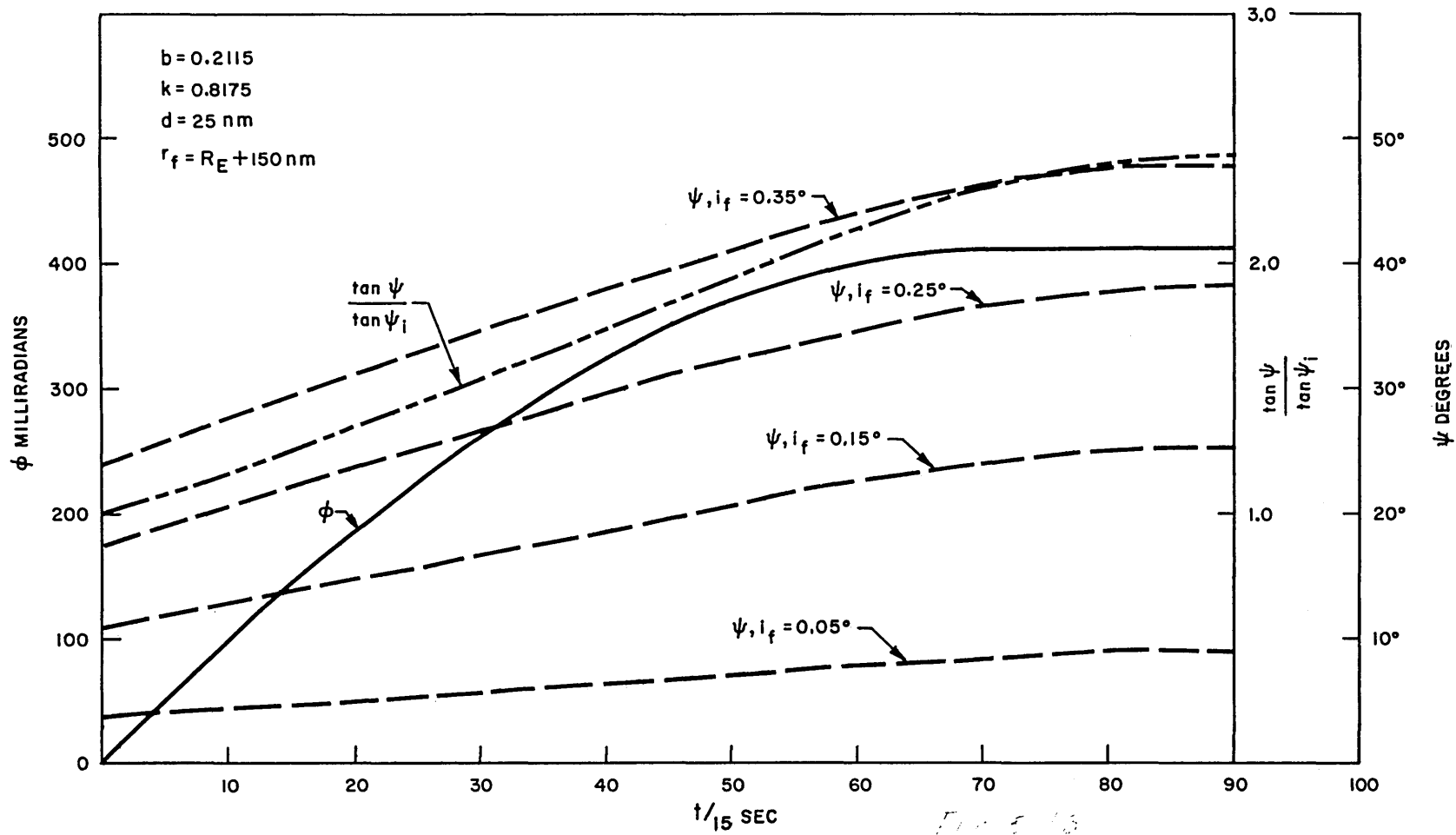


Fig. 5-18 Selected Standard Trajectory  $\phi$  vs  $t$ ,  $\psi$  vs  $t$ , and  $\tan_N \psi$  vs  $t$

### 5.7 Trajectory Selection Considerations

Since the techniques presented in this investigation are based on the simplifications derived through the use of a nominal intercept trajectory, to avoid further timing restrictions an arbitrary location of the relative line of nodes must also be accepted. If the inclination is such as to require a significant portion of the allowable velocity change capability, then two impulse transfers that traverse near  $180^\circ$  must be avoided to allow for the most unfavorable location of the line of nodes.

In the literature much attention has been devoted to determining optimum fuel transfers between exactly defined orbits but unfortunately little effort has been directed toward determining minimum fuel transfers under various guidance techniques in the face of varying uncertainties in the knowledge of the orbits and including various guidance, measurement and correction errors. Since the prime effort of the author's study is to present line-of-sight guidance techniques, the method of finding an intercept with near-minimum velocity requirements has been rather crude. Essentially, it has been to take a given maximum relative inclination and a total allowable velocity change capability and to attempt to find the combination of radius change and intercept trajectory that will allow the largest uncertainties in orbit knowledge with a given set of significant guidance errors. Then, if the orbit uncertainties closely match the maximum expected, one knows

that the selected trajectory is close to the optimum. This procedure obviously involves considerable intuition and educated guesswork and the excuse offered for this lack of precision is that the purpose is not to find the absolute optimum but merely a reasonably economical trajectory that illustrates the principles presented for line-of-sight guidance.

In addition to the desire for minimum fuel and a large tolerance to orbit errors several other factors merit consideration in trajectory selection. For a given trajectory to be suitable for an intercept maneuver the required thrust directions and magnitudes and their relations to the line of sight as well as the guidance correction techniques must be compatible with the configuration and capabilities of the interceptor vehicle. Initial ranges should not be so great as to allow insufficient time for target acquisition and observation prior to initiating the intercept maneuver. Whenever possible, the initial velocity change application should not involve the loss of visual contact with the target. Interceptor maneuvering during the guidance phase should be held to a minimum and again the target should remain in sight at all times. The line of sight should not approach the horizon where optical contact with the target might be lost. The final closing velocities should be kept as low as possible so that the braking phase may be started at closer ranges. The entire maneuver should be completed in as short a time possible to avoid, among other things,

overtaxing human powers of concentration. Although in general the guidance philosophy developed herein allows any total variation in the line of sight there may be some limits on its travel especially if, in an emergency, the stars themselves are to be used as the inertial reference. Since obviously all of the above considerations cannot be completely satisfied, a reasonable degree of compromise must be expected. This serves to emphasize the point that the entire system including a selected trajectory must be as flexible as possible as more is learned concerning the critical phases of operation.

Some general observations can be made from a brief study of the three approximate graphs of angles and velocities versus  $b$  and  $k$  and the series of exact line-of-sight variations obtained from the computer studies. For low values of  $b$  or conditions of near-tangential departure from the waiting orbit,  $\phi$  tends to increase throughout the maneuver, the final velocity increment is higher than the initial, and the initial ranges and line-of-sight angles are greater. The converse of this is true for higher values of  $b$  or conditions of near-tangential arrival at the target. For values of  $b$  near .5 the total in-plane velocity changes are lower for a given angle traversed or total time. Values of  $b$  somewhat greater than .5 result in the minimum  $\phi$  variation.  $\beta_i$  is about equal to  $\alpha_i$  when  $f_i$  is near  $15^\circ$ .

Another interesting fact is evident from the  $\phi$  versus  $f$  curves and that is that there appears to be a maximum value for  $\phi_f$ . Taking the approximate expression for  $\phi_f$ :

$$\begin{aligned}\phi_f &= f_f + \beta_f \\ &\cong f_f + \arctan\left(\frac{1}{2} \cot f_f\right)\end{aligned}$$

and differentiating to find the value of  $f_f$  for which  $\phi_f$  is a maximum, it is found that:

$$\phi_{f \max} \cong 109.5^\circ$$

for:

$$f_f \cong 144.5^\circ$$

and this appears to agree quite closely with the  $\phi$  versus  $t$  curves. This feature is somewhat misleading and its significance is still not completely understood by the author. This will be discussed further in Chapter 7.

All of the above considerations for intercept trajectory selection can be applied directly to intercepts involving elliptic target orbits especially if the coapsidal elliptic waiting orbit technique

is used. When the circular waiting orbit technique is used the appropriate transformation will permit the use of the same considerations for line-of-sight motion. However, the magnitude of  $\Delta V_{ip}$ , the angle  $\alpha_1$ , and the effective radial separation distance  $d$  must be considered as functions of target true anomaly. Section 8.17 and Figure 8-13 discuss the effects of these considerations as applied to a specific application.





## CHAPTER 6

## DERIVATION OF GUIDANCE PHILOSOPHY

6.1 Visual Orbital References

In order to make use of line-of-sight guidance techniques for effecting rendezvous, several reference directions will be needed. These are the local vertical, the plane of the orbital motion of the interceptor, and an inertial reference. The local vertical in conjunction with the plane of motion is needed to make the out-of-plane angle measurements  $\psi_1$  and  $\psi_2$  when the target reaches the appropriate in-plane  $\beta$  angles from the local vertical, and also when the target reaches the  $\beta_i$  angle to provide a reference for applying the velocity change needed to initiate the intercept trajectory. The inertial reference in conjunction with the plane of motion is needed to compare the anticipated nominal line-of-sight motion with the actual motion of the target to form a basis for the guidance corrections as derived in the succeeding sections.

The local vertical is probably best obtained through the use of horizon scanners. This indication should be as accurate as possible;

however, the usual accuracies of from  $.3^{\circ}$  to  $.5^{\circ}$  that are quoted for these devices are sufficiently adequate. The plane of orbital motion can be obtained by several means especially if a stabilized platform is available and torqued to the local vertical. As an alternative for possible back up use, the author would like to briefly describe an optical method for determining the orbital plane. Referring to Fig. 6-1a, if at any point A in orbital motion, a star is sighted along the local vertical and at some subsequent time, say  $30^{\circ}$ - $40^{\circ}$  later at point B, the same star is observed, then the star's apparent displacement with respect to the present local vertical will define the orbital plane, and its direction of motion will be opposite that of the actual motion of the interceptor. A simple telescopic star-tracking device with a field of view as shown in Fig. 6-1b would initially be sighted along the local vertical. Any easily identifiable star in the close vicinity to the local vertical would then be selected and its closest distance of passage from the center noted. At some subsequent time, say  $30^{\circ}$ - $40^{\circ}$  of orbital travel, the telescope would be positioned on the same star, offsetting it from center the same amount as the earlier noted distance. (The indexed cross-plane line would be mechanically held perpendicular to the arc travel from the local vertical.) The plane determined by the local vertical and the telescope axis would then be fed into the inertial reference system as the orbital plane. The accuracies obtainable by

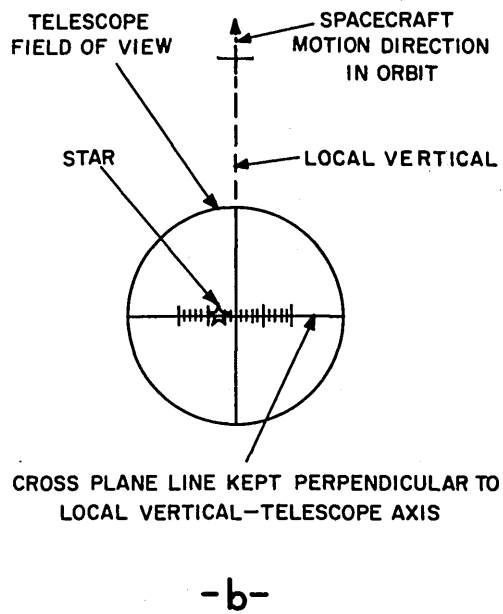
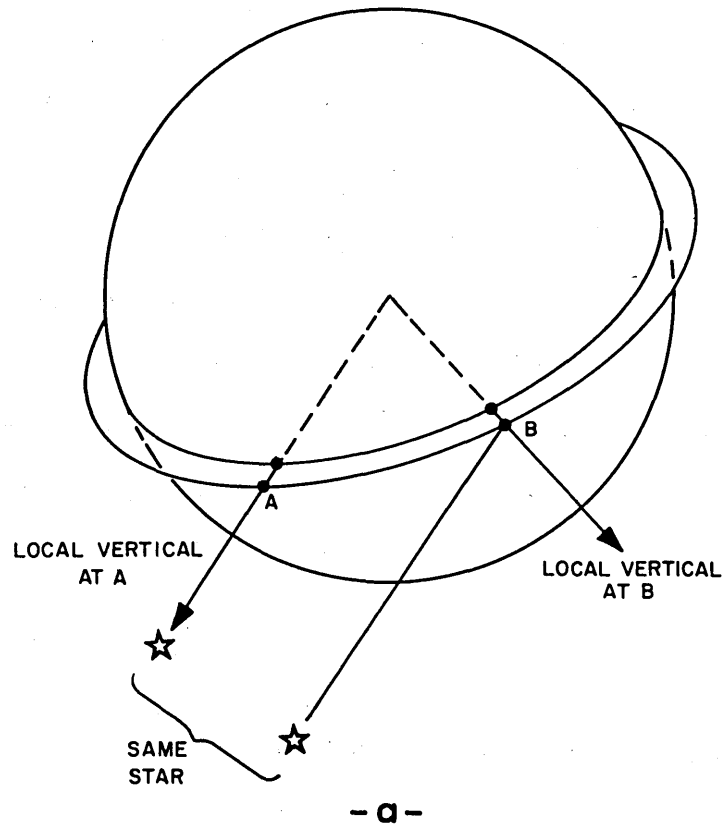


Fig. 6-1 Optical Plane-of-Orbit Determination

this method should be of the order of the accuracies of the local vertical divided by the sine of the angle between the local vertical and the telescope axis. The instrumentation required to maintain an inertial reference direction for the basis of comparing anticipated target motions with actual target motion could be obtained from many types of gyro packages. Again the author would suggest using the telescope to track bright stars as a drift correction device to the inertial package. It appears as though drift rates of around  $5^{\circ}$  per hour are reasonably tolerated by the proposed guidance technique. More will be said of this later in the discussion of the simulations, but it appears as though high precision inertial reference packages are not needed.

## 6.2 The Optical Rendezvous Sight

The purpose of the optical sight is to provide the pilot with a reticle of prescribed dimensions which when centered on the target after entering the intercept trajectory will indicate subsequent deviations of the line of sight to the target from the line-of-sight motions that should exist if the interceptor is on the selected nominal trajectory. To provide this reticle motion for the nominally selected trajectory the reticle image must be driven with respect to inertial space in accordance with the appropriate  $\phi$  vs.  $t$  and the unnormalized  $\tan \psi$  vs.  $t$  curves. Having the  $\psi$  vs.  $t$  relation for the existing out-of-plane situations in terms of  $\tan \psi$  may actually prove to be an advantage,

since mechanically obtaining  $\psi$  may well prove to be simpler knowing  $\tan \psi$  than  $\psi$  itself. The author would envision the use in practice of potentiometers rewound with the selected  $\phi$  vs.  $t$  and  $\tan_N \psi$  vs.  $t$  curves and a constant time drive. The reticle must also have a manual override which will permit the pilot to recenter the reticle on the target after making guidance corrections. Provisions should also be made for a Beta Index Marker that can be set to various in-plane angles from the local vertical. This together with a read out capability of the out-of-plane angle  $\psi$  will permit the computations of the  $\Delta V_{iz}$  quantity and the application of the velocity change required to embark on the intercept trajectory at the angle  $\beta_i$ .

The attitude of the spacecraft with respect to the inertially oriented reticle will depend on the method of applying velocity corrections from the guidance theory and the location of the thrust units of the spacecraft. As will be mentioned in the next section and in Chapter 7 it has been found advantageous to make the velocity corrections for  $\psi$  deviations perpendicular to the line of sight and velocity corrections for  $\phi$  deviations at some pitch down angle  $\alpha_p$  from the perpendicular to the line of sight. Since in the Gemini spacecraft, four thrust units are located perpendicular or transverse to the longitudinal axis of the vehicle, the correct attitude for velocity corrections would be to have the vertical axis of the spacecraft in its orbital plane

and the longitudinal axis pointed toward the target then pitched down or forward the angle  $\alpha_p$  parallel to the orbital plane. If the sight now is equipped with a vehicle fixed set of reference lines offset up an angle  $\alpha_p$  from the longitudinal axis of the vehicle, the pilot can easily maintain the proper attitude for velocity corrections by centering the vehicle fixed reference lines on the inertial reticle through the vehicle attitude control system. A schematic of the sight field of view in relation to the orbit plane, local vertical, and vehicle longitudinal axis for the early portion of a typical rendezvous is portrayed in Fig. 6-2. It should be recalled that the  $\phi$  variation of the reticle is always referenced to the initial  $\phi$  direction at the start of the intercept, i. e.,  $\phi_i = 0$ . The vehicle attitude for the initial velocity change application could easily be attained through reference to the sight by setting the Beta Index Marker to the angle  $\alpha_i - \alpha_p$ , manually positioning the reticle to the computed out-of-plane angle  $\psi = \chi$  and also aligning it over the Beta Index Marker and then centering the fixed reference lines on the reticle.

The field of view of the sight might typically encompass about  $10^\circ$  and the possible use of some low powers of magnification certainly should be thoroughly investigated. A provision to cover the possibility of inertial platform failure could be incorporated by having the copilot continually track two stars and use this as a substitute inertial reference. In Fig. 6-2, the sight field of view and attitude reference

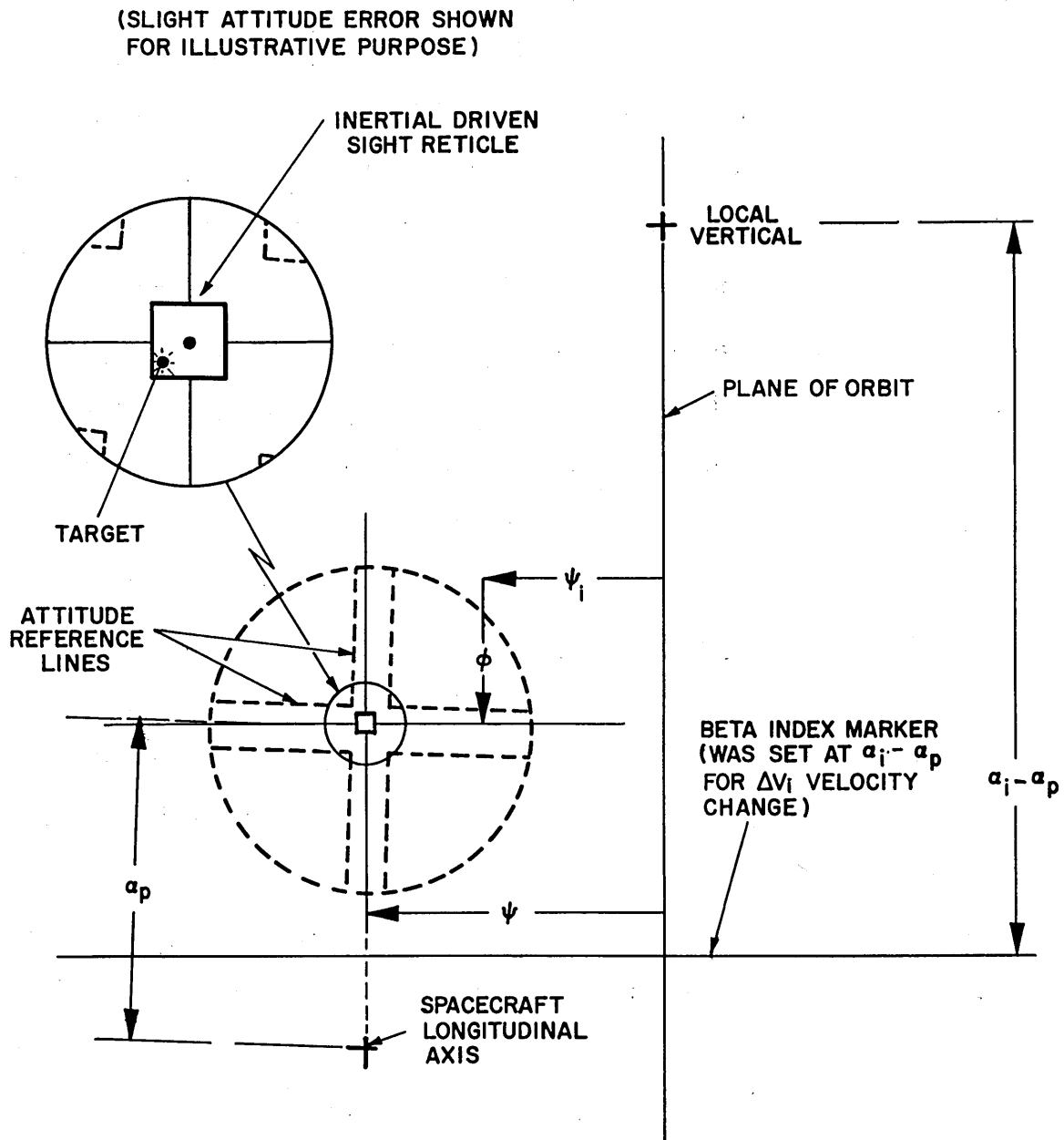


Fig. 6-2 The Optical Rendezvous Sight

image lines that are fixed to the spacecraft are shown as dotted lines, whereas the inertially referenced sight reticle images and the Beta Index Marker which would be projected into the vehicle mounted sighting device are shown in solid lines. If the  $\alpha_p$  angle is a constant, as is tentatively recommended, it is easy to see that when the vehicle attitude is correct the reticle image will always appear at a fixed position relative to the vehicle axes, thereby simplifying the projection problem. With respect to inertial space and the orbit plane the reticle should have limits of travel to at least  $70^\circ$  to either side of the orbit plane and  $30^\circ$  to  $40^\circ$  of travel in the  $\phi$  direction for intercept trajectories that are herein recommended. The purpose of the square reticle will be explained in the next section.

### 6.3 Guidance Correction Theory

The basic guidance logic proposed to control the line of sight is essentially a proportional navigational technique which can be simply stated as follows. If the angular position error of the actual line of sight in comparison with that expected for the selected nominal trajectory reaches a prescribed value, then a velocity correction will be applied with a component perpendicular to the line of sight to null out the angular rate error that exists. The amount of velocity correction needed can be arrived at essentially by two methods. Either the correction can be applied until the angular rate error becomes zero or an attempt can be made to predict the correction needed based on



previous observations. The first method would involve the closed loop ability of the pilot to detect a condition of zero relative motion between the reticle and the target, whereas the latter method would involve the use of guidance equations and some computation to arrive at the required correction. Instead of attempting to investigate both methods the author selected the prediction method as perhaps being more susceptible to a complete analysis under a digital computer simulation situation. In order to produce valid results, the first method really should be tested under conditions of actual human controller participation. It was initially felt by the author after observing and studying the results of the pilot simulation work done at the Langley Research Center (24) that the prediction method would offer better results especially in the initial phases at greater ranges. However, as will be mentioned later in Chapter 8, it is now felt that direct pilot control throughout the intercept may promise equally good or even better results and naturally with considerable simplification benefits. Unfortunately the press of time has prevented the inclusion of this promising investigation as a part of this study.

Turning now to the formulation of a set of guidance equations for the velocity correction prediction method, the general approach is to obtain a value for the average angular rate error that has existed since the sight was last aligned with the target and to make the velocity correction component perpendicular to the line of sight equal to this

value times the existing range to the target. The average rate error will be taken as the angular deviation divided by the time interval since the last correction. From a study of Fig. 6-3, where in 6-3a the interceptor is pointed directly at the target and in 6-3b where it remains aligned in its orbital plane, it can be seen that when corrections are made for in-plane deviations in  $\phi$ , the out-of-plane motion is not directly disturbed. The same holds true for out-of-plane corrections due to  $\psi$  deviations when the interceptor remains aligned with its orbital plane. When the interceptor is pointed at the target however, as in Fig. 6-3a, a cross-coupling situation exists and corrections due to  $\psi$  deviations contribute directly to the in-plane motion as the sine of the  $\psi$  angle. Initially it was thought that this cross-coupling should be avoided, however; after considerable rendezvous simulations were carried out it was realized that the cross-coupling was always beneficial and indeed good use could be made of this situation.

Now if the attitude of the vehicle is pointed at the target and pitched down an angle  $\alpha_p$  in the plane of its radius vector and the line-of-sight vector as shown in Fig. 6-3c, then cross-coupling is seen to exist now between the  $\phi$  correction and the  $\psi$  motion and though this will be shown to be adverse coupling it is of order  $\sin \chi \alpha_p$  times  $\sin \psi$  and its effect is rather small. A further explanation of these coupling effects and the reasons for the  $\chi \alpha_p$  pitch down will be given

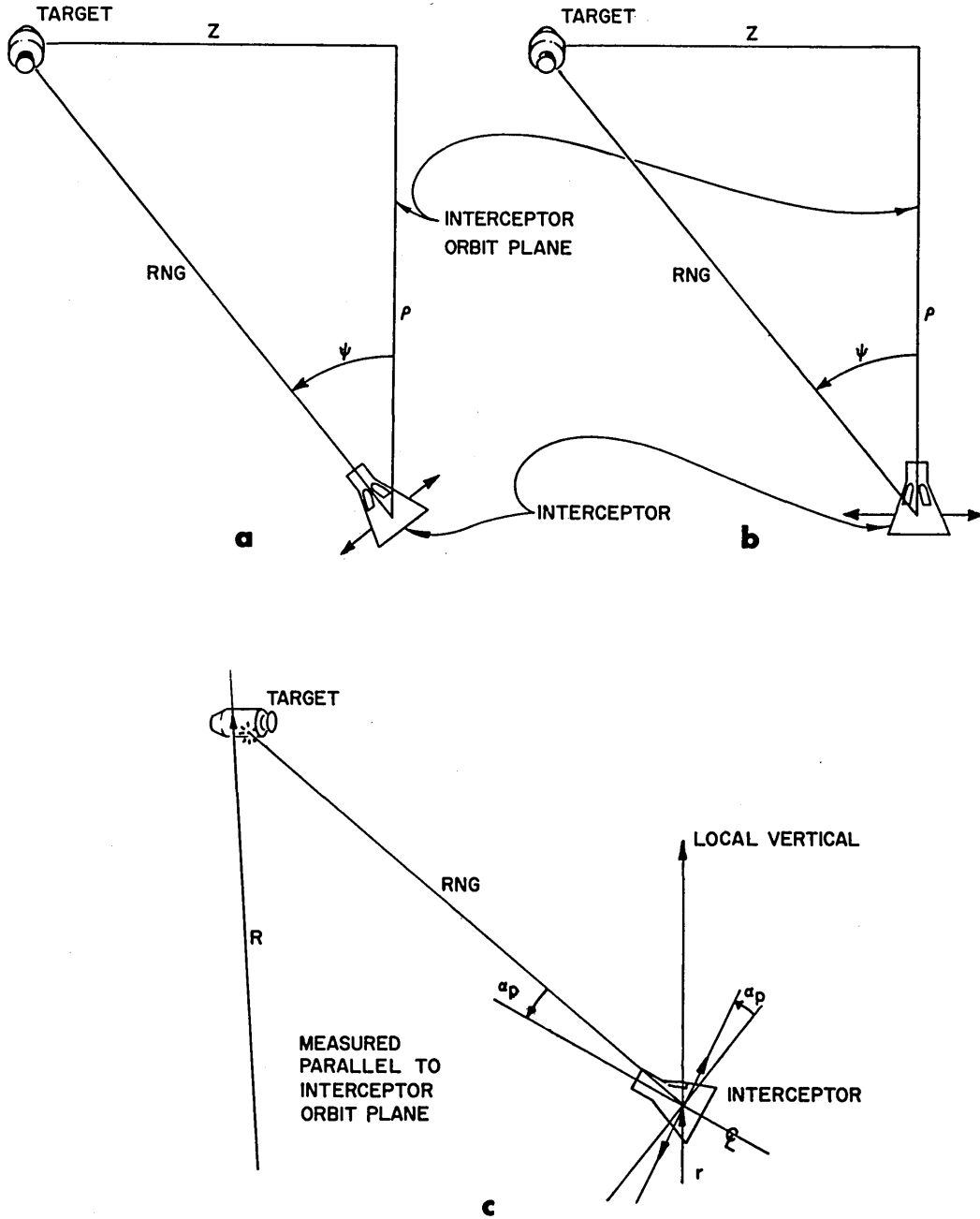


Fig. 6-3 Velocity Correction Coupling Effects

in the next chapter.

With the attitude of the vehicle pointed toward the target and pitched down the angle  $\alpha_p$  the general guidance equations for planar corrections due to  $\phi$  deviations and  $\psi$  corrections due to  $\psi$  deviations can now be written as,

$$\Delta V_{\phi} = \frac{\Delta\phi \text{ Rng}}{\Delta t \cos \alpha_p}$$

$$\Delta V_{\psi} = \frac{\Delta\psi \text{ Rng}}{\Delta t}$$

or when a square reticle is used whose sides are  $\Delta S$  radians from the center point and when corrections are made whenever the target reaches this tolerance deviation angle

$$\Delta V_{\phi} = K_{\phi} \frac{\Delta S \text{ Rng}}{\Delta t \cos \alpha_p}$$

$$\Delta V_{\psi} = K_{\psi} \frac{\Delta S \text{ Rng}}{\Delta t}$$

where  $K_{\phi}$  and  $K_{\psi}$  are the respective guidance sensitivity parameters. When radar range information is available, as is assumed in most of the rendezvous simulations, these are the guidance equations that are used.

If radar is not available, some function approximating  $\rho_{\text{nom}}/\cos \psi$  must be substituted for Rng. Instead of using the existing

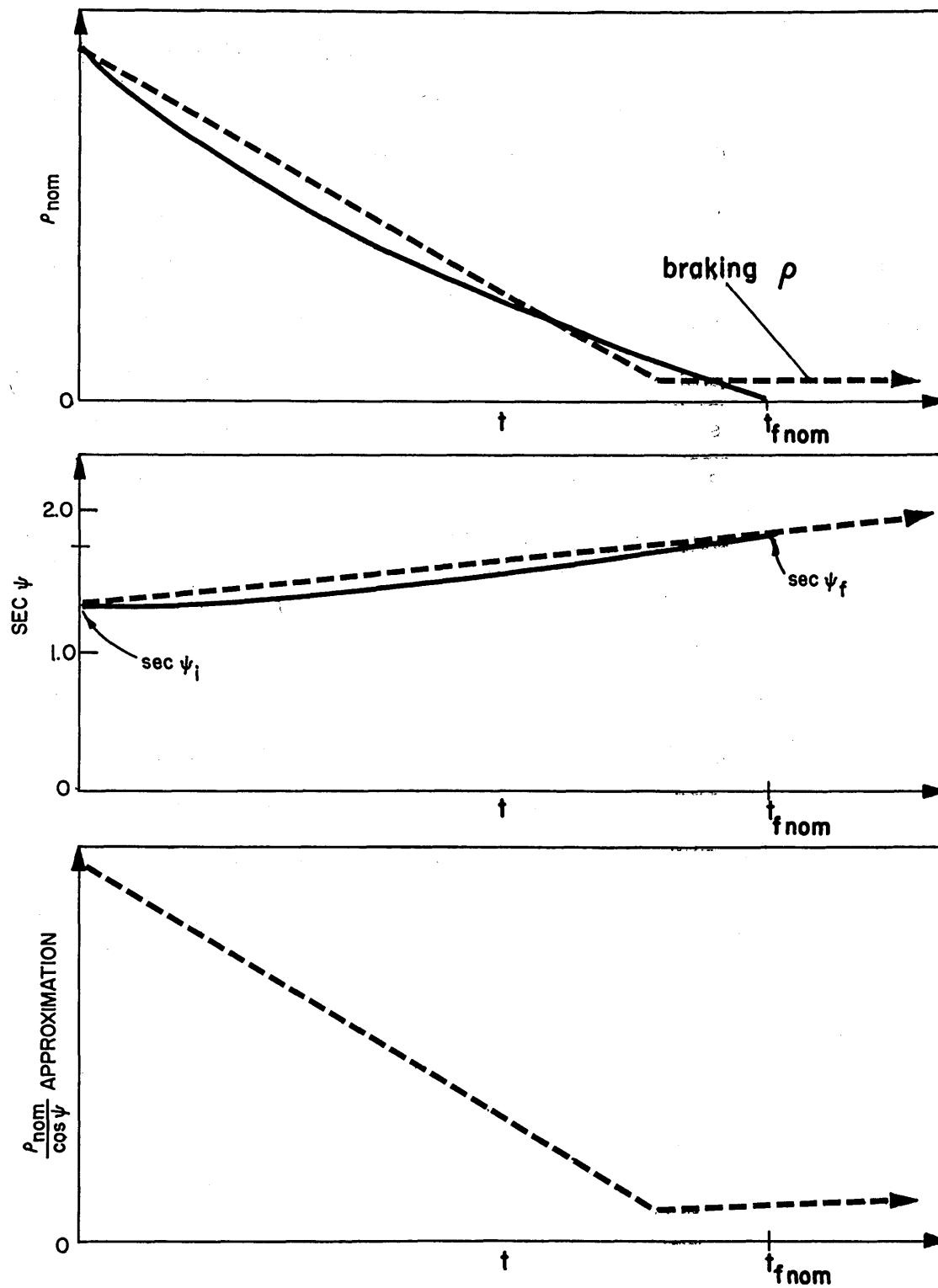


Fig. 6-4 Guidance Equation Approximation - No Radar Option

values of  $\rho_{nom}$  and  $\psi$  which would involve a rather complicated computation, linear functions of time representing the dotted lines on Fig. 6-4 were used in simulations where radar was not available. Since obviously if the intercept took longer than anticipated, a  $\rho_{nom}$  of zero would mean no velocity correction, a final value of  $\rho_b$  equal to the nominal braking range was used as the terminal time was approached. This  $\rho$  linearization is completely defined once a nominal trajectory is selected. Also  $\psi_f$  is known as a function of  $\psi_i$  for a given trajectory so that the  $\cos \psi$  approximation is readily obtainable at the start of the intercept. Both these time functions plus the divisions by  $\Delta t$  could be incorporated into a simple special purpose computer modified to give as the output, when a time mark button was pushed, the thrusting time for the required velocity correction. These approximations may seem at first a bit crude but when compared with the tested errors in initial conditions which in many cases exceed 50% errors in  $\rho$  they work quite well. One of the reasons that radar was used on most of the simulations was that in the author's opinion this gave a closer feel for the results that might be expected from a complete pilot control of the velocity correction by terminating the correction when the rate error approached zero.

These guidance equations, with or without radar, when used in conjunction with the sight reticle determination of an angular motion

error constitute in effect a variable time-of-flight navigation in contrast to a fixed time to rendezvous and do not attempt to force the interceptor onto a fixed trajectory. Instead, since after a correction in a given direction, the sight reticle is realigned with zero deviation in that direction, the result is to place the interceptor on a neighboring trajectory which will have approximately the same line-of-sight variation characteristics.





## CHAPTER 7

## RENDEZVOUS SIMULATIONS

7.1 Computer Program

The line-of-sight techniques for rendezvous that have been developed were tested by digital simulation runs on the Instrumentation Laboratory MH 800 computer. The runs were made under the assumption of a single spherical attracting body and the exact three-dimensional orbital motion of the two vehicles was determined by use of the subroutine Orbit Pos which is discussed in the appendix. The nominal trajectory input conditions consist of the discrete 15-second interval values of  $\phi$ ,  $\tan \psi$  normalized, and  $\rho$  as determined from the computer program that ran backwards in time from a rendezvous condition. In addition, the in-plane velocity change direction  $a_i$ , the velocity magnitude  $\Delta V_{ip}$ , and the various angles  $\beta_1$ ,  $\beta_2$ ,  $\beta_i$ ,  $\gamma_{12}$ ,  $\gamma_{21}$ ,  $\Delta f_i$ ,  $\Delta f_t$ , and distances  $\rho_1$ ,  $\rho_2$ ,  $R_1$ ,  $R_2$  to compute the  $\Delta V_{iz}$  and to start the intercept maneuver are also supplied as nominal values. The operating conditions fed into the program consist of the sight dimension  $\Delta S$ , the guidance sensitivities  $K_\phi$  and  $K_\psi$ , the pitch down angle  $a_p$ , the terminal braking range  $\rho_b$ , and decision parameters to indicate whether radar is assumed available

and whether the simple or slightly more involved computation technique is to be used for obtaining  $\Delta V_{iz}$ . Also included in the operating conditions are delay times for partially offsetting the impulsive velocity additions made initially and for subsequent corrections and a series of one-sigma values for interceptor measurement and action errors. These error inputs will be explained in a later section of this chapter.

The actual starting conditions for the simulation consisted of having the relative positions of the vehicles such that the  $\beta$  angle is slightly greater than  $\beta_1$  and the initial conditions consisted of the semi-major axes of the target and the interceptor waiting orbit, their respective eccentricities and true anomalies, the relative inclination of the orbital planes and the angle  $\gamma_i$  from the line of nodes. The true anomalies and the  $\gamma_i$  angle are fed in so that if the angle  $\beta_i$  occurred at exactly the angle  $\gamma_{12} + \gamma_{2i}$  after the starting point,  $f_i$ ,  $f_{it}$ , and  $\gamma_i$  would be as read in. In other words the sum of  $\gamma_{12}$  plus  $\gamma_{2i}$  is subtracted from  $f_i$ ,  $f_{it}$ , and  $\gamma_i$  to produce the actual starting conditions.

Once the inertial positions and velocities of the two vehicles are obtained through standard orbital equations and trigonometric relations, their relative positions and angles as seen from the interceptor are recorded at 15-second intervals in their orbits.  $\psi_1$  is noted when  $\beta$  first becomes less than  $\beta_1$ . The observation of  $\psi_2$  depends on which type of computation option is to be used. For the simple slide-rule-type  $\Delta V_{iz}$  calculation  $\psi_2$  is noted when the time

interval indicates that the target should have nominally traversed the angle  $\psi_{12}$ . For the more involved computation option,  $\psi_2$  is noted when  $\beta$  first becomes less than  $\beta_2$  and the time interval from the  $\psi_1$  observation is used to obtain a new value of  $\psi_{12}$  to be used in the  $\Delta V_{iz}$  computation. Either of these options can be used with radar in which case the range at the time of the  $\psi_1$  and  $\psi_2$  observations are also noted. If radar is not available, the appropriate  $\rho_{nom}$  values for the nominal target and waiting orbits are used instead. Whatever the option selected, the computation is made as outlined in Section 5.4 and, when  $\beta$  is less than  $\beta_i$ , the combined velocity change is added to the interceptor after the appropriate time delay interval.

After applying this initial velocity change, at subsequent 15-second intervals the inertial line-of-sight variation is compared with the stored discrete values for  $\phi$  and  $\psi$ , the latter having been processed from the  $\tan \psi$  normal values through multiplication by  $\tan \psi_i$  and converted to angular values. Whenever the comparison yields a difference greater than  $\Delta S$  then the appropriate guidance equation is utilized to obtain the velocity correction. After this correction is made following the appropriate delay time, the cumulative angular error is set to zero in the direction for which the correction was made. This process is continued and a complete set of target deviations, angles,  $\rho$  values and velocity corrections are printed out for each 15-second interval. The simulation ends when the existing  $\rho$  value is less than the nominal braking  $\rho_b$ . At this time the closing velocity, the velocity perpendicular to the line of sight, the relative

velocity, the total velocity changes added to the interceptor including the final relative velocity and the total number of in-plane and out-of-plane corrections are obtained and printed out. The program then reads in the next set of initial conditions and proceeds as before.

## 7.2 Summary of Various Approaches

In addition to the standard single intersecting, nominal, two-impulse intercepts between nominally circular orbits many simulations have been conducted for:

- (1) Rendezvous situations in which the target applies the initial velocity change and the interceptor then makes all the subsequent corrections
- (2) Nominal three-impulse maneuvers where the relative line of nodes is shifted to cross prior to the in-plane rendezvous.
- (3) Long time multiple intersecting intercepts in which the interceptor goes outside the target orbit and traverses about  $270^{\circ}$  prior to final rendezvous.
- (4) Nominally elliptic target orbits with the interceptor departing a nominally circular waiting orbit and using the same line-of-sight variation regardless of the target true anomaly at the start of the maneuver
- (5) Nominally elliptic target orbits with the interceptor departing a nominally coapsidal elliptic waiting orbit

of near-constant radial separation from the target orbit and using the identical trajectory input conditions as if the rendezvous was to be accomplished between two nominally circular orbits.

Initially it was felt that with the rather limited maneuver capability of the Gemini spacecraft, a good way to utilize line-of-sight guidance techniques and still allow for significant uncertainties in the initial target and spacecraft orbits would be to command the target to apply the initial velocity change to depart its circular orbit so as to intersect the spacecraft's circular orbit. Subsequent corrections and the braking maneuver would then be executed using the spacecraft's maneuver fuel. Though this concept proved to be quite satisfactory it was subsequently rejected as too specialized a maneuver when changes in the guidance concept and trajectory selection indicated that the spacecraft alone was capable of accomplishing the rendezvous even in the face of appreciable orbit errors. The significant lesson learned in this investigation was that with a given set of initial condition errors, whether the target departed its orbit on an intercept trajectory or the interceptor did all the maneuvering made little difference in the relative motion, and the timing and magnitude of correction needed was essentially identical. Hence it appears that if required for some specialized mission, these line-of-sight guidance techniques could be applied with either vehicle doing the tracking and likewise, either vehicle doing the correcting maneuvers.

Next, three-impulse maneuvers were investigated as a possible solution to the apparent field of view problem. If, as was originally thought by the author, coupled corrections were to be avoided at all costs, then depending on the relative inclinations, as the vehicles approach rendezvous, the target may be more than  $60^\circ$  to the side of the spacecraft's longitudinal axis. This impractical situation could be avoided by the three-impulse maneuver described in Section 5.4. For a nominal in-plane trajectory and arbitrary  $\gamma_1$ , a little reflection produces the conclusion that for minimum fuel usage the angle from intercept initiation to the new nodal crossing should be not much less than  $90^\circ$ . This means that considering the Z thrusting times needed to adapt the interceptor to the target's plane at the nodal crossing, the accuracies in relocating the line of nodes and the time needed for the braking maneuver, the overall intercept should be planned for at least  $120^\circ$ . Many simulations were conducted for various intercept trajectories using this three-impulse technique. Even though  $\psi$  guidance control was not needed until after the nodal crossing, the total velocity changes needed for given initial orbit errors were considerably higher than for the nominal two-impulse maneuvers. One of the major reasons for this was that the low acceleration levels of the spacecraft required longer time maneuvers with a higher final true anomaly at rendezvous and as will be seen later, in general, the closer  $f_f$  is to  $180^\circ$  the more sensitive is the intercept to orbit errors. When it was

finally realized that the coupled  $\psi$  corrections that resulted from pointing the interceptor at the target were beneficial, no further investigations of three-impulse maneuvers were made.

Several simulations were made for intercept trajectories that traversed about  $270^\circ$  to establish the validity of the line-of-sight techniques over extended periods of time. Though these maneuvers were impractical from an optical standpoint, in that the target passed through the horizon at ranges of 30 to 60 nm and the rendezvous terminated with the Earth in the background of the target, they nonetheless demonstrated that line-of-sight techniques could be applied to longer duration multiple intersecting intercepts. In general, the velocity change requirements for initial orbit errors were somewhat higher than for the shorter single intersecting intercepts; yet, the author feels that through better optimization of the pitch angle,  $\alpha_p$ , perhaps by making it variable instead of a constant, these types of long duration missions could be made almost as economical as the shorter intercepts. Optical properties, however, would continue to argue against such maneuvers.

In all the rendezvous simulations made with nominally elliptic target orbits the general conclusion reached is that even if the ellipticity is small in comparison with the distance  $d$ , it is better to adapt the interceptor waiting orbit to be elliptical and coapsidal with the target and then execute a complete nominal intercept as if the two orbits were

circular, than it is to have the interceptor in a circular waiting orbit where the initial velocity magnitude and direction and the final velocity magnitude are functions of the target true anomaly. Both of these approaches would use a fixed set of  $\phi$  and  $\tan_N \psi$  curves and initiate the intercept at a given  $\beta_i$  angle. Both of these techniques for handling elliptic targets will be compared in detail and simulation results presented in Chapter 8. Since the recommended procedure for rendezvous with an elliptic target orbit employs line-of-sight motion and velocity changes that are essentially identical with the treatment for circular targets, complete analysis of the latter can be interpreted as applying to any and all practical rendezvous situations. This extension will also be more fully understood following the treatment of elliptic target orbits in Chapter 8.

### 7.3 Preliminary Conclusions Obtained from Simulations

After completing many rendezvous simulations for various types of rendezvous situations, several line-of-sight guidance technique characteristics became apparent which indicated strengths and weaknesses in the original concept and suggested some of the modifications which have already been mentioned briefly.

In one instance, a program error caused the direction of the  $\Delta V_{iz}$  component to be reversed. The  $\psi$  guidance control naturally detected this immediately and in two correction applications the error was rectified. The fuel penalty for this error was only slightly greater than twice the magnitude of the  $\Delta V_{iz}$  component indicating



that the error was essentially nulled and the correct amount of velocity change applied before the error had much effect. In another instance, the first data card for the nominal  $\phi$  values was in error giving rise to grossly incorrect velocity changes in the first six 15-second intervals. Again, once the correct  $\phi$  values were available, the errors were immediately rectified by compensating velocity changes. In general the closed loop guidance afforded by the continuous monitoring of the line-of-sight motion is quite tight and quick to detect and compensate errors. In fact, the author has even considered but not investigated the possibility of completely doing away with the initial velocity application and its associated computation. This possibility would perhaps be better handled in a direct pilot controlled simulator where the pilot thrusts in a specified direction until the relative rate of motion of the target and the sight become zero.

Second to the overall close control afforded by the basic guidance concept, was the next important conclusion concerning the desirable final true anomaly of the intercept trajectory. Even before conducting simulations, the author had a strong feeling that an  $f_f$  of  $180^\circ$  or a tangential arrival at the target was undesirable from an error standpoint for the simple reason that if for some reason insufficient velocity was imparted initially, the interceptor would fall short of reaching the radial distance of the target. It was felt that line-of-sight guidance, or for that matter any guidance scheme, might not note this soon

enough. Certainly corrections near perpendicular to the line of sight as the interceptor was falling short would be rather ineffective. The author at first attempted to attach some beneficial significance to the situation described at the end of Section 5.7 concerning the existence of an apparent  $\phi_f$  maximum by the argument that neighboring intercept trajectories on either side of a nominal which had a  $\phi_f$  maximum would result in small line-of-sight deviations and hence small corrections. It appears that the argument is essentially correct but the results of it should be interpreted as being not at all beneficial. The fact of the matter is that the most fuel savings are realized when the final rendezvous occurs as close as possible to the selected angle. If it has a tendency to occur later then the possibility of falling short exists and if it occurs earlier, then the final relative velocities increase considerably. Hence the condition of an  $f_f$  of near  $144^\circ$  for a near  $\phi_f$  maximum is actually least sensitive to controlling the point of rendezvous. Since an  $f_f$  of between  $144^\circ$  and  $180^\circ$  would still be susceptible to the falling short condition, the best  $f_f$  must be somewhat less than  $144^\circ$ . This essentially boils down to saying that the higher the angle of intersection of the two orbits the more positive will be the control of the intersection point. Obviously the lower  $f_f$  is the higher the in-plane characteristic velocity is and the greater are the initial ranges. Clearly some compromise is needed and if the out-of-plane considerations are significant then the total angle traversed should be near  $90^\circ$ .

as reasoned earlier. A trajectory that seems to be about the best all around is the one selected of  $b = 0.2115$ ,  $k = 0.8175$  which has an  $f_f$  of about  $105^\circ$  and  $f_i$  of about  $15^\circ$ .

The next conclusion reached from the preliminary simulations revealed the beneficial aspects of the  $\psi$ -coupled corrections that resulted if the spacecraft remained oriented to point toward the target and made  $\psi$  corrections perpendicular to the line of sight. To see this more clearly the reader is referred to Fig. 6-3a. Consider a hypothetical rendezvous where the  $\Delta V_{iz}$  is correct to cause the line of nodes to occur at the preselected angle but the initial orbit eccentricities are such as to cause the in-plane rendezvous to have a tendency to occur late. As the maneuver progresses,  $\rho$  will have a tendency to be greater than it should be resulting in a  $\psi$  rotation to the right of the nominal motion. This will call for a  $\psi$  correction which has a coupled component to decrease  $\rho$  and cause the rendezvous to occur sooner. The reverse condition is also beneficial in that if the in-plane motion is as it should be but the line of nodes has a late tendency, then the larger Z value results in a  $\psi$  rotation to the left of the nominal motion. This will call for a correction which has a coupled component to delay the rendezvous thus avoiding the tendency for more  $\psi$  corrections. It is easy to see that, if the coupled components were in the opposite direction, unstable tendencies would be present. The tracking simplifications and field-of-view sight considerations, brought

about by continually orienting the spacecraft toward the target, completely eliminate the necessity to resort to three-impulse maneuvers and eliminate any transition point from line-of-sight control to the braking maneuver.

Whereas  $\psi$  corrections appear to be more practical and efficient when applied perpendicular to the line of sight, such is not the case in general for  $\phi$  corrections. In the original rendezvous simulations that traversed about  $90^\circ$ , considerable benefit was derived by applying the first  $\phi$  correction (if it occurred within about 2 minutes) in a near-vertical direction with the component perpendicular to the line of sight as determined by the guidance equation. The reasoning behind this was that the most efficient velocity correction to change the orbital radius  $90^\circ$  later was in the vertical direction. It was later observed that a tendency to rendezvous late resulted in corrections for negative  $\phi$  deviations and a tendency to rendezvous early resulted in positive  $\phi$  deviations. This immediately suggested that if negative  $\phi$  corrections were pitched forward from the top of the spacecraft, compensating benefits would be derived. The same rotation of the correction direction with respect to the line of sight would also compensate for positive  $\phi$  corrections. The effect would be to add or subtract velocity components along the line of sight according to the observed tendency to rendezvous late or early respectively.

A more analytical determination of the appropriate pitch angle

$a_p$  can be derived by an approach similar to a differential correction analysis. To carry out this analysis assume that at the instant of applying the initial velocity correction to embark on the intercept trajectory the waiting orbit has superimposed on it an error eccentricity. The initial velocity change adapted the circular portion of the waiting orbit onto the desired trajectory, now an additional velocity change must be found to adapt the error eccentricity onto the desired trajectory. This will be derived by first converting the error eccentricity into a circular velocity at the radial distance corresponding to the error true anomaly  $f_\epsilon$  and then adapting this onto the desired trajectory. Figure 7-1 depicts a planar view centered on the interceptor with the local vertical at the top and the direction of the line of sight to the target and the initial velocity change direction as indicated. The intercept trajectory with  $b = 0.2115$  and  $k = 0.8175$  has been found to be well-suited to the proposed line-of-sight guidance techniques. The dotted line 2 by 1 ellipse represents the locus of velocity vectors from the center needed to circularize an error eccentricity for a given  $f_\epsilon$ . Note that this has been normalized to unity for an  $f_\epsilon$  of  $90^\circ$  and  $270^\circ$ . Now, to convert a given circular velocity to the desired intercept trajectory, a velocity change is needed in the direction of nominal  $\Delta V_{ip}$  proportional to the radial eccentricity error divided by the nominal distance  $d$ . For the normalized  $\Delta V$  error of the dotted ellipse this can be shown to be very nearly equal to  $\cos f_\epsilon \Delta V_{ip} / 2 \Delta V_H$ .

In Fig. 7-1 examples of the sum of velocity corrections needed for an  $f_{\epsilon}$  of  $0^{\circ}$  and  $180^{\circ}$  are given. (For this trajectory  $\Delta V_{ip}/\Delta V_H = 0.9$  from Fig. 5-4.) Note that for an  $f_{\epsilon}$  of  $90^{\circ}$  or  $270^{\circ}$  the radial error is zero and only the circularizing velocity component is needed. When this process is carried out for other values of  $f_{\epsilon}$  the locus of velocity vectors from the center forms the solid line envelope. This now gives a good indication of the direction in which velocity corrections should be made initially to counteract eccentricity errors in the waiting orbit. Target orbit eccentricity errors will be subsequently seen to be transferable to the waiting orbit with a  $180^{\circ}$  phase shift in the true anomaly. Semi-major axis errors in the waiting orbit or for that matter the target orbit require proportional corrections simply along the direction of the initial velocity change.

Now the same line of reasoning can be applied to subsequent points along the intercept trajectory by assuming that the actual trajectory that the interceptor is on consists of a desired trajectory plus an error eccentricity and a semi-major axis error. However, the velocity change direction and magnitude needed here to replace  $\Delta V_{ip}$  is that required to depart a circular orbit onto the remainder of the nominal trajectory. These quantities may be calculated by obtaining a new set of rendezvous parameters  $b'$  and  $k'$ . These can readily be calculated by recalling that:

$$\frac{b'}{k'} = \frac{b}{k} = -\cos f_f$$

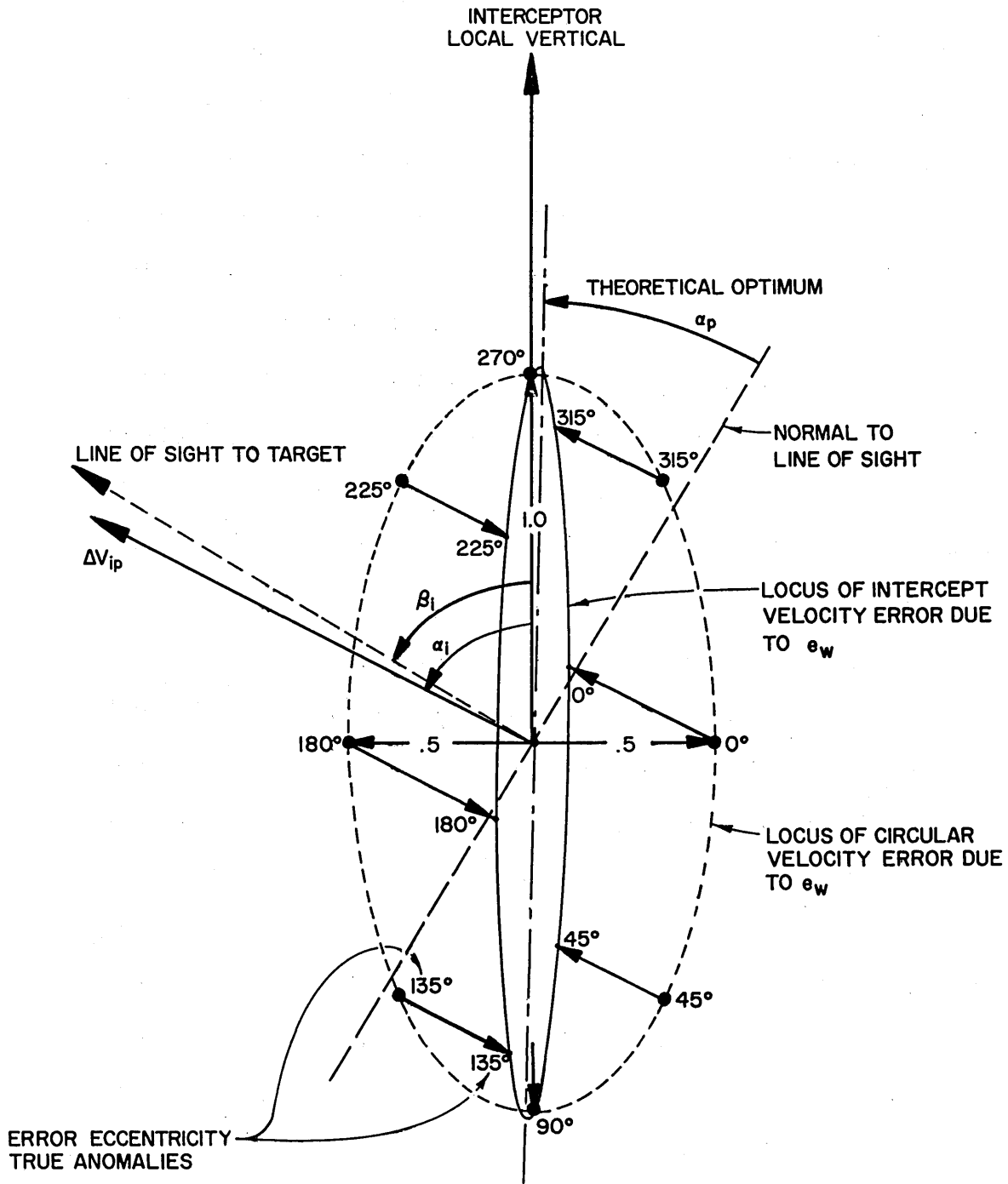


Fig. 7-1 Analytical Determination of Initial Pitch Down Angle  $\alpha_p$

$$k' = \frac{1}{\cos f_i - \cos f_f}$$

Figure 7-2 is a similar diagram for the same intercept trajectory but at a true anomaly of  $60^\circ$  or about half way through the maneuver. The validity of applying this approach much past the initial stages seems somewhat open to question since the relative positions of the two vehicles as indicated by the  $\beta$  angle would no longer be exactly correct. In addition, the goal is not necessarily to stay on a given trajectory but rather to adapt to a neighboring one with hopefully similar line-of-sight variations. Further, no consideration is given in this analysis toward minimizing the total velocity changes including the final relative velocity. It is rather evident that in the terminal stages this analysis would call for corrections very nearly along the line of sight. Simulation experience does indicate that some  $\alpha_p$  angle is beneficial throughout the intercept. Limiting considerations to a constant angle, for this intercept trajectory an  $\alpha_p$  of about  $20^\circ$  has been found to be best. It is not too surprising that this is less than even the  $\alpha_p$  that might be indicated from Fig. 7-1 when consideration is given to the slight cross-coupling effects plus the obvious fact that the greater  $\alpha_p$  is the greater will be the magnitude of each  $\phi$  correction.

One final preliminary conclusion from the initial simulations seems well worthy of mention at this point. It concerns the possible





benefits that might be derived by the use of a radar range determination at the arrival of  $\beta_i$  to modify the magnitude of the in-plane velocity change  $\Delta V_{ip}$ . It has been found that if the waiting orbit errors consist only of eccentricity errors, the true anomalies at the start of the intercept that produce higher closing velocities and greater total velocity requirements are those in the vicinity of  $0^\circ$  and conversely the true anomalies that produce tendencies to fall short or rendezvous late are in the vicinity of  $180^\circ$ . Now if through the use of radar range at  $\beta_i$  the increased range in the former case or decreased range in the latter case were interpreted as a semi-major axis errors and the  $\Delta V_{ip}$  increased or decreased respectively, obviously these tendencies would be aggravated. Hence the important conclusion that unless some other information is available to indicate whether the source of range errors is due to eccentricity errors or semi-major axis errors it would be best to ignore the radar range information.

#### 7.4 Prologue to the Presentation of Results

The exact manner of the presentation of results for a rendezvous study such as that undertaken in this investigation has been a continued source of consternation to the author. The scope is broad, the field is relatively new and the precedents are few. The form ultimately selected is believed to be as economical and concise as the time and depth of investigation permit, and logical in nature when viewed under the consideration of the probably progress of events in

this country's manned space programs.

At the outset the standard intercept trajectory along with its guidance parameters and mode of operation that has been found to demonstrate to fullest advantage the techniques of line-of-sight guidance will be presented. Next some relationships between initial condition errors in the target orbit and interceptor waiting orbit will be formulated. Then the validity of the extension of rendezvous between circular orbits and coapsidal elliptic orbits will be established. As a final part of this chapter a selection will be made of random observational measurement and action errors.

With the foregoing as background, Chapter 8 will then deal with the standard trajectory and guidance principles under various modes of operation, under varying conditions of the guidance parameters, and in comparison with other possible intercept trajectories. A comparison will then be made of two methods of dealing with elliptic target orbits. Finally through a technique of scaling, the results of this investigation will be shown to be readily extendible to other possible missions in the manned space program including some observations applicable to the Lunar Orbit Rendezvous problem.

Chapter 9 will then attempt to present in a concise mission profile form a general theory of rendezvous applicable to most all conceivable orbital operations utilizing line-of-sight techniques.

#### 7.5 The Recommended Form of Intercept Guidance

The reader is reminded at this point that the prime criteria

used in the selection of a standard intercept trajectory, mode of operation, and guidance parameters was to achieve the greatest tolerance to initial condition orbit errors with an anticipated reasonable maximum out-of-plane situation, and to be able to accomplish the rendezvous within the physical constraints and velocity change limitations of such an interceptor as the Gemini spacecraft in the face of significant measurement and action errors.

The trajectory found to best satisfy these criteria has the following characteristics:

- (1) Rendezvous parameters

$$b = 0.2115$$

$$k = 0.8175$$

- (2) Radial distance traversed (between circular orbits)

$$d = 25 \text{ nm, target altitude } 150 \text{ nm,}$$

$$\text{waiting orbit altitude } 125 \text{ nm}$$

- (3) Central angle traversed

$$\Delta f_i \cong 90^\circ$$

- (4) Initial and final true anomalies

$$f_i \cong 15^\circ$$

$$f_f \cong 105^\circ$$

## (5) Line-of-sight details

$$\beta_i \cong 59.3^\circ$$

$$\rho_i \cong 48.5 \text{ nm}$$

$$\beta_f \cong -7.6^\circ$$

Total  $\phi$  variation  $\cong 24^\circ$

## (6) In-plane velocity changes

$$\Delta V_{ip} \cong 79 \text{ fps} \quad \left( \frac{\Delta V_{ip}}{\Delta V_H} \cong 0.88 \right)$$

$$\alpha_i \cong 62.5^\circ$$

$$\Delta V_{fp} \cong 141 \text{ fps} \quad \left( \frac{\Delta V_{fp}}{\Delta V_H} \cong 1.58 \right)$$

$$\alpha_f \cong 172.4^\circ$$

## (7) Noncoplanar parameter

$$\frac{\tan \psi_f}{\tan \psi_i} \cong 2.437$$

(8)  $\Delta V_{iz}$  determination parameters

$$\beta_{1i} \cong 66.0^\circ$$

$$\rho_{1i} \cong 60.2 \text{ nm}$$

$$\gamma_{12} \cong 16.0^\circ$$

$$\beta_2 \cong 61.0^\circ$$

(8) (cont.)

$$\rho_2 = 50.8 \text{ nm}$$

$$\gamma_{2i} = 4.0^\circ$$

The mode of operation suggested utilized radar range information for  $\Delta V_{iZ}$  determination and guidance corrections and the "computation" option for  $\Delta V_{iZ}$  determination or in other words a variable  $\gamma_{12}$ .

The guidance parameters found to be most satisfactory are:

(1) Square sight reticle 5 mils from center to edge

(2) Guidance sensitivity constants

$$K_\phi = 1.0$$

$$K_\psi = 1.0$$

(3) Constant pitch down angle

$$\alpha_p = 20^\circ$$

(4)  $\psi$  correction made perpendicular to line of sight

(5)  $\tan_N \psi$  curve derived from  $i_f \approx 0.25^\circ$  ( $\Delta V_{fZ} = 111 \text{ fps}$ )

This trajectory, the mode of operation, and these guidance parameters will now be used to establish relationships between orbit errors and then in the next chapter, using measurement and action errors, certain variations will be explored.

## 7.6 Noncoplanar Situation Used for Testing

A relative inclination between the target orbit and the interceptor waiting orbit of  $0.35^\circ$  was selected as a reasonable maximum to be expected. This allows for considerable flexibility in the launch window and orbit injection errors. Between circular orbits at an attitude of 150 nm this amounts to about a 155 fps Z-velocity component. For relative inclinations slightly greater or less than this, the tolerances to other orbit errors would be correspondingly decreased or increased under the same velocity change limitations. It is felt that these effects can be readily inferred to reasonably good accuracy by simple manual calculations. So for standardization and comparison purposes this relative inclination was used in all the subsequent simulations except some of the last scaling comparison runs.

A standard  $\gamma_i$  or angle from the start of the intercept back to the relative line of nodes would also help make comparisons more meaningful. In selecting this angle, a condition that would reflect a near-maximum velocity change requirement was desired. In addition this condition should fully test both the  $\Delta V_{iz}$  computation and the  $\psi$  guidance performance. If  $\gamma_i$  were  $0^\circ$  or  $180^\circ$ , the maximum burden would be on the computation and little testing of the guidance would result. Conversely, a  $\gamma_i$  of  $90^\circ$  or  $270^\circ$  would not test the computation as much and the guidance would be conducted under maximum  $\psi$  angles. Since the selected trajectory traverses about  $90^\circ$ , the total velocity requirements are essentially identical for equal angles on either side of a  $\gamma_i$  of  $90^\circ$ . For example, a  $\gamma_i$  of  $60^\circ$  is comparable to  $120^\circ$  and  $30^\circ$  is

comparable to  $150^\circ$ . (If this is not clear to the reader, Fig. 5-8b should be consulted.)

Figure 7-3 shows the results of rendezvous simulations of the standard trajectory and parameters under no error conditions indicating the total velocity requirements for  $i = 0.35^\circ$  as a function of  $\gamma_i$ . The theoretical requirements are also shown as cross marks for comparison. Though maximum velocity requirements for no errors are seen to exist for  $\gamma_i$  of  $0^\circ$  or  $180^\circ$ , under conditions of orbit errors and measurement and action errors, a  $\gamma_i$  in the vicinity of  $45^\circ$  or  $135^\circ$  seems to produce near-maximum requirements. These  $\gamma_i$  also test both the computation and guidance control aspects to a considerable degree. In view of this, a  $\gamma_i$  of  $45^\circ$  has been selected as the condition to be used for all subsequent simulation runs.



STANDARD TRAJECTORY, MODE AND GUIDANCE,  $i_T = 0.35^\circ$  NO ERROR  
COMPARED WITH (X) THEORETICAL VELOCITY REQUIREMENTS

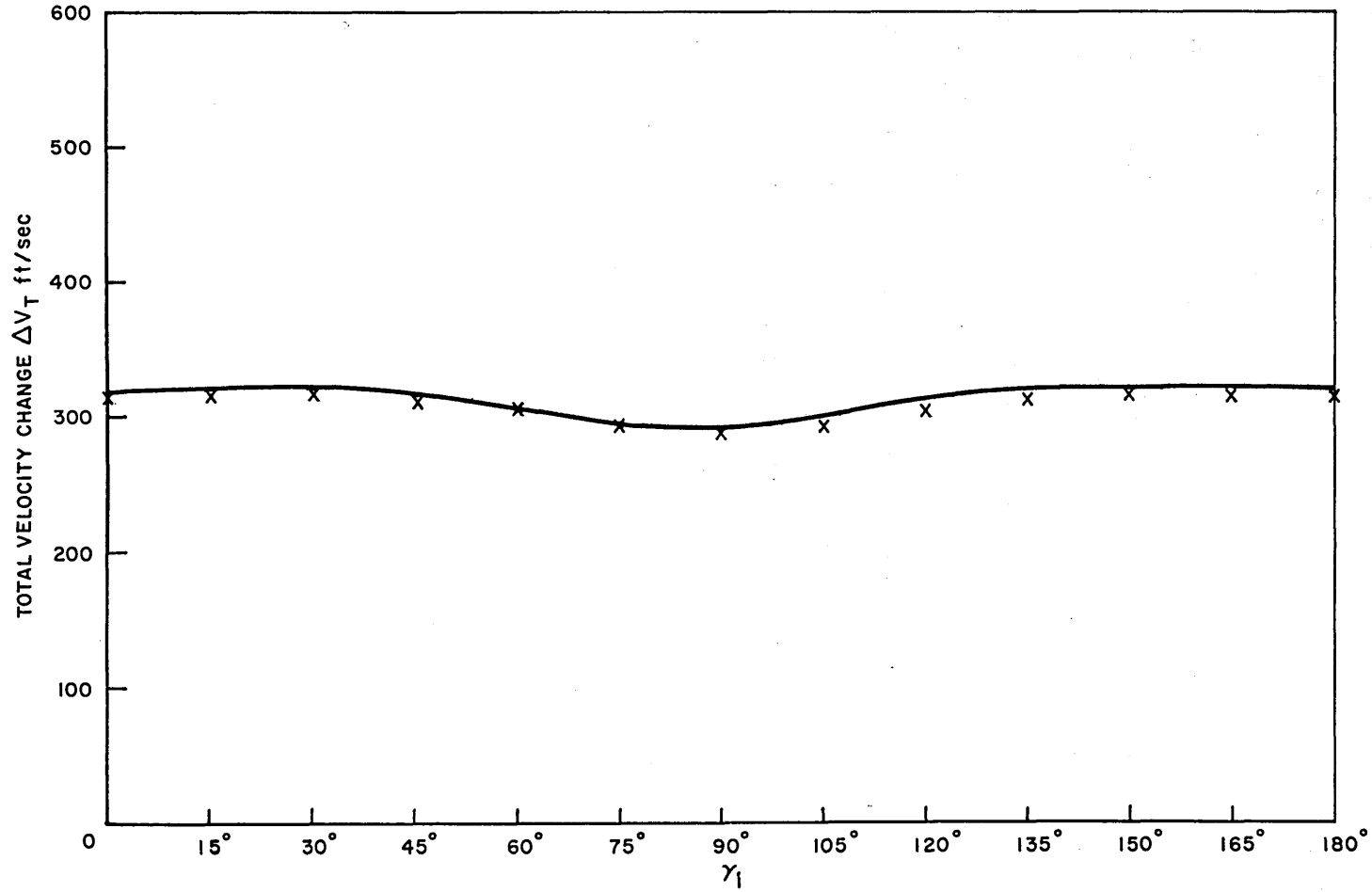


Fig. 7-3 Effects of Variable  $\gamma_i$

## 7.7 Waiting Orbit Errors

Initial condition errors in the interceptor waiting orbit can consist of departures from circular orbit conditions or eccentricity errors with associated true anomalies at the start of the intercept and errors in the semi-major axis of the waiting orbit. Figure 7-4 shows the effects of these errors on the total velocity requirements. Three conditions are displayed representing  $\delta a_w$  of 0, +3 nm, -3 nm for an eccentricity  $e_w$  of 0.001 as a function of  $f_{iw}$ . This eccentricity is characterized by a radial variation up and down from the semi-major axis of about 3.6 nm for the nominal conditions of intercept between 125 nm and 150 nm orbits. Along with the identification of each line are given the velocity requirements for the semi-major axis error with no eccentricity error. It can be seen that for a given true anomaly  $f_{iw}$  the addition of one or the other  $\delta a_w$  errors requires more velocity capability than with no  $\delta a_w$  error.

STANDARD TRAJECTORY, MODE, GUIDANCE AND RELATIVE INCLINATION CONDITION  
 $e_w = 0.001$      $\delta a_w = 0, +3nm, -3nm$

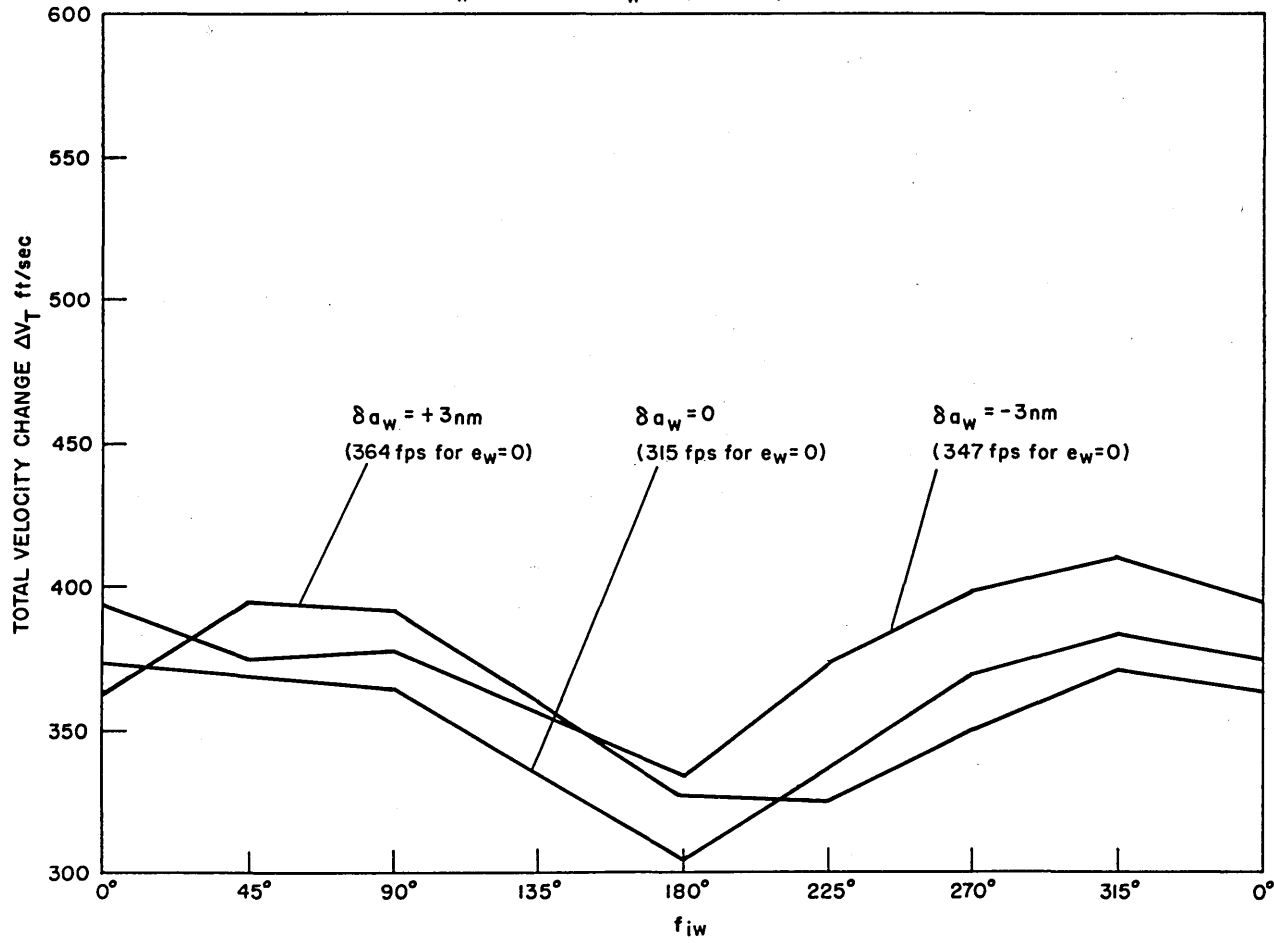


Fig. 7-4 Effects of Waiting Orbit Errors

## 7.8 Target Orbit Errors

The effects of initial condition errors consisting of target orbit eccentricities and their total velocity requirements as a function of the target true anomaly at the start of the intercept are presented in Fig. 7-5. It can readily be seen that for a given true anomaly of the target eccentricity the magnitude of the velocity requirements behave in a very nearly linear fashion. The peaks are consistently about  $45^\circ$  on either side of  $180^\circ$ . The reasons for the small effect of the eccentricity at true anomalies near  $0^\circ$  is that the error effects cause the target to move in a similar fashion to the interceptor. To put it another way, the initial true anomaly of the target is close to the initial true anomaly of the interceptor and as has been mentioned previously, this produces line-of-sight motion similar to that for a rendezvous with a circular target.

The cross marks indicate a comparison with waiting orbit errors of 0.001 from the preceding Fig. 7-4 with the true anomalies phase shifted by  $180^\circ$ . The close agreement suggests the interchangeability of target and waiting orbit eccentricity errors through a mere phase shifting process. In addition to simplifying the error analysis as discussed in Section 7-9, this extremely important interchange capability opens up tremendous possibilities for executing a rendezvous with an elliptic target orbit as will be mentioned in Section 7-10.

To the right side of Fig. 7-5 is a tabulation of an attempted comparison of ellipticity errors and semi-major axis errors. Corresponding to each value of ellipticity there is a maximum radial deviation from the semi-major axis that is given by the product  $a e$ . This

STANDARD TRAJECTORY, MODE, GUIDANCE AND RELATIVE INCLINATION CONDITION  
 VARIOUS  $e_t$ ,  $\delta a_t = 0$ , COMPARISON FOR  $e_w = 0.001$

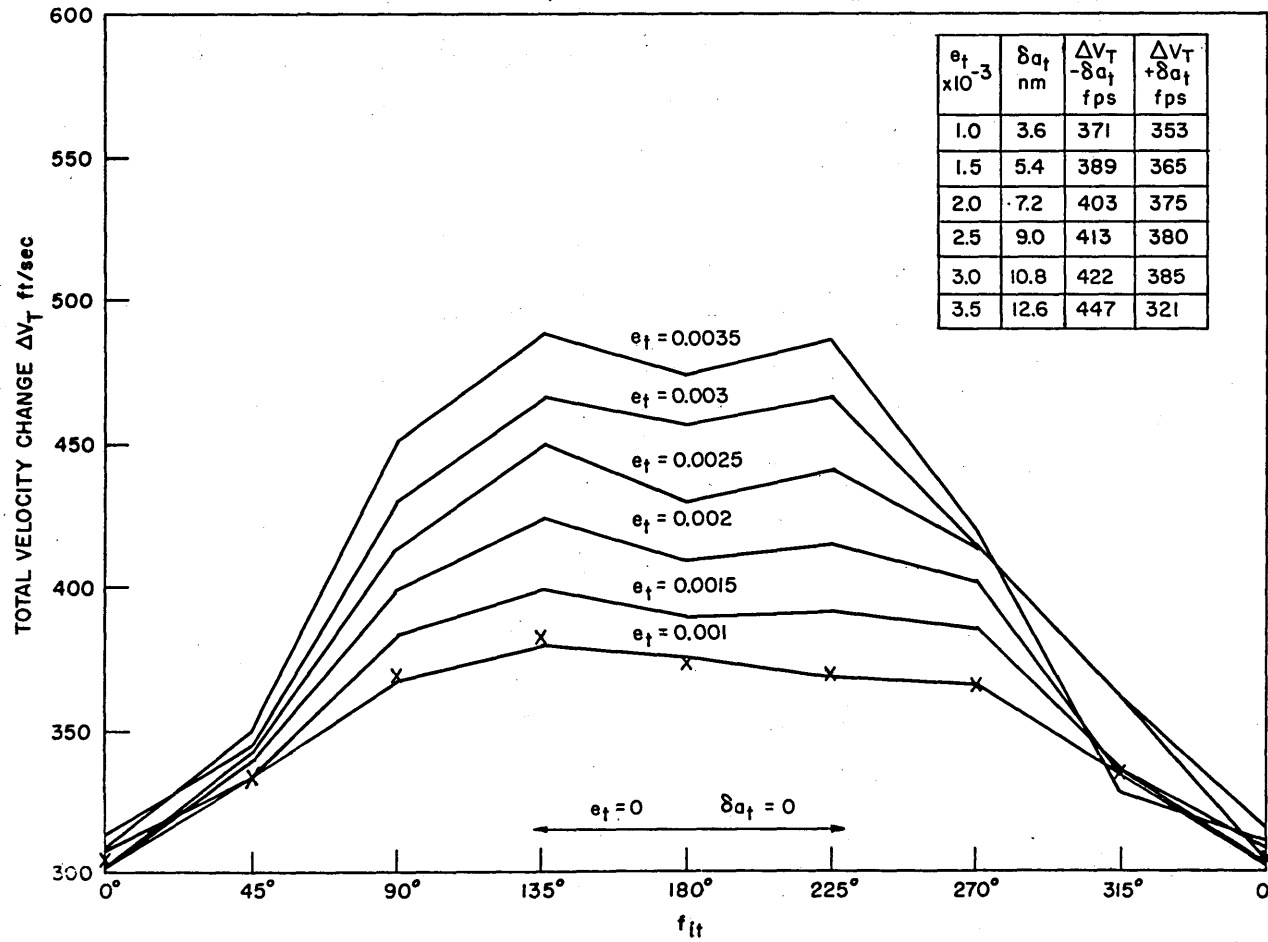


Fig. 7-5 Effects of Target Orbit Errors

radial error was used as a semi-major axis error with no eccentricity error. The velocity requirements for errors of plus and minus this quantity  $\delta a_t$  are given in the table. In every case it is seen that the maximum eccentricity penalties are greater than the semi-major axis errors corresponding to the same displacement.

#### 7.9 Target Orbit Errors as Combined Errors - Superposition

Figure 7-6 shows by the solid lines the velocity change requirements as a function of true anomaly for a constant target eccentricity of 0.0025 for three different conditions of waiting orbit semi-major axis errors. (The  $\delta a_w = 0$  case is a repeat from the previous graph.) It is noted that increases in radial separation  $d$  produce higher velocity requirements for all true anomalies except those near  $225^\circ$  and  $270^\circ$ . The decrease in radial separation produces the highest requirements for these true anomalies. (The fact that the two peaks are about equal is due to the selection of the pitch down angle  $\alpha_p$ .) The cross marks at  $90^\circ$  intervals indicate the results of simulations where the total combined eccentricity was equal to 0.0025 but 0.001 of it was shifted to the waiting orbit by a true anomaly phase shift of  $180^\circ$ . The close agreement of this comparison results in the conclusion that the highest velocity requirement cases of combined orbit eccentricities which occur when the true anomalies are  $180^\circ$  apart can be analyzed by simply adding the eccentricities together and considering their effects at either of the orbits. For comparison, the horizontal lines indicate the effects of semi-major axis errors

STANDARD TRAJECTORY, MODE, GUIDANCE AND RELATIVE INCLINATION CONDITION  
 $e_t = 0.0025$ ,  $\delta a_w = 0, -3nm, +3nm$   
 X INDICATES SEPARATED ERRORS  $e_w = 0.001$  ( $180^\circ$  PHASE SHIFT)  $e_t = 0.0015$  FOR COMPARISON

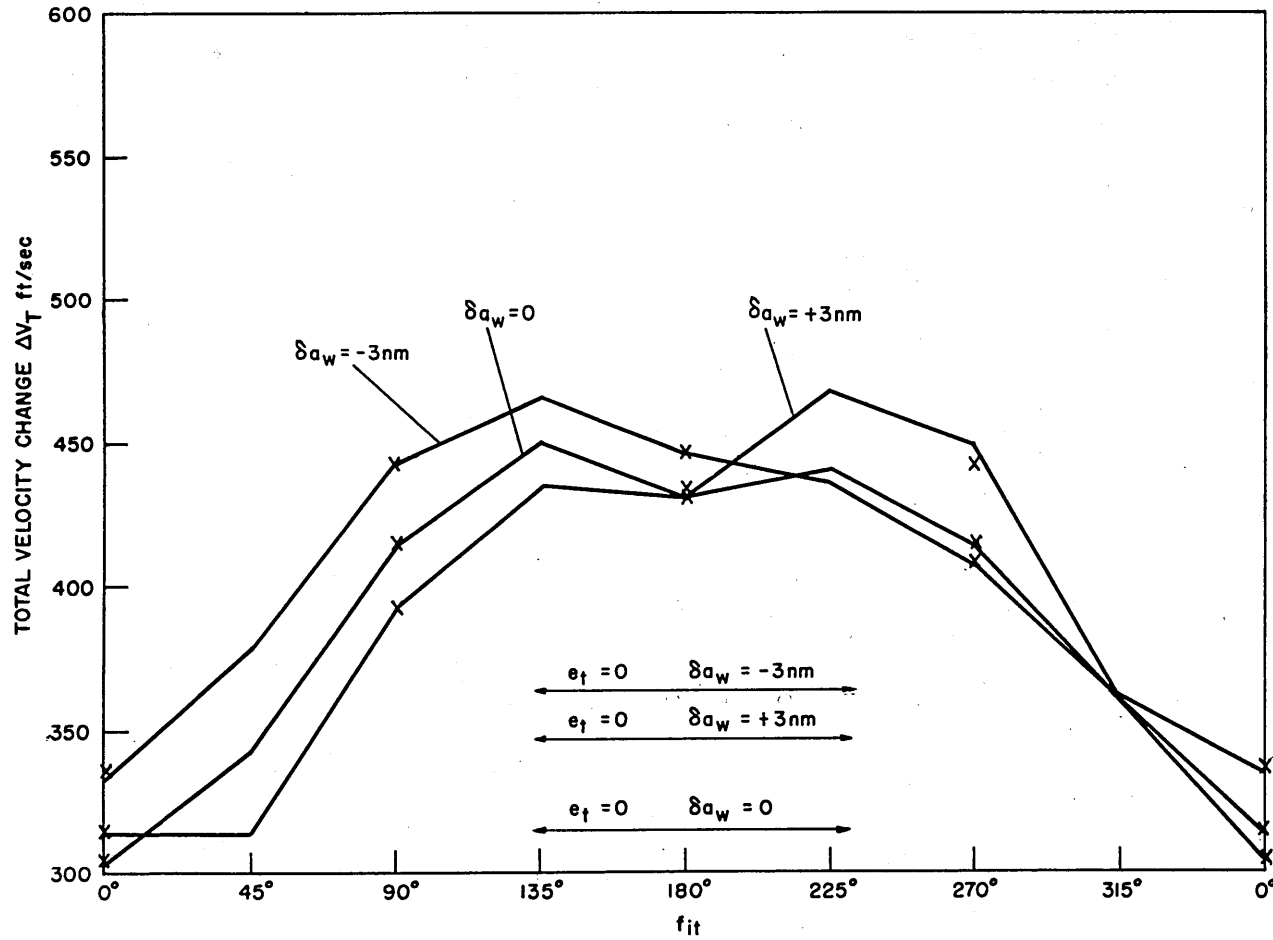


Fig. 7-6 Target Orbit Errors Reflecting Combined Errors

without eccentricity errors. By comparing the results in this graph with the previous one it is seen that the sum of the eccentricity error of 0.0025 and the semi-major axis error of 3 nm, which corresponds to about an eccentricity of 0.001, produces less velocity requirements than either an eccentricity of 0.003 or 0.0035 alone. The conclusion can be inferred that combinations of eccentricity and  $\delta a$  produce less velocity requirements than an eccentricity alone which corresponds to the same maximum radial displacement. Though this property could be used to eliminate any need for considering semi-major axis errors the author has chosen to retain the identity of  $\delta a$  in the event that unforeseen factors might predominate. The conditions used for testing subsequent variations will be a  $\delta a_w$  of -3 nm for all  $f_{it}$  except  $225^\circ$  and  $270^\circ$  where a  $\delta a_w$  of +3 nm will be used. The eccentricity errors will be lumped at the target as  $e_t = 0.0025$ .

#### 7.10 Eccentricity Phase Shift Applied to Nominally Elliptic Targets

The potentialities of phase shifting the eccentricities of the target and waiting orbits offer great significance to the problem of rendezvous with a nominally elliptic target orbit. Consider the case of copasidal target and waiting orbits of equal eccentricity. By the reasoning established in the preceding analysis, if the target eccentricity were phase shifted by  $180^\circ$  into the waiting orbit the result would be that both orbits would now be circular and a nominal intercept could be used starting at any true anomaly.

To test the validity of this argument, the author took the very



same standard trajectory curves and guidance parameters including  $\beta$  angles,  $\alpha$  angle, and  $\Delta V_{ip}$  magnitude derived for circular orbits and used them for a rendezvous to a target of ellipticity 0.01 which had altitudes of perigee of 114 nm and apogee of 186 nm, the semi-major axis remaining at 150 nm. The interceptor was placed in a coapsidal elliptic waiting orbit with a semi-major axis of 125 nm. To be strictly correct in having the radial distances near equal all around the orbit the eccentricity of the waiting orbit was obtained from the relation:

$$a_w e_w = a_t e_t$$

which gave  $e_w = 0.01007$  with altitudes of perigee of 89 nm and apogee of 161 nm. The vehicles were put into relative rendezvous position at progressive  $45^\circ$  intervals around the orbits. The results of this no-error simulation are presented in Fig. 7-7. The results speak for themselves. The maximum velocity requirement is only 12 fps higher than for the no-error transfer between circular orbits!

In an effort to see just how far this relationship could be applied, the author then picked a situation that would encompass the extremes of any foreseeable manned orbital rendezvous in the vicinity of the Earth. Standard curves and parameters were derived for an intercept trajectory with the same values of  $b$  and  $k$  but between circular orbits at 275 nm and 300 nm. These values were then used for a no-error simulation with the same inclination of  $0, 35^\circ$  and  $\gamma_i$

of  $45^\circ$  for a target of ellipticity 0.05 with a perigee altitude of 113 nm, semi-major axis at 300 nm, and an apogee altitude of 487 nm! The interceptor was put into a coapsidal orbit of ellipticity 0.05034 with a perigee altitude of 88 nm, semi-major axis at 275 nm and an apogee altitude of 462 nm. These results are presented in Fig. 7-8. Again there is only a small difference in the total required velocity to conduct a rendezvous at any initial true anomaly when compared to the same no-error condition for an intercept between circular orbits. Here the maximum velocity requirement is only 21 fps higher than for the transfer between circular orbits. The superposition of errors in eccentricity and semi-major axis will be further investigated at the end of Chapter 8.

#### 7.11 Measurement and Action Errors

To be a valid investigation of any guidance and control concept the system under study must be demonstrated to perform satisfactorily in the face of reasonable errors in the operating conditions. Since in the proposed system of optical control of satellite rendezvous utilizing line-of-sight techniques, the sources of errors and frequency of occurrence are most numerous, any attempt to examine their effects on an individual basis under the spectrum of possible initial condition errors would indeed be a monumental task. Since the system is, by nature, closed loop in its operation, it inherently possesses its own error compensating features. The author has felt from the outset

STANDARD TRAJECTORY, MODE, GUIDANCE AND RELATIVE INCLINATION CONDITION

(DERIVED FROM CIRCULAR ORBITS)

$e_t = 0.01$  , ALTITUDES: PERIGEE 114 nm, APOGEE 186 nm, SEMI-MAJOR AXIS 150 nm  
 $e_w = 0.01007$  from  $a_w e_w = a_t e_t$  , ALTITUDES: PERIGEE 89 nm, APOGEE 161 nm, SEMI-MAJOR AXIS 125 nm

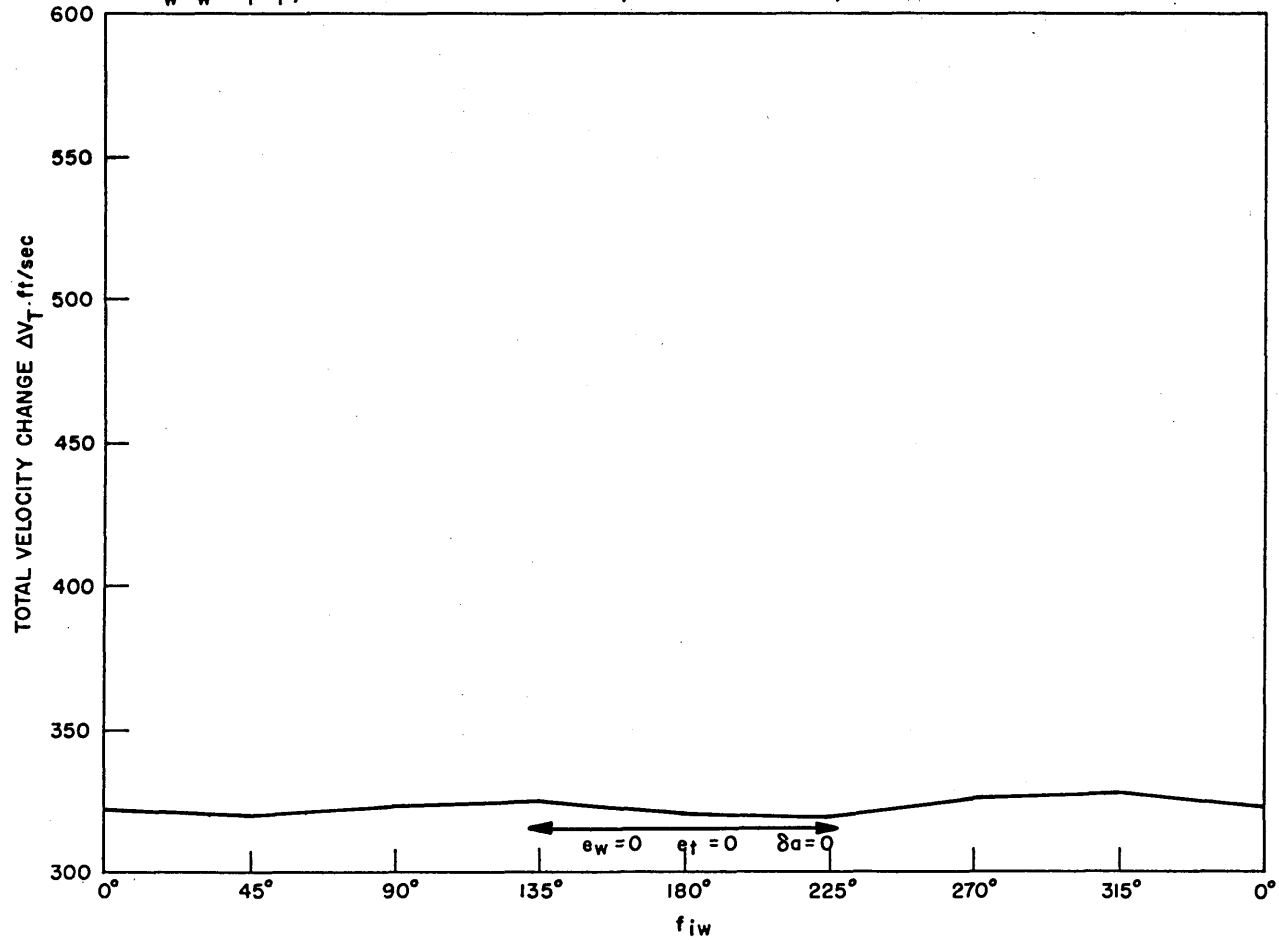


Fig. 7-7 Rendezvous Between Coapsidal Elliptic Orbits - No Errors

that even large errors in the operating conditions would have a small effect in comparison with the wide range of initial condition errors that have been examined. With the above considerations in mind the computer rendezvous simulation programs were rewritten to incorporate various random errors in the simulated observational measurements taken from the interceptor and in the actions taken as a result of these measurements. The one-sigma values of these random errors were arranged to be read into the program along with the other input data. The error values selected are believed to represent the slightly pessimistic side of reasonably anticipated system performance.

These one-sigma error values are listed and explained as follows:

(1) Orbit Plane Bias Error - 10 mils

This represents the error in determination of the interceptor orbit plane and affects the  $\psi_1$ ,  $\psi_2$ , and  $\psi_i$  observation. As a bias the random number is selected once and applied to each of these observations. The  $\psi_1$  and  $\psi_2$  observations determine  $\Delta V_{iz}$  and the  $\psi_i$  observation is used to unnormalize the  $\tan_N \psi$  curve. In addition to this bias error these observations are also subject to the sight tracking error.

(2) Spacecraft Attitude Error - 20 mils

This error affects the direction of application of the initial velocity change  $\Delta V_i$  and the subsequent velocity corrections. As a random number it is applied to each component of the velocity change coordinate system. The error value may seem low when

STANDARD TRAJECTORY, MODE, GUIDANCE AND RELATIVE INCLINATION CONDITION  
 (DERIVED FROM CIRCULAR ORBITS)

$e_t = 0.05$  , ALTITUDES: PERIGEE 113 nm, APOGEE 487 nm, SEMI-MAJOR AXIS 300 nm  
 $e_w = 0.05034$ , ALTITUDES: PERIGEE 88 nm, APOGEE 462 nm, SEMI-MAJOR AXIS 275 nm

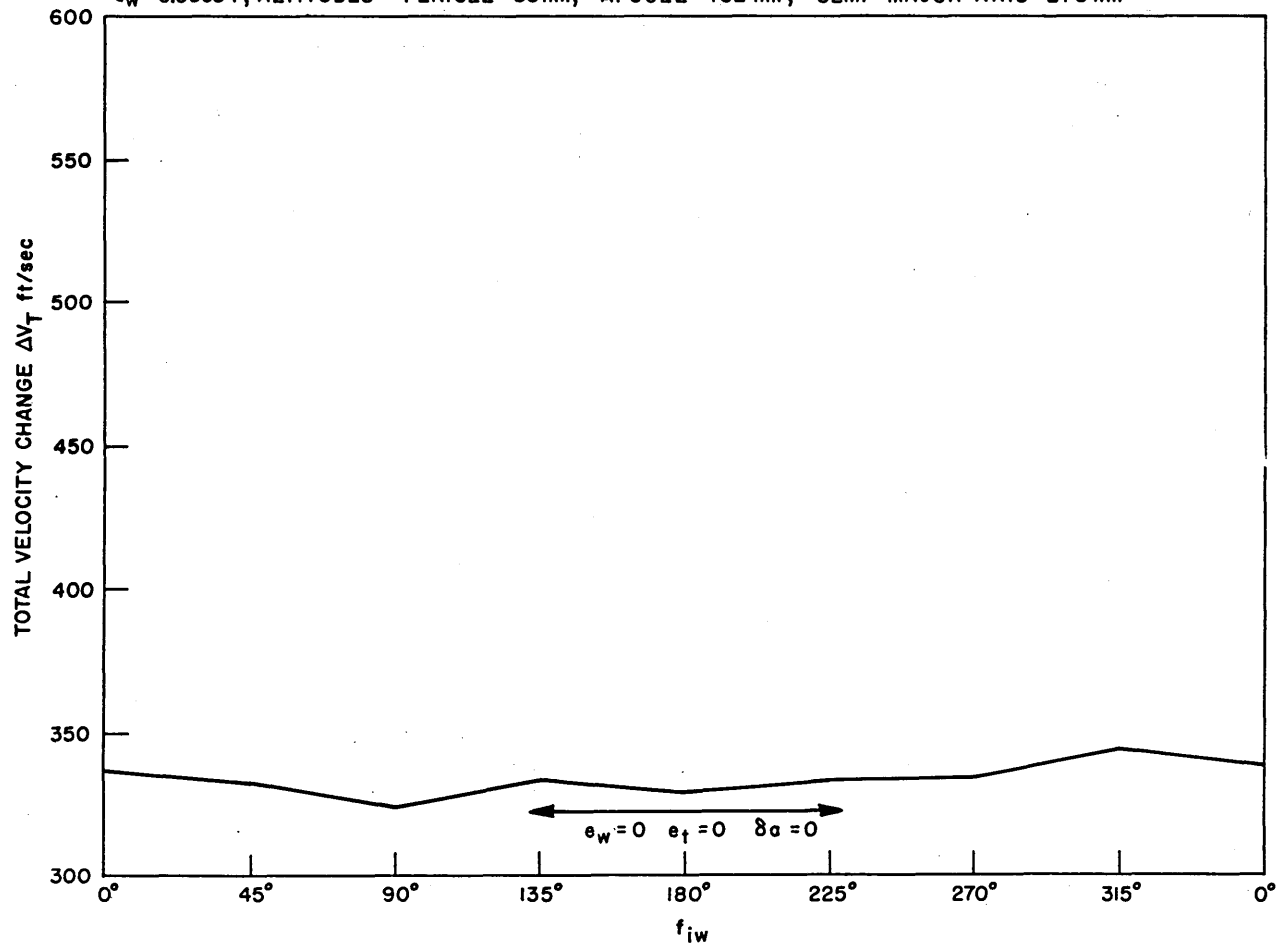


Fig. 7-8 Rendezvous Between Extreme Coapsidal Elliptic Orbits - No Errors

thinking of usual attitude indicating systems but considering the reference lines in the proposed optical sight it appears to be on the pessimistic side.

(3) Sight Tracking Error - 0.5 mils

The effect of this error is essentially in the timing of the decision to make a velocity correction. It reflects the inaccuracies of aligning the axes of the sight reticle on the target and also of deciding when the target has crossed the edges of the reticle square. It is not actually a tracking error since no actual tracking is performed but rather a relative position determination error. From the author's experience in tracking a near-6 mil aerial gunnery target with a 2 mil pipper under rapidly changing 3 to 4 g acceleration levels, a three-sigma relative position determination of 1.5 mils is not at all unreasonable for the near-static conditions of the proposed stabilized sight reticle.

(4) Thrust and Computation Bias - 3 percent

The effect of this error is reflected in the magnitude of the initial velocity change and in the subsequent velocity corrections. It lumps together the inaccuracies of nonstandard thrust devices and errors of computation for  $\Delta V_{iz}$  and the guidance equation computations. The significantly large errors in velocity application that result from the no-computation and no-radar modes to be examined later will testify to the noncritical effects of this error source. If too small a

correction is made at one time, it simply means that another will be called for sooner, and conversely if too great a correction is made either another correction will not be needed as soon or a correction will be called for in the opposite direction. Only in the no-radar mode where errors of correction are of the order of 50% do significant tendencies for undercorrection or instabilities become evident. The few instabilities that have been observed are usually caused by the sampling interval rather than overcorrection.

(5) Thrust Cutoff - 0.25 ft/sec.

The effect of this error is negligible on all but the very last terminal corrections when the velocity change magnitudes are on the order of one or two feet per second. Even here the effects are essentially undetectable. In fact for the thrust devices envisioned for the Gemini vehicle which have cut off timing accuracies on the order of milliseconds, this value as a one-sigma value is quite excessive. It would not be until the docking phase that this error would come into play.

(6) Radar Range Error - one percent

This error affects the  $\Delta V_{iz}$  computation and the guidance equation computation when the radar mode of operation is selected. The one-sigma value for the error is a standard figure quoted for several types of equipment that furnish only range information, especially considering its use with friendly targets, probably transponder equipped, at ranges less than 100 nm.

(7) Local Vertical Error for Determination of  $\beta$  Angles

Errors in the local vertical that affect the orbit plane determination have already been accounted for by the Orbit Plane Bias Error. The 15-second sampling interval inherently involves errors in the determination of the arrival of a specified  $\beta$  angle. Since for the trajectory selected and the  $\beta$  angles to be observed the sampling interval involves  $\beta$  changes of from  $0.3^\circ$  to  $0.5^\circ$  and these are very nearly the accuracies anticipated of horizon scanner devices, no further errors were imposed on the  $\beta$  angle determination. It should be recalled that once the intercept is started the local vertical is no longer required since only relative motion between the target and the reticle is of concern.

All of the above errors have been applied to all of the simulation rendezvous runs that will be subsequently examined. None of these have produced any significant difficulties. The over-all effect is that velocity requirements have increased slightly. In a few cases surprisingly enough the velocity requirements have actually decreased. This is evidently due to the coincidental compensating effects of the random errors and the initial condition errors. This would certainly be rather difficult to establish in a rigorous analytical fashion.



## CHAPTER 8

## COMPLETE RESULTS OF SIMULATIONS

8.1 Effects of Measurement and Action Errors on the Standard Trajectory

The one-sigma random errors discussed in the last chapter were added to the critical combination of lumped eccentricity errors and  $\delta a_w$  errors. A portrayal of their effects on the standard trajectory are presented in Figure 8-1. The critical combination of initial condition orbit errors that come from the analysis of Figure 7-6 are a positive  $\delta a_w$  of 3 n. m. for  $f_{it}$  of  $225^\circ$  and  $270^\circ$  and a negative  $\delta a_w$  of 3 n. m. for all other  $f_{it}$ .

The addition of these errors can be seen not to alter significantly the velocity requirements as a function of initial condition orbit errors. The general effect could be likened to the superposition of noise on the no error results. Similar comparisons with other conditions and trajectories indicates a tendency for these measurement and action errors to increase slightly the velocity requirements for all initial condition errors. For some unknown reason this tendency is not particularly evident in Figure 8-1. The cross marks are the results of earlier studies with

the same measurement and action errors but where the eccentricity errors were not all lumped at the target but with  $e_w = 0.001$  and  $e_t = 0.0015$ . For these conditions  $f_{iw}$  was  $180^\circ$  different from  $f_{it}$ .

One point should be stressed to the reader in the event that it has become lost in the shuffle of eccentricities. That is that the velocity requirements of this graph and all succeeding graphs do not present in a statistical sense the likelihood of the occurrence of velocity requirements; instead, they represent the extremes of effective error eccentricity that result when the true anomalies are  $180^\circ$  apart. When these are not  $180^\circ$  apart a lesser effective lumped eccentricity would result with attendant lower velocity requirements. For example, as derived previously, when the eccentricities are equal and the true anomalies are in phase, an effective lumped eccentricity of zero results.

The range of closing velocities for these runs was 138.6 fps for  $f_{it} = 90^\circ$  and 222.6 fps for  $f_{it} = 225^\circ$ .

## 8.2 Detailed Presentation of a Rendezvous Simulation

At this point it appears appropriate to present in a detailed graphical form the complete results of a particular rendezvous simulation. The one selected for presentation does not reflect any average or typical set of conditions but rather a more critical example requiring a near maximum in performance and velocity requirements.

STANDARD TRAJECTORY, MODE, GUIDANCE AND RELATIVE INCLINATION CONDITION  
 $e_t = 0.0025$ ,  $\delta a_w = +3$  n.m. FOR  $f_{it}$  OF  $225^\circ, 270^\circ$ ;  $\delta a_w = -3$  n.m. FOR ALL OTHER  $f_{it}$   
 X- SEPARATED ECCENTRICITY ERRORS,  $e_w = 0.001$ ,  $e_t = 0.0015$ , WITH MEASUREMENT  
 AND ACTION ERRORS

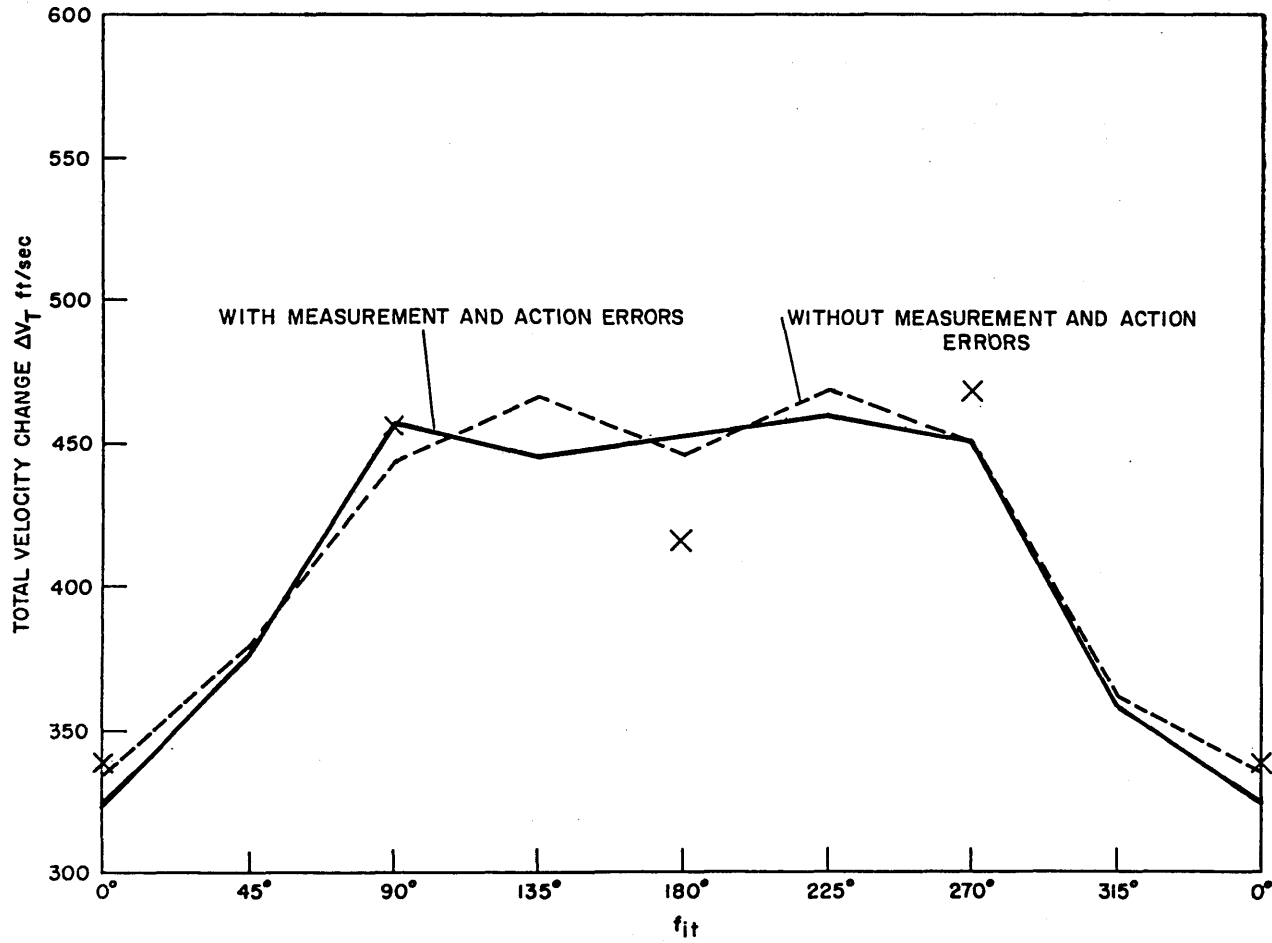


Fig. 8-1 Effects of Measurement and Action Errors on the Standard Trajectory

The example selected uses the standard trajectory with characteristics as summarized in Section 7.5 for a rendezvous between a target in a nominally circular orbit at an altitude of 150 n.m. and an interceptor in a nominally circular waiting orbit at an altitude of 125 n.m. The initial condition orbit errors consist of a  $\delta a_w$  of +3 n.m. placing the semimajor axis of the waiting orbit at 128 n.m. and a lumped eccentricity of the target of  $e_t = 0.0025$  with a nominal  $f_{it}$  of  $270^\circ$  which might be interpreted as  $e_t = 0.0015$ ,  $f_{it} = 270^\circ$  and  $e_w = 0.001$ ,  $f_{iw} = 90^\circ$ . (The relative velocity error corresponding to this error eccentricity amounts to very nearly  $eV_c$  or about 63.5 fps!) The relative inclination of the orbits is  $.35^\circ$  with a nominal  $\gamma_i$  of  $45^\circ$ . The mode of operation is radar with the computation option for  $\Delta V_{iz}$ , and the complete set of random measurement and action errors described in Section 7.11 are employed.

The  $\Delta V_{iz}$  determination phase for this rendezvous is summarized as follows. The central angle traversed by the interceptor from just prior to the  $\beta_1$  angle to the  $\beta_1$  angle was about  $40^\circ$  instead of the nominal  $20^\circ$ . This is caused by the orbit error effects and means that the actual  $f_{it}$  and  $\gamma_i$  that exist at the start of the intercept are about  $20^\circ$  greater than the nominal selected as the initial condition. This means that  $\gamma_{12}$  and  $\gamma_{2i}$  are correspondingly greater than the values for the nominal intercept.  $\psi_1$  and  $\psi_2$  were observed by the interceptor

as about  $8^\circ$  and  $24^\circ$  (the Orbit Plane Bias Error caused these both to be about  $1^\circ$  less than the actual values). The  $\Delta V_{iz}$  computation for the selected mode yielded 71.5 fps. The value of  $\Delta V_{iz}$  for all four possible modes of operation are tabulated below:

<u>Mode</u>	<u><math>\Delta V_{iz}</math> fps</u>
Computation and Radar	71.5
Computation and No Radar	123.4
No Computation and Radar	106.5
No Computation and No Radar	112.5

Due to the thrust bias error the actual value of  $\Delta V_{ip}$  was about 2 fps greater than the nominal and the total velocity change applied to start the intercept maneuver was 108.2 fps. This was applied at a  $\beta_i$  angle that was about  $.6^\circ$  greater than it should be. The out-of-plane velocity change angle  $\chi$  was  $41.4^\circ$ , and the existing  $\rho$  distance at this point was 37.3 n. m. compared to the nominal no error value of 48.5 n. m.

The sequence of events occurring in the guidance phase is portrayed in Figures 8-2a and 8-2b. In the former, the angles  $\beta$ ,  $\beta_{nom}$  and  $\phi$  and the cumulative in-plane velocity corrections are given as a function of time whereas in the latter, the angle  $\psi$ , the distances  $\rho$  and  $\rho_{nom}$  and the cumulative out-of-plane velocity corrections are presented. Along with the actual values of  $\phi$  and  $\psi$  is shown the sight

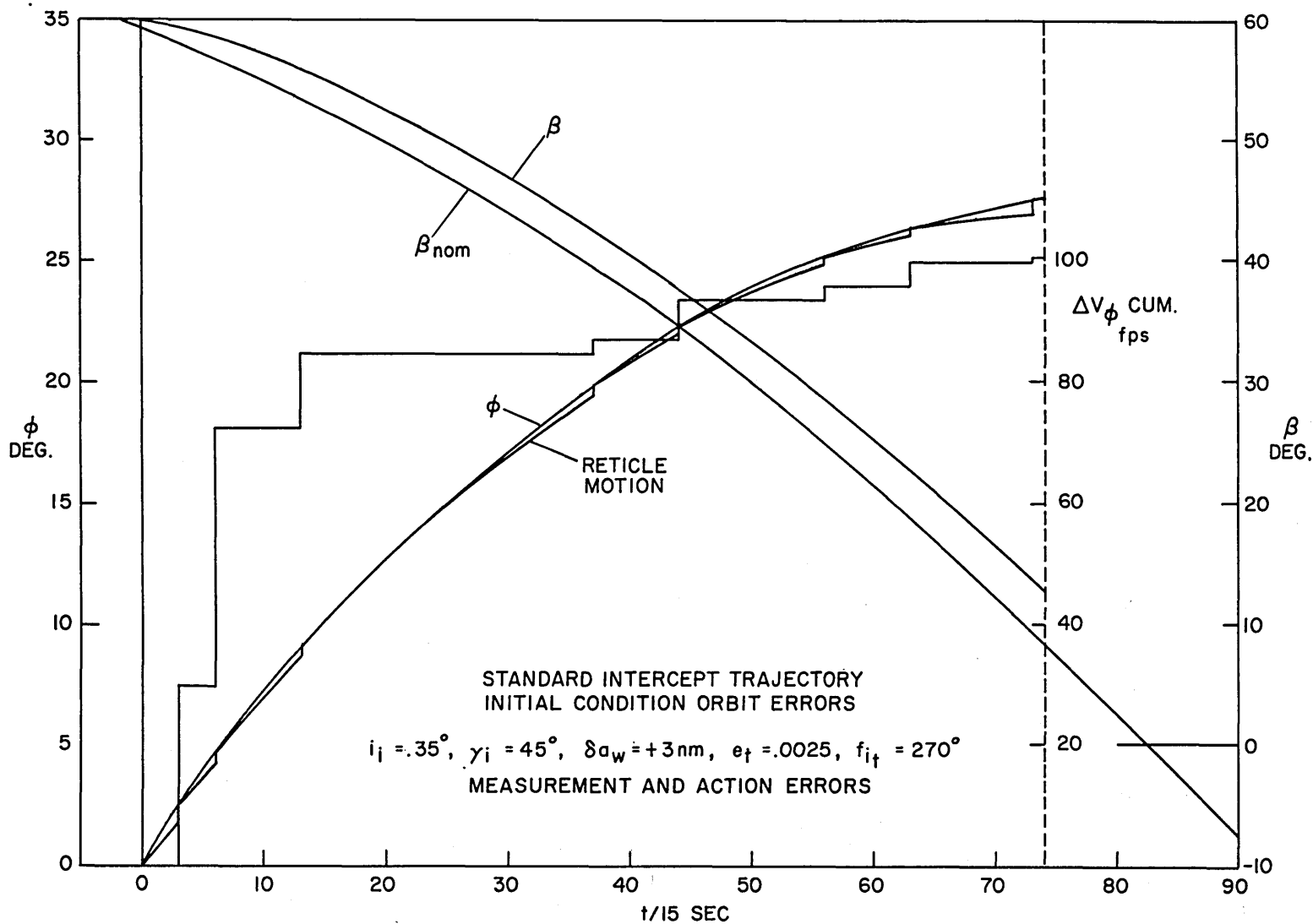


Fig. 8-2a Detailed Presentation of a Rendezvous Simulation

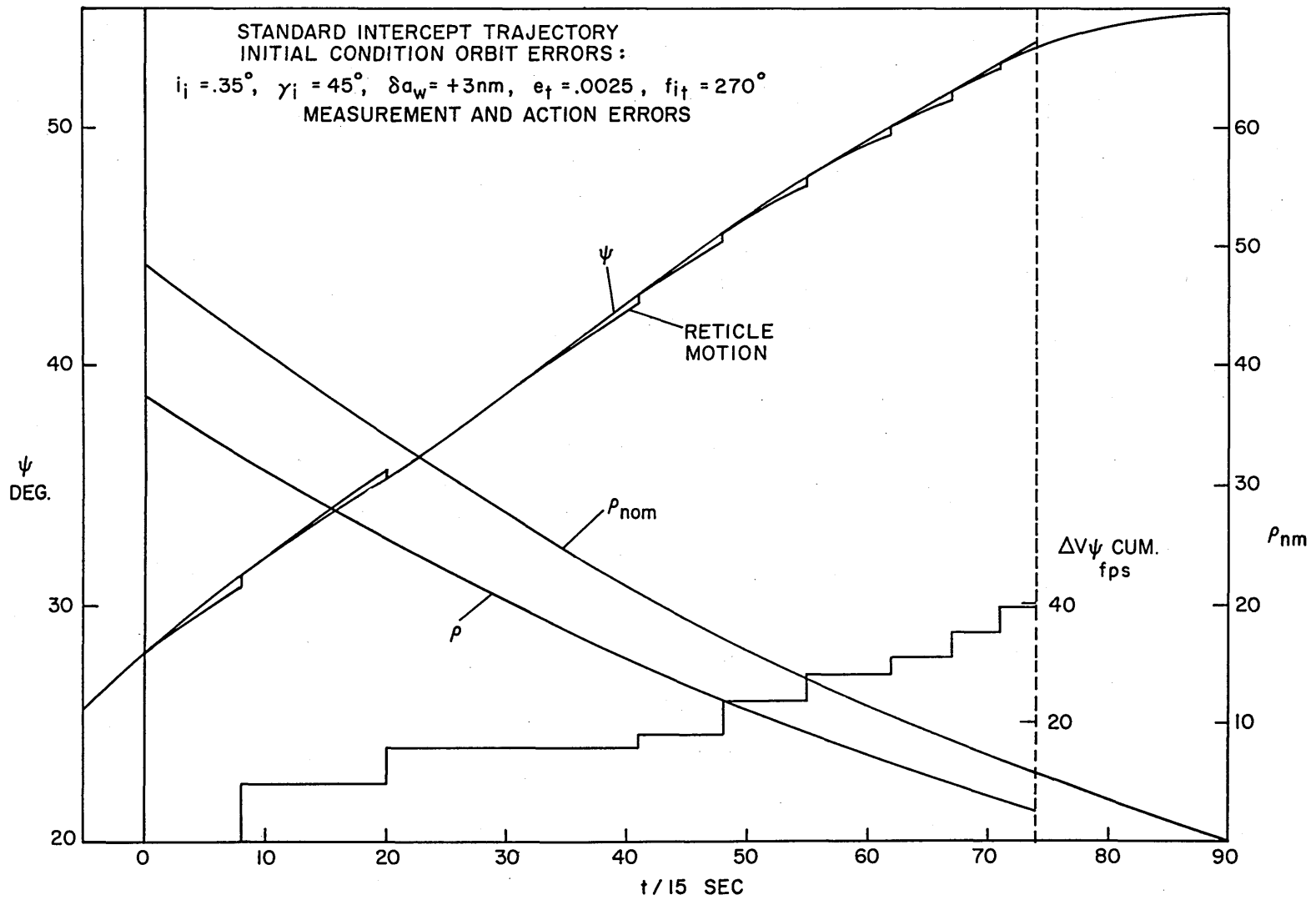


Fig. 8-2b Detailed Presentation of a Rendezvous Simulation ( continued )

reticle motion as it is centered initially then follows the nominal  $\phi$  and  $\psi$  variation until being re-aligned following a velocity correction. The simulation is terminated when  $\rho$  becomes less than about 2.5 nm, which is the approximate range at which a braking maneuver would commence. At this point the relative velocity of the two vehicles is 195.1 fps of which 194.9 fps is along the line of sight and 9.1 fps is perpendicular to the line of sight. (Usually the perpendicular velocity is of the order of 3 or 4 fps.) Eight  $\phi$  corrections have been made totaling 100.5 fps and eight  $\psi$  corrections totaling 39.4 fps. The total velocity change requirement including the final relative velocity is 443.2 fps.

The first  $\phi$  correction was made one interval late due to the random tracking error and when it was made the reticle deviation was 13.2 mils. The additional interval  $\Delta t$  in the guidance equation made the correction too small and this explains the larger second correction. With nonimpulsive thrusting, at the acceleration levels of the Gemini vehicle, much of the first three or so minutes of the intercept would be spent under a thrusting condition. The long time interval between the third and fourth  $\phi$  corrections and the size of the fourth correction in comparison with the size of the fifth correction and its time interval are worthy of note. The guidance equations assume a linear variation between time intervals which obviously is far from correct for the fourth correction. The resulting undercorrection then calls for a larger correction after a shorter time interval. The initial condition errors for this simulation produce a distinct tendency to rendezvous too soon.



Considering the  $\alpha_p$  angle and the direction of  $\psi$  corrections it can be seen that both  $\phi$  and  $\psi$  corrections have components away from the target and therefore tend to delay the rendezvous. However, from the  $\rho$  curve it can be seen that the rendezvous will still occur some 135 seconds or about 9 degrees early.

With this evidence of how the guidance system corrects itself for any misapplication of corrections plus the rate at which deviation errors build up and in consideration of the low thrust levels for velocity corrections, perhaps now the reader will at least partially agree with the conclusion of the author that possibilities definitely exist for direct pilot control of the corrections thereby dispensing with the guidance equations altogether and eliminating the need for radar during the guidance phase. Then, if the initial condition orbit errors can be held to a sufficiently low level or through the use of a nominal relative inclination and a  $\gamma_i$  as a function of time, the computation and radar requirements of the  $\Delta V_{iz}$  determination can be eliminated, a simple low power radar would only be needed for the braking phase.

The effects of rather large drift rates in the inertial reference unit of the sight reticle can now be better understood. A low precision drift rate of  $5^\circ/\text{hr}$  would produce a deviation of 5 mils in about 14 time intervals of the time scales shown in Figs. 8-2a and 8-2b. Though undoubtedly this drift error would affect the magnitude and spacing of corrections, the effect would not be cumulative since the reticle is re-centered after each correction. The overall effect would be that the  $\phi$  and  $\psi$  functions would no longer represent the nominal trajectory, but instead would closely resemble some neighboring intercept trajectory.

### 8.3 A Comparison of Modes of Operation

The four modes of operation under comparison are the combinations of the presence or absence of the variable  $\gamma_{12}$  computation for  $\Delta V_{iz}$  and the use or nonuse of radar range information for the same computation and in the guidance equations. Figure 8-3 presents all four of these modes of operation for the standard intercept trajectory under the same sets of conditions used previously. The comparison shows that with the exception of the initial condition represented by a target true anomaly of  $270^\circ$ , the velocity requirements follow the same pattern, with the computation and radar mode producing slightly more economical results. The reasons for the higher requirements for the no-radar modes are a combination of a slightly higher  $\Delta V_{iz}$  result and a slight  $\phi$  overcorrection in the terminal phases. The higher than needed  $\Delta V_{iz}$  component requires an early  $-\psi$  correction which causes the rendezvous to occur earlier with higher closing velocities. (Reference the detailed simulation in the previous section.) Direct pilot guidance should compensate for some of these tendencies in the no-radar modes in the author's opinion.

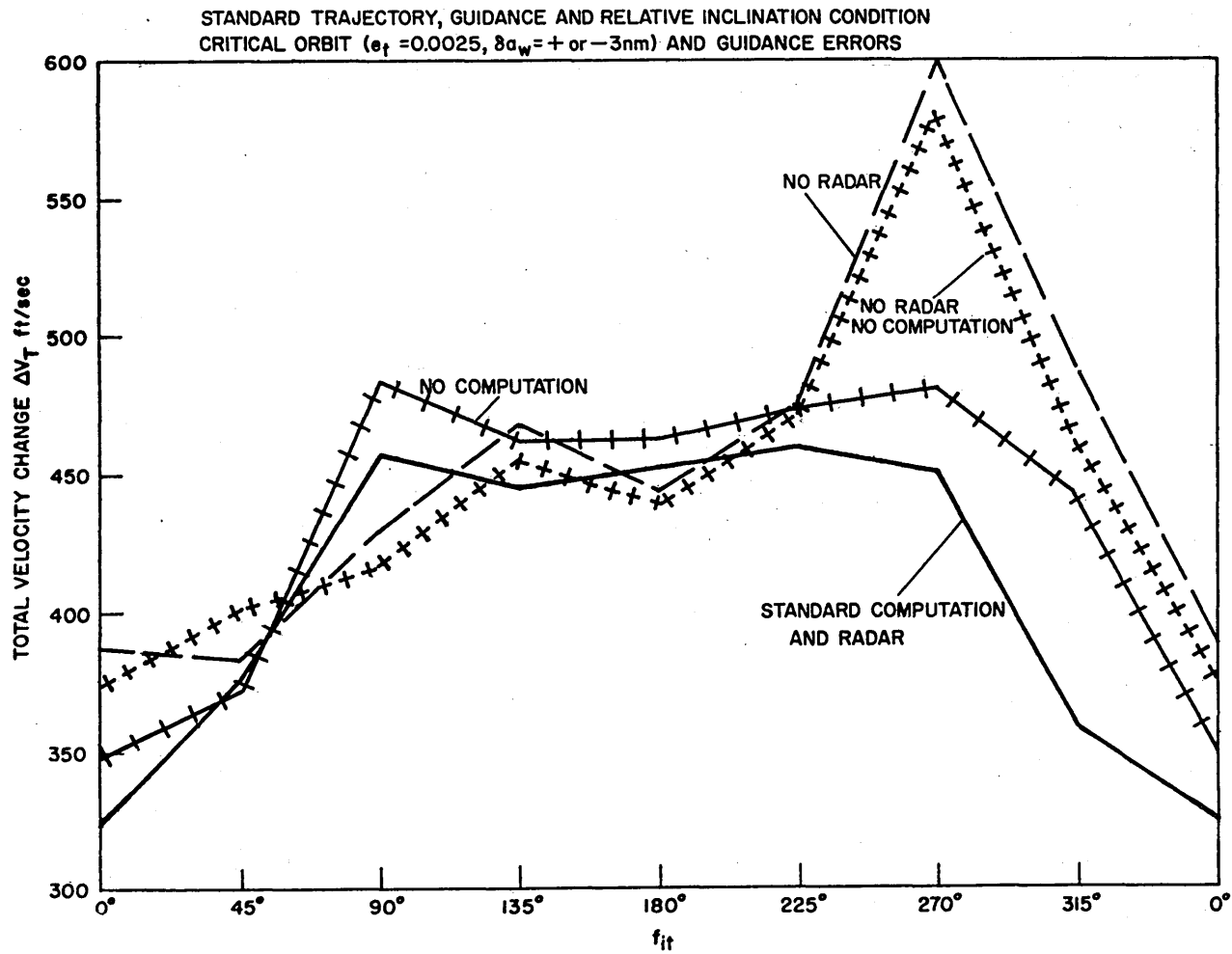


Fig. 8-3 Comparison of Modes of Operation

#### 8.4 Standard Intercept Compared with Other Trajectories

The intercept trajectories selected for comparison with the standard intercept all nominally traversed about  $90^\circ$ . This value was used in consideration of the relatively large portion of total velocity requirements needed to handle the out-of-plane situation. The intercepts ranged from tangential departure from the waiting orbit to tangential arrival at the target orbit. The  $a_p$  values were determined from an analysis similar to that of Fig. 7-1. The rendezvous parameters and  $a_p$  angles for the intercepts whose simulation results are given in Fig. 8-4 are as follows:

- |                  |              |                    |                            |
|------------------|--------------|--------------------|----------------------------|
| 1. $b = 0,$      | $k = 1.0$    | $a_p = 20^\circ$   | (Tangent to waiting orbit) |
| 2. $b = 0.2115,$ | $k = 0.8175$ | $a_p = 20^\circ$   |                            |
| 3. $b = 0.5,$    | $k = 0.715$  | $a_p = 30^\circ$   | (Minimum planar velocity)  |
| 4. $b = 0.73,$   | $k = 0.78$   | $a_p = 35^\circ$   |                            |
| 5. $b = 0.9931,$ | $k = 1.0$    | $a_p = 47.5^\circ$ | (Tangent to target orbit)  |

The combination of eccentricity and semi-major axis errors and inclination and  $\gamma_i$  were kept the same as those previously found most critical for the standard intercept. Certainly these are not necessarily the most critical conditions for the other intercepts. (The two tangential intercepts would be more critical with  $\gamma_i$  resulting in higher out-of-plane components at the points of tangency.) Nonetheless, the velocity requirement results clearly demonstrate the superiority of the standard trajectory. The horizontal lines indicate the velocity requirements with no initial condition orbit errors. As intimated previously, the intercept most sensitive to guidance control is the one

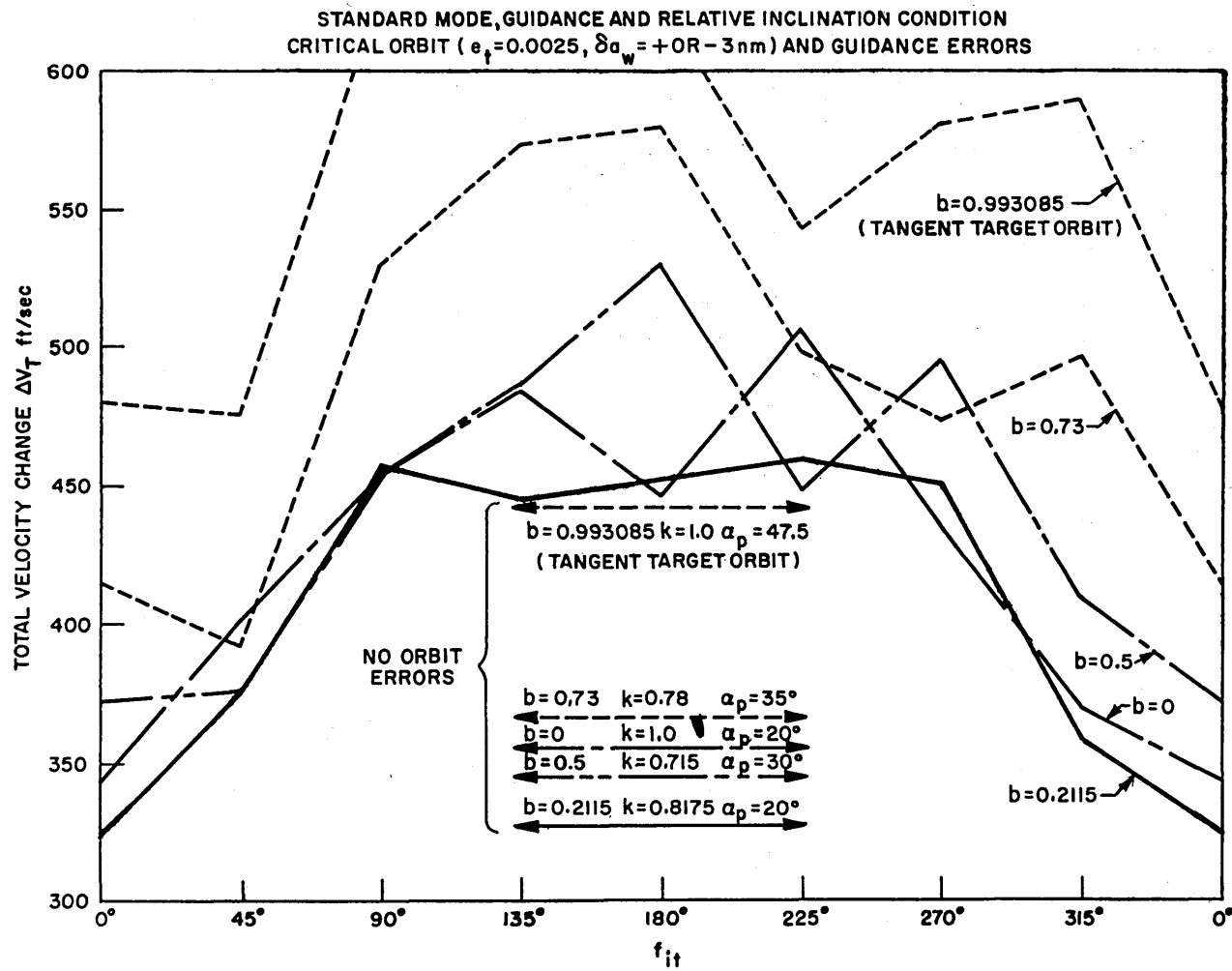


Fig. 8-4 Standard Trajectory Compared with Other Trajectories

with a tangential arrival at the target. The intercept of  $b = 0$ ,  $k = 1$  representing a tangential departure from the waiting orbit is second best to the standard intercept in terms of velocity requirements; however, the initial ranges and  $\beta$  angles are greater as are the terminal closing velocities - both undesirable characteristics. This type of intercept will be mentioned later in Chapter 10 in connection with the Apollo lunar landing abort rendezvous problem. The selected  $\alpha_p$  angles may not be exactly optimum for the other intercepts but they are certainly not much in error.

As part of the intercept trajectory comparison, several simulations were made of rendezvous maneuvers going outside the target orbit and traversing a nominal  $270^\circ$ . Though these are impractical from an optical standpoint since the target passes through the horizon and the terminal conditions have the Earth in the background, the purpose was to demonstrate that the derived guidance system is not necessarily limited to short duration intercepts. The initial  $\alpha_p$  analysis for the selected trajectories gave angles of  $40^\circ$  which naturally led to greater correction velocity requirements. For these longer duration missions a constant  $\alpha_p$  is certainly not as good an approximation as for the  $90^\circ$  intercepts. The correction pattern was similar to the shorter missions in that several large initial corrections were followed by long intervals of no corrections, terminating in several small quick corrections. Initial condition errors did not produce large changes in the final true anomaly as might be expected from total intercept time, rather these changes were comparable to those produced in single

intersecting orbits. The results of these simulations for the same  $i = 0.35^\circ$ ,  $\gamma_i = 45^\circ$ , and nominal orbital radii are tabulated below:

<u>Rendezvous Parameter Orbit Errors</u>				<u>Velocity Requirements</u>
<u>b</u>	<u>k</u>	<u><math>\delta a_w</math></u>	<u><math>f_{it}</math> (<math>e_t = 0.0025</math>)</u>	<u><math>\Delta V_T</math></u>
0.2115	0.8175	0	—	409
		-3 nm	$90^\circ$	681
		+3 nm	$180^\circ$	424
		+3 nm	$270^\circ$	439
0.300	0.762	0	—	436
		-3 nm	$90^\circ$	526
		+3 nm	$180^\circ$	517
		+3 nm	$270^\circ$	447

Upon closer analysis it appears that a constant  $a_p$  of about  $30^\circ$  should produce better results. If one were interested in investigating these longer intercepts in more detail, strong consideration should be given to merely forgetting about the  $\Delta V_{iz}$  computation and make the plane change whenever the relative line of nodes occurred. The penalties associated with such a three-impulse maneuver might well be less than allowing for an arbitrary  $\gamma_i$  and accepting  $\psi$  guidance throughout the intercept.

Finally, in an attempt to compare these techniques of variable line-of-sight guidance with schemes whereby the angular rate of the line of sight is continually corrected to zero, some simulations were made with all zeros fed in as the  $\phi$  and  $\psi$  curves. From a quick analysis of the line-of-sight motion for various intercepts the conclusion

is reached that if the interceptor is initially on a trajectory which has a  $b < 0.5$ , the initial correction to keep the line-of-sight constant will soon cancel out the relative closing velocity. The first runs were for an intercept with  $b = 0.73$  and  $k = 0.78$  for which the total  $\phi$  variation is small. With zero relative inclination and zero orbit errors the velocity requirement was 396 fps and when only the same inclination  $i = 0.35^\circ$ ,  $\gamma_i = 45^\circ$  was introduced this rose to 822 fps. Next, runs were made for  $b = 0.9931$ ,  $k = 1.0$ , or nominally tangent to the target orbit. The requirement for zero relative inclination and zero orbit errors was 347 fps and this rose to 637 with the same inclination conditions. When an orbit error of  $\delta a_w = -3\text{nm}$  and  $e_t = 0.0025$ ,  $f_{it} = 135^\circ$  was introduced, the vehicles did not even come close to a rendezvous.

#### 8.5 Effects of Variations in the Pitch Down Angle $\alpha_p$

The general trend observed in Fig. 8-5 which shows the results of variations in the angle  $\alpha_p$  for the standard intercept trajectory is to shift the orbit error conditions which produce the maximum velocity requirements. When  $\alpha_p$  is increased the sensitivity to negative  $\delta a_w$  errors which occur near  $f_{it}$  of  $135^\circ$  is increased and the effect of positive  $\delta a_w$  errors remains about the same. (Refer to Fig. 7-6.) Conversely when  $\alpha_p$  is decreased the sensitivity to positive  $\delta a_w$  errors which occur near  $f_{it}$  of  $225^\circ$  and  $270^\circ$  is increased and the effect of negative  $\delta a_w$  errors remains essentially the same. Another effect which is actually part of the explanation of the previous one is that the



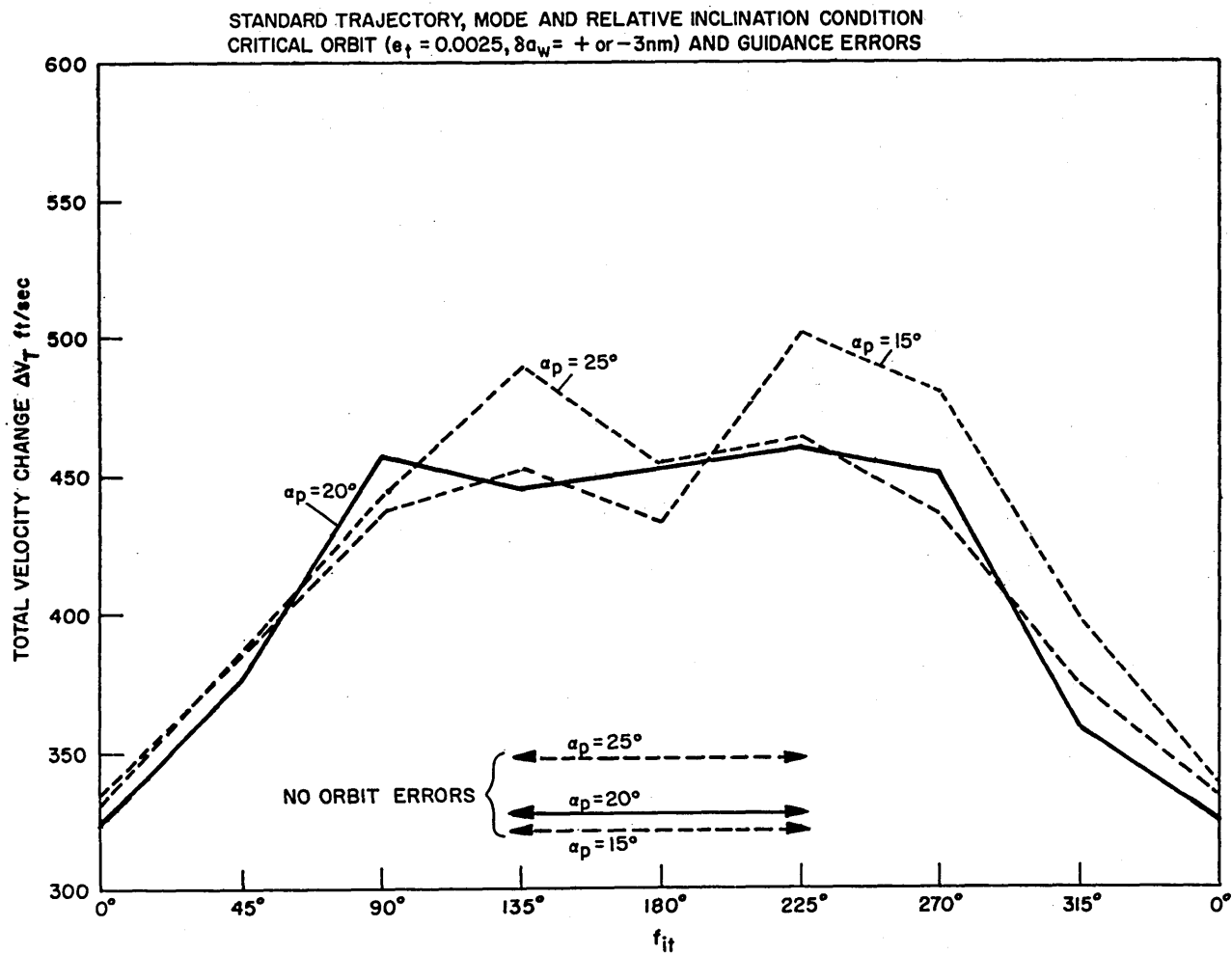


Fig. 8-5 Effects of Variations in Pitch Down Angle  $\alpha_p$

magnitude of the  $\phi$  corrections is increased as  $\alpha_p$  increased due to the division by  $\cos \alpha_p$  in the guidance equation. This is evident in the no-orbit error cases portrayed by the horizontal lines in Fig. 8-5.

#### 8.6 Effects of Variations in the Radial Distance d

The purpose of this analysis is to see what the tolerances in the nominal distance d are under the same orbit error conditions with a view toward updating the interceptor's knowledge of his semi-major axis as the result of ground supplied information. The considerations are that as d increases the error effects decrease but the nominal fuel requirements increase and as d decreases, though the nominal fuel decreases, the orbit errors should have a greater disturbing effect. The effects of 5 nm changes in d are portrayed in Fig. 8-6. The results show that the nominal d of 25 nm is less sensitive to decreases than increases. The higher requirements for an  $f_{it}$  of  $225^\circ$  and  $270^\circ$  where it should be recalled that  $\delta a_w$  is +3 nm also suggests in view of the analysis of the previous section that perhaps  $\alpha_p$  should be increased slightly. These results also clearly indicate that quite beneficial results can be obtained by updating the nominal d and hence the magnitude of  $\Delta V_{ip}$  on the basis of ground supplied tracking information. In these examples if d was not corrected  $\delta a_w$  would be 8 nm in some cases, and these errors would probably be intolerable.

STANDARD TRAJECTORY, MODE AND RELATIVE INCLINATION CONDITION  
 CRITICAL ORBIT ( $e_T = 0.0025$ ,  $\delta a_w = + \text{ or } - 3\text{nm}$ ) AND GUIDANCE ERRORS

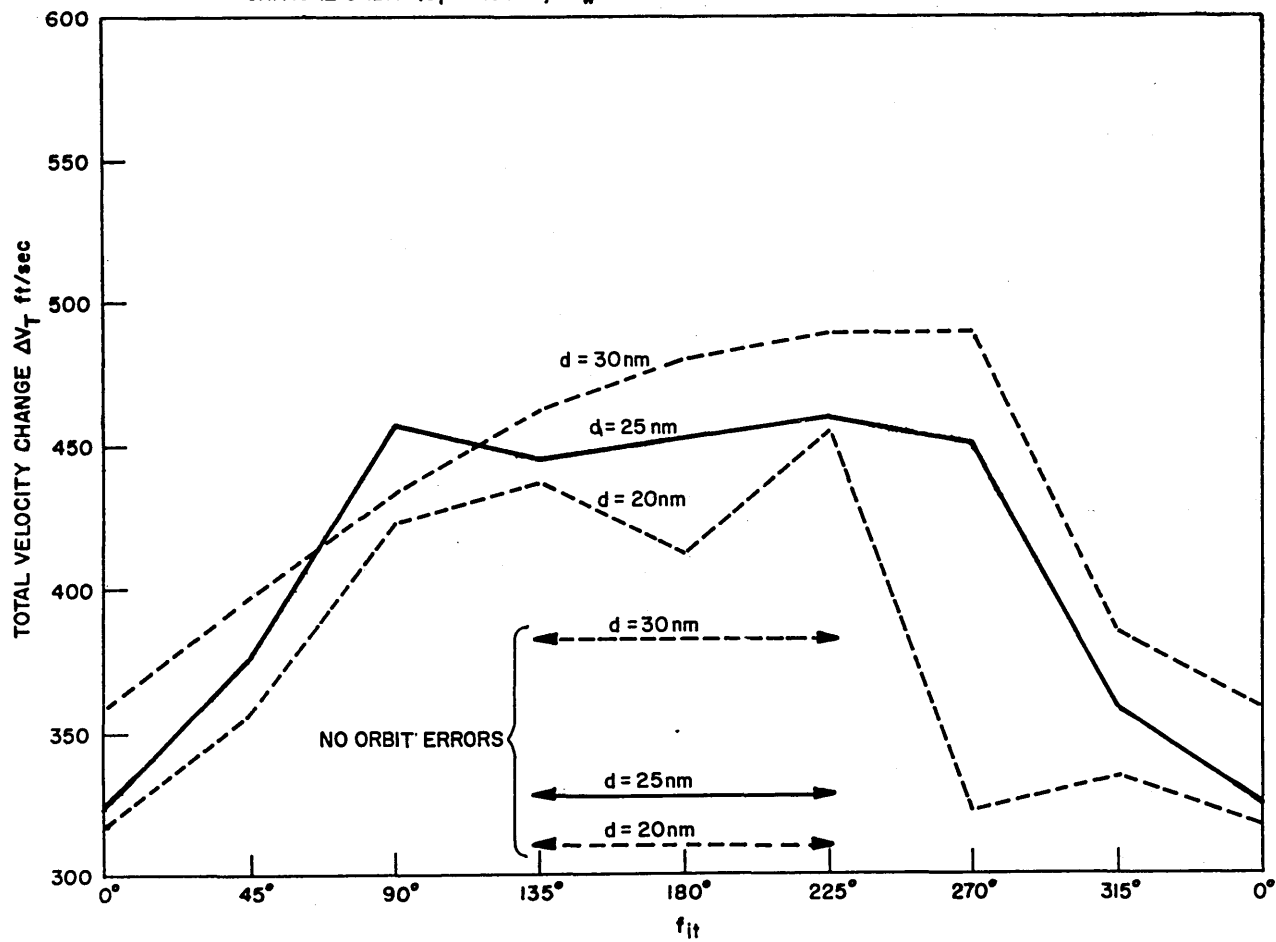


Fig. 8-6 Effects of Variations in Nominal Radial Distance  $d$

### 8.7 Effects of Variations in Reticle Size

Results of simulations run for the standard intercept with the same standard errors as portrayed in Fig. 8-7 seem to indicate that considerable latitude exists in the choice of reticle size. The 5-mil reticle originally selected is felt to be about the minimum size commensurate with human optical tracking capabilities. Naturally the smaller the size the tighter the control, with more corrections of a smaller magnitude. Twice the size reticle does not mean necessarily twice the size of the correction and half as many, since it takes longer for the deviation to occur, making the correction less than proportional to the reticle size, and errors have longer to build up which tends to require subsequent corrections sooner. Some beneficial results do however seem to be attainable through an increase to about 7.5 mils. Also indicated by the 7.5 mil results is the indication, as in the previous section, that some increase in  $\alpha_p$  may be warranted.

### 8.8 Effects of a Circular Reticle

The possibility of using a circular reticle and thereby economizing on the number and total magnitude of velocity corrections has been kept in mind ever since the original concept of the optical sight was conceived. The changes that permitted pointing the spacecraft at the target in the  $\psi$  direction made this all the more practical; however, the additional use of a constant pitch down angle involves some compensating disadvantages. Such a technique would require

STANDARD TRAJECTORY, MODE AND RELATIVE INCLINATION CONDITION  
 CRITICAL ORBIT ( $e_t = 0.0025$ ,  $\delta a_w = + \text{ or } -3\text{nm}$ ) AND GUIDANCE ERRORS

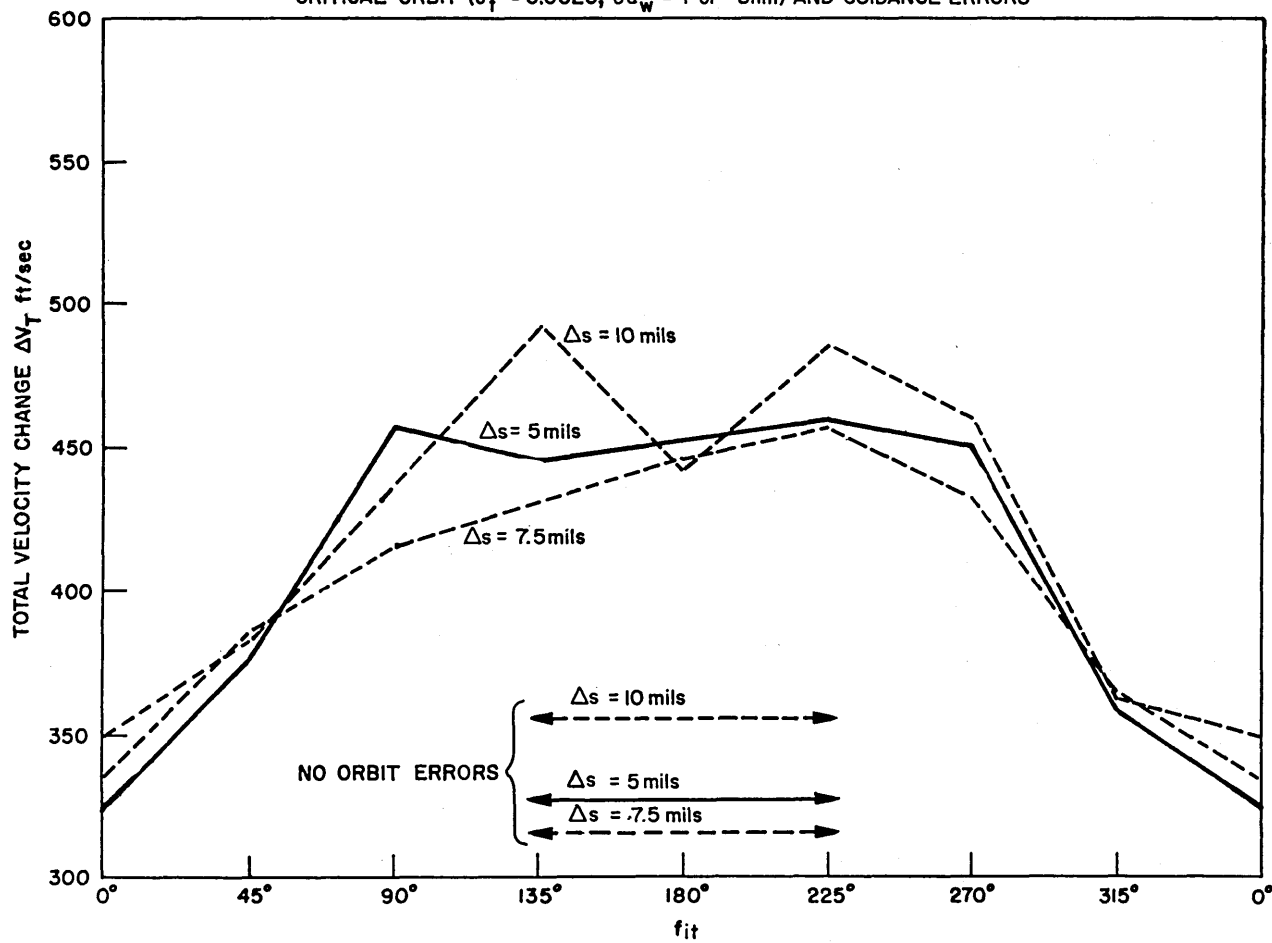


Fig. 8-7 Effects of Variations in Size of Square Reticle

rolling the spacecraft to align one of the four thrust nozzles opposite to the desired velocity correction. This naturally takes fuel plus additional attention to attitude control.

In an effort to investigate just how great the benefits might be from such a technique the simulation program was rewritten to incorporate this mode of operation. To account for the increased inaccuracies in roll attitude the one-sigma attitude error in this direction was multiplied by a factor of five making its value about  $5.8^\circ$ . The results of these simulation runs for the standard trajectory with a 5-mil circular reticle are compared with the 5-mil square reticle results in Fig. 8-8. The angles for each run indicate the total roll angle needed for attitude changes. These figures are obtained by rolling the spacecraft from the normal upright attitude through the smallest angle to align the thrust nozzle, then returning to the upright attitude and summing the total angles traversed. Though the total number of corrections needed decreased somewhat, the total velocity requirements were only slightly less. In consideration of the fuel needed for attitude changes plus the attendant complications required for the sight to indicate the desired direction of correction it seems not at all worth while to incorporate the circular reticle mode of operation.

#### 8.9 Effects of Variation in $\gamma_1$

Since most all of the simulations have been conducted under the assumption that a  $\gamma_1$  of  $45^\circ$  reflects a near maximum in critical

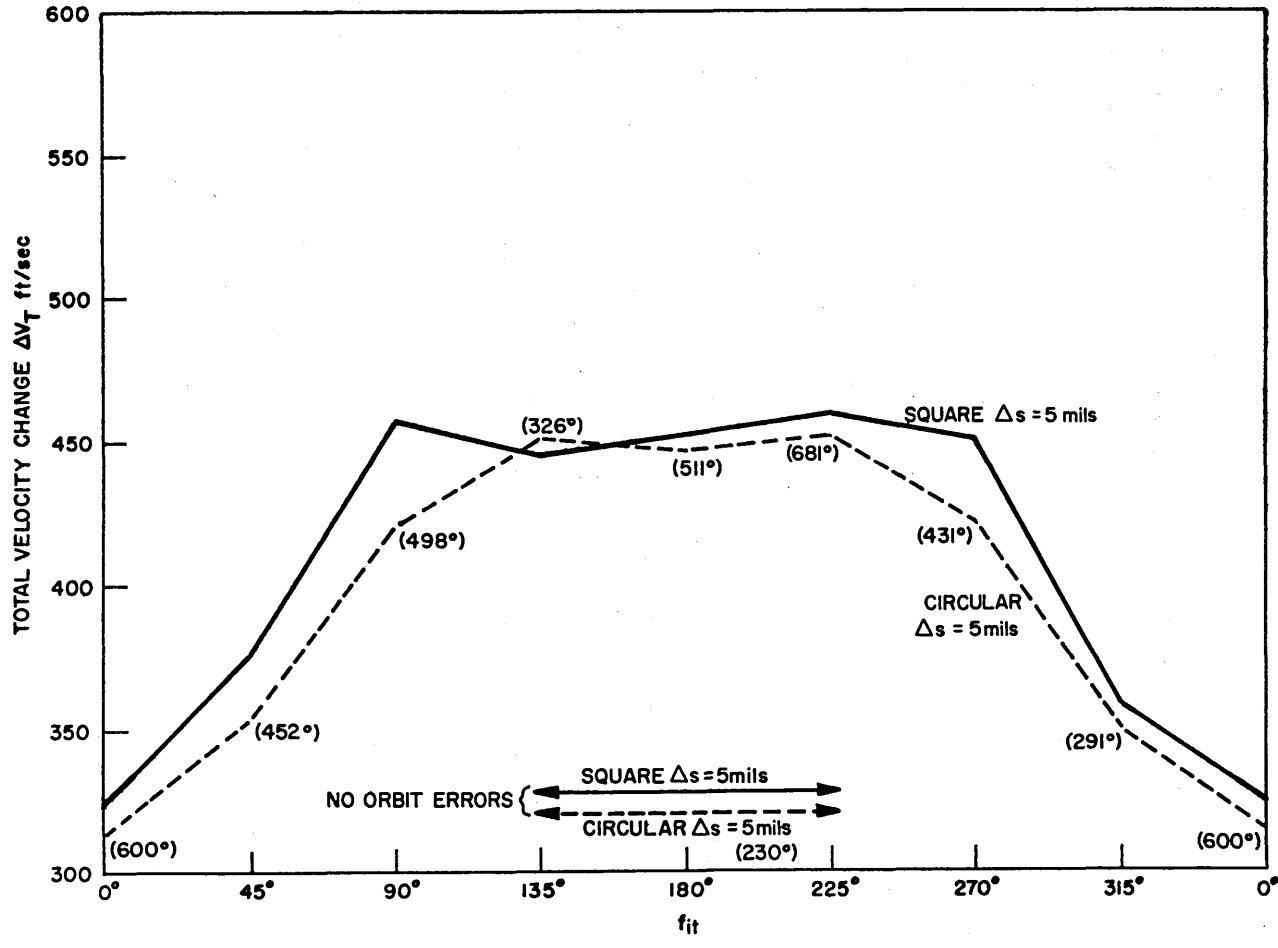


Fig. 8-8 Effects of a Circular Reticle

requirements for velocity change, a check on this appears in order. To do this the critical initial condition orbit errors of  $\delta a_w = +3$  nm and a lumped  $e_t = 0.0025$  with  $f_{it} = 225^\circ$  were selected since they indicate a near-maximum requirement for  $\gamma_i = 45^\circ$ . The results for  $\gamma_i$  variations from  $0^\circ$  to  $180^\circ$  are presented in Fig. 8-9 along with the no-error results previously given. For  $\gamma_i$  of  $180^\circ$  to  $360^\circ$ , the results would be identical, assuming a symmetrical astronaut.

Theoretically, due to the fact that the nominal trajectory traverses  $90^\circ$  (rather than due to any astronaut characteristics), angles less than  $180^\circ$  should produce the same results as the same angles from  $0^\circ$ . That this is not the case is undoubtedly due to the  $\Delta V_{iz}$  computation. It appears as though the orbit plane bias error producing errors in  $\psi_1$  and  $\psi_2$  give rise to greater errors in the inherent computation of the magnitude of the relative inclination. When  $\psi$  is decreasing prior to a  $\gamma_i$  near  $180^\circ$  its changes with time are less; hence it is more sensitive to observational error than for a  $\gamma_i$  the same angle from  $0^\circ$  where  $\psi$  is increasing prior to reaching  $\psi_i$ . ("Live and learn", as the saying goes. If one had the insight to figure all this out from the beginning, there would be little point in going through all this analysis.)



STANDARD TRAJECTORY, MODE AND GUIDANCE,  $i_t = 0.35^\circ$   
 CRITICAL ORBIT ERROR ( $e_t = 0.0025 f_{it} = 225^\circ$ ,  $\delta a_w = 3 \text{ nm}$ ) AND GUIDANCE ERRORS  
 COMPARED WITH NO ERRORS

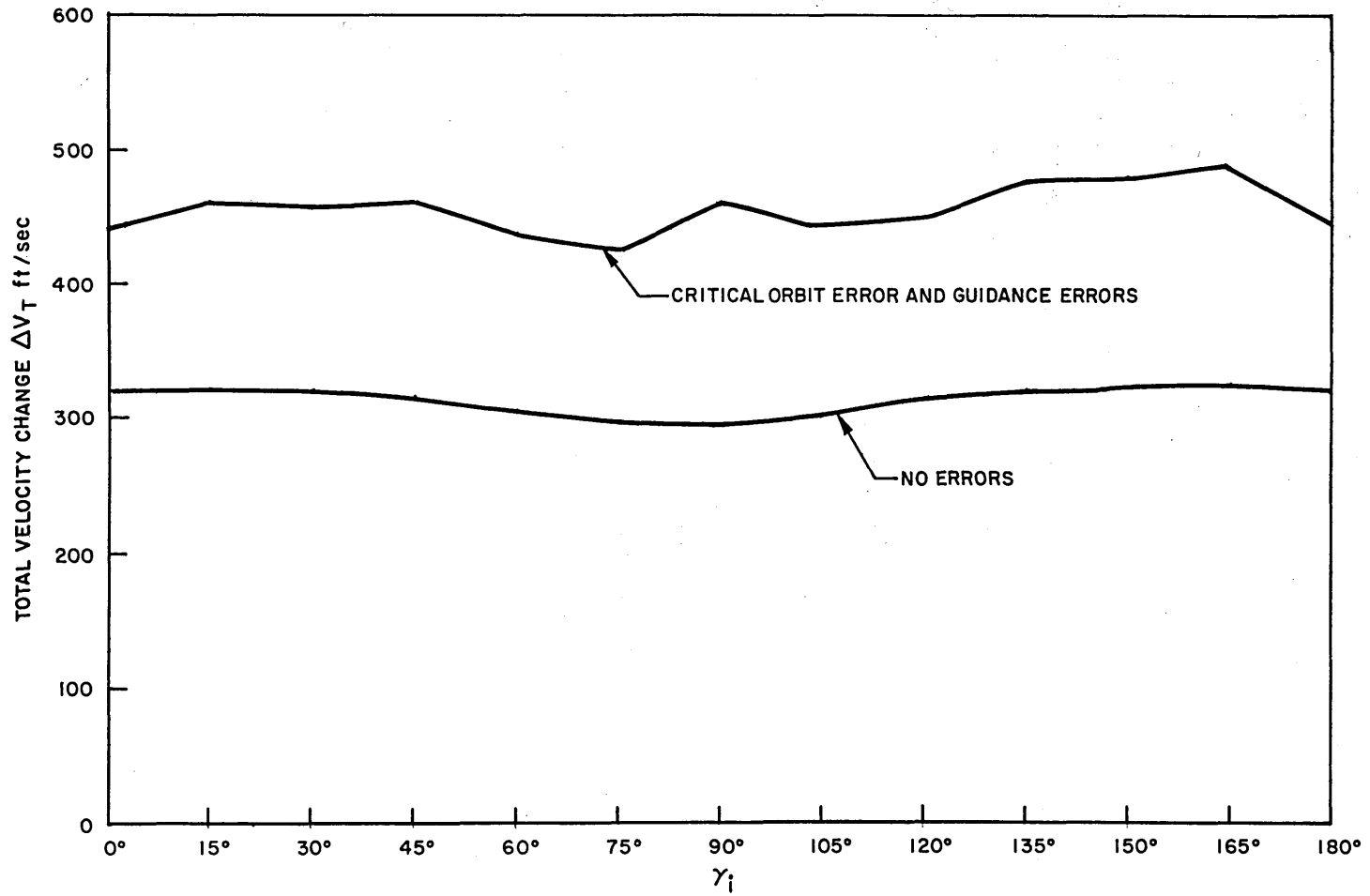


Fig. 8-9 Effects of Variations in  $\gamma_i$  on a Critical Orbit Error

#### 8.10 Extension of Results to Other Earth Missions

To demonstrate how well the results of the preceding specific Gemini mission application can be generalized to other Earth orbit rendezvous missions, the author has selected two other missions and applied similar sets of error conditions to observe their performance. The first extension supposes the target in the same nominally circular orbit at an altitude of 150 nm but now it is desired for the intercept to be made from a nominally circular orbit at a 100 nm altitude traversing twice the radial distance as before. The contention is that by doubling all the orbit errors including the relative inclination, the velocity requirements should also be doubled following the same distribution pattern with error true anomaly. The second extension changes the altitude of the target but keeps the radial distance traversed the same. For this mission the target is at 300 nm and the interceptor waiting orbit is at 275 nm which might be typical conditions for an orbiting space station assembly (now that the Apollo earth orbit rendezvous option is defunct). For this mission the contention is that if the errors are kept the same the velocity requirements should be essentially the same.

The results of these extension simulations are presented in Fig. 8-10 where for ease in comparison the actual results of the 100 nm to 150 nm rendezvous mission have been divided by two. The validity of the contention thus appears to be reasonably established. For some

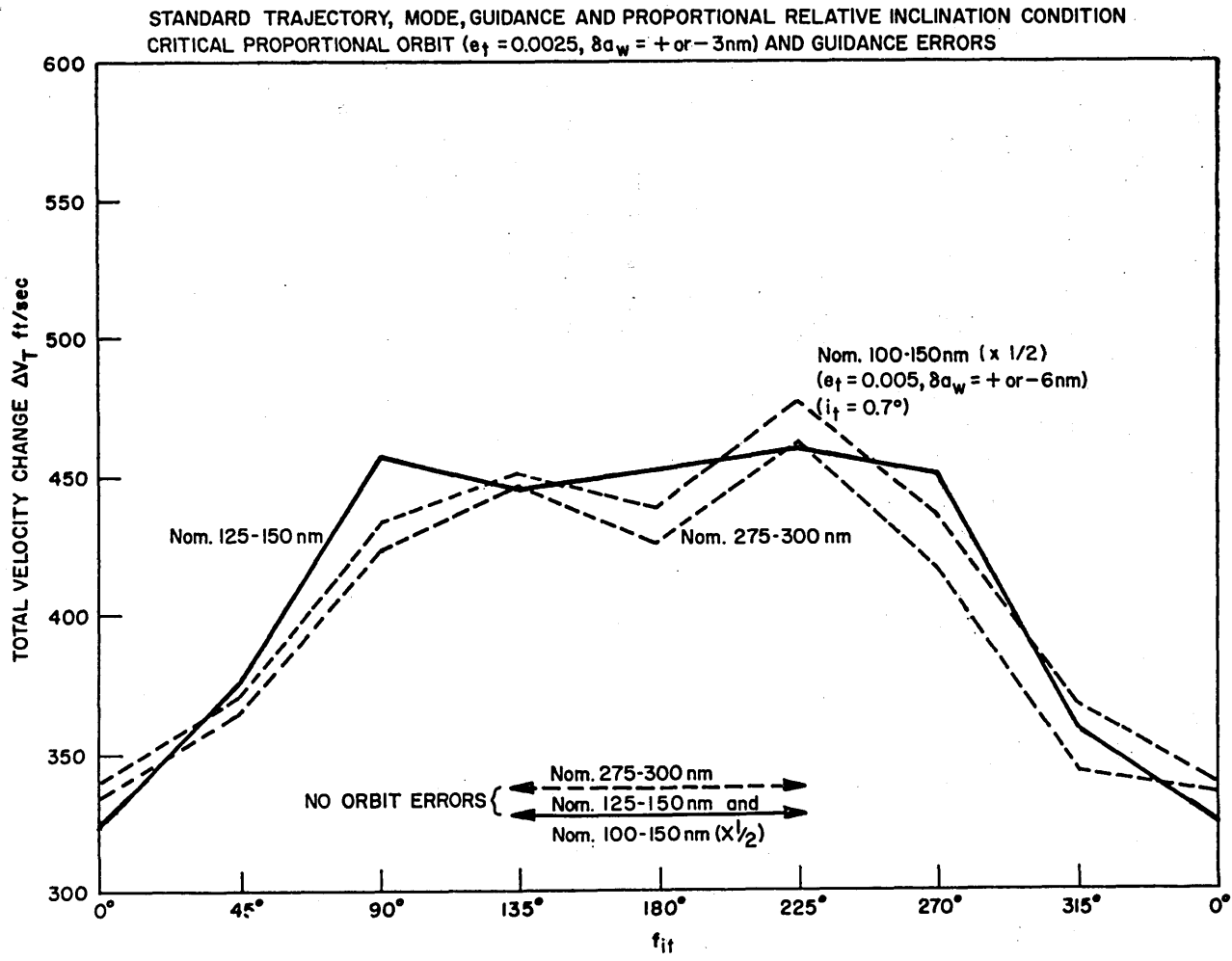


Fig. 8-10 Extension of Results to Other Earth Orbit Missions

unknown reason the two extensions appear to be actually more similar to each other than to the model from which they are extended. The slightly lower requirements at the higher altitude is clearly due to the slightly lower absolute velocities of the two vehicles involved. Extensions to other missions appear only to be simply a matter of scaling the radial distances and the radial orbit errors. The theoretical effects of different inclinations can be readily obtained from simple calculations and the actual effects should be near linear unless they greatly exceed the proportions examined here.

#### 8.11 Extension of Results to Lunar Orbit Missions

In demonstrating the extension of the results to lunar orbits, the desire is to find a practical mission that would have essentially the same velocity requirements at the Moon as the specific Gemini mission has around the Earth. Then the same scaling effects would be applicable. An interceptor waiting orbit altitude of near the surface is desired as being meaningful in view of the Apollo mission. The determination of the distance  $d$  to give the same nominal velocity requirement, which in effect would be a relative comparison of the maneuver capability around the Moon with that around the Earth, came as a considerable surprise to the author. The considerations that usually first come to mind are the fact that the orbital velocities are about 5 times smaller around the Moon and the gravitational attraction at the surface of the Moon is about  $1/6$  that of the Earth. The fact that

the radius of orbital motion is less than 1/3 usually does not immediately come to mind. The approximate formula, derived previously, for the Hohmann characteristic velocity should give a very close indication of relative maneuver capability.

$$\Delta V_H = V_c \frac{d}{2 r_f}$$

Equating characteristic velocities for near-surface radial maneuver capabilities the surprising conclusion is reached that they are in the ratio of 7 to 5 for Moon to Earth. In other words the velocity needed for a 25-nm radial maneuver capability around the Earth would result in only a 35-nm capability around the Moon. It is just not true, as some people seem to believe, that maneuvering around the Moon is far easier than around the Earth.

To test the extension of the developed line-of-sight guidance techniques to lunar missions in view of the above result, a target altitude of 100 nm and an interceptor waiting orbit of 65 nm above the surface was selected. The scaling of the relative inclination conditions of  $0.35^\circ$  to produce the same velocity requirements produced a relative inclination for the lunar orbits of  $1.7^\circ$ . For the  $\delta a_w$  errors the round number of 4 nm was chosen instead of the more precise 4.2 nm. The eccentricity errors scaled to give the same ratio of radial displacements of 7:5 resulted in very nearly 5 times the Earth value and

an  $e_t$  of 0.0125 was selected. Curves were derived for the same rendezvous parameters as the standard Earth intercept trajectory. The increased size of the ratio  $d/r_f$  by a factor of about 5 produced slight changes in the trajectory. Instead of traversing  $90.7^\circ$  it now covered  $93.1^\circ$ . All the other properties are very nearly identical; the  $\Delta V_{ip}$  being only 1/2 fps less. Naturally the maneuver took longer - 31.5 minutes instead of 22.5 minutes.

The results of the simulations are compared with the standard Earth mission in Fig. 8-11. The close agreement is not only in total velocity requirements but also in the total number, the magnitude, and the spacing of velocity corrections. The time intervals between corrections are roughly in the same ratio as the respective orbital periods or about 3 to 2 thus easing the situation somewhat when consideration is given to nonimpulsive thrust maneuvers.

STANDARD TRAJECTORY, MODE, GUIDANCE AND PROPORTIONAL RELATIVE INCLINATION CONDITION  
 CRITICAL PROPORTIONAL ORBIT ( $e_t = 0.0025$ ,  $\delta_{aw} = +$  OR  $-3$  n.m.) AND GUIDANCE ERRORS

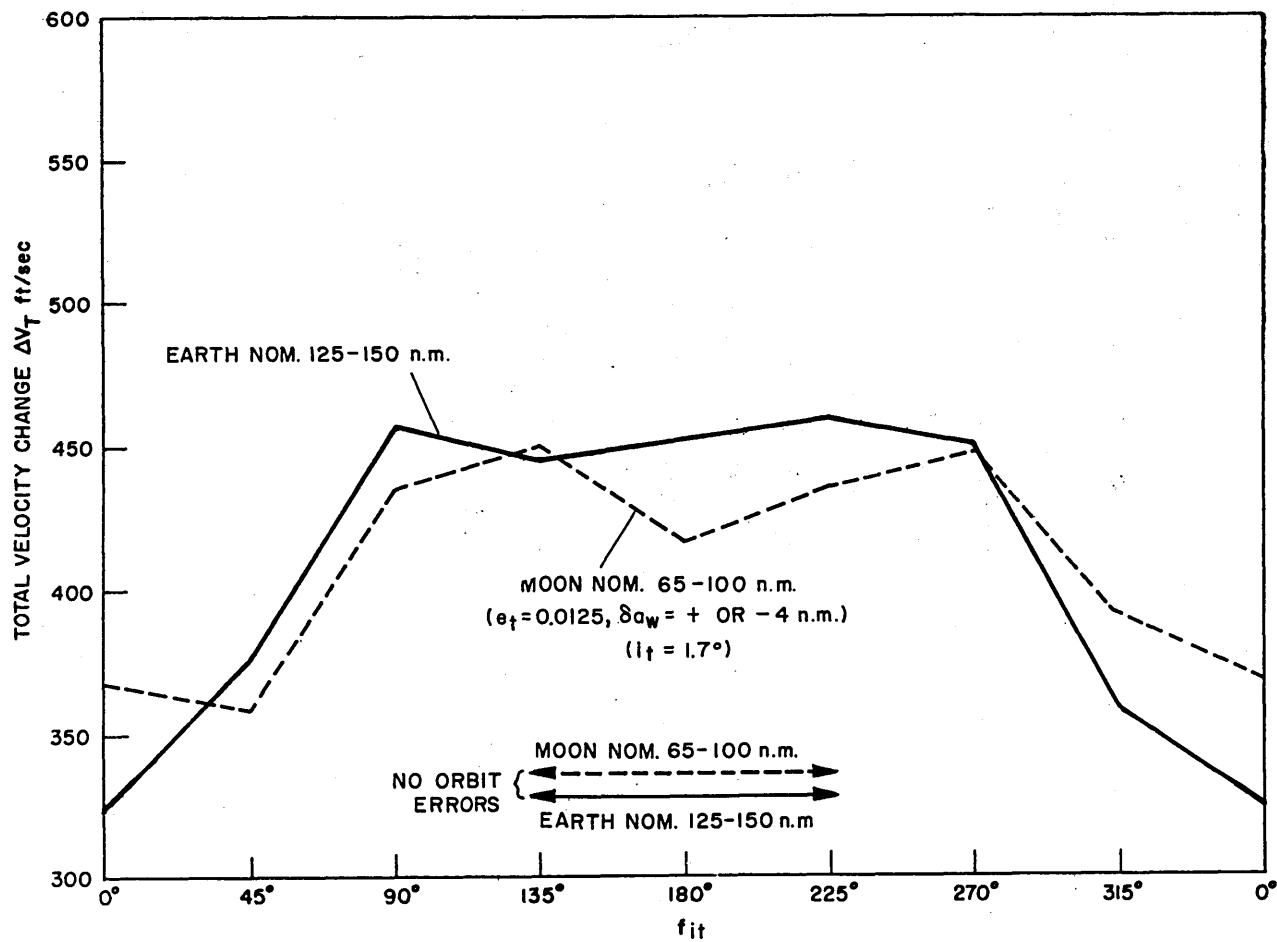


Fig. 8-11 Extension of Results to Lunar Orbit Missions

## 8.12 Error Effects on Extreme Coapsidal Elliptic Orbits

This section and the succeeding section deal with two different approaches to rendezvous with targets in elliptic orbits. The next section treats intercepts which originate from a nominally circular waiting orbit whereas this section examines intercepts departing a nominal coapsidal elliptic waiting orbit of near-equal ellipticity. The advantages of economy, simplicity and generality make the coapsidal elliptic waiting orbit the far superior method. Both approaches are included to make this fact more evident.

In order to superimpose an error ellipticity onto an elliptic orbit so that the resulting orbit will reflect the same range of velocity and position errors, an approximate analysis is needed to determine how the nominal eccentricity and true anomaly should be changed to reflect the changes due to a selected condition of error eccentricity and true anomaly. The model used in the following analysis assumes a simple sinusoidal radial variation with true anomaly. The eccentricity values themselves make this a close approximation and the fact that the model is used only in the near-vicinity of perigee makes it even better.

With this model then,

$$\Delta r_o = -a e_o \cos f_o$$

$$\Delta r_\epsilon = -a e_\epsilon \cos f_\epsilon$$

$$\Delta r = -a e \cos f$$

$$\Delta r = \Delta r_o + \Delta r_\epsilon$$



where the subscript o is the condition without errors,  $\epsilon$  refers to the error condition resulting from the error eccentricity and no subscript signifies the combined effect of the others. Now, differentiating the resulting expression for  $\Delta r$  with respect to  $f$  and setting this to zero to find the relation of  $f_o$  to  $f_\epsilon$  at actual perigee gives:

$$a e_o \sin f_o \frac{df_o}{df} + a e_\epsilon \sin f_\epsilon \frac{df_\epsilon}{df} = 0$$

For small  $e_\epsilon$  the changes of  $f_o$  and  $f_\epsilon$  for changes in  $f$  will be very nearly equal, hence:

$$\sin f_{op} = - \frac{e_\epsilon}{e_o} \sin f_\epsilon$$

where  $f_{op}$  is the true anomaly of  $f_o$  at actual perigee, so:

$$f = f_o - f_{op}$$

Now, substituting  $f = 0$  in the expression for  $\Delta r$  and dividing by  $-a$ :

$$e = e_o \cos f_{op} + e_\epsilon \cos f_\epsilon$$

Finally, the above three equations permit the calculation of  $e$  and  $f$  for say the waiting orbit given the no-error conditions  $e_o$  and  $f_o$  and desired error eccentricity conditions  $e_\epsilon$  and  $f_\epsilon$ .

Using the above relations with the same  $\delta a_w$  errors and  $e_w$  of 0.0025 together with the most critical case of Fig. 7-8 represented by  $f_{oiw}$  of  $315^\circ$ , actual values for  $e_w$  and  $f_{iw}$  were computed and simulations of intercepts to a target of eccentricity  $e_t = 0.05$  with perigee altitude of 113 nm and apogee altitude of 487 nm, again using the guidance information as if the orbits were nominally circular, are compared in Fig. 8-12 with the previous scaling results of the critical  $\delta a_w$  for an intercept between actual nominally circular orbits at 275 nm and 300 nm altitudes. The velocity requirement curves now as a function of  $f_{iw}$  instead of  $f_{it}$  show in addition to the  $180^\circ$  phase shift, a slight additional phase shift for the elliptic orbits which undoubtedly is due to the locations of the intercept maneuver near the perigee of the elliptic orbits rather than the eccentricity error application. The two peaks are again evident; one for the negative  $\delta a_w$  error, and one for the positive  $\delta a_w$  error.

The tremendous importance of these results is that they verify that coplanar elliptic target and waiting orbits with eccentricities defined by:

$$a_w e_w = a_t e_t$$

can be treated as circular orbits as far as line-of-sight rendezvous intercept techniques are concerned without introducing significant errors. The sensitivities of these rendezvous intercepts can then be obtained simply by analyzing the sensitivities of the circular orbits to  $\delta a_w$  errors and superimposed eccentricity errors.

STANDARD TRAJECTORY, MODE, GUIDANCE AND RELATIVE INCLINATION CONDITION  
(DERIVED FROM CIRCULAR ORBIT)

$e_t = 0.05$ , ALTITUDES: PERIGEE 113 n.m., APOGEE 487 n.m., SEMI-MAJOR AXIS 300 n.m.  
 $e_w = 0.05034$ , ALTITUDES: PERIGEE 88 n.m., APOGEE 462 n.m., SEMI-MAJOR AXIS 275 n.m.  
 CRITICAL INITIATION POINT:  $f_{it} = 315^\circ$ , SUPERIMPOSED ORBIT ERRORS ( $e_{ew} = 0.0025$ ,  $\delta a_w = +$  AND  $-3$  n.m.)  
 GUIDANCE ERRORS. COMPARED WITH RESULTS FROM NOMINALLY CIRCULAR ORBITS  
 180° PHASE SHIFT DUE TO WAITING ORBIT ERRORS INSTEAD OF TARGET ORBIT ERRORS

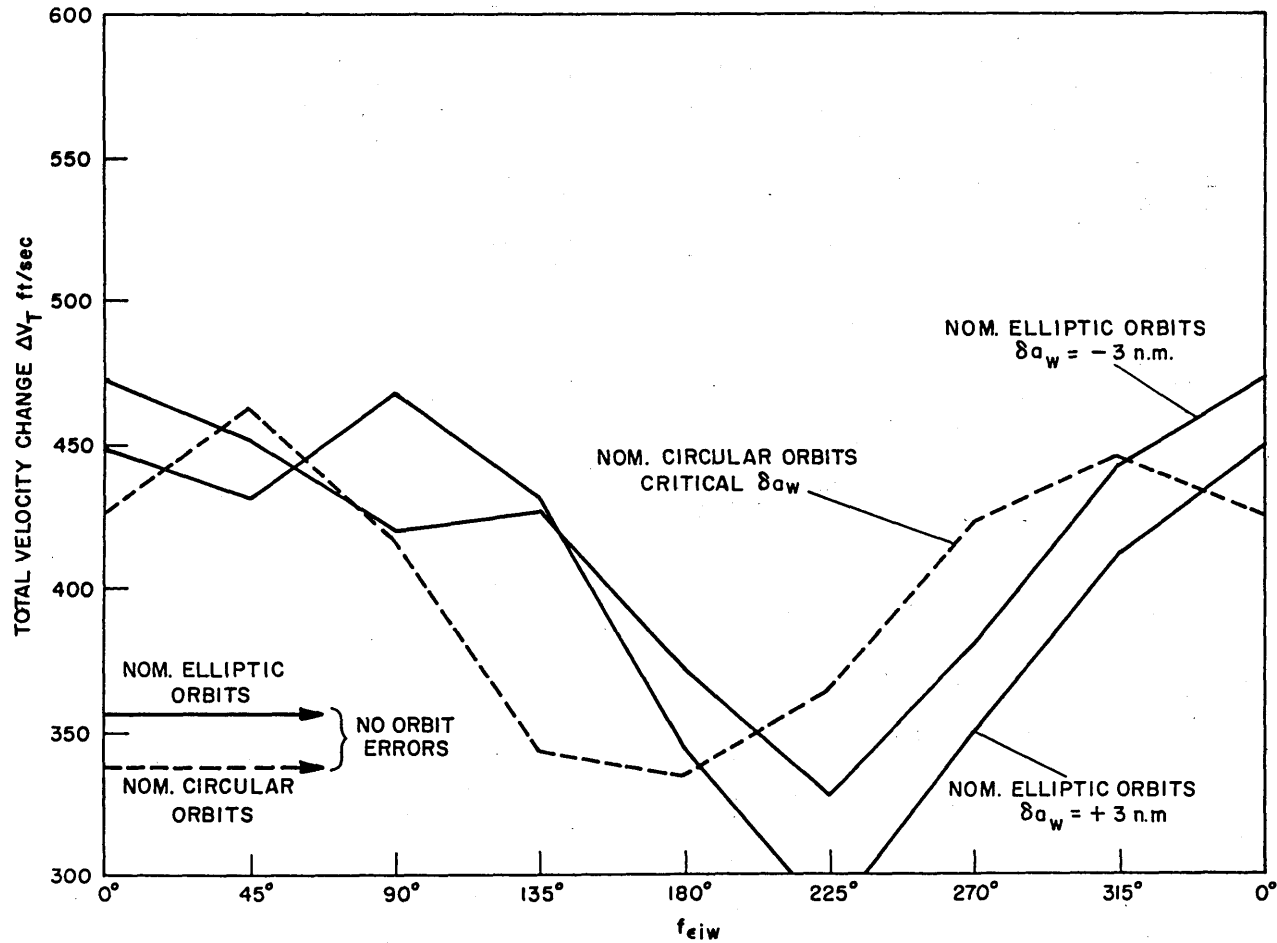


Fig. 8-12 Error Effects on Extreme Coapsidal Elliptic Orbits

### 8.13 Standard Intercept Line-of-Sight Motion for Elliptic Targets and Circular Waiting Orbits

Despite the definite superiority of using the coapsidal elliptic waiting orbit technique for rendezvous intercepts to elliptic orbit targets, the author has deemed it worth while to present briefly the error effects on the principle evolved in Section 5.3 whereby, through a transformation of the rendezvous parameters, an intercept from a circular waiting orbit to an elliptic target orbit can be found that has very nearly identical line-of-sight properties to a selected intercept between circular orbits. As a result of this principle, a constant set of  $\phi$  and  $\tan_N \psi$  curves can be used in the sight, and only the magnitude of  $\Delta V_{ip}$  and the angle  $\alpha_i$  are functions of the target true anomaly that exists at the start of the intercept.

As a model for testing this principle under orbit error conditions a nominally elliptic target orbit with eccentricity of 0.0025 and semi-major axis altitude of 150 nm and a nominally circular waiting orbit at an altitude of 125 nm was selected. By specifying the final target true anomaly and the pseudo intercept with a circular target as having the standard rendezvous parameters of:

$$b'' = 0.2115$$

$$k' = 0.8175$$

curves and parameters were obtained following the transformation of  $b'$  and  $k'$  for the actual intercept. As explained in Section 5.3 the  $\phi$  and  $\tan_N \psi$  curves thusly obtained do agree very closely with the circular case. The curves actually used for the simulations were in fact those derived from circular orbits and were identical for each condition of target true anomaly. The values of  $\Delta V_{ip}$  and  $a_i$  as a function of the nominal target final true anomaly are portrayed in Fig. 8-13. The values of  $b$  and  $k$  and  $d^f$  are also given for each  $45^\circ$  of target final true anomaly. The value  $d^f$  gives a relative measure of the magnitude of the final relative velocity and also indicates, in a sense, the sensitivity of the intercept to orbit errors as explained in Section 8.6. It can be surmised from Fig. 8-13, that intercepts with a nominal target final true anomaly near  $225^\circ$  should be the highest in velocity requirements whereas those with a true anomaly near  $45^\circ$  should be the lowest.

The initial conditions for the simulations consisted of the same relative inclination of  $0.35^\circ$  and  $\gamma_i$  of  $45^\circ$  as used previously and orbit errors of  $\delta a_w = \pm 3$  nm and  $e_w = 0.002$  instead of 0.0025. The results of these simulations in terms of velocity requirements versus  $f_{iw}$  are presented in Figs. 8-14a through 8-14h for nominal target final true anomalies at  $45^\circ$  intervals from  $0^\circ$  to  $315^\circ$ . In general the results indicate that the combinations of target nominal eccentricity of 0.0025 and semi-major axis errors of  $\pm 3$  nm with lumped error eccentricity

of 0.002 are slightly too large for the velocity change criteria originally established for the specific mission application. The only specific comment to be made is that in several cases where the target final true anomaly was  $0^\circ$  or  $45^\circ$  the error combinations resulting in reduced ranges delayed the arrival of  $\beta_i$  quite significantly making the angle  $\gamma_{li}$  much larger than it should be. In some cases the  $\beta$  angle actually reversed its motion and increased before decreasing again to  $\beta_i$ . In one case  $\gamma_{li}$  was as large as  $160^\circ$  instead of the nominal  $20^\circ$ . The effects of this situation are to make the  $\Delta V_{iz}$  computation considerably in error and to make the  $\Delta V_{ip}$  magnitude and angle  $\alpha_i$  also erroneous. For these extreme cases the angle  $\gamma_{li}$  is given in parenthesis next to the velocity requirement.

Though all these simulations do establish in general the validity of the transformation concept, other than being an interesting and neat trick, its use for rendezvous with elliptic orbit targets is limited to certain rather low values of target eccentricity and it involves time-varying conditions of departure from the waiting orbit with attendant complications and uneconomical operation. In the author's opinion, the most practical way to rendezvous with an elliptic orbit target from a waiting orbit using line-of-sight guidance techniques, is to use the copasidal elliptic orbit approach shown to be so general and simple in its operation.

SOLUTION OBTAINED BY TRANSFORMATION OF RENDEZVOUS PARAMETERS  
 $b^i=0.2115$   $k^i=0.8175$  FOR PSEUDO INTERCEPT TO CIRCULAR ORBIT TARGET

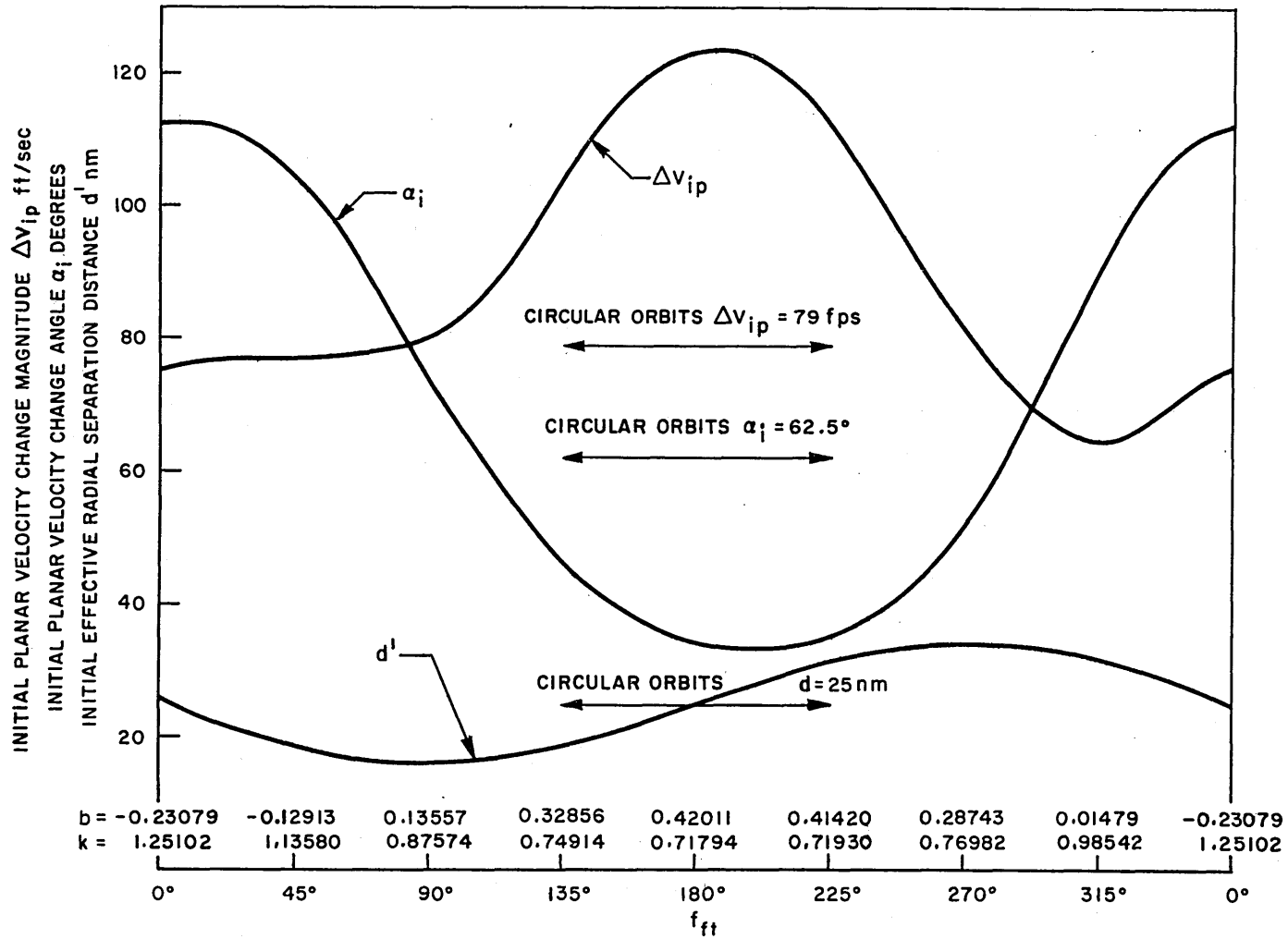


Fig. 8-13 Initial Maneuver for Standard Intercept Line-of-Sight Motion - Intercepts from Circular Waiting Orbit to Elliptic Target Orbit

STANDARD TRAJECTORY, MODE, GUIDANCE AND RELATIVE INCLINATION CONDITION  
 CRITICAL ORBIT ( $e_w = 0.002$ ,  $\delta a_w = +$  and  $-3$  nm) AND GUIDANCE ERRORS  
 NOMINAL ORBIT CONDITIONS:  $e_w = 0$ ,  $e_t = 0.0025$ ,  $a_t - a_w = 25$  nm

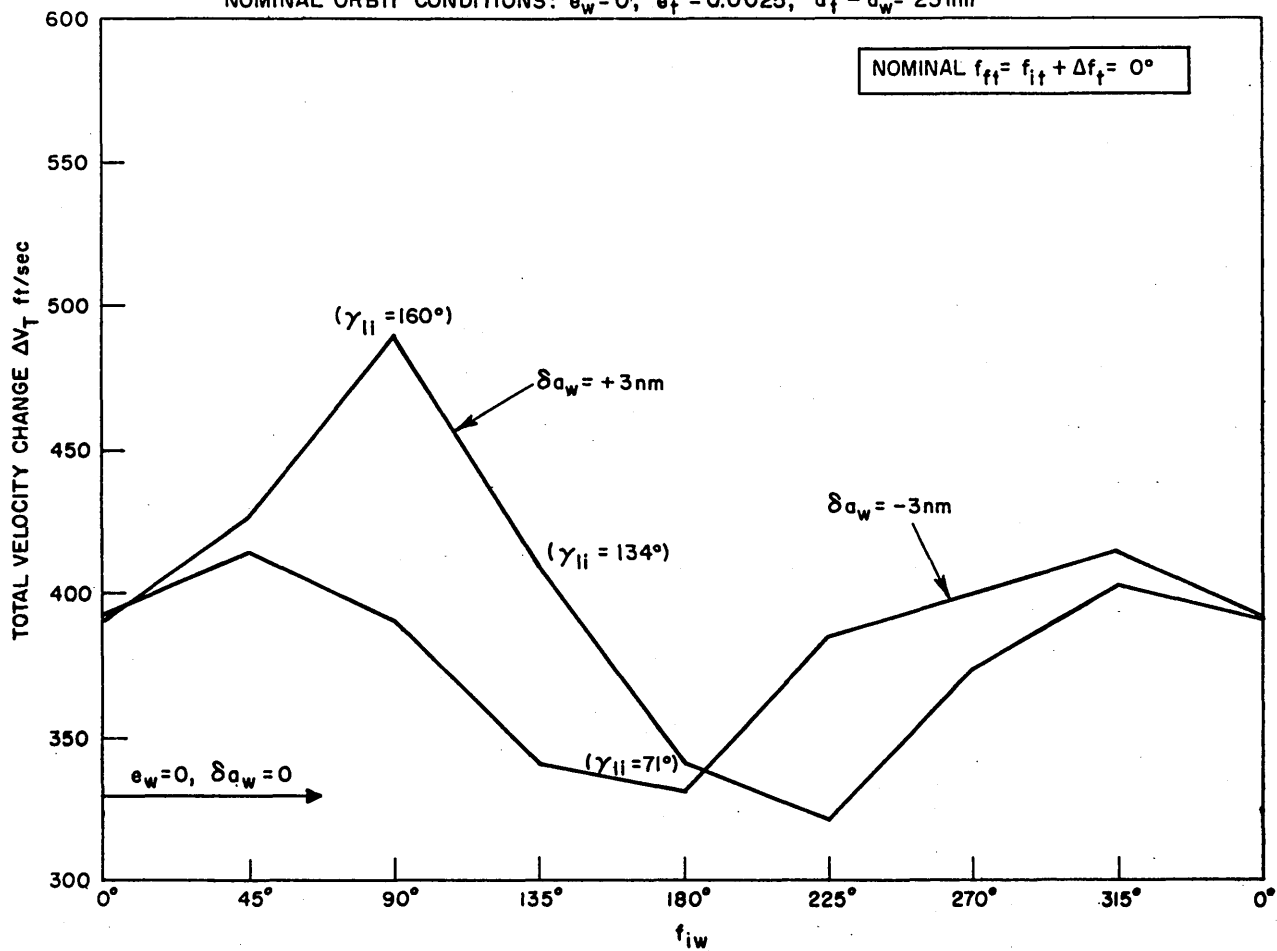


Fig. 8-14a Error Effects on Intercepts from Circular Waiting Orbits to Elliptic Target Orbit (cont.)



STANDARD TRAJECTORY, MODE, GUIDANCE AND RELATIVE INCLINATION CONDITION  
 CRITICAL ORBIT ( $e_w = 0.002$ ,  $\delta a_w = +$  and  $-3\text{nm}$ ) AND GUIDANCE ERRORS  
 NOMINAL ORBIT CONDITIONS:  $e_w = 0$ ,  $e_t = 0.0025$ ,  $a_t - a_w = 25\text{nm}$

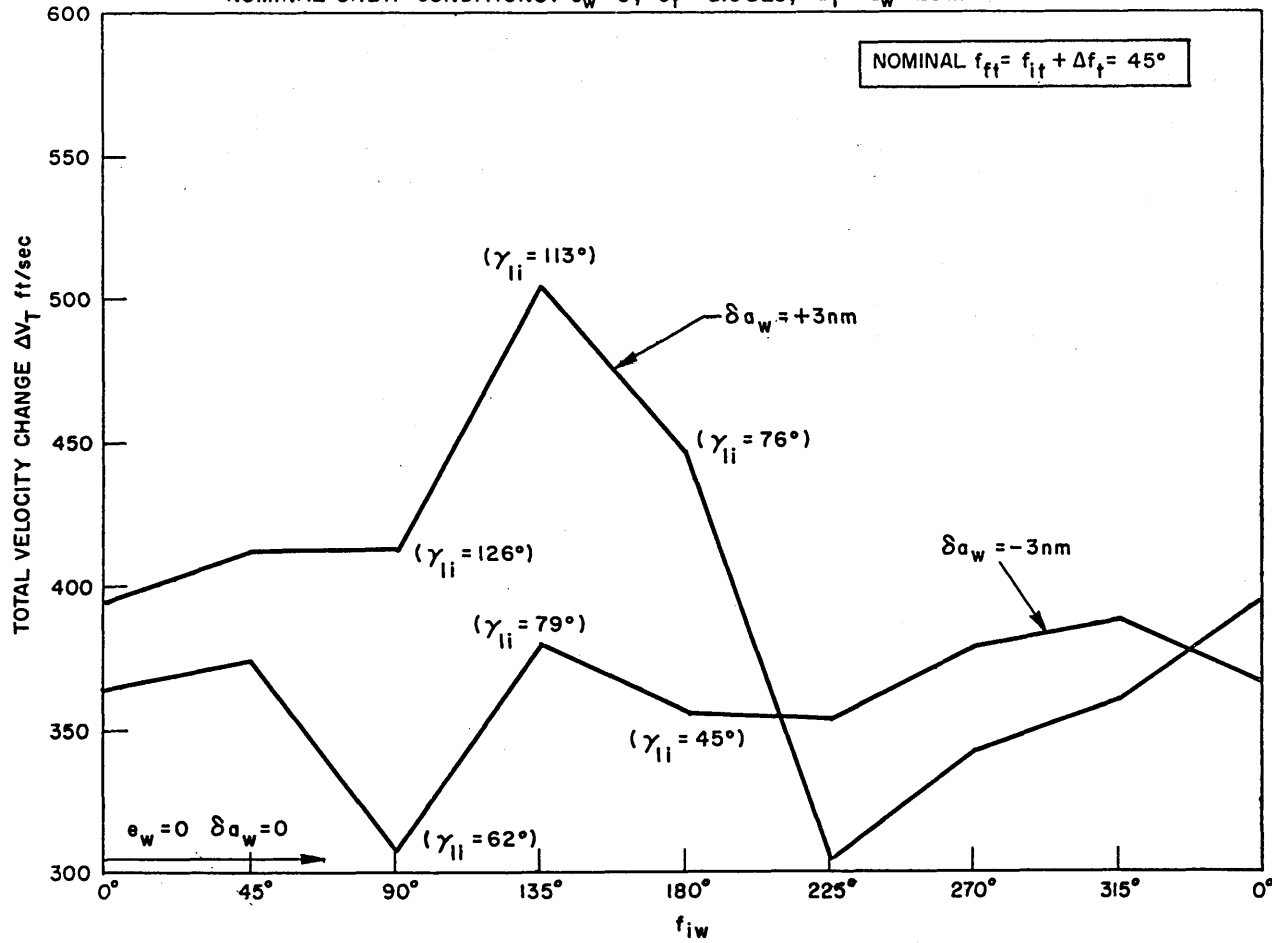


Fig. 8-14b Error Effects on Intercepts from Circular Waiting Orbits to Elliptic Target Orbit (cont.)

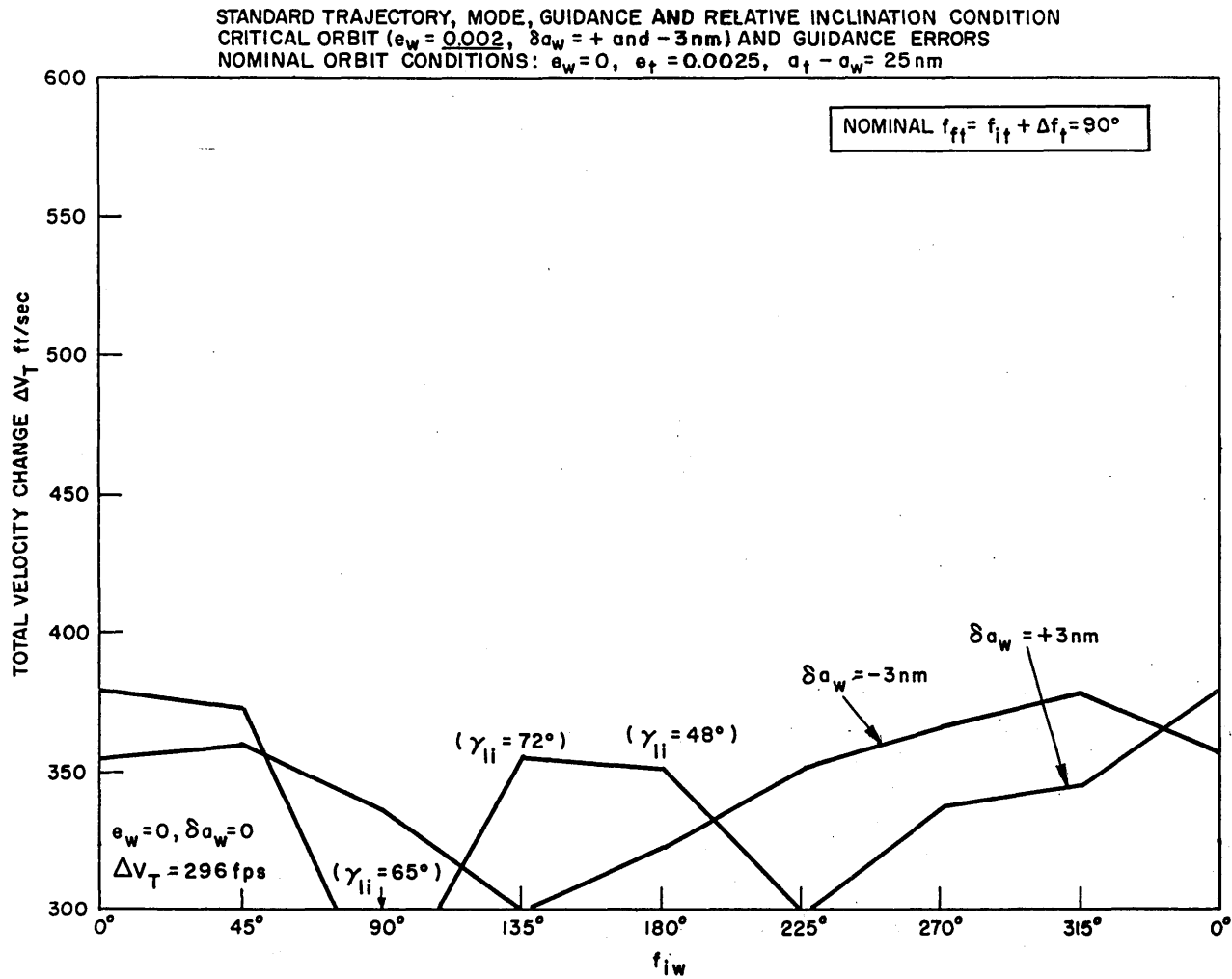


Fig. 8-14c Error Effects on Intercepts from Circular Waiting Orbits to Elliptic Target Orbit (cont.)

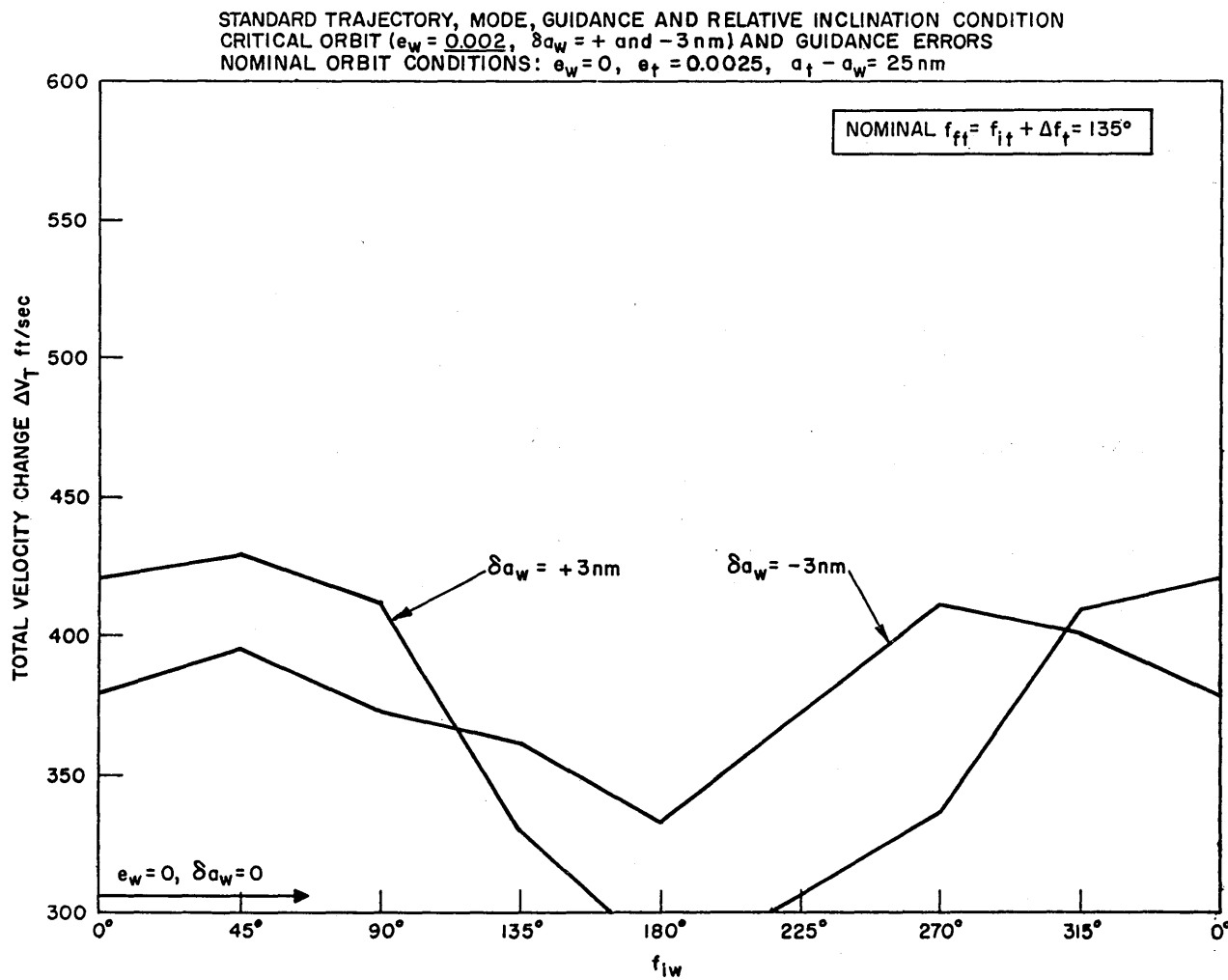


Fig. 8-14d Error Effects on Intercepts from Circular Waiting Orbits to Elliptic Target Orbit (cont.)

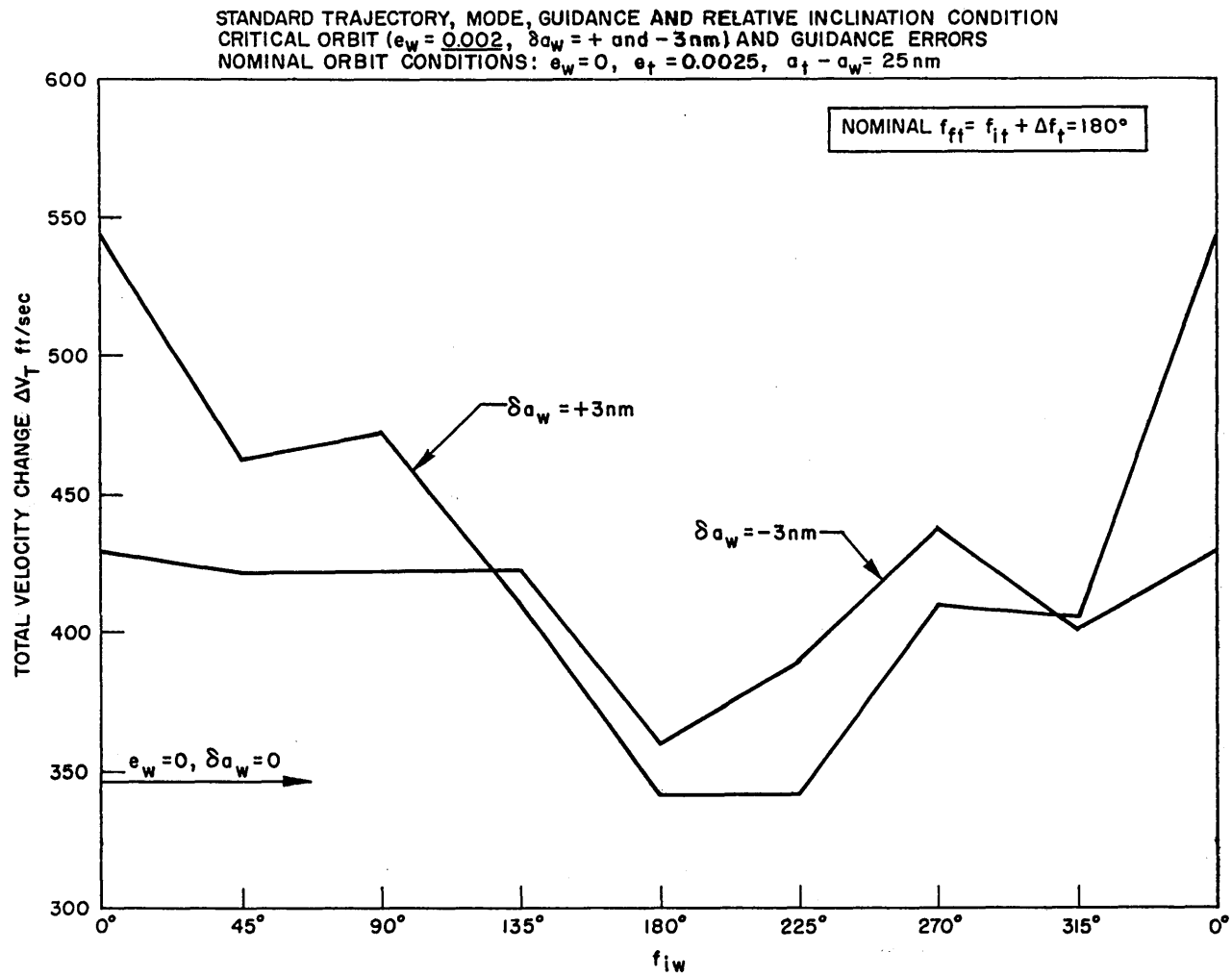


Fig. 8-14e Error Effects on Intercepts from Circular Waiting Orbits to Elliptic Target Orbit (cont.)

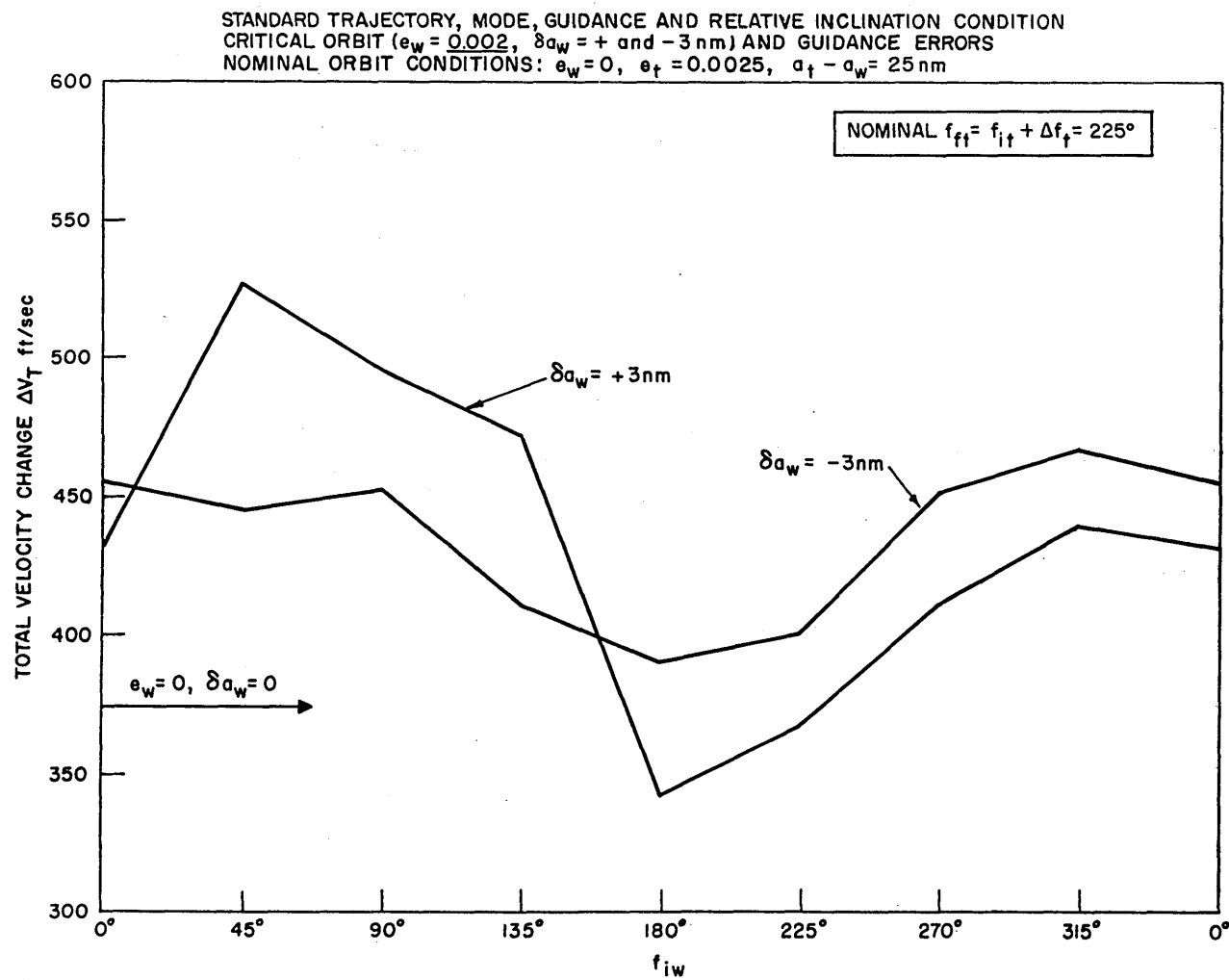


Fig. 8-14f Error Effects on Intercepts from Circular Waiting Orbits to Elliptic Target Orbit (cont.)

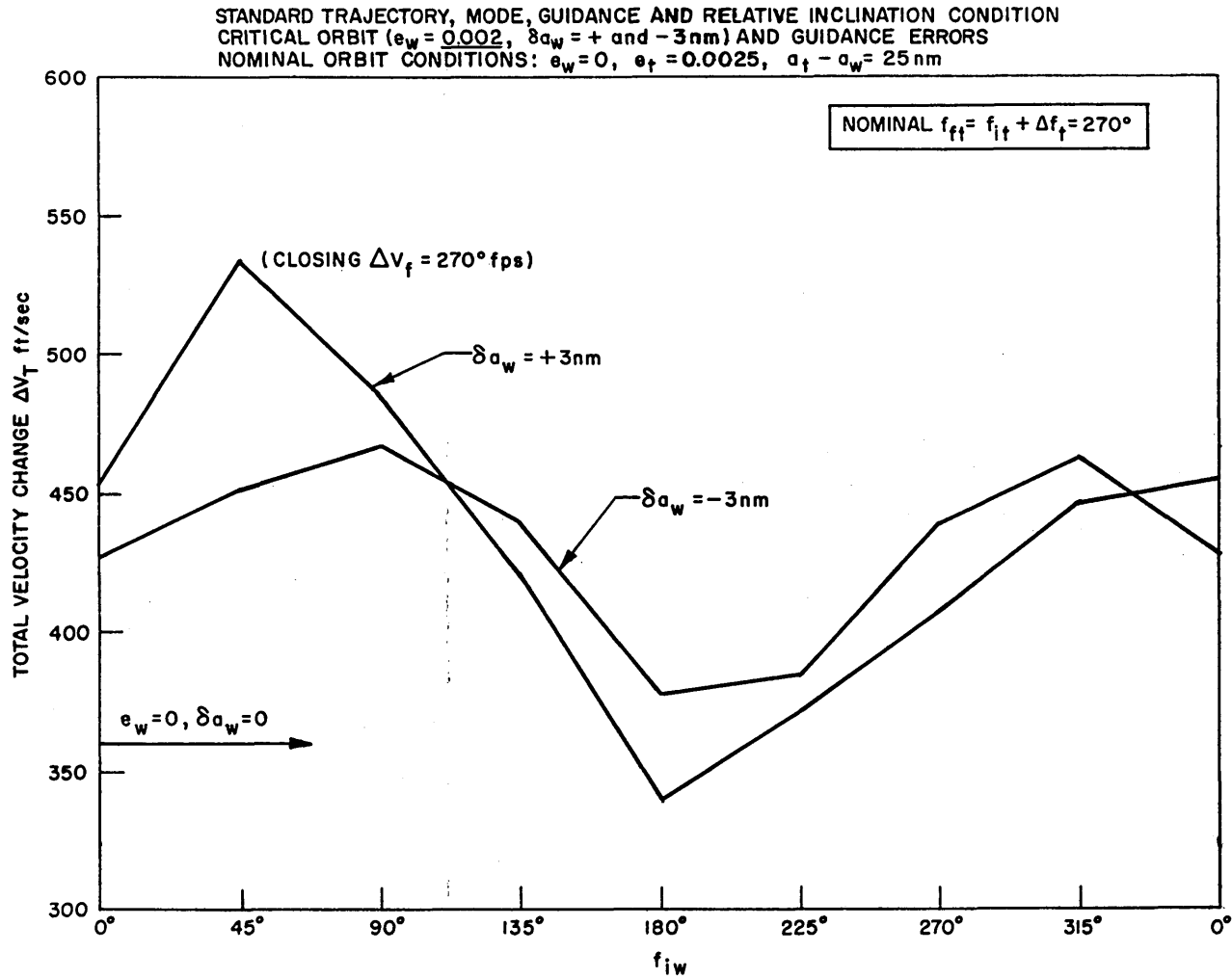


Fig. 8-14g Error Effects on Intercepts from Circular Waiting Orbits to Elliptic Target Orbit (cont.)

STANDARD TRAJECTORY, MODE, GUIDANCE AND RELATIVE INCLINATION CONDITION  
 CRITICAL ORBIT ( $e_w = 0.002$ ,  $\delta a_w = +$  and  $-3$  nm) AND GUIDANCE ERRORS  
 NOMINAL ORBIT CONDITIONS:  $e_w = 0$ ,  $e_t = 0.0025$ ,  $a_t - a_w = 25$  nm

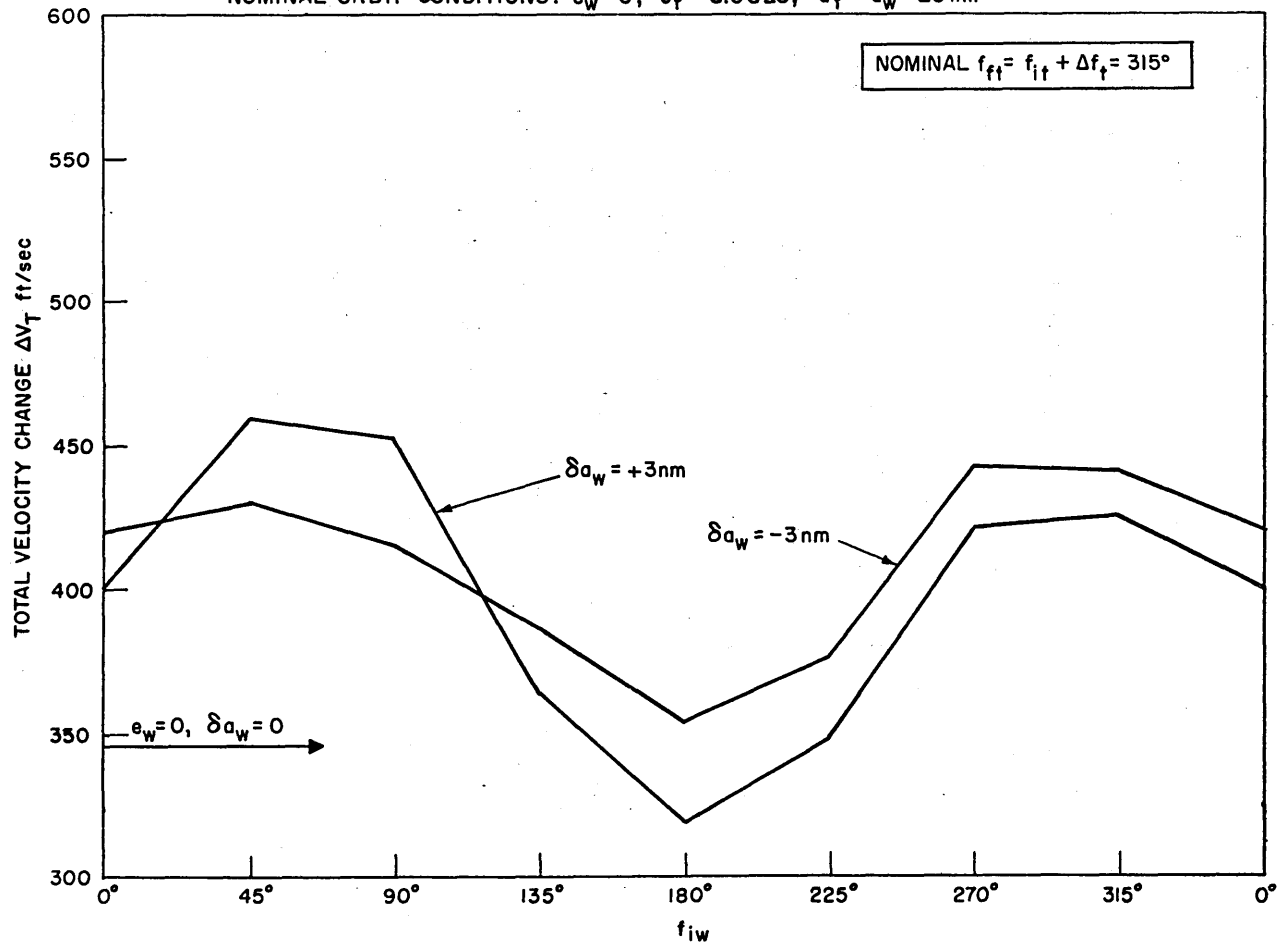


Fig. 8-14h Error Effects on Intercepts from Circular Waiting Orbits to Elliptic Target Orbit (cont.)

#### 8.14 General Remarks on Rendezvous Simulations

Through the technique of using the coapsidal elliptic waiting orbit, all the preceding analyses of rendezvous intercepts between circular orbits have been demonstrated to be applicable to elliptic target orbits in the complete range of conceivable manned operations in near-Earth space. Through the scaling technique, the radial distances traversed in the intercept have been demonstrated to be readily extendible to the limits of reasonable optical observations. These techniques also permit an analogous extension to lunar orbit maneuvers.

For the specific Gemini mission application, and through the above extension for a wide variety of other space rendezvous missions, a standard intercept trajectory has been selected and demonstrated to be reasonably close to the best trajectory from among the range of possibilities available for acceptable optically controlled maneuvers. Various modes of operation of the proposed guidance technique have been examined and though the mode that performed best involved the use of radar range and a modest single computation ability, if the orbit errors were not too great a simpler computation could be used and radar not employed except as needed for the braking phase. The potentialities for further simplification through the future study of direct pilot control simulations, ultimately dispensing with the use of guidance equations, have been clearly indicated. The benefits to be derived by updating the interceptor's knowledge of the waiting orbit



semi-major axis have also been demonstrated. The selected guidance parameters associated with the reticle size and pitch down angle have been shown to produce near-optimum performance; however, possible further refinements have been indicated.

In essence, the analysis of the proposed line-of-sight guidance techniques appears to be complete in the depth afforded by this type of an investigation, and the tolerances of this system to orbit errors in view of the selected velocity change capability are fairly well-established. The way is now open for future investigations of specific orbit injection equipment and the performance accuracies of subsequent orbit maneuvering to see how well these tolerances can be met. These investigations are highly dependent on specific hardware and the incorporation of such an analysis is unfortunately beyond the scope of this investigation.



## CHAPTER 9

## GENERAL THEORY OF RENDEZVOUS

9.1 Nominal Mission Profile-A Function of Target Orbit

In this chapter an attempt will be made to formulate a generalized approach to rendezvous utilizing line-of-sight techniques. Though specific missions may require special deviations, the general rules are basic to the solution of the rendezvous problem. This chapter will also serve as a brief review of the rendezvous principles set forth in this investigation.

The overall mission profile for rendezvous is primarily a function of the target orbit parameters. Its inclination relative to the launch site latitude, the semi-major axis, and eccentricity all have major effects on the approach to rendezvous. The most difficult conditions result from targets with high inclinations, high eccentricities and low perigee altitudes. Of secondary importance in the mission profile are the anticipated interceptor orbit errors, optical acquisition ranges, thrust capabilities, and thrust levels. These latter factors will primarily determine the nominal radial separation distance,  $d$ .

The general theory of rendezvous involves the use of a three-orbit approach to the target consisting of:

- (1.) An elliptic waiting orbit oriented to be coapsidal with the target and with:

$$a_w = a_t - d$$

$$e_w = \frac{a_t e_t}{a_w}$$

- (2.) An elliptic parking orbit with a perigee equal to the optimum injection burn out altitude and an apogee altitude equal to the perigee altitude of the waiting orbit.
- (3.) A circular transfer orbit connecting the apogee of the parking orbit with the perigee of the waiting orbit.

Fig. 9-1 depicts an inertial view of an exaggerated example utilizing this general approach to rendezvous. Launch and injection into the parking orbit are arranged and timed so that the plane of the parking orbit will closely coincide with the plane of the target. As discussed in the next section, a small intentional relative inclination may be desired. The time of entering the transfer orbit will depend upon the phase angle and the phase rates of the parking and transfer orbits. The time of entering the waiting orbit likewise depends on the phase

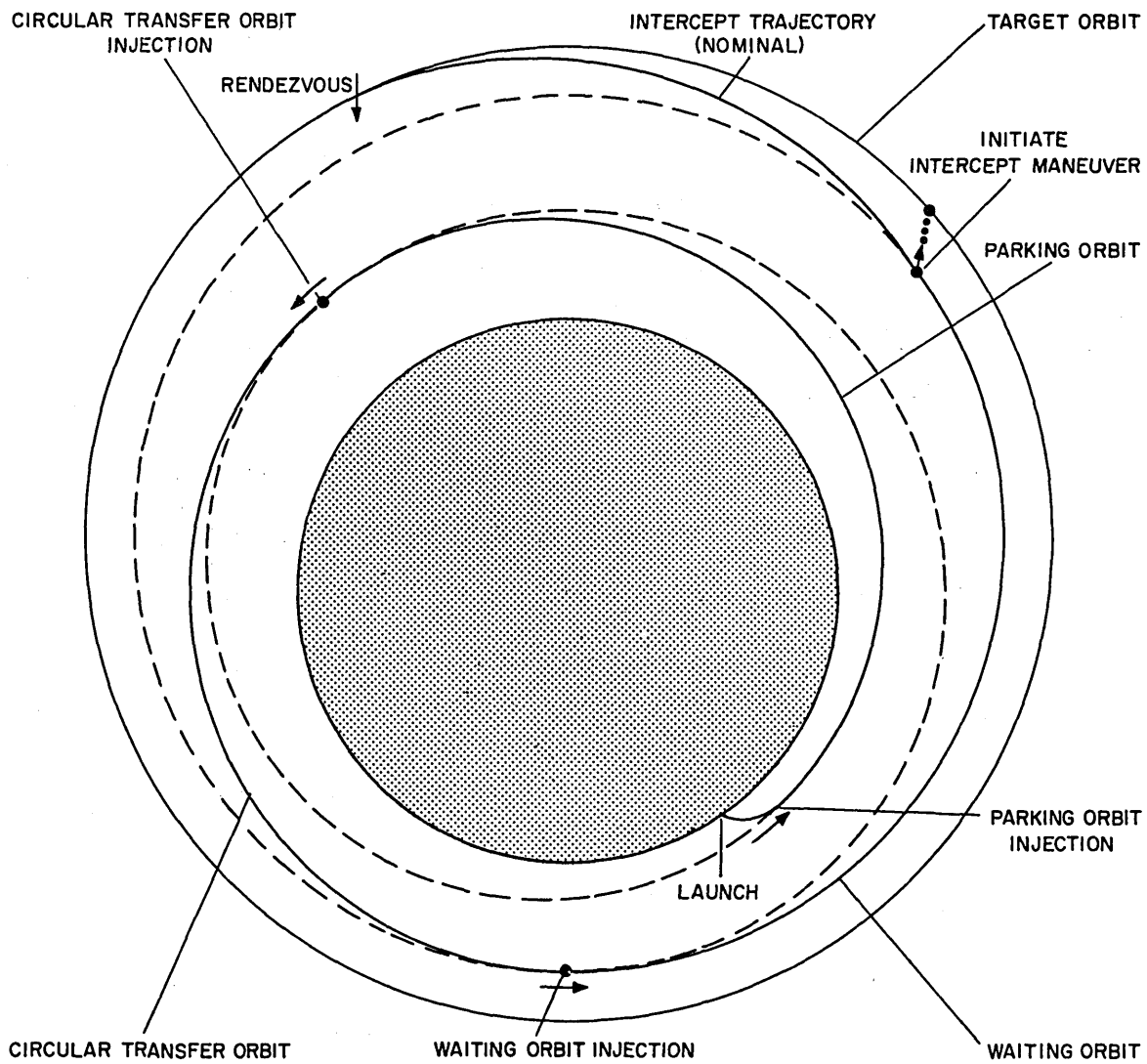


Fig. 9-1 Generalized Approach for Rendezvous Intercept

angle and the phase rate of the transfer orbit. Ideally, both of these orbit changes must be made at discrete times. Prior to injection a thorough analysis along the lines of Fig. 4-8 and 4-10 is essential. Once in the waiting orbit a standard nominal intercept is accomplished when a prescribed  $\beta$  angle is reached.

The Russian space mission involving Cosmos 3 and Cosmos 4 represents an application of this general rendezvous theory with several modifications. In this case the parking and transfer orbits were omitted entirely and the injection of Cosmos 4 was made directly into a near-coapsidal elliptic waiting orbit of near constant radial separation from Cosmos 3. Since the semi-major axis altitude of Cosmos 3 was slightly higher and it was injected into orbit slightly ahead of Cosmos 4, the latter could be termed the interceptor as it overtook and eventually preceded the former. However, since evidently neither vehicle undertook orbital maneuvering, this designation is irrelevant. The orbit of Cosmos 3 was not precisely a Rendezvous Compatible Orbit; hence a slight non-coplanar relative motion existed between the vehicles. Perhaps due to this consideration and also the possibility of a slight launch delay, which apparently did not materialize, the decision was made to strive for an injection of Cosmos 4 into an orbit slightly above and ahead of Cosmos 3.

## 9.2 Nominal Injection Plane

For rendezvous missions utilizing line-of-sight guidance techniques there are two factors that affect the selection of the nominal injection plane for the parking orbit. The first of these concerns the relationship of the phase angle to the target from the injection point and the target orbit plane orientation relative to the injection point as functions of injection time. In other words, for a given target orbit as in Fig. 3-2, there is a fixed relationship between phase angle and relative inclination--as one varies so does the other. Some control of this can be exercised through selection of the target period. The second factor concerns the line of sight for various relative inclinations and its relation to the sun, which is to be excluded from possible line-of-sight fields of view. From Fig. 4-9, if the injection occurs in the mid-morning, it is readily seen that for the quasi-direct ascent rendezvous, the sun would not interfere with the line of sight. However, for different locations of the initial and final points of the intercept, the sun could interfere with the line of sight. If as in Fig. 9-2, the injection is made at mid-morning and the standard intercept trajectory is used, the initial point of the intercept should not be in the region from A to B if it is desired that the sun always be at least  $20^{\circ}$  away from the line of sight. However, considering that the launch site latitude always remains north of the

sun even on June 21, if the relative inclination of the waiting orbit were such that it was to the south of the target plane in the region from A to B, say with a line of nodes along C D, then the resulting  $\psi$  angle would always insure that the sun was well clear of the line of sight. Fortunately, this situation occurs naturally as a consequence of an injection parallel to the target plane when the target plane is north of the latitude of the launch site. (Refer to Fig. 3-2.) Fortunately again, for the Gemini mission with a target altitude of 150 nm, the conditions for near-direct ascent of the interceptor occur when the target plane is well north of the launch site.

This same intentional out-of-plane injection consideration can and should be applied to any other type of rendezvous situation utilizing line-of-sight techniques.

### 9.3 Elliptic Parking Orbit

The elliptic parking orbit should be subject to the following considerations. If the perigee of the target, or altitude in the event of a circular target, is quite low, the parking orbit may have to be circular and thus become, in effect, the transfer or waiting orbit immediately. In such a case the launch timing would become more critical due to the decreased phase rate, and error sensitivities at injection would increase. The orbit would also be subject to greater atmospheric drag.



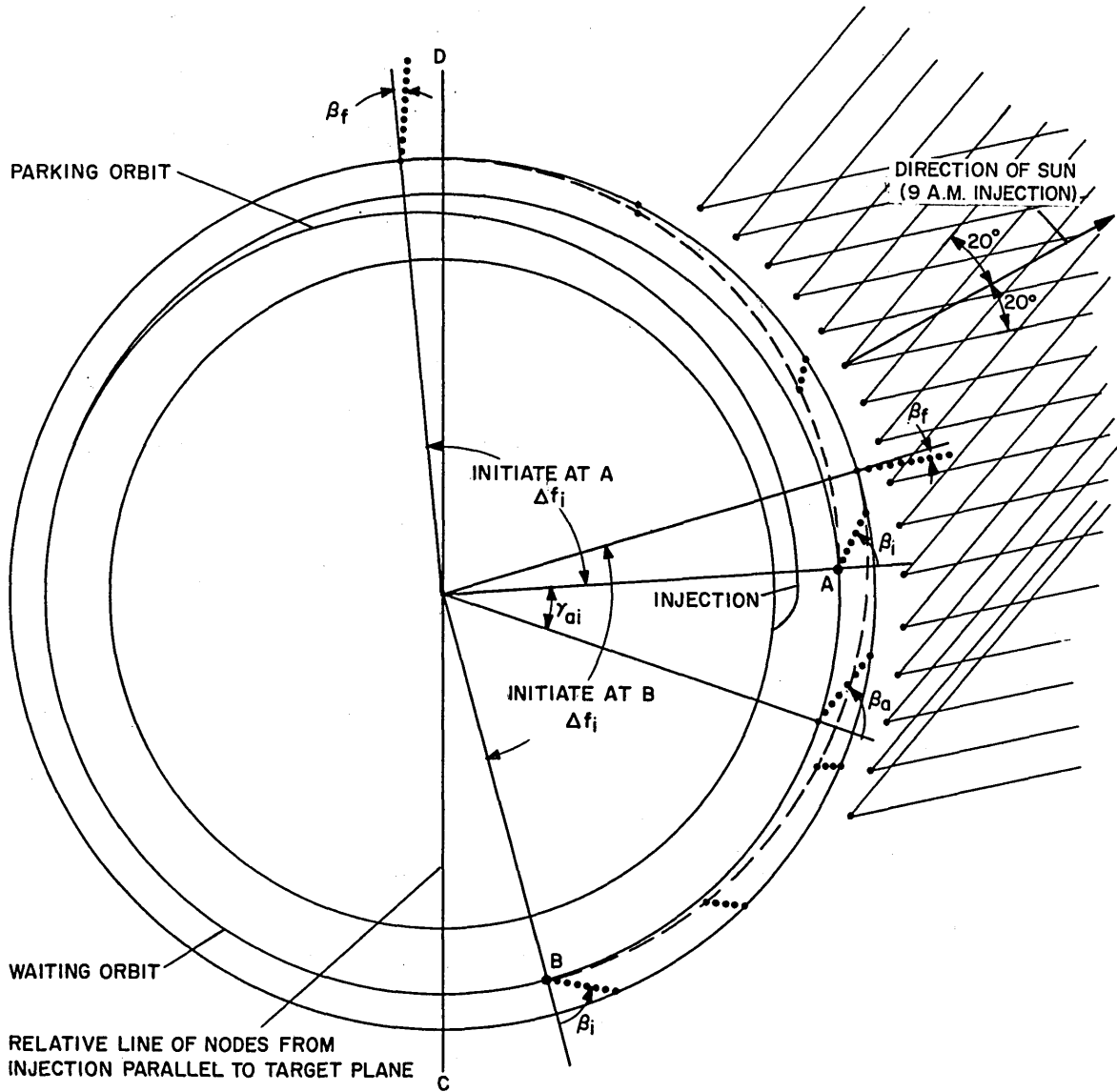


Fig. 9-2 Intentional Non-Coplanar Injection

For more normal elliptic parking orbits the residence time of the interceptor would depend on the phase angle and phase rate. Sufficient time should be spent in the orbit for ground tracking to compute the time and magnitude of the velocity change needed to maneuver to the transfer orbit. One-half a period would probably be insufficient if high accuracy is desired. One and one-half periods would probably be a better residence time.

#### 9.4 Circular Transfer Orbit

If the target orbit is circular, the transfer orbit automatically becomes the waiting orbit. For elliptic target orbits the residence time in the transfer orbit has discrete values depending on the inertial orientation of the apogee of the parking orbit and the desired perigee of the waiting orbit. Again, the total time spent will depend on the phase angle and phase rate. If ground tracking is to be used for orbit updating, as it should whenever possible, sufficient time should be spent in this orbit to enable an adequate computation of the time and magnitude of the velocity change needed to enter the elliptic waiting orbit. The more elliptic the target orbit is the more critical this timing becomes. For the extreme elliptic target orbit used in the simulations, a timing error alone of 30 seconds would result in the full error eccentricity being superimposed on the nominal waiting orbit. However, with good ground tracking one could expect to do much better than this.

### 9.5 Elliptic Waiting Orbit

As evidenced from the previous simulation results indicating velocity requirements for intercept, the ultimate success or failure of the rendezvous attempt depends directly on the accuracy of attaining the desired waiting orbit with near-constant radial separation from the target orbit. Since, in effect, the precision of this orbit, whether it be nominally elliptic or circular, is the key to rendezvous, every available resource should be directed toward attaining this orbit with the lowest error tolerances possible. If satisfactory error tolerances can be met with a quasi-direct ascent, so much the better. If not, then a time versus orbit accuracy determination trade-off is necessary. The residence time in this orbit prior to initiating the intercept phase is a function of the injection time and the phase angle and phase rates of the parking and transfer orbits. Since entry into this orbit and into the transfer orbit can only be made at discrete times, if optimum maneuvering is to be made, an analysis similar to Fig. 4-8, but including the transfer orbit, would give the nominal residence time in the waiting orbit as a function of injection or launch time. The minimum residence time should allow for orbit correction, if deemed necessary, accurate orbit plane determination, target acquisition, and  $\Delta V_{iz}$  determination. If small errors are detected in this waiting orbit as a result of either ground tracking or

on-board computation, it may very well be better to modify  $\Delta V_{ip}$  and  $\alpha_i$  as a function of time instead of correcting the orbit.

#### 9.6 Intercept Maneuvers

The intercept maneuver utilizing line-of-sight guidance techniques would be similar to the examples presented in this investigation with possible modification incorporating direct pilot control of the correction magnitudes and the use of a nominal or ground supplied relative inclination and  $\gamma_i$  angle. The actual nominal intercept trajectory would depend on the vehicle capabilities, optical acquisition ranges and maximum expected non-coplanar effects and orbit errors, and would probably not differ much from the standard intercept trajectory selected in this investigation. Since the intercept maneuver is the only portion of the total rendezvous maneuver that is not very near the deterministic optimum, every effort should be made to keep the distance  $d$  as low as expected orbit errors will allow. This investigation has demonstrated that the distance  $d$  should be slightly greater than twice the maximum relative radial displacement error due to either semi-major axis errors or eccentricity errors in both the target or waiting orbits. If further investigation establishes that radar range information is definitely not required in the guidance phase and the mission calls for frequent ferry-type rendezvous intercepts with a space station, some advantages may be

gained by having the radar needed for the braking and docking phase located in the space station instead of the interceptor. Closing range and range rate could then be relayed to the interceptor for use in initiating the braking maneuver. However, this concept might not satisfy emergency or rescue missions in the event of space station malfunctions.

#### 9.7 Braking and Docking Maneuver

Since this phase of the rendezvous maneuver has not been included in this investigation, little of a specific factual nature can be recommended. It does appear though that sight magnification could be of a distinct advantage in assisting the initiation of this maneuver. A provision should probably be made for relocating the sight axis relative to the longitudinal axis of the spacecraft so that  $\alpha_p$  is zero for the braking phase enabling the use of the sight and attitude control of the vehicle to attain and maintain a zero rotation of the line of sight while the forward-directed thrusters are reducing the relative velocity to zero. As the range approaches a few thousand feet the pilot should be able to view the target directly without interference of the sight so that the terminal approach and maneuvering for docking can be controlled in much the same way as an aircraft formation join-up or aerial refueling operation. Intensive pilot controlled simulation should establish the best techniques for the

transition from visual control through the sight to direct observation through the windshield. The author feels that with considerable intensive practice, continually emphasizing the virtues of patience, the braking and docking maneuver can be executed under direct pilot control in a manner that smoothly transitions from the preceding line-of-sight guidance phase. It is further felt that these maneuvers can be accomplished without requiring a significantly greater total velocity change capability than the closing velocity at the start of the braking maneuver.

## CHAPTER 10

## SUMMARY AND CONCLUSIONS

10.1 Review of Significant Developments

In tracing through all the research embodied in this investigation of line-of-sight guidance techniques for manned orbital rendezvous there are seven concepts that have been evolved that warrant reiteration in retrospect. Since the number is seven, the author feels compelled to dedicate one to each of the original seven Mercury Astronauts. In the order of their development which is also somewhat the order of their application, yet certainly not the order of importance, for this has yet to be established, they are:

(1) The Concept of Maneuver Approach in Stages

This concerns the use of the parking, transfer and waiting orbits to place the interceptor into a favorable position from which a nominal intercept maneuver may be performed. This approach by stages permits the circumventing of stringent injection timing restrictions, yet allows near-optimum maneuvers to approach optical acquisition ranges in an expeditious manner for rendezvous missions to targets in either circular or elliptic orbits.

(2) Guidance Based on Nominal Inertial Variations of the Line-of-Sight

The basic concept of employing a sight reticle programmed to vary inertially as the line of sight should vary for a nominal intercept, and basing the guidance corrections on the deviations of the observed target motion, permits simple, reliable and economical intercepts to be performed. These intercepts can be performed without undue on-board computation and in a manner that is vastly superior to the constant line-of-sight techniques for visual control of rendezvous that have previously been proposed.

(3) The Introduction of Rendezvous Parameters

The use of the rendezvous parameters  $b$  and  $k$  has been demonstrated to greatly assist the classification of possible intercept trajectories in a manner that has far more significance than the usual orbital elements of an intercept trajectory. Their use in approximately derived expression enables the immediate visualization of the properties of a particular trajectory and how these properties change for neighboring trajectories. They facilitate the derivation of a guidance correction theory and through transformation permit analogies to be drawn concerning the similarities of intercepts to circular target orbits and elliptic target orbits. Through the coapsidal elliptic waiting orbit concept they can be applied unchanged to intercepting targets of varying degrees of orbit ellipticity.



(4) The  $\Delta V_{iz}$  Computation

Through an analysis, valid for low relative inclination and arbitrary target and interceptor waiting orbits, the velocity change needed to relocate the relative line of nodes to a predetermined position has been demonstrated to be readily obtainable through a simple calculation based on two previous angular position observations of the target. This computation can be employed in varying degrees of the complexity of equipment and sensing devices to compensate for the effects of orbit errors, thus offering a flexibility in the mode of operation that could cope with malfunctions without altering the concept of rendezvous.

(5) The Use of a Single Normalized Out-of-Plane Guidance Function

The demonstrated near-linearity of the  $\tan_N \psi$  function for various relative inclinations of intercept for a nominal in-plane maneuver under conditions of an arbitrary location of the relative line of nodes permits the use of only two functions for line-of-sight guidance based on the programmed motion of the sight reticle. This enables the initiation of the intercept maneuver at any appropriate point in the waiting orbit by obtaining the nominal out-of-plane motion through a simple unnormalizing process.

(6) The Effects of Coupled Guidance Corrections

The demonstrated beneficial effects that are obtained

through coupled out-of-plane corrections in comparison to the earlier preferred technique of corrections normal to the plane of motion enables significant practical and economical modifications in the guidance correction theory. This greatly simplifies the sight field of view presentation and guidance equation utilization. The additionally demonstrated benefits from non-perpendicular to the line-of-sight corrections for in-plane deviations through the pitch down angle  $\alpha_p$  results in a more nearly optimum guidance correction theory.

(7) The Coapsidal Waiting Orbit Concept for Intercepts to Elliptic Target Orbits

The far-reaching consequence of this simple concept is perhaps the most important single development that enables the extension of the results of the specific mission application to almost any conceivable rendezvous mission suitable for manned orbital operations in the near-Earth space environment. The near-complete cancellation of the ellipticity effects of the target orbit that result when the interceptor is in a coapsidal elliptic waiting orbit of near-constant radial separation enables the use of a nominal intercept trajectory derived from circular orbit considerations and the uniform application of these parameters to the intercept of a target in an elliptic orbit regardless of the point of initiating the maneuver.

The application of these seven significant developments to a line-of-sight guidance technique and the testing of these principles through extensive digital computer simulations under a wide range of error conditions has demonstrated the potentialities of further extensions of man's direct participation in rendezvous maneuvers both for the specific Gemini rendezvous mission and a wide range of other potential rendezvous missions.

#### 10.2 Applications Through Future Investigations to Various Rendezvous Missions

The extent to which the principles outlined in this investigation could or should be applied to future manned orbital operations will depend on a multitude of factors, many of which are simply not well understood at the present time. Among these, the important question concerning the proper allocation of the human resources to either direct participation controlling or a mere monitoring role in the overall mission is as yet not completely settled. To assist in the accumulation of evidence applicable to this question, several possible future applications of line-of-sight guidance techniques will be enumerated and discussed briefly.

##### (1) Gemini Rendezvous Mission

Since in the initial long-duration missions planned as part of the Gemini program, the spacecraft already has the capabilities of slight maneuvering to circularize the initial injection orbit,

much valuable data can be gathered from these missions concerning the maneuver accuracies to attain a specified waiting orbit. The expected tolerances for entering a specified elliptic waiting orbit through the use of parking and transfer orbits can be also thoroughly evaluated. If velocity change capability in these early missions is critical, the apogee of the initial parking orbit could be lowered so that an elliptic waiting orbit with the same semi-major axis as the proposed circular orbit could eventually be entered. This maneuver would involve very nearly the same total velocity change. Also in these early missions a small target equipped with a flashing light beacon could be ejected into an equal period orbit to provide an indication of optical tracking ranges. These target orbits would simulate rendezvous intercepts with rendezvous parameters of  $b=0$  and  $k=1$  with a final intercept true anomaly of approximately  $90^\circ$  or  $270^\circ$  depending on whether the target left the spacecraft in a downward or upward direction. These intercepts are rather close to the standard intercept trajectory found in this investigation to give the best overall results.

Enough has been said already in the body of this study concerning the actual rendezvous mission phase of the Gemini program. These missions should eventually include simulations of the Apollo landing abort intercepts and the ascent from launch as discussed later in

this section as well as intercepts to intentional elliptic target orbits using the coapsidal elliptic waiting orbit concept.

(2) Space Station Assembly and Ferry Mission

Much of the preceeding can be seen to apply directly to missions associated with the assembly, resupply and ferrying to space stations. Since the target orbit would be desired to be more permanent in nature the semi-major axis would most likely be in the vicinity of 300 nm and the orbit very nearly circular. This higher altitude would permit more maneuver space in the approach phase with a higher phase rate for the parking orbit. Since these missions would be conducted on a near-routine basis, operational complexity and equipment weights should be kept as low as possible to afford a maximum payload. The use of standardized intercept maneuvers here would be a distinct advantage. Certain equipment of a computational nature and also radar range equipment could be located in the space station and necessary instructions relayed to the intercepting ferry pilot as needed. The possibility definitely exists in these type missions to have unmanned ferry vehicles commanded to depart a lower waiting orbit and execute a multiple intersecting intercept going outside the target orbit and commanding ferry corrections based on visual observations made by controllers located in the space station.

(3) Lunar Landing Abort Rendezvous

From the detached viewpoint of the author, the most critical phase of the Apollo Lunar Landing mission is associated with the maneuvers required of the Lunar Excursion Module, LEM, to abort at any time from the landing maneuver and intercept the Command Module, CM, which has remained in lunar orbit. In the author's opinion, which is influenced considerably by fighter pilot experiences, abort situations should call for the execution of simple, reliable and straight forward responses to extricate the vehicle from the undesirable situation with the least possibility of further compounding the difficulty. It is well known from surveys of aircraft accidents that the overwhelming majority of mishaps result from not one malfunction but a series of contributing causes. If the apparent best solution for a particular mission involves placing a vehicle and its crew in a situation from which abort recovery becomes rather critical, then consideration should be given to alternate solutions that may be slightly less optimum in the abort free condition, but which give a greater chance of success in the event that an abort becomes necessary.

With the above remarks in mind a potential solution that, among others, is receiving current consideration for the lunar landing concept will be briefly described along with its associated

abort situations. Then a possible alternate solution will be suggested with a view toward making the abort situation less critical. Figure 10-1a presents a rotating coordinate frame portrayal of both solutions with their associated typical abort trajectories. The present concept in dashed lines calls for the LEM to depart the CM, which remains in a circular orbit, by applying a downward velocity increment about  $95^\circ$  prior to the nominal desired landing site so that the LEM will attain a synchronous, or equal period, elliptic orbit with the CM and have a perilune just short of the landing site. The purpose of the synchronous orbit is so that the LEM can return to the CM at any time prior to starting the landing maneuver by simply remaining in this orbit which will return periodically to the close vicinity of the CM. Then, after perhaps one pass over the landing site in this elliptic orbit, at the next arrival at perilune the descent to landing maneuver would be initiated. The approximate trace of this landing trajectory including a period of hover is again portrayed in Fig. 10-1a by the dashed lines indicating the motion relative to the orbiting CM. It should be noted that abort trajectories from various points in the landing maneuver all involve different trajectories and the best intercepts from the given initial conditions seem to involve longer time maneuvers that go outside the CM orbit. To embark on these intercepts would most likely involve extensive storage of trajectory

information, considerable digital computation and an almost certain use of a full tracking radar capability since the line of sight would have the lunar surface as a background and this might well be in sunlight or Earthshine.

As an alternate solution the author suggests departing the CM orbit by an upward directed velocity increment to the LEM about  $265^\circ$  prior to the landing site. Now at any time prior to entering the landing maneuver the LEM can return to the CM as before but in this case in a shorter time interval from a perilune condition. The resulting nominal intercept from perilune has rendezvous parameters of  $b=0$  and  $k=1$ , the ranges are always decreasing and the line of sight does not pass through the horizon but remains directed well away from the Moon (and also from the Sun and Earth in a presently conceived situation). At any subsequent abort situation during the landing maneuver up to the termination of the hovering period, the LEM now need only inject into a near-circular waiting orbit and await the arrival of the appropriate line-of-sight angle from the local vertical to the target to initiate the same nominal intercept as before. Using the line-of-sight techniques evolved in this investigation, one needs only two sight functions, a modest computational capability, and a radar which, at close ranges, supplies only range and range rate.



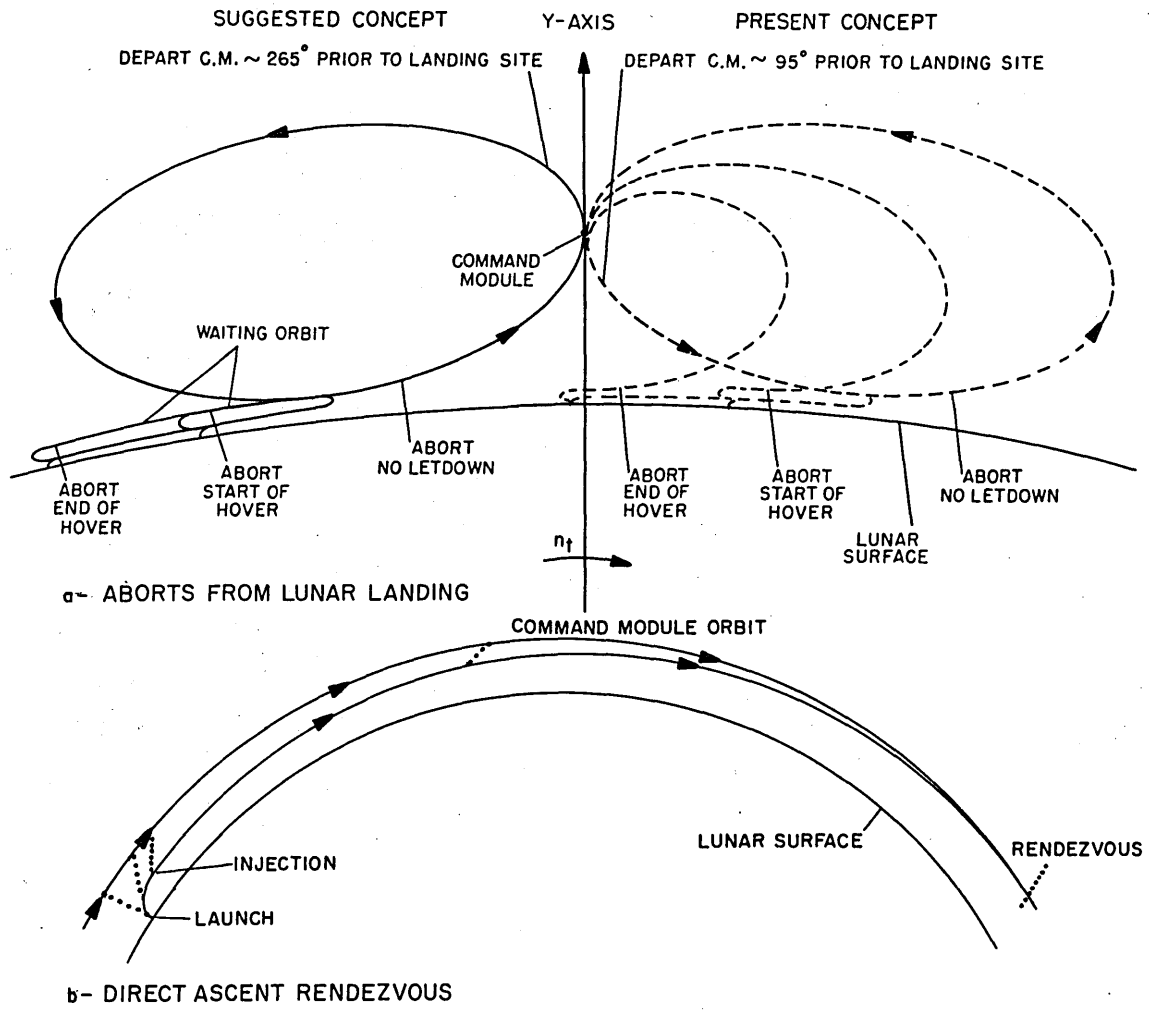


Fig. 10-1 Applications to Lunar Orbit Rendezvous Mission

The above comparison is admittedly not as simple as it may seem, since in the interests of brevity many complicating details that affect both solutions have been omitted. Yet it does appear that significant simplifications of the abort intercepts can be derived through the suggested departure of the LEM from the CM orbit. Two basic penalties are paid for these simplifications. The first concerns the decreased precision in the knowledge of the LEM orbit approaching perilune since a longer time has been spent in this orbit. The second concerns the questionable advantage of having the CM in close position to witness the actual touchdown maneuver. The author feels that the first disadvantage can be overcome through the use of a ground check point selected in the first pass over the landing site, and used as a dead reckoning fix prior to initiating the landing maneuver. The second penalty must be accepted as the price to pay for abort simplification.

The abort intercepts suggested here could and should be rehearsed as part of the Gemini rendezvous program.

(4) Lunar Ascent Rendezvous

Without resorting to a long discourse, the line-of-sight guidance techniques of this investigation could also be applied to the post-injection phase of a direct-ascent rendezvous from the lunar surface to the CM orbit. In addition due to the higher acceleration levels of launch, the lack of atmospheric complications and the

considerably lower injection velocities, the possibility exists for controlling the injection into an intercept trajectory through the application of line-of-sight techniques using a programmed nominal reticle motion throughout the thrusting portion of the launch maneuver. The author feels that this is a most fruitful area for future investigation to prove or disprove the above contention. If this concept proved feasible, it could be blended directly into the nominal coasting intercept as studied herein. A typical ascent rendezvous from the lunar surface is portrayed in inertial coordinates in Fig. 10-1b.

(5) Application to Passive Targets

Targets that do not emit radiation suitable for optical discrimination obviously cannot be intercepted by the techniques presented in this investigation. The possibility does exist, however, to illuminate such targets through bursts of laser radiation at modest ranges. Whether the return from such radiation is suitable for visual observation or whether in fact the emitted radiation could be aimed toward the target assisted by a crude direction finding radar are facts unknown to the author. Whatever the means of determining the inertial line-of-sight direction, if the accuracies obtained are of the same order as human visual observations, then these same techniques could be applied.

(6) Active Maneuvering Targets

The situation, now to be discussed briefly, no longer concerns a target in a highly predictable orbit, but rather intercepts to a target that may take intentional evasive action to frustrate the intercept. From the error analysis section of this investigation one concludes that if the interceptor orbit has the same error as the target orbit the nominal intercept remained essentially unchanged. This is the principle that fostered the coapsidal elliptic waiting orbit concept. Applying this concept to a maneuverable target one concludes that whatever action the target takes in its orbit, if the interceptor takes a similar action at the same point over the Earth, then the resulting relative motion will not change substantially. This immediately brings to mind the analogy to aerial dog fighting where the goal is to get in trail with the target aircraft and then imitate his actions while maintaining a closing velocity.

To implement this technique the total intercept maneuver should be as short as possible. During the approach phase, ground tracking must relay appropriate orbit changes to the interceptor and naturally these must be continuously available. After acquisition of the target by the interceptor a combination of line-of-sight and range rate comparisons with anticipated motions could form the basis for velocity corrections similar to those of this investigation. The

addition of range rate information is needed since evasive velocity changes along the line of sight would otherwise go undetected for longer periods of time and result in much greater velocity changes required of the interceptor when eventually the target velocity changes become noticeable. An infrared radiation detector might be of assistance in discerning thrust maneuvers of the target. Since the actions taken by the interceptor should take place ideally at the same position over the Earth as those of the target, the basic intercept trajectory should have a low value of the rendezvous parameters  $b$  so the interceptor would not get ahead of the target until the terminal stages where orbital motions can be neglected.

The complete treatment of this problem is most complex yet if the above comments are kept in mind many simplifications can be made in future investigations.

### 10.3 Areas for Immediate Future Study

Since the basic principles of line-of-sight guidance techniques appear to be fairly well established for exact orbital motion under the assumption and restrictions inherent in the digital simulation investigation, the need is now apparent to remove these restrictions to attain a closer simulation of the actual physical situation involved. To do this and still retain the exact orbital motions would indeed be a difficult task involving both digital and analog computation adapted

to pilot control in real time. In the opinion of the author the areas that need immediate investigation do not require the exact orbital motions of the respective vehicles. What is needed are the trends and overall effects of removing various restrictions and conducting a more physical simulation. These effects on approximate orbital motions could then be appropriately related to the exact orbital motions.

With the above remarks in mind the areas that need further investigation are the effects of nonimpulsive velocity corrections using acceleration levels appropriate to the vehicle under consideration, the continuous display of relative target and sight motions instead of discrete sampling and the direct participation of pilot observations and reactions to the guidance and control environment. The results to be sought concern the possibilities of dispensing with the guidance equations for corrections in favor of correction thrust termination based on an observed nulling of the relative motion of the sight reticle and the target light source, and the potentialities of utilizing a nominal relative inclination and  $\gamma_1$  angle to dispense with the  $\Delta V_{iz}$  computation. Naturally, prior to attempting any of this direct pilot control simulation, the basic design and fabrication of an optical sight to present the vehicle attitude reference and the inertially programmed reticle must be accomplished.

When all this is completed the author is confident that a rendezvous concept will evolve utilizing line-of-sight techniques for manned intercepts that will compete favorably with other concepts presently in existence.





## APPENDIX A

DERIVATIONS OF EXACT AND APPROXIMATE ORBITAL  
AND RELATIVE MOTION EXPRESSIONSA.1 Organization

The expressions derived in this appendix can be divided into two main categories: those that are derived in terms of the exact relations between the rendezvous parameters  $b$  and  $k$  and the usual orbital parameters  $a_i$  and  $e_i$ , and those derived from approximations to relative motion valid for low orbit eccentricities and radial distance ratios  $d/r_f$ . The first category extends through Section A. 6 and deals with orbital relations for intercepts between coplanar circular orbits using the rendezvous parameter relations:

$$a_i = r_f - bd$$

$$e_i = k \frac{d}{r_f}$$

The approximations to the exact expressions to be herein derived were listed in Chapter 5 and the means by which these results can be

extended to noncoplanar elliptic orbits were also discussed. In the derivation of these expressions reference should be made to Fig. 5-1 or page 67. The second category uses a sinusoidal relative position approximation together with some relations derived in Chapter 4 to obtain approximate line-of-sight motion expressions for coplanar intercepts to an elliptic target orbit and to formulate a transformation of rendezvous parameters. This transformation establishes that intercepts to elliptic orbit targets can be considered as essentially identical to the line-of-sight motion that exists for a pseudo intercept to a target in a circular orbit.

#### A. 2 Expressions for Tangential Departure and Arrival for Circular Orbits - Hohmann Transfer

In order for intercept trajectories to be valid between circular orbits of radius  $r_i$  and  $r_f$  where:

$$r_i = r_f - d$$

the intercept orbit must intersect or be tangent to the circular orbits. In other words, the perigee radius  $r_p$  must be at or below  $r_i$  and the apogee radius  $r_a$  must be at or above  $r_f$  and the following inequalities must hold:

$$r_p = a_i (1 - e_i) \leq r_f - d$$

$$r_a = a_i (1 + e_i) \geq r_f$$

where the condition of equality applies to conditions of tangency.

For the departure from the circular waiting orbit:

$$a_i (1 - e_i) \leq r_f - d$$

$$(r_f - bd) \left(1 - k \frac{d}{r_f}\right) \leq r_f - d$$

$$r_f - bd - kd + bk \frac{d^2}{r_f} \leq r_f - d$$

$$-b \left(1 - k \frac{d}{r_f}\right) \leq k - 1$$

or;

$$b \geq \frac{1 - k}{1 - k \frac{d}{r_f}}$$

and when the equality holds the departure is tangential.

For the arrival at the target orbit:

$$a_i (1 + e_i) \geq r_f$$

$$(r_f - bd) \left(1 + k \frac{d}{r_f}\right) \geq r_f$$

$$r_f - bd + kd - bk \frac{d^2}{r_f} \geq r_f$$

$$-b \left(1 + k \frac{d}{r_f}\right) \geq k$$

or;

$$b < \frac{k}{1 + k \frac{d}{r_f}}$$

and now when the equality holds the arrival is tangential.

For the Hohmann transfer where both departure and arrival are tangential,

$$a_i (1 - e_i) = r_f - d$$

$$a_i (1 + e_i) = r_f$$

Addition yields:

$$2a_i = 2r_f - d$$

$$a_i = r_f - \frac{1}{2} d$$

which from the definition of  $b$  produces:

$$b = \frac{1}{2}$$


---

while subtracting yields:

$$2 a_i e_i = d$$

$$2(r_f - bd) k \frac{d}{r_f} = d$$

$$k = \frac{1}{2 - 2b \frac{d}{r_f}}$$

which, upon substituting for  $b$  produces:

$$k = \frac{1}{2 - \frac{d}{r_f}}$$


---

### A. 3 Expression for Initial and Final Intercept True Anomalies

Taking the standard conic formula:

$$r = \frac{a(1 - e^2)}{1 + e \cos f}$$

and solving for  $\cos f$  yields:

$$\cos f = \frac{\frac{a(1-e^2)}{r} - 1}{e}$$

Substituting the initial conditions and the  $b$  and  $k$  definitions:

$$\begin{aligned} \cos f_i &= \frac{\frac{(r_f - bd)(1 - k^2 d^2 / r_f^2)}{r_f - d} - 1}{kd / r_f} \\ &= \frac{r_f - bd - k^2 d^2 / r_f + bk^2 d^3 / r_f^2 - r_f + d}{kd(1 - d / r_f)} \end{aligned}$$

and finally;

$$\cos f_i = \frac{\left[ \frac{(1-b)}{k} - k \frac{d}{r_f} + bk \frac{d^2}{r_f^2} \right] \left(1 - \frac{d}{r_f}\right)^{-1}}{\underline{\underline{\hspace{10em}}}}$$

or expanding in a series:

$$\cos f_i = \frac{(1-b)}{k} + \frac{(1-b) - k^2}{k} \frac{d}{r_f} + \frac{(1-b)(1-k^2)}{k} \frac{d^2}{r_f^2} + \dots$$

and the first order approximation:

$$\underline{\underline{\cos f_i \cong \frac{(1-b)}{k}}}}$$

Now substituting the final conditions and the b and k definitions into the transformed conic formula:

$$\begin{aligned} \cos f_f &= \frac{\frac{(r_f - bd)(1 - k^2 d^2 / r_f^2)}{r_f} - 1}{kd / r_f} \\ &= \frac{r_f - bd - k^2 d^2 / r_f + bk^2 d^3 / r_f^2 - r_f}{kd} \end{aligned}$$

and finally;

$$\cos f_f = \frac{b}{k} - k \frac{d}{r_f} + bk \frac{d^2}{r_f^2}$$

or the first order approximation:

$$\cos f_f \approx \frac{b}{k}$$

#### A.4 Expressions for Initial and Final Velocity Change Angles

The expression for the velocity change angle at either the initial or final points is:

$$\tan \alpha = \frac{V_\theta - V_c}{V_r}$$

where  $V_{\theta}$  and  $V_r$  apply to conditions in the intercept orbit and  $V_c$  applies to the respective circular orbit. From Chapter 4 these are given by:

$$V_{\theta} = \sqrt{\frac{\mu}{p}} (1 + e \cos f)$$

$$V_r = \sqrt{\frac{\mu}{p}} e \sin f$$

$$V_c = \sqrt{\frac{\mu}{r}}$$

Now, substituting these expressions:

$$\tan \alpha = \frac{\sqrt{\frac{\mu}{p}} (1 + e \cos f) - \sqrt{\frac{\mu}{r}}}{\sqrt{\frac{\mu}{p}} e \sin f}$$

$$= \frac{1 + e \cos f - \sqrt{\frac{p}{r}}}{e \sin f}$$

finally;

$$\tan \alpha = \frac{1 + e \cos f - (1 + e \cos f)^{1/2}}{e \sin f}$$


---



---



Expanding in a series to obtain an expression for low eccentricities which avoids the difference between two comparable size numbers:

$$\tan \alpha = \frac{1 + e \cos f - 1 - \frac{e \cos f}{2} + \frac{e^2 \cos^2 f}{8} - \frac{e^3 \cos^3 f}{16} + \dots}{e \sin f}$$

$$= \frac{1}{2} \cot f \left( 1 + \frac{e}{4} (\cos f - \frac{e}{2} \cos^2 f + \dots) \right)$$

or the first order approximations:

$$\tan \alpha_i \cong \frac{1}{2} \cot f_i$$

$$\tan \alpha_i \cong \frac{1 - b}{2 \sqrt{k^2 - (1 - b)^2}}$$

and;

$$\tan \alpha_f \cong \frac{1}{2} \cot f_f$$

$$\tan \alpha_f \cong - \frac{b}{2 \sqrt{k^2 - b^2}}$$

### A.5 Expressions for Initial and Final Velocity Change Magnitudes

Since in many cases it becomes more meaningful to express velocity change magnitudes in terms of the characteristic velocity change required for a Hohmann transfer, exact and approximate expressions for that velocity change will now be derived. For this maneuver all the velocities are horizontal and:

$$\Delta V_H = V_{ct} - V_a + V_p - V_{cw}$$

where t and w refer to the target and waiting orbits, and a and p refer to apogee and perigee conditions. The compact form of the vis viva integral:

$$V^2 = \mu \left( \frac{2}{r} - \frac{1}{a} \right)$$

will be used to obtain expressions for these velocities.

$$\begin{aligned} V_p^2 &= \mu \left( \frac{2}{r_p} - \frac{1}{a_i} \right) \\ &= \mu \left( \frac{2}{r_f - d} - \frac{1}{r_f - d/2} \right) \\ &= \mu \frac{2r_f - d - r_f + d}{(r_f - d)(r_f - d/2)} \end{aligned}$$

A shorthand notation is now introduced for clarity:

$$\sigma = \frac{d}{r_f}$$

$$V_p^2 = \mu \frac{r_f}{r_f^2 (1 - \sigma) (1 - \sigma/2)}$$

$$V_p^2 = V_{cf}^2 \frac{1}{(1 - \sigma) (1 - \sigma/2)}$$

In a similar manner:

$$V_a^2 = \mu \left( \frac{2}{r_f} - \frac{1}{r_f - d/2} \right)$$

finally yields;

$$V_a^2 = V_{cf}^2 \frac{(1 - \sigma)}{(1 - \sigma/2)}$$

and;

$$\begin{aligned} V_{cw}^2 &= \frac{\mu}{r_f - d} \\ &= V_{cf}^2 \frac{1}{1 - \sigma} \end{aligned}$$

and;

$$V_{ct} = V_{cf}$$

Now substituting these expressions to obtain  $\Delta V_H$ ,

$$\Delta V_H = V_{cf} - V_{cf} \left( \frac{1 - \sigma}{1 - \sigma/2} \right)^{1/2} + V_{cf} \frac{1}{((1 - \sigma)(1 - \sigma/2))^{1/2}} - \frac{V_{cf}}{(1 - \sigma)^{1/2}}$$

$$= V_{cf} \left[ 1 - \frac{1 - \sigma}{(1 - \sigma)^{1/2} (1 - \sigma/2)^{1/2}} + \frac{1}{(1 - \sigma)^{1/2} (1 - \sigma/2)^{1/2}} \right]$$

$$- \frac{1}{(1 - \sigma)^{1/2}}$$

$$= V_{cf} \left[ 1 - \frac{\left( \frac{1 - \sigma}{(1 - \sigma/2)^{1/2}} - \frac{1}{(1 - \sigma)^{1/2}} \right)}{(1 - \sigma)^{1/2}} \right]$$

$$\Delta V_H = V_{cf} \left[ 1 - \frac{\left( 1 - \frac{\sigma}{(1 - \sigma/2)^{1/2}} \right)}{(1 - \sigma)^{1/2}} \right]$$


---



---

Expanding this in a series to obtain an approximate form;

$$\begin{aligned}\Delta V_H &= V_{cf} \left[ 1 - \left\{ 1 - \sigma \left( 1 + \frac{\sigma}{4} + \frac{3\sigma^2}{32} + \dots \right) \right\} \left( 1 + \frac{\sigma}{2} + \frac{3\sigma^2}{8} + \frac{5\sigma^3}{16} + \dots \right) \right] \\ &= V_{cf} \left[ 1 - 1 - \frac{\sigma}{2} + \sigma + \frac{\sigma^2}{4} + \frac{\sigma^2}{2} - \frac{3\sigma^2}{8} + \frac{3\sigma^3}{32} + \frac{\sigma^3}{8} + \frac{3\sigma^3}{8} - \frac{5\sigma^3}{16} + \dots \right] \\ &= V_{cf} \left[ \frac{\sigma}{2} + \frac{3\sigma^2}{8} + \frac{9\sigma^3}{32} + \dots \right]\end{aligned}$$

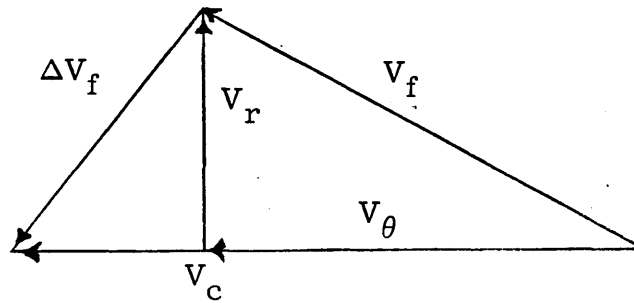
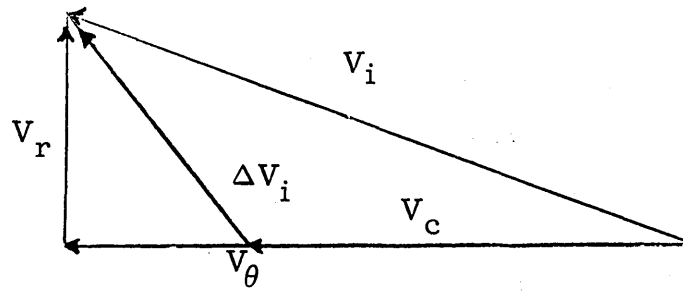
yielding the first order approximation:

$$\underline{\underline{\Delta V_H \approx V_{cf} \frac{d}{2r_f}}}$$

Now for nontangential departures or arrivals the velocity change at either end is given by:

$$\Delta V^2 = V_r^2 + (V_\theta - V_c)^2$$

where  $V_r$  and  $V_\theta$  as before pertain to the intercept trajectory and  $V_c$  to the respective circular orbit. For clarity initial and final vector sketches are given



Now carrying out the square operation:

$$\Delta V^2 = V_r^2 + V_\theta^2 - 2V_\theta V_c + V_c^2$$

$$= V^2 + V_c^2 - 2V_\theta V_c$$

These values are obtained by:

$$V^2 = \mu \left( \frac{2}{r} - \frac{1}{a} \right)$$

$$V_c^2 = \frac{\mu}{r}$$

$$V_\theta = \frac{h}{r} = \frac{\sqrt{\mu p}}{r}$$

Substituting these in yields:

$$\Delta V^2 = \mu \left( \frac{2}{r} - \frac{1}{a} + \frac{1}{r} - \frac{2}{r} \sqrt{\frac{p}{r}} \right)$$

$$\Delta V^2 = V_c^2 \left( 3 - \frac{r}{a} - 2 \sqrt{1 + e \cos f} \right)$$


---

To obtain approximate expressions in terms of the rendezvous parameters the final condition will be evaluated first since it is somewhat simpler.

$$\begin{aligned} \Delta V_f^2 &= V_{cf}^2 \left( 3 - \frac{r_f}{r_f - bd} - 2 \sqrt{1 + k \frac{d}{r_f} \cos f_f} \right) \\ &= V_{cf}^2 \left( 2 - \frac{bd}{r_f - bd} - 2 \left( 1 + k \frac{d}{r_f} \cos f_f \right)^{1/2} \right) \end{aligned}$$

Now expanding in series, substituting the expression for  $\cos f_f$  and again employing  $\sigma = \frac{d}{r_f}$ :

$$\begin{aligned}
\Delta V_f^2 &= V_{cf}^2 \left[ 2 - b\sigma(1 + b\sigma + b^2\sigma^2 + \dots) - 2 - k\sigma\left(-\frac{b}{k} - k\sigma + bk\sigma^2\right) \right. \\
&\quad \left. + \frac{1}{4} k^2 \sigma^2 \left(\frac{b^2}{k^2} + 2b\sigma + \dots\right) - \frac{1}{8} k^3 \sigma^3 \left(-\frac{b^3}{k^3} + \dots\right) + \dots \right] \\
&= V_{cf}^2 \left[ -b^2 \sigma^2 - b^3 \sigma^3 + k^2 \sigma^2 - bk^2 \sigma^3 + \frac{1}{4} b^2 \sigma^2 + \frac{1}{2} bk^2 \sigma^3 \right. \\
&\quad \left. + \frac{1}{8} b^3 \sigma^3 + \dots \right] \\
&= V_{cf}^2 \frac{\sigma^2}{4} \left[ 4k^2 - 3b^2 - \left(\frac{7}{2} b^3 + 2bk^2\right) \sigma + \dots \right]
\end{aligned}$$

and the first order approximations:

$$\Delta V_f \cong V_{cf} \frac{d}{2r_f} \sqrt{4k^2 - 3b^2}$$

which upon substituting the  $\Delta V_H$  approximation becomes;

$$\underline{\underline{\Delta V_f \cong \Delta V_H \sqrt{4k^2 - 3b^2}}}$$

Now, for the initial velocity change:

$$\Delta V_i^2 = V_{ci}^2 \left[ 3 - \frac{r_f - d}{r_f - bd} - 2 \sqrt{1 + k \frac{d}{r_f} \cos f_i} \right]$$



$$\begin{aligned}
&= V_{ci}^2 \left[ 2 + \frac{(1-b)\sigma}{1-b\sigma} - 2(1+k\sigma \cos f_i)^{1/2} \right] \\
&= V_{ci}^2 \left[ 2 + (1-b)\sigma (1+b\sigma + b^2\sigma^2 + \dots) - 2 \right. \\
&\quad \left. - k\sigma \left\{ \frac{(1-b)}{k} + \frac{(1-b) - k^2}{k} \sigma + \frac{(1-b)(1-k^2)}{k} \sigma^2 + \dots \right\} \right. \\
&\quad \left. + \frac{1}{4} k^2 \sigma^2 \left\{ \frac{(1-b)^2}{k^2} + 2 \frac{(1-b)^2 - k^2(1-b)}{k^2} \sigma + \dots \right\} \right. \\
&\quad \left. - \frac{1}{8} k^3 \sigma^3 \left\{ \frac{(1-b)^3}{k^3} + \dots \right\} + \dots \right] \\
&= V_{ci}^2 \left[ (1-b)b\sigma^2 + (1-b)b^2\sigma^3 - (1-b)\sigma^2 + k^2\sigma^2 - (1-b)(1-k^2)\sigma^3 \right. \\
&\quad \left. + \frac{1}{4}(1-b)^2\sigma^2 + \frac{1}{2}(1-b)^2\sigma^3 - \frac{1}{2}k^2(1-b)\sigma^3 \right. \\
&\quad \left. - \frac{1}{8}(1-b)^3\sigma^3 \right] \\
&= V_{ci}^2 \frac{\sigma^2}{4} \left[ 4k^2 - 3(1-b)^2 - \left\{ \frac{(7b+5)(1-b)^2}{2} - 2(1-b)k^2 \right\} \sigma + \dots \right]
\end{aligned}$$

Now converting  $V_{ci}^2$  to  $V_{cf}^2$  with the series of  $(1-\sigma)^{-1}$ :

$$\Delta V_i^2 = V_{cf}^2 \frac{\sigma^2}{4} [4k^2 - 3(1-b)^2 - \left\{ \frac{(7b+5)(1-b)^2}{2} - 2(1-b)k^2 \right\} \sigma + \dots] (1 + \sigma + \sigma^2 + \dots)$$

The first order approximation to this is:

$$\Delta V_i \cong V_{cf} \frac{d}{2r_f} \sqrt{4k^2 - 3(1-b)^2}$$

which upon substituting the  $\Delta V_H$  approximation becomes:

$$\underline{\underline{\Delta V_i \cong \Delta V_H \sqrt{4k^2 - 3(1-b)^2}}}$$

#### A. 6 The Expression for the Initial Line-of-Sight Angle

The basic expression in terms of the phase angle  $\theta$  separating the two vehicles is obtained from simple trigonometry as:

$$\tan \beta_i = \frac{r_f \sin \theta_i}{r_f \cos \theta_i - r_i}$$

or;

$$\tan \beta_i = \frac{\sin \theta_i}{\cos \theta_i - 1 + \frac{d}{r_f}}$$

The angle  $\theta$  can be found by taking the time for the intercept, applying this to the target mean motion and subtracting the angles traversed by both vehicles. For an exact treatment of the time of intercept the reader is referred to Reference (28). This expression is so involved that its use is almost completely restricted to machine computation.

To find a relatively simple expression for  $\tan \beta_i$  in terms of the rendezvous parameters to the first order of  $d/r_f$  is a most difficult task in itself. Though this has been carried out by the author the complete derivation will not be included here. Since the resulting expression is comparable to the one obtained through the rotating coordinate frame approximations of the next section, only a brief outline of the inertial frame analysis will be presented now.

To get  $\theta_i$  in terms of known values set:

$$\theta_i = (f_f - f_i) - n_t (t_f - t_i)$$

but;

$$t_f - t_i = \frac{M_f - M_i}{n_i}$$

where  $M_f$  and  $M_i$  are the final and initial mean anomalies of the interceptor.

Now setting:

$$\begin{aligned}\gamma &= \frac{n_t}{n_i} = \left(\frac{a_i}{r_f}\right)^{3/2} \\ &= (1 - b\sigma)^{3/2} \\ &= 1 - \lambda\end{aligned}$$

the following skeleton outline will indicate the steps necessary for evaluation:

$$\tan \beta_i = \frac{\sin \theta_i}{\cos \theta_i - 1 + \sigma}$$

$$\theta_i = (f_f - f_i) - \gamma (M_f - M_i)$$

$$= (f_f - \gamma M_f) - (f_i - \gamma M_i)$$

$$= F_f - F_i$$

$$\sin \theta_i = \sin F_f \cos F_i - \cos F_f \sin F_i$$

$$\cos \theta_i = \cos F_f \cos F_i + \sin F_f \sin F_i$$

$$\sin F_f = \sin f_f \cos \gamma M_f - \cos f_f \sin \gamma M_f$$

etc.

using Kepler's equations,  $M = E - e \sin E$ ,

$$\sin \gamma M_f = \sin \gamma E_f \cos (\gamma e \sin E_f) - \cos \gamma E_f \sin (\gamma e \sin E_f)$$

etc.,

$$\sin \gamma E_f = \sin E_f \cos \lambda E_f - \cos E_f \sin \lambda E_f$$

etc.,

$$\sin (\gamma e \sin E_f) \cong \gamma e \sin E_f$$

$$\cong e \sin E_f - \lambda e \sin E_f$$

$$\cos (\gamma e \sin E_f) \cong 1 - \frac{(\gamma e \sin E_f)^2}{2}$$

$$\cong 1 - \frac{e^2 \sin^2 E_f}{2}$$

etc.,

$$\sin \lambda E_f = \lambda E_f$$

$$\cos \lambda E_f = 1 - \frac{\lambda^2 E_f^2}{2}$$

etc.,

To evaluate all these expressions in reverse order,  $\cos f_f$  and  $\cos f_i$  are already known in terms of  $b$ ,  $k$ , and  $\sigma$  and  $\sin f_f$  and  $\sin f_i$  can be readily obtained.  $\cos E_f$  and  $\cos E_i$  are given by the simpler expressions:

$$\begin{aligned}\cos E_f &= \frac{a_i - r_f}{a_i e_i} \\ &= -\frac{b}{k} (1 + b\sigma + b^2 \sigma^2 + \dots)\end{aligned}$$

$$\begin{aligned}\cos E_i &= \frac{a_i - r_i}{a_i e_i} \\ &= \frac{(1 - b)}{k} (1 + b\sigma + b^2 \sigma^2 + \dots)\end{aligned}$$

and  $\sin E_f$  and  $\sin E_i$  can be readily obtained from these.  $\lambda$  is obtained from the series expansion for  $\gamma$ . Since there are no rapidly convergent expansions for the angles  $E_f$  and  $E_i$  they must be left as is.

If the expansion is only desired to first order then some simplifications can be made when one realizes that if the highest order term in the power series for  $\sin \theta_i$  is in fact a term of order  $\sigma$  (as it is), then the series for  $\cos \theta_i$  will be of the form:

$$\cos \theta_i = 1 - (\dots) \sigma^2 + \dots$$

Comparing this with the original expression for  $\tan \beta_i$  it can be seen that the first term will be:

$$\tan \beta_i = (\text{1st term of } \sin \theta_i) \frac{r_f}{d}$$

When all of this has been carried out the resulting expression has the form:

$$\tan \beta_i \approx \frac{3}{2} b (E_f - E_i) + 2 \sqrt{k^2 - b^2} - 2 \sqrt{k^2 (1 - b)^2}$$


---

and to the order for which this is valid the angle  $f$  can be considered equal to  $E$ .

#### A. 7 Rotating Coordinate Frame Approximation - Elliptic Orbits

The trace of a vehicle in an elliptic orbit in a coordinate frame rotating with the mean motion of the vehicle was shown in Chapter 4 to have limits of travel in the approximate ratio of 2 to 1. This motion now will be shown to be approximated by a sinusoidal variation which does in fact imply an approximate 2 by 1 ellipse. Using this sinusoidal approximation together with the phase rate expression, also from Chapter 4, the relative motion of any coplanar

intercept to any elliptical orbiting target can be obtained and to the same approximation the rendezvous parameters can be transformed to liken the maneuver to a pseudo intercept of a vehicle in a circular orbit.

The eccentric anomaly  $E$  instead of the true anomaly  $f$  will be used to establish the approximate sinusoidal variation. The expression for the orbit radius in terms of  $E$  from basic orbital mechanics is:

$$\begin{aligned} r &= a (1 - e \cos E) \\ &= a - a e \cos E \end{aligned}$$

and it is immediately seen that the radial variation around the semi-major axis  $a$  is exactly sinusoidal with  $E$  and has an amplitude of  $a e$ . It is now desired to show that the variation along the circular arc of radius  $a$  given by:

$$S = a (f - M)$$

is approximately sinusoidal with  $E$  and has an amplitude of  $2 a e$ . To do this some expressions relating  $f$  to  $E$  will be needed. The standard conic formula in terms of the true anomaly is:

$$r = \frac{a(1 - e^2)}{1 + e \cos f}$$



Equating this to the formula involving the eccentric anomaly and canceling out a gives:

$$1 - e \cos E = \frac{1 - e^2}{1 + e \cos f}$$

$$1 + e \cos f = \frac{1 - e^2}{1 - e \cos E}$$

$$e \cos f = \frac{e(\cos E - e)}{1 - e \cos E}$$

and finally:

$$\cos f = \frac{\cos E - e}{1 - e \cos E}$$

and also:

$$\sin f = \frac{\sqrt{(1 - e \cos E)^2 - (\cos E - e)^2}}{1 - e \cos E}$$

$$= \frac{\sqrt{1 - 2e \cos E - e^2 \cos^2 E - \cos^2 E + 2e \cos E - e^2}}{1 - e \cos E}$$

$$\sin f = \frac{\sqrt{1 - e^2} \sin E}{1 - e \cos E}$$

Kepler's equation  $M = E - e \sin E$  is now substituted into the arc distance expression to give:

$$S = a(f - E) + a e \sin E$$

and apparently half the task is accomplished exactly. Now since for small eccentricity the angle  $f - E$  is small, it can be approximated by its sine function giving:

$$\begin{aligned} S &= a \sin (f - E) + a e \sin E \\ &= a \sin f \cos E - a \cos f \sin E + a e \sin E \end{aligned}$$

Now further substitution of the expressions for  $\sin f$  and  $\cos f$  just derived above gives:

$$\begin{aligned} S &= \frac{a \sqrt{1 - e^2} \sin E \cos E}{1 - e \cos E} - \frac{a(\cos E - e) \sin E}{1 - e \cos E} + a e \sin E \\ &= \frac{a \sin E \cos E (\sqrt{1 - e^2} - 1)}{1 - e \cos E} + \frac{a e \sin E}{1 - e \cos E} + a e \sin E \end{aligned}$$

Expanding the square root and the denominators in series yields,

$$\begin{aligned} S &= a \sin E \cos E \left(-1 + 1 - \frac{e^2}{2} - \frac{e^4}{8} - \dots\right) (1 + e \cos E + e^2 \cos^2 E + \dots) \\ &\quad + a e \sin E (1 + e \cos E + e^2 \cos^2 E + \dots) + a e \sin E \\ &= 2 a e \sin E - a \frac{e^2}{2} \sin E \cos E (1 + e \cos E + e^2 \cos^2 E) \left(1 + \frac{e^2}{4} + \dots\right) \\ &\quad + a e^2 \sin E \cos E (1 + e \cos E + e^2 \cos^2 E + \dots) \end{aligned}$$

or more simply:

$$S = 2 a e \sin E + a \frac{e^2}{2} \sin E \cos E + \text{order } (e^3)$$

and finally the first order approximation:

$$S \cong 2 a e \sin E$$

Therefore one concludes that for low eccentricity the trace of an elliptic orbit in a coordinate frame rotating with the mean motion of the orbit is indeed very nearly represented by a 2 by 1 ellipse.

A. 8 Approximate Expressions for Line-of-Sight Motion Throughout a Coplanar Intercept to a Target in an Elliptic Orbit

In order to obtain approximate expressions for the line-of-sight motion in a simple closed-solution form certain approximations are necessary. In addition to the sinusoidal variation approximations for elliptic orbits, in many cases it is necessary to further assume that the eccentricities are sufficiently small to permit the interchanging of the anomalies  $f$ ,  $E$ , and  $M$ . Further it is assumed that the phase angles separating the vehicles are sufficiently small to permit neglecting the curvature effects on the rotating coordinate frame representation. In some cases the assumption will also be made that the central angles traversed by the vehicles are the same for equal time intervals. The result of these approximations makes the analysis quite comparable to other rotating frame analyses found in the

current literature except that here the angles and constants are related to actual orbital parameters instead of existing initial conditions.

With these approximations in mind, refer now to Fig. A-1, where the relative motion of the target  $t$  and the interceptor  $i$  is portrayed as they proceed toward the rendezvous point  $R$ . The coordinate frame rotates with the mean motion of a fictitious vehicle in a circular orbit at a radius  $r_f$  and hence  $R$  appears stationary while the 2 by 1 ellipses that generate the actual vehicle traces appear to translate - the target ellipse to the right, and the interceptor ellipse to the left. For the target vehicle, the semi-major axis length  $a_t$  is greater than  $r_f$  by the positive amount  $a_t e_t \cos f_{ft}$  and from the relations of Chapter 4 the distance that this ellipse translates to the left during the intercept is:

$$S_{3-4} = -\frac{3}{2} a_t e_t \cos f_{ft} (f_{ft} - f_{it})$$

On the other hand, the intercept orbit semi-major axis length  $a_i$  is less than  $r_f$  by the positive amount  $-a_i e_i \cos f_f$ . The distance that this ellipse translates to the left during the intercept is:

$$S_{1-2} = -\frac{3}{2} a_i e_i \cos f_f (f_f - f_i)$$

Now disregarding the translation of the ellipses during the intercept the target vehicle moves to the left due to elliptic motion an amount:

$$S_{4-R} = 2 a_t e_t (\sin f_{ft} - \sin f_{it})$$

and the interceptor vehicle moves to the left the amount:

$$S_{2-4} = 2 a_i e_i (\sin f_f - \sin f_i)$$

Considering now the radial motion, the target vehicle moves upward during the intercept the amount:

$$\Delta r_{4-R} = - a_t e_t (\cos f_{ft} - \cos f_{it})$$

and the interceptor vehicle moves upward the amount :

$$\Delta r_{2-R} = - a_i e_i (\cos f_f - \cos f_i)$$

The approximate expression for the relative line-of-sight angle from the interceptor's local vertical to the target at the start of the intercept is now clearly given by:

$$\tan \beta_i = \frac{S_{1-2} - S_{3-4} + S_{2-R} - S_{4-R}}{\Delta r_{2-R} - \Delta r_{4-R}}$$

As a matter of fact the expression is not limited to the initial point in the intercept; by removing the i subscripts and substituting the appropriate values of  $f_t$  and  $f$ , the expression is equally valid for any time during the intercept. Dividing numerator and denominator

by  $a_i e_i$  and setting:

$$Q = \frac{a_t e_t}{a_i e_i}$$

yields;

$$\tan \beta \approx \frac{-\frac{3}{2}[\cos f_f(f_f - f) - Q \cos f_{ft}(f_{ft} - f_t)] + 2[\sin f_f \sin f - Q(\sin f_{ft} - \sin f_t)]}{-(\cos f_f - \cos f) + Q(\cos f_{ft} - \cos f_t)}$$


---

Now when  $f_{ft}$  is equal to  $f_f$  or to  $f_f + 180^\circ$  and to the extent that the angles traversed by the target  $f_{ft} - f_t$  are approximated by  $f_f - f$  both numerator and denominator are seen to contain the common factor  $(1 - Q)$  and when this is eliminated the result is the same as if the target orbit had no ellipticity. The result for this condition or for  $e_t = 0$  is simply:

$$\tan \beta = \frac{-\frac{3}{2} \cos f_f(f_f - f) + 2(\sin f_f - \sin f)}{-(\cos f_f - \cos f)}$$

To show that this result agrees with that obtained in the previous derivation of A. 6 for the initial conditions, the following approximations are needed:

$$\cos f_f = -\frac{b}{k}$$

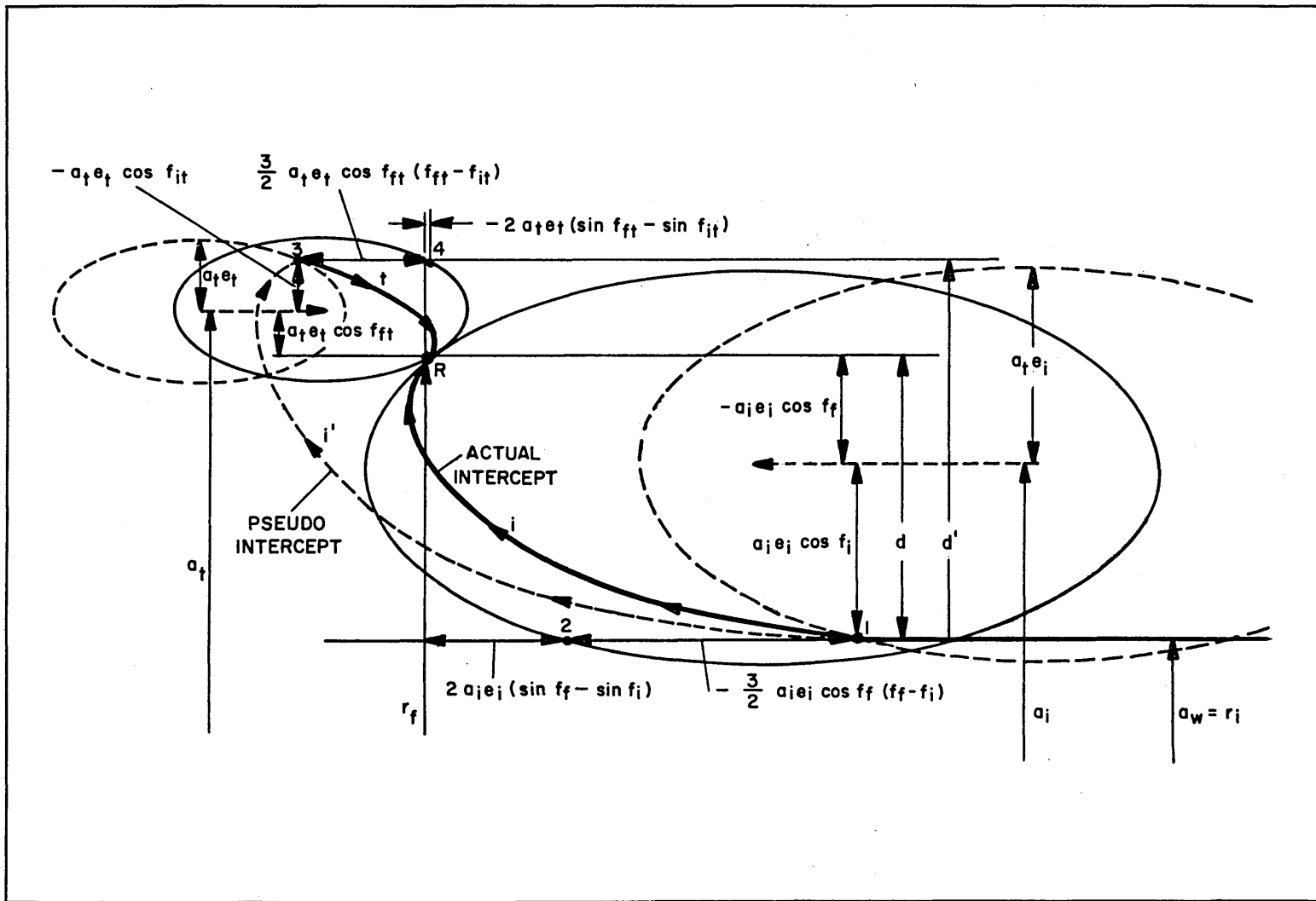


Fig. A-1 Approximate Relative Motion in a Rotating Coordinate Frame

$$\cos f_i = \frac{(1 - b)}{k}$$

$$\sin f_f = \frac{\sqrt{k^2 - b^2}}{k}$$

$$\sin f_i = \frac{\sqrt{k^2 - (1 - b)^2}}{k}$$

The denominator then becomes:

$$\begin{aligned} -(\cos f_f - \cos f_i) &= -\left[-\frac{b}{k} - \frac{(1 - b)}{k}\right] \\ &= \frac{1}{k} \end{aligned}$$

and the expression becomes:

$$\tan \beta_i = \frac{\frac{3}{2} b (f_f - f_i) + 2 \sqrt{k^2 - b^2} - 2 \sqrt{k^2 - (1 - b)^2}}{\quad}$$

which upon interchanging f and E is identical to the result obtained in Section A. 6

Further approximate line-of-sight relations derived by the author, though not used in this investigation, will now be listed in the hopes that they may be of use to others. The inertial line-of-sight angle  $\phi$



is given by:

$$\phi = f + [\beta]_r + \theta$$

where  $[\beta]_r$  indicates the rotating frame derivation and  $\theta = f_c - f$ , where  $f_c$  is the inertial angle of the fictitious target at radius,  $r_f$ , from the perigee of the intercept trajectory.  $\phi$  now becomes:

$$\phi = f_c + [\beta]_r$$

The angular rate of the line of sight now becomes:

$$\begin{aligned} \dot{\phi} &= \dot{f}_c + [\dot{\beta}]_r + \dot{f}_c \\ &= 2\dot{f}_c + [\dot{\beta}]_r \end{aligned}$$

where the second  $\dot{f}_c$  is due to the rotation of the frame in which  $\beta$  is obtained. To get a fairly simple solution one assumes  $\dot{f} = \dot{f}_c = \dot{f}_t$  to yield:

$$\dot{\phi} \approx \dot{f}_c \left[ 2 - \frac{\frac{3}{2}(\cos f_f - Q \cos f_{ft}) - 2(\cos f - Q \cos f_t) + \tan \beta (\sin f - Q \sin f_t)}{(1 + \tan^2 \beta)[(\cos f_f - \cos f) - Q(\cos f_{ft} - \cos f_t)]} \right]$$

The out-of-plane angle  $\psi$  can be obtained either by:

$$\tan \psi \approx \frac{a_t \sin i_f \sin (f_f - f) \cos \beta}{-a_i e_i (\cos f_f - \cos f) + a_t e_t (\cos f_{ft} - \cos f_t)}$$

or:

$$\sin \psi \approx \frac{a_t \sin i_f \sin (f_f - f)}{R_{ng}}$$

#### A.9 Transformations of Rendezvous Parameters for Intercepts to a Target in an Elliptic Orbit

The goal of this section is to derive the required expressions for transforming an intercept to an elliptic orbit target into a pseudo intercept to a circular orbit target that has essentially identical line-of-sight motion characteristics and vice versa. This amounts to determining the phase and amplitude changes necessary to make one sinusoidal variation the same as the sum of two other sinusoidal variations. To do this in a simple manner the approximation is made that:

$$\dot{f} = \dot{f}'_t = \dot{f}'_i$$

where here and subsequently the prime denotes conditions and properties of the pseudo intercept to a circular orbit target.

Now if the following expression equating the radial variation of the pseudo intercept to the actual intercept:

$$-a'_i e'_i (\cos f'_f - \cos f'_i) = -a_i e_i (\cos f_f - \cos f) + a_t e_t (\cos f_{ft} - \cos f_t)$$

is differentiated once, multiplied by minus one and the above equality of angular rates employed the following results:

$$a_i' e_i' \sin f' = a_i e_i \sin f - a_t e_t \sin f_t$$

(The same result is obtained by twice differentiating the equated expression for arc travel variation.)

From Fig. A-1:

$$d = -a_i e_i (\cos f_f - \cos f_i)$$

$$d = \frac{a_i e_i}{k}$$

or,

$$a_i e_i = kd$$

and likewise;

$$a_i' e_i' = k'd'$$

Now defining:

$$f' = f + \Delta f_p$$

$$f_t = f + f_{ft} - f_f$$

and substituting these values the following results:

$$k'd' \sin (f + \Delta f_p) = kd \sin f - a_t e_t \sin (f + f_{ft} - f_f)$$

Evaluating this for  $f = -\Delta f_p$  to eliminate  $k' d'$  gives:

$$0 = -kd \sin \Delta f_p - a_t e_t \sin (f_{ft} - f_f - \Delta f_p)$$

$$kd \sin \Delta f_p = -a_t e_t \sin (f_{ft} - f_t) \cos \Delta f + a_t e_t \cos (f_{ft} - f_t) \sin \Delta f_p$$

or;

$$\tan \Delta f_p = \frac{-a_t e_t \sin (f_{ft} - f_f)}{kd - a_t e_t \cos (f_{ft} - f_f)}$$

From Fig. A-1:

$$d = a_t - r_i - a_t e_t \cos f_{ft}$$

$$d' = a_t - r_i - a_t e_t \cos f_{it}$$

Now the rendezvous parameters of the pseudo intercept from 1 to 3 (the trace shown in Fig. A-1 by the dashed line is appropriate for a frame that rotates with the mean motion of 3 instead of R) can be obtained from:

$$k' = \frac{1}{\cos (f_i + \Delta f_p) - \cos (f_f + \Delta f_p)}$$

$$b' = -k' \cos (f_f + \Delta f_p)$$

To obtain the rendezvous parameters of an actual intercept to an elliptic orbit target so that the line-of-sight motion is essentially the same as a desired pseudo intercept to a circular orbit target the unknown angles  $f$  and  $f_f$  must be changed to the known values  $f'$  and  $f_f'$  by:

$$f = f' - \Delta f_p'$$

$$f_f = f_f' - \Delta f_p'$$

producing:

$$k'd' \sin f' = kd \sin (f' - \Delta f_p') - a_t e_t \sin (f' + f_{ft}' - f_f')$$

Now evaluating this for  $f' = \Delta f_p'$  to eliminate  $kd$ :

$$k'd' \sin \Delta f_p' = -a_t e_t \sin (f_{ft}' - f_f' + \Delta f_p')$$

$$k'd' \sin \Delta f_p' = -a_t e_t \sin (f_{ft}' - f_f') \cos \Delta f_p' - a_t e_t \cos (f_{ft}' - f_f') \sin \Delta f_p'$$

or:

$$\tan \Delta f_p' = \frac{-a_t e_t \sin (f_{ft}' - f_f')}{k'd' + a_t e_t \cos (f_{ft}' - f_f')}$$

Again from Fig. A-1:

$$d' = a_t - r_i \perp a_t e_t \cos f_{it}$$

Now the rendezvous parameters of the actual intercept including the initial velocity change characteristics to depart the circular waiting orbit can be computed from:

$$k = \frac{l}{\cos (f_i' - \Delta f_p') - \cos (f_f' - \Delta f_p')}$$

$$b = -k \cos (f_f' - \Delta f_p')$$

The resulting intercept, for the specified target ellipticity and expected final true anomaly, will have line-of-sight motion that is essentially identical with the selected pseudo intercept to a circular orbit target. The required velocity change magnitude,  $\Delta V_{ip}$ , and the direction  $\alpha_i$  can be obtained as functions of the expected final target true anomaly as in Fig. 8-13 or, more appropriately, as functions of the initial target true anomaly or time. This maneuver, executed at the appropriate  $\beta_i$  angle, would then place the interceptor on an intercept trajectory that has essentially the same line-of-sight motion regardless of the true anomaly of the target. The pseudo radial distance  $d'$  would be a measure of the sensitivity to orbit errors and the anticipated final closing velocity,  $\Delta V_{fp}$ .

## APPENDIX B-1

DESCRIPTION OF COMPUTER SUBROUTINE ORBIT POSB.1. General Description of Operation

This orbital position subroutine was written for general use on the MH 800 of the personnel of the Apollo Space Guidance Analysis Division of the MIT Instrumentation Laboratory by two staff engineers - P. G. Felleman and R. D. Goss. As written by these individuals, the general instructions for use are as follows:

" The purpose of Orbital Pos is to compute position and velocity vectors for two vehicles, an interceptor and a target, at a specified time  $T$ . It is assumed that the vehicles are acted upon by a single gravitational body. The initial conditions, i. e., the position and velocity vectors of the vehicles at time  $T = 0$  are input quantities which are read into the subroutine. These input vectors must be expressed in a common right-hand axis system with origin at the center of the gravitational body. (There are no other constraints on the choice of the common axis system.)

" The inputs to Orbit Pos must be written into a file in the following order:

$$\bar{R}_I, \bar{R}_T, \bar{V}_I, \bar{V}_T, T, MU, Q$$

$\bar{R}_I$  and  $\bar{R}_T$  are the initial position vectors for the interceptor and target respectively.  $\bar{V}_I$  and  $\bar{V}_T$  are the corresponding initial velocity vectors.  $T$  is the time at which position and velocity are desired.  $MU$  is the gravitational constant of the appropriate body.  $Q$  is a quantity which is zero if the subroutine is being used for the first time or if a new set of initial conditions are to be used.  $Q$  is one if the subroutine is being used for other than the first time and the same initial conditions apply, but a new elapsed time is being used.

" The output quantities of Orbit Pos are the position and velocity vectors of the interceptor and the target expressed in the target's local vertical coordinate system. The origin of this system is at the center of the attracting body with the Y-axis passing through the target and the Z-axis in the direction of the cross product of the Y-axis and the target velocity vector. The X-axis forms a right-handed system. Another output is the target position vector expressed in its initial local vertical coordinate system. The output quantities are read out of the file in the following order:

$$\bar{R}_{IT}, \bar{V}_{IT}, \bar{R}_{TR}, \bar{V}_T, \bar{R}_{TP}$$

These are the interceptor's final position and velocity vectors in the target's local vertical system, the target's position and velocity vectors in its own local vertical system, and the target's position at



at time  $T$  expressed in the target's local vertical coordinate system at time  $T = 0$ . (Note that in defining velocity vectors for this subroutine, the axis systems are assumed to be nonrotating about the gravitational body.)"

The subroutine first computes the initial orbital parameters of both vehicles including the time from perigee,  $T_p$  for the initial position using rather standard orbital mechanics expressions. The final time  $\tau = T + T_p$  is then computed and the final mean anomaly

$$M = n \tau$$

is obtained. Through an iterative solution of Kepler's equation  $M = E - e \sin E$  the final positions and velocities of the vehicles are eventually obtained in their respective perigee coordinate system. A system of various matrices then convert these values into the desired output form. The techniques of the iteration are as follows: The first value taken for the eccentric anomaly is:

$$E_0 = M$$

This is then iterated using the Newton-Raphson technique by the expression:

$$E_{k+1} = E_k + \frac{M - E_k + e \sin E_k}{1 - \cos E_k}$$

until the epoch error quantity:

$$\tau = \frac{E_{n+1} - e \sin E_{k+1}}{n}$$

is less than 0.00001 seconds or whatever time units are being used for near-Earth orbits where the velocities are on the order of 25,000 fps this would roughly translate into a position error of less than 1/4 of a foot. Also for these types of orbits usually only two or three iterations are necessary.

## B.2 Use of the Subroutine Orbit Pos

Since the output desired for both the trajectory analysis programs and the intercept simulation programs of this investigation were in terms of measurements and observations relative to the interceptor's local vertical and plane of motion, the actual roles of interceptor and target were reversed. That is to say the interceptor in the investigation was in fact the target in the nomenclature of the subroutine. This facilitated the initial specification of relative positions, subsequent relative position determination, and determination of motion of the interceptor reference frame through the last vector output of the subroutine.

Use was continually made of the feature of setting Q equal to one, when no velocity corrections were made, by having the initial position and velocity vectors be those immediately following the last change in velocity. Not only did this serve to increase the accuracy

of motion determination but it also resulted in a considerable saving of computation time. Despite this saving, the computation time needed for a typical intercept traversing a nominal angle of about  $90^{\circ}$  was very nearly one minute.

As an indication of the accuracies with which the simulation program specified initial relative positions and velocities and the subroutine then determined relative motion, when an exact circular target orbit was desired, the resulting target radius never deviated by more than three points in the tenth significant figure meaning that its orbital position was accurate to better than one inch! It should be recalled that in the interceptor's local vertical coordinate system this meant the accurate specification of all six components of position and velocity. Under conditions of relative orbit inclination only the interceptor vehicle has zero values for some of its position and velocity components. So the fact that the target orbit was circular did not, in effect, greatly simplify its subsequent motion determination.



## REFERENCES

1. Bender, D. F., "Optimum Co-Planar Two Impulse Transfers Between Elliptic Orbits," IAS Paper No. 62-4, 1962.
2. Braham, H. S., and Skidmore, L. J., "Guidance Error Analysis of Satellite Trajectories," IAS Paper No. 61-9, 1961.
3. Brissenden, R. F., Burton, B. B., Foudriat, E. C., and Whitten, J. B., "Analog Simulation of a Pilot-Controlled Rendezvous," NASA TN D-747, 1961.
4. Brissenden, R. F., and Lineberry, E. C., Jr., "Visual Control of Rendezvous," IAS Paper No. 62-42, 1962.
5. Carney, T. M., and Lineberry, E. C., Jr., "Automatic Terminal Guidance Logic for Rendezvous Vehicles," NASA TN D-923, 1961.
6. Cicolani, L. S., "Trajectory Control in Rendezvous Problems Using Proportional Navigation," NASA TN D-772, 1961.
7. Clohessy, W. H., and Wiltshire, R. S., "Terminal Guidance Systems for Satellite Rendezvous," IAS Paper No. 59-93, 1959.
8. Connors, T. L., Hugget, W. A., and Lawson, A. C., Jr., "Line-of-Sight Criteria for Interplanetary Navigation," Proc. 10th IAF Cong., Springer Verlag, Vienna, 1960.
9. Czarnik, M. R., "Guidance and Control Mechanics, Gemini Design Note No. 2, Subject: Terminal Guidance Equations," Unpublished Note of McDonnell Aircraft Corporation presented at NASA meeting in Houston, Texas, July 1962.
10. Darby, W. O., "Correction for the Effects of Finite Thrusting Time In Orbit Changing Maneuvers," IAS Paper No. 61-154-1848, 1961.
11. Duke, W. M., Goldberg, E. A., and Pfeffer, I., "Error Analysis Considerations for a Satellite Rendezvous," ARS Preprint No. 1198-60, 1960.
12. Eggleston, J. M., and Beck, H. D., "A Study of the Positions and Velocities of a Space Station and a Ferry Vehicle During Rendezvous and Return," NASA TR R-87, 1960.

13. Eggleston, J. M., "The Trajectories and Some Practical Guidance Considerations for Rendezvous and Return," IAS Paper No. 61-36, 1961.
14. Eggleston, J. M., and Dunning, R. S., "Analytical Evaluation of a Method of Midcourse Guidance for Rendezvous with Earth Satellites," NASA TN D-883, 1961.
15. Eggleston, J. M., "Optimum Time to Rendezvous," ARS Journal 30 No. 11, 1960.
16. Ehricke, K. A., Space Flight, Vol. I, Environment and Celestial Mechanics, D. Van Nostrand Co. N. J., 1960.
17. Felleman, P. G., "Analysis of Guidance Techniques for Achieving Orbital Rendezvous," M.I.T. Inst. Lab., Internal Dist. Report E-1106, 1962.
18. Felleman, P. G., and Sears, N. E., Jr., "A Guidance Technique for Achieving Rendezvous," Aero/Space Engr., Vol. 19, No. 5, 1960, p. 76.
19. Garber, T. B., "Ascent Guidance for a Satellite Rendezvous," Aero/Space Engr. Vol. 19, No. 5, 1960, p. 74.
20. Hollister, W. M., "The Design of a Control System for the Terminal Phase of a Satellite Rendezvous," S.M. Thesis, M.I.T., 1959.
21. Hord, R. A., "Relative Motion in the Terminal Phase of Interception of a Satellite or a Ballistic Missile," NASA TN 4399, 1958.
22. Houbolt, J. C., "Lunar-Orbit Rendezvous and Manned Lunar Landing," Astronautics, Vol. 7, No. 4, 1962, p. 26.
23. Houbolt, J. C., "Problems and Potentialities of Space Rendezvous," Astronautica Acta, Vol. III, 1961.
24. Kurbjun, M. C., Brissenden, R. F., Foudriat, E. C., and Burton, B. B., "Pilot Control of Rendezvous," IAS Paper No. 61-37, 1961.
25. Levin, E., and Ward, J., "Manned Control of Orbital Rendezvous," RAND P-1834, 1959.

26. Lineberry, E. C., Jr., "Study of an Automatic System for Control of the Terminal Phase of Satellite Rendezvous," NASA TR R-128, 1962.
27. Lineberry, E. C., Jr., Brissenden, R. F., and Kurbjun, M. C., "Analytical and Preliminary Simulation Study of a Pilot's Ability to Control the Terminal Phase of a Rendezvous with Simple Optical Devices and a Timer," NASA, TN, D-965, 1961.
28. Miller, J. G., Grotz, R. M., and Hellman, N. N., "Incremental Velocity Change Versus Time for Intersecting Transfers Between Circular Coplanar Orbits," ARS Preprint No. 2076-61, 1961.
29. Moulton, F. R., Celestial Mechanics, second revised edition, MacMillan Co., N. Y., 1914.
30. Mueller, R. R., "Some Optimizations on a Satellite-Based AICBM Interceptor," ARS Preprint No. 2134-61, 1961.
31. Munick, H., "Optimum Orbital Transfer Using N-Impulses," ARS Preprint No. 2078-61, 1961.
32. Nason, M. L., "Terminal Guidance Technique for Satellite Interception Utilizing a Constant Thrust Rocket Motor," ARS Jour. 30, No. 9, 1960.
33. Nason, M. L., "Terminal Guidance and Rocket Fuel Requirements for Satellites," ARS Paper No. 777-59, 1959.
34. Nelson, A. W., "Manned Orbital Rendezvous," ARS Paper No. 1493-60, 1960.
35. Paiewonsky, B. H., "Transfer Between Vehicles in Circular Orbits," Jet Propulsion, 1958, p. 121.
36. Peske, A., and Ward, M., "Techniques for Error Analysis of Trajectories," ARS Preprint 1926-61, 1961.
37. Peterson, N. V., "Orbital Assembly and Launch for Lunar Operations," IAS Paper No. 62-81, 1962.
38. Peterson, N. V., and Swanson, R. S., "Rendezvous in Space-Effects of Launch Conditions," Aero/Space Engr. Vol. 19, No. 5, 1960.

39. Sears, N. E., Jr., "Satellite Rendezvous Guidance System," (Secret, Unclassified Title), M.I.T. Inst. Lab., Report R-257, 1959.
40. Sears, N. E., Jr., and Felleman, P. G., "Terminal Guidance for a Satellite Rendezvous," ARS Preprint No. 778-59, 1959.
41. Sears, N. E., Jr., "Satellite Rendezvous Guidance System Study," (Confidential, Unclassified Title), M.I.T. Inst. Lab., Report R-344, 1962.
42. Smart, W. M., Celestial Mechanics, Longmans, Green and Co., London, 1953.
43. Soule, P. W., "Rendezvous with Satellites in Elliptical Orbits of Low Eccentricity," AAS Preprint No. 60-71, 1960.
44. Spradlin, L. W., "The Long-Time Satellite Rendezvous Trajectory," Aero/Space Engr., Vol. 19, No. 6, 1960.
45. Spradlin, L. W., "Terminal Guidance for Satellite Rendezvous," S. M. Thesis M.I.T., 1960.
46. Stapleford, R. L., "A Study of the Two Basic Approximations in the Impulsive Guidance Techniques for Orbital Rendezvous," ASD TDR 62-82, 1961.
47. Steinhoff, E. A., "Orbital Rendezvous and Guidance," Aero/Space Engr., Vol. 19, No. 5, 1960, p. 70.
48. Straly, W. H., "Utilizing the Phasing Technique in Rendezvous," ARS Preprint No. 2295-61, 1961.
49. Swanson, R. S., and Peterson, N. V., "The Influence of Launch Conditions on the Friendly Rendezvous of Astrovehicles," AAS Preprint No. 59-16, 1959.
50. Swanson, R. S., Peterson, N. V., and Hoover, L. R., "An Astrovehicle Rendezvous-Guidance Concept," AAS Preprint No. 60-12, 1960.
51. Thompson, H. B., and Stapleford, R. L., "A Study of Manual and Automatic Control Systems for the Terminal Phase of Orbital Rendezvous," ASD TR-61-344, Part I, 1962.



52. Tufts College Institute for Applied Experimental Psychology, Handbook of Human Engineering Data, Second Edition, (Revised), U.S. Naval Training Device Center, Port Washington, N. Y., 1960.
53. Wheelon, A. D., "An Introduction to Midcourse and Terminal Guidance," JPL Report No. 145, 1958.
54. Wolowitz, C. H., Drake, H. M., and Videan, E. N., "Simulator Investigation of Controls and Display Required for Terminal Phase of Coplanar Orbital Rendezvous," NASA TN D-511, 1960.
55. Wrigley, W. "Guidance and Control" Chap. 9 of Orbital and Satellite Vehicles Vol. 2, M.I.T., Cambridge, Mass., 1958.



## BIOGRAPHY

Edwin Eugene Aldrin, Jr. was born in Glen Ridge, New Jersey on January 20, 1930. He lived in Montclair, New Jersey and attended elementary, junior high, and high schools there. He was graduated number three in his class and awarded the degree of Bachelor of Science from the United States Military Academy at West Point, N. Y. in June 1951. He was immediately commissioned as an officer in the United States Air Force.

Following pilot training in Florida and Texas, he received his wings in August 1952. He flew F-86's in combat in Korea from December 1952 to July 1953 where he was credited with destroying two MIG-15 aircraft in aerial combat and awarded the Distinguished Flying Cross and Air Medal with two Oak Leaf Clusters. After a tour as fighter gunnery instructor at Nellis Air Force Base, Nevada, he was assigned as aide to the Dean of Faculty at the United States Air Force Academy in Colorado. Prior to attending MIT, he served for three years as a flight commander in an F-100 tactical fighter squadron in Germany where he was awarded the Air Force Commendation Medal for his duties performed as Alert Commander.

In 1959 he entered MIT under a two-year master's level program of study in Astronautics sponsored by the Air Force Institute of Technology. Subsequently he extended his program of study toward the degree of Doctor of Science.

Major Aldrin, known to many under the nickname "Buzz", is a member of Sigma Gamma Tau and Tau Beta Pi.